The Formation and Function of the Brain Ventricular System

By
Jessica T. Chang

B.S. Molecular and Cellular Biology
The Johns Hopkins University, 2006

Submitted to the Department of Biology
in Partial Fulfillment of the Requirements for the Degree of

Doctor of Philosophy in Biology
at the
Massachusetts Institute of Technology

June 2012

Signature of author……
Department of Biology
May 4, 2012

Certified by……..
Hazel L. Sive
Professor of Biology
Associate Dean, School of Science
Thesis Supervisor

Accepted by ……
Robert T. Sauer
Salvador E. Luria Professor of Biology
Chairman, Graduate Student Committee

The Formation and Function of the Brain Ventricular System

By
Jessica T. Chang

Submitted to the Department of Biology
on April 13, 2012 in Partial Fulfillment of the Requirements for the
Degree of Doctor of Philosophy in Biology at the Massachusetts Institute of Technology

ABSTRACT

The brain ventricular system is composed of a highly conserved set of cavities that contain cerebrospinal fluid (CSF), a protein-rich fluid essential for brain function. However, little is known about the function of embryonic CSF (eCSF), or the mechanisms of CSF production, retention, and circulation that regulate brain ventricle shape and size. Here we present data that begins to dissect the mechanisms governing CSF dynamics during zebrafish embryonic development.

Our data indicate that the Na,K-ATPase regulates three aspects of brain ventricle development essential for normal function - neuroepithelial formation, permeability, and CSF production. Formation of a cohesive neuroepithelium requires both the alpha subunit (Atp1a1) and the regulatory subunit, Fyxd1, while only Atp1a1 modulates neuroepithelial permeability. Further, RhoA regulates both neuroepithelium formation and permeability, downstream of the Na,K-ATPase. Finally, we identified a RhoA-independent process, likely CSF production, which requires Atp1a1, but not Fxyd1. Therefore, formation of the vertebrate brain ventricles requires both production and retention of CSF.

Although the embryonic brain ventricles contain large quantities of eCSF little is known about the function of the fluid or the mechanisms that drive fluid production. We developed a method to manually drain eCSF from zebrafish brain ventricles and show that eCSF is necessary for cell survival within the neuroepithelium. Further, increased retinol binding protein 4 (Rbp4), retinoic acid synthesis, and retinoic acid signaling via the PPARγ (peroxisome proliferator-activated receptor gamma) receptors, prevents neuroepithelial cell death. Thus, we present a novel role for Rbp4 and retinoic acid synthesis and signaling during embryonic brain development.

Finally, we also developed an assay to visualize CSF flow in the embryonic zebrafish. We found that the midbrain-hindbrain boundary acts as a barrier preventing CSF movement between the midbrain and hindbrain, while CSF moves freely between the midbrain and forebrain. Additionally, the heartbeat contributes to CSF movement increasing mixing between the hindbrain and forebrain/midbrain compartments. Furthermore, we determined that

hydrocephalic phenotypes observed in zebrafish are due to abnormalities in CSF production, retention and flow.

These data demonstrate the importance of CSF dynamics during development and further suggest that disruption of these processes can all result in hydrocephalus.

Thesis Supervisor: Hazel L. Sive
Title: Member, Whitehead institute for Biomedical Research
Associate Dean, School of Science
Professor of Biology, MIT

To my parents who have provided endless support, love, and encouragement.

TABLE OF CONTENTS:

Tables and Figures

ACKNOWLEDGEMENTS:

I would like to thank those who have helped both scientifically and personally throughout my graduate career.

To my advisor Hazel Sive who has always been there to challenge and push me. I am thankful for the guidance she provided in addition to the opportunity to explore and pursue new ideas. I will always be grateful for her never ending mentorship.

To Jen Gutzman who took me under her wing as a rotation student and will forever be a close friend. I am indebted to her for teaching me everything I know about zebrafish biology, providing me with fantastic scientific and non-scientific conversations and advice, and for making the Sive lab a fun place to work.

I would also like to thank the rest of the Sive lab. In particular, Heather Ferguson, who has been an incredible and organized administrative assistant, and Olivier Paugois for taking excellent care of the fish (and providing endless amounts of bubble wrap) and without whom, none of these experiments would have been possible.

To my thesis committee members, Troy Littleton, Peter Reddien, and Iain Cheeseman, who have provided insightful and rigorous comments and criticisms along the way and Maria Lehtinen for kindly agreeing to be on my thesis defense committee.

Additionally, I'd like to thank the girls, Jen Gutzman, Chelsea Backer, Isabel Brachmann, Dina Esposito, Alicia Blaker-Lee, and Jasmine McCammon for being amazing, supportive friends and for the rules, special coffee breaks, swimming, setting things on fire, St. Patty's day parades and races, sparkle shoes, the Jen dance, hearts, dinners, and making the day to day so enjoyable.

Most importantly, I'd like to thank my family, my Mom, Dad, and brother Jeremy, for all their support, encouragement, enthusiasm about science, and their stories about graduate school.

Finally, to Joey Davis, who over the years has provided support, love, and laughter, and most importantly, is a constant reminder that there is life outside of the lab.

Curriculum Vitae — Jessica T. Chang

Education

- Massachusettes Institute of Technology 2006-present
  PhD candidate
- Johns Hopkins University 2002-2006
  B.S. Cellular and Molecular Biology with a Minor in Psychology
  Major GPA = 3.93 Overall GPA: 3.89

Research Experience

- Formation and function of the zebrafish brain ventricular system. 2006-present
  - PhD Candidate in the lab of Dr. Hazel Sive at MIT.
  - I studied the role of the Na,K-ATPase during brain ventricle formation and identified a function for the CSF during neuroepithelial cell survival.
- WASP and its effect on secretion in mammalian T cells. Summer 2006
  - Research associate in the lab of Dr. Jim Miller at the University of Rochester
  - Used live imaging and molecular biology to study the WASP protein and its effect on secretion in mammalian T cells.
- Role of TGF-β signaling during *Drosophila* sex determination and gonad morphognesis. 2004-2006
  - Undergraduate research associate in the lab of Dr. Mark VanDoren at The Johns Hopkins University.
  - Identified a sex specific activity of TGF-β signaling which inhibits premature differentiation of embryonic germ cells.
- Bone formation in psoriatic and rheumatoid arthritis. . Summer 2002
  - Volunteer in the Lab of Dr. Chris Ritchlin at the University of Rochester
  - Introduction to immunology, molecular biology, blood cell separation, and tissue culture lab practices.

Awards

- Recipient of NSF Graduate Research Fellowship program 2006-2010
- Recipient of the William D. McElroy Award for Outstanding Undergraduate Research in Biology 2006
- Recipient of Howard Hughes Undergraduate Research Fellowship Summer 2005
- Member of Johns Hopkins Women's Swim Team 2002-2006
  - CoSIDA Academic All American College Division District II Women's At Large Team Award (2004).
  - Competed at NCAA National Meet and All American (2003-2005)

Teaching Experience

- Teaching Assistant for Introduction to Biology (7.013) Spring 2008
  - Two classes of around 25 students that met twice a week for an hour. I also prepared study material and graded test, quizzes and problem sets.

- Teaching Assistant for Cellular Neuroscience (7.29J/9.09J) Spring 2010
    - Class of around 50 students met for an hour a week. I also prepared study material, practice questions and graded tests and problem sets.
- Supervised MIT Undergraduate Research Student Fall 2008
    - Examined mRNA expression pattern of zebrafish Fxyd1 in vivo.
- Supervised University of Puerto Rico student in summer MSRP program. Summer 2011
    - Visualization of embryonic zebrafish CSF flow using a photoconvertible Kaede protein in vivo.

Professional Society Memberships _____

- Member of the American Society of Cell Biology 2011- present
- Member of the Society of Neuroscience 2010-present
- Member of Phi Beta Kappa – Johns Hopkins University 2006
- Treasurer of Tri Beta Biology Honors Society – Johns Hopkins University 2005-2006

Publications _____

- Chang, J.T., Lowery, L.A., and Sive, H. (2012). Multiple roles of Na,K-ATPase during brain ventricle development. Developmental Biology. Submitted to Developmental Biology.
- Chang J.T., and Sive, H. (2012). Embryonic cerebrospinal fluid and retinoic acid are required for embryonic zebrafish neuroepithelial cell survival. In progress.
- Chang, J.T. and Sive, H. (2012). Manual drainage of zebrafish embryonic cerebrospinal fluid. J Vis Exp. Accepted.
- Chang, J.T. and Sive, H. (2012). An assay for permeability of the zebrafish embryonic neuroepithelium. J Vis Exp. Accepted.

Invited Talks _____

- Chang, J.T., Lowery, L.A., Sive, H. The Na,K-ATPase: a bifunctional protein complex that regulates brain ventricle formation. Invited Talk, NE SDB Meeting, March 25-27th 2011.
- Chang, J.T., Lowery, L.A., Sive, H. A dual role for the Na,K-ATPase during brain ventricle development. Invited talk, WI Forum, April 15th 2011.

Abstracts _____

- Chang, J.T., Lowery, L.A., Sive, H. Multiple roles of the Na,K-ATPase during brain ventricle development. Poster presentation, ASCB 2011, Denver, CO, December 3-7th 2011.
- Chang, J.T., Lowery, L.A., Sive, H. Multiple contributions of the NaKATPase to brain ventricle development. Poster presentation, SFN Neuroscience 2010, San Diego, CA November 13-17th 2010.
- Chang, J.T., Lowery, L.A., Sive, H. Multiple contributions of the NaKATPase to brain ventricle inflation. Poster presentation, Neural Development Gordon Conference, Newport, RI August 8-15th 2010.
- Chang, J.T., Lowery, L.A., Sive, H. Regulation of brain ventricle inflation. Poster presentation, 6th European Zebrafish Genetics and Development Meeting, Rome, Italy July 15-19th 2009.

- Chang, J.T., Lowery, L.A., Sive, H. Regulation of zebrafish brain ventricle formation by the Na+K+ ATPase. Poster presentation, NE SDB Meeting, April 24-26th 2009.

CHAPTER ONE

The brain ventricular system and cerebrospinal fluid dynamics

Contributions: I wrote the introductory chapter.

The human brain is one of the most complex structures within the body and to begin to comprehend its function, we must understand how it develops. The construction of the brain begins during early embryogenesis and continues into later life. Defects in brain development often result in severe disorders such as neural tube defects, autism, or mental retardation. The study of brain development classically focuses on the brain tissue, examining the role of tissue shape, differentiation, and neuronal migration. However, the cerebrospinal fluid (CSF) is also a critically important component of the brain, and yet, it receives far less attention. Here, we focus on the intimate connection between the brain and CSF during development and adulthood.

Formation and maintenance of the brain ventricular system

The structure of the vertebrate embryonic brain is highly conserved, and has characteristic bends and folds that allow the brain to pack into the skull. Neurulation, the process of forming the neural tube, starts with a sheet of epithelial cells called the neural plate that, during the course of development, folds and fuses to form the neural tube (Figure 1.1A) (Harrington et al., 2009; Lowery and Sive, 2004). Once a closed neural tube is formed, the central lumen of the tube inflates with CSF to form three distinct fluid-filled compartments termed the embryonic forebrain, midbrain, and hindbrain ventricles, which are maintained into adulthood (Figure

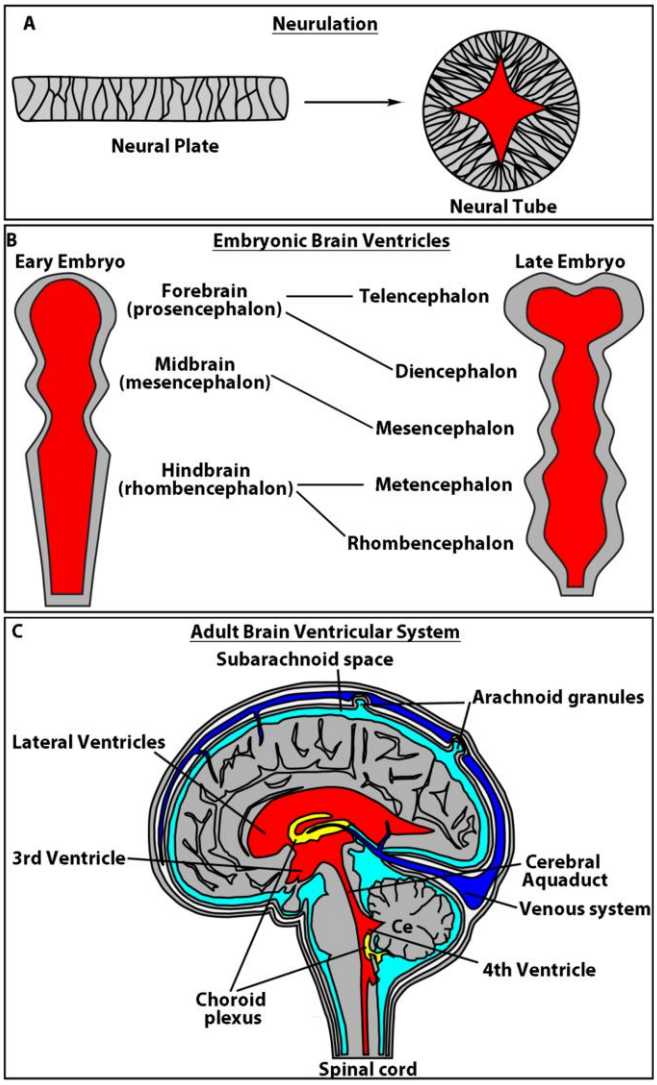

Figure 1.1 The brain ventricular system. (A) Neurulation, the folding and fusing of the neural plate to form a neural tube. (B) Embryonic brain ventricles in the early and late embryo. (C) Adult brain ventricles. Red indicates CSF. Grey= brain or neuroepithelium.

1.1B-C) (Harrington et al., 2009; Lowery et al., 2009; Lowery and Sive, 2004).

CSF is a protein-rich fluid that is present in the early embryonic brain (embryonic CSF – eCSF) and persists into adulthood. It is jointly produced by the neuroepithelium (epithelium that forms the neural tube), ependymal cells lining the brain ventricles, and the choroid plexus, specialized, vascularized ependymal cells (Brown et al., 2004; Pollay and Curl, 1967; Speake et al., 2001; Welss, 1934). Once CSF is secreted into the ventricles, it circulates signaling molecules and removes waste and other metabolites (Czosnyka et al., 2004; Sawamoto et al., 2006). eCSF has three-fold more protein compared to adult CSF (Zheng and Chodobski, 2005) suggesting an important role during embryonic development. Indeed, several studies have identified a requirement for eCSF during cell division, survival, and neurogenesis (Gato et al., 2005; Lehtinen et al., 2011; Miyan et al., 2006; Salehi and Mashayekhi, 2006).

Careful regulation of CSF dynamics is required for normal brain development and homeostasis. We and others have shown that eCSF production and retention as well as neuroepithelial shape are all necessary for proper brain ventricle inflation (Chapter 2) (Gutzman et al., 2008; Gutzman and Sive, 2010; Lowery et al., 2009; Lowery and Sive, 2005; Nyholm et al., 2009; Zhang et al., 2010). Additionally, CSF circulation maintains CSF volume and brain ventricle size where defects can result in hydrocephalus, an accumulation of CSF within the brain ventricles (Mashayekhi et al., 2002). Furthermore, specific factors within the CSF are essential for proper brain development (Gato et al., 2005; Miyan et al., 2006; Salehi and Mashayekhi, 2006). Here, we review the requirements for neuroepithelial formation, brain ventricle development, and contributions of CSF production, retention, circulation, and function.

Neural tube morphogenesis and brain ventricle inflation

Neuroepithelial formation is a prerequisite for brain ventricle inflation and maintenance of brain ventricle size. For neural tube morphogenesis to proceed, the neuroepithelium must regulate its rigidity and plasticity to accommodate the changing neural tissue. This process requires the polarization of the epithelium, the formation of an open neural tube, and coordinated changes in tissue and cell shape.

Epithelial polarization

Formation of a polarized epithelium, which is required for directional transport of ions and solutes across an epithelium and for the generation of discrete compartments within the lumen of the neural tube (Cereijido et al., 2004), occurs in two stages. First, a polarization axis is established in response to external cues, and second, molecular asymmetry is generated along the axis (Drubin and Nelson, 1996). Together, these processes generate apical and basal polarity and junctions. While the exact mechanism directing formation of the apical complex is still being determined, studies have begun to identify important components of this process (Drubin and Nelson, 1996; Nelson, 2003; Niessen, 2007). Establishment of apical polarity and junctions are critically required for normal brain development. In amniotes, the neural plate already has apical polarity and junctions (Figure 1.2A) while anamniotes form a polarized epithelium during neurulation as cells intercalate to form a closed neural rod (Figure 1.2A). Further, mice unable to form apical polarity fail to separate the cerebral hemispheres resulting in a phenotype similar to holoprosencephaly (Chen et al., 2006). Additionally, studies in mouse, zebrafish, and *Drosophila* have identified a role for apical-basal polarity during mitotic spindle orientation during neural progenitor cell division (Cabernard and Doe, 2009; Ohata et al., 2011; Yingling et al., 2008). Thus, generation of a polarized epithelium is crucial for further developmental processes required to form the mature brain.

Neural tube opening

Subsequent to epithelial polarization, formation of an open neural tube commences. During vertebrate embryonic development, the central lumen of the neural tube gives rise to the brain ventricular system. There are two types of vertebrate neurulation: “lumen first”, as in amniotes such as chickens and mice, where the lumen forms as the neural tube closes (Colas and Schoenwolf, 2001), and “lumen later”, observed in anamniotes including *Xenopus* and zebrafish, where the lumen forms after the closure of the neural tube (Figure 1.2A) (Davidson and Keller, 1999; Hong and Brewster, 2006). Interestingly, opening of the zebrafish neural tube is similar to closure of the neural tube in amniotes. In amniotes such as chick, mouse, and human, neural tube closure occurs in a sequential multi-site process rather than a single site

that bi-directionally zippers from anterior to posterior (Figure 1.2B, left) (Golden and Chernoff, 1993; Van Allen et al., 1993; Van Straaten et al., 1996). Similarly, Gutzman and Sive demonstrate that in zebrafish, there is a multi-site sequential opening of the hindbrain ventricle (Figure 1.2B, right) (Gutzman and Sive, 2010). This process begins at the rhombomere boundaries and then extends to within the rhombomeres (transient morphological segments with distinct gene expressions) (Lumsden, 2004). The first opening occurs around 18 hpf (hours post fertilization) at the rhombomere 0/1 boundary (r0/1), the second at the r3/4 boundary and subsequently the r4/5 boundary. At 20 hpf, the lumen of the neural tube opens both anterior and posterior to r1 and at the final boundary, r2/3. Finally between 22-24 hpf, sequential separation of the midline occurs at r2, then r4, and finally r3 and r5 (Gutzman and Sive, 2010). Thus, opening of the

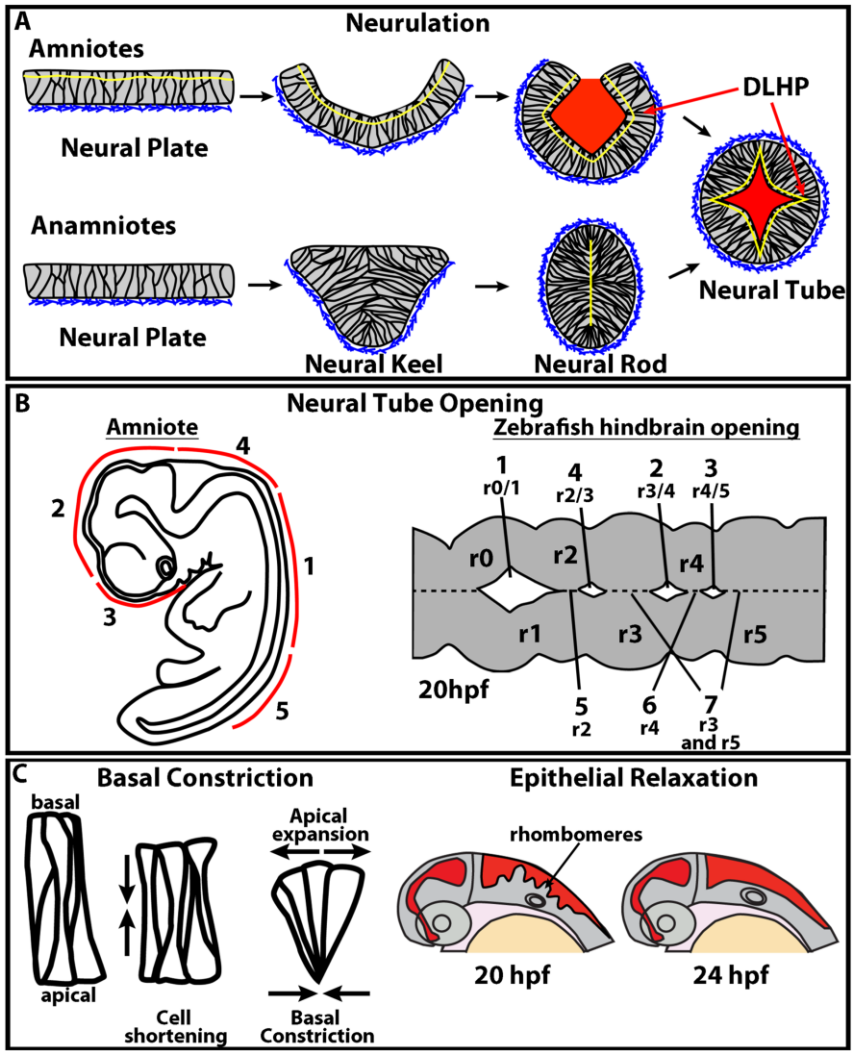

Figure 1.2 Changes in neuroepithelium and cell shape. (A) Amniotic vs. anamniotic neurulation, the amniote neural plate has apical junctions (yellow) and connection with exrtracellular matrix (ECM, blue) and rolls to form a closed and inflated neural tube (A top). The anamniote neural plate is in contact with the ECM (blue), and deepens to form the neural keel. Next, cells intercalate and form apical junctions resulting in a closed neural rod. Subsequently, the neural rod undergoes cell shape changes and inflation to form the neural tube (A bottom). DLHP = dorsal lateral hinge-points. (B) Neural tube closure in amniotes (left) compared to zebrafish hindbrain opening (right). R= rhombomere. # indicates order of closure/opening (C) Cell shape changes basal constriction (left) and epithelial relaxation of rhombomeres (right). Representative clusters of cells from MHB (C, left). Red in A and C = CSF.

zebrafish neural tube does not occur like a zipper as hypothesized, but rather, in a fashion similar to the multi-site process of amniote neural tube closure. Further investigation into the mechanisms that drive neural tube opening in zebrafish compared to neural tube closure in mice will conclusively determine whether these are in fact similarly regulated processes.

Neuroepithelium and cell shape changes

As the embryonic brain develops, the neuroepithelium begins to bend and fold generating the highly conserved shape of the neural tube (Lowery et al., 2009). As the neural tube closes in mice, the neuroepithelium bends to form dorsal lateral hinge-points (DLHP) that allow the tissue to fold and form a tube (Figure 1.2A) (Ybot-Gonzalez et al., 2007). Similarly, in zebrafish as the neural tube opens, dorsal lateral hinge-points begin to form (Nyholm et al., 2009). Nyhlom et al., 2009 proposed that formation of the dorsal lateral hinge-points occur in a similar manner during mouse and fish neural tube development by promoting actin-myosin contraction. Notably however, the timing of this event differs between amniotes and anamniotes (Figure 1.2A). The formation of the DLHP is crucial for the proper ventricle shape and subsequent filling with eCSF. Without the DLHP, the tube would fail to form or appear to have reduced brain ventricle inflation as a result of incomplete tissue morphogenesis.

Additional changes in neural tube morphology are driven by changes in neuroepithelial cell shape. In zebrafish, a combination of apical and basal constriction is thought to drive epithelial bending. Apical constriction is very well studied and its role during development is extensively reviewed (Sawyer et al., 2010). Basal constriction on the other hand is relatively understudied process. Gutzman et al., identified a role for basal constriction in the formation of the midbrain-hindbrain boundary (MHB) constriction (Gutzman et al., 2008). This study identified a cluster of 3-4 cells in the MHB that first shorten, then basally constrict, and finally apically expand (Figure 1.2C, left) (Gutzman et al., 2008). Further identification of the mechanisms which drive basal constriction is ongoing. A second type of cell shape change that is crucial for proper neuroepithelial morphogenesis and subsequent brain ventricle opening is the process of epithelial relaxation. Gutzman and Sive identified that a mutation in the zebrafish *myosin phosphatase 1* gene prevents relaxation of the actin-myosin complex within the rhombomeres.

In zebrafish, the rhombomeres appear as distinct bumps within the hindbrain neuroepithelium from 19-21 hpf, and lose their characteristic shape by 24 hpf, thus leaving the neuroepithelium smooth (Figure 1.2C, right). This loss of morphology corresponds to a decrease in phosphorylated myosin and subsequent changes in cell shape. In this study, the authors identified a correlation between myosin contraction and ventricle expansion, postulating that regulating the elasticity of the epithelium is necessary for normal ventricle expansion (Gutzman and Sive, 2010).

As described, many of the steps required for the formation of a cohesive, intact and dynamic neuroepithelium have been identified, however, the mechanisms of some critical transitions remain. Given that proper formation of the neuroepithelium is a crucial first step in the formation of the brain ventricular system, failure at this point results in neural tube defects and an inability to properly regulate CSF dynamics.

CSF production

About 50-70% of adult CSF is produced by the choroid plexus, a highly branched and vascularized secretory structure that forms the blood-CSF barrier (BCSFB) (Wright et al., 1977). CSF is also produced by the ependyma, the layer of cells immediately adjacent to the brain ventricles (Pollay and Curl, 1967). In the developing embryo, eCSF is present immediately after neural tube closure and prior to choroid plexus development. In amniotes, amniotic fluid is initially incorporated into the central lumen of the neural tube and contributes to early eCSF (Figure 1.2A) (Harrington et al., 2009; Lowery et al., 2009; Lowery and Sive, 2004). Studies using explanted chick neuroepithelium also demonstrated that this tissue is secretory suggesting that the neuroepithelium can also produce eCSF (Welss, 1934).

CSF production has been extensively studied in the context of the choroid plexus. The choroid plexus epithelium is polarized and facilitates diffusion of ions down the electrochemical gradient thus driving movement of water into the ventricles. To date, the Na,K-ATPase, Na^+-K^{+-} $2Cl^-$ co-transporter, (NKCC), Na^+-H^+ exchanger (NHE), carbonic anhydrase, and the Na^+-HCO_3^- co-transporters have been implicated in adult CSF production (Banizs et al., 2007; Davson and Segal, 1970; Jacobs et al., 2008; Keep et al., 1994; Maren, 1988; Murphy and Johanson, 1989;

Pollay et al., 1985; Wu et al., 1998). However, many other channels that regulate K^+ and Cl^- levels are expressed in the choroid plexus and may regulate CSF production through as yet undetermined mechanisms. (Brown et al., 2004; Damkier et al., 2010; Johanson et al., 2008). Here, we will specifically focus on the role of Na^+, HCO_3^-, and water movement during CSF production.

Na^+ transport

Regulation of Na^+ transport in the choroid plexus is critical for CSF production. The Na,K-ATPase is expressed on the apical membrane of the choroid plexus and pumps 3 Na^+ ions out of the cell in exchange for movement of 2 K^+ into the cell, thereby keeping cellular Na^+ low and establishing a favorable gradient for Na^+ co-transporters to mediate Na^+ movement into the cell from the basolateral side (Figure 1.3, left). Inhibition of the Na,K-ATPase pump with the inhibitor ouabain, decreases CSF secretion and the movement of Na^+ into the CSF of rats, rabbits and dogs (Davson and Segal, 1970; Pollay et al., 1985). Similarly, the Na^+-K^+-$2Cl^-$ co-transporter (NKCC) is apically localized in the choroid plexus epithelium (Figure 1.3, left) (Plotkin et al., 1997; Wu et al., 1998) and pharmacological inhibition of the NKCC not only reduces CSF formation but also reduces the choroid plexus epithelial cell volume, thus demonstrating a role in ion transport into the choroid plexus (Keep et al., 1994; Wu et al., 1998). Furthermore, the Na^+-H^+ exchangers (NHE) are required to regulate intracellular pH and cell volume in addition to contributing to

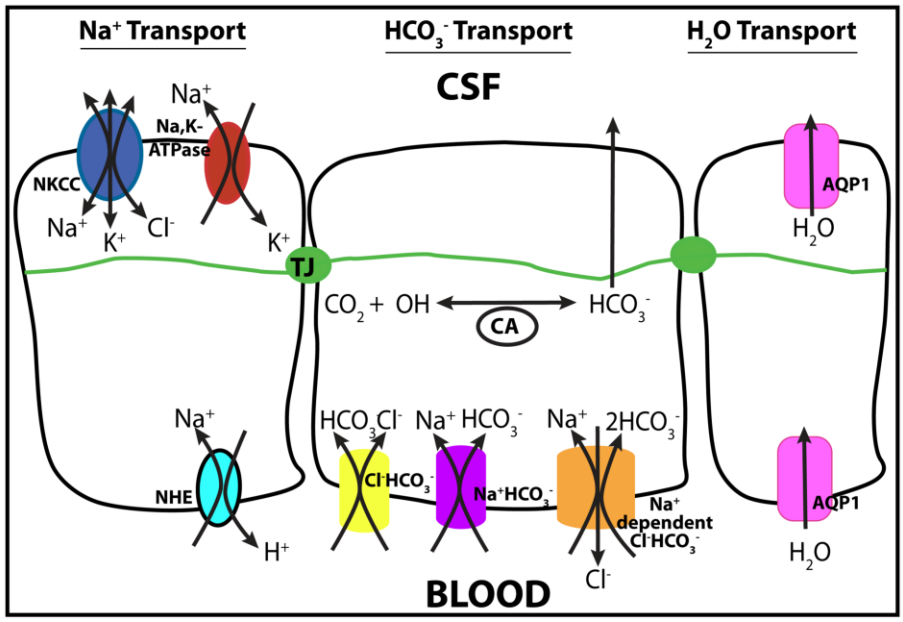

Figure 1.3: Ionic gradient regulating CSF production. CSF production requires Na^+ transport (left cell), HCO_3^- transport (center cell), and water movement (right cell). CA = carbonic anhydrase.

transepithelial Na^+ transport (Orlowski and Grinstein, 2004). Murphy and Johnson (1989) demonstrate that inhibition of NHE by amiloride reduces Na^+ transport into the CSF. These studies suggest that the NHE is localized to the basal membrane and likely imports Na^+ from the blood providing the Na^+ for the Na,K-ATPase to extrude into the CSF (Figure 1.3, left) (Murphy and Johanson, 1989). However, further studies are required to identify the localization of the NHE in the choroid plexus. Taken together, these studies demonstrate the necessity of Na^+ transport during adult CSF production.

In contrast to adult CSF production, few studies have examined the requirement of Na^+ transport during eCSF production. We have identified a role for the Na,K-ATPase during early embryonic brain ventricle inflation (Chapter 2) (Lowery and Sive, 2005). The Na,K-ATPase is required for three distinct processes of brain ventricle development including neural tube formation, neuroepithelial permeability regulation, and CSF production (Chapter 2) suggesting a critical role for this protein during brain ventricle inflation both in adults and embryos. While studies have identified roles for the NKCC and NHE in embryonic fluid transport (Bara et al., 1990; Vanden Heuvel et al., 2006) and these transporters have been identified in the embryonic brain, their role during CSF production or other aspects of brain development have yet to be addressed.

HCO_3^- transport

The transport of HCO_3^- is crucial for CSF secretion (Saito and Wright, 1983; Saito and Wright, 1984). In the choroid plexus, there are three major HCO_3^- transporters: $Cl^-HCO_3^-$, Na^+-HCO_3^-, and Na^+-dependent Cl^--HCO_3^- (Figure 1.3, center). These co-transporters are expressed on the basolateral side of the choroid plexus membrane and promote the accumulation of Na^+, HCO_3^-, and Cl^-, which are necessary for CSF secretion (Lindsey et al., 1990; Praetorius et al., 2004; Segal, 1993). The Na^+-HCO_3^- co-transporter moves HCO_3^- molecules into the cell down the concentration gradient of Na^+ created by the Na,K-ATPase (Choi et al., 2000), whereas the Na^+-dependent Cl^--HCO_3^- co-transporter exchanges Cl^- for movement of Na^+ and two HCO_3^- into the cell. Furthermore, knockout of the Na^+-dependent Cl^--HCO_3^- co-transporter results in mice with smaller brain ventricles (Jacobs et al., 2008), while the transport activity of the Na^+-HCO_3^- is

increased in hydrocephalic mice (Banizs et al., 2007) consistent with a role during CSF production. Although a direct connection between the Cl^--HCO_3^- and CSF production has not been made, this transporter is thought to be required for CSF production as it is expressed in the choroid plexus and chemical inhibition of the Cl^--HCO_3^- exchanger using DIDS, an anion transporter inhibitor, reduces Cl^- transport into the CSF (Deng and Johanson, 1989; Frankel and Kazemi, 1983).

Further support for a role of HCO_3^- in fluid secretion comes from studies inhibiting carbonic anhydrase, a crucial enzyme required for cellular hydration of CO_2 to produce H^+ and HCO_3^- (Figure 1.3 center). Although this enzyme is not directly involved in the movement of ions, it is thought to have an important role in CSF secretion. Acetazolamide, a carbonic anhydrase inhibitor, is commonly used to therapeutically reduce CSF production (Maren, 1988; Vogh et al., 1987) and can decrease CSF pressure in children with hydrocephalus (Cowan and Whitelaw, 1991). Carbonic anhydrase is expressed during embryonic development in mice, rat, human, and fish (De Vitry et al., 1989; Gilmour and Perry, 2009; Johansson et al., 2008a). However, the mechanism by which carbonic anhydrase promotes fluid secretion and the developmental stage during which it is required for fluid secretion remains to be determined.

Water transport

Establishment of an osmotic gradient drives movement of water through aquaporins into the brain ventricles. Aquaporins (AQP) are small integral membrane proteins and provide the major pathway for water transport in secretory tissues such as the brain (Verkman and Mitra, 2000). Recent studies have identified that AQP are not only permeable to water but also to certain ions and small molecules (Boassa et al., 2006) that may further modulate CSF production. To date, three aquaporin isoforms, AQP1, AQP4, and AQP9 have been detected within the mammalian brain (Gunnarson et al., 2004). AQP1 is expressed on the apical surface of the choroid plexus and at lower levels on the basolateral surfaces (Figure 1.3, left) (Johansson et al., 2005; Speake et al., 2003). APQ1 knockout mice have reduced CSF secretion and smaller ventricles (Oshio et al., 2003), suggesting a crucial role during brain ventricle inflation. Although both AQP4 and AQP9 are expressed in astrocytes, AQP4 is intimately linked to CSF reabsorption

by the blood brain barrier (BBB), whereas little is known about AQP9 (Gunnarson et al., 2004). Water movement via AQP4 is required to buffer the outflow of K^+ ions due to action potentials and promote K^+ clearance by astrocytes of the BBB (Amiry-Moghaddam and Ottersen, 2003). Conversely, in some pathological conditions, a reduction of AQP4 can prevent brain edemas that usually lead to permanent brain damage (Amiry-Moghaddam et al., 2003; Manley et al., 2000; Vajda et al., 2002).

In the embryonic chick, AQP1, AQP4 and Kir4 (K^+ channel) are highly expressed at the rudimentary blood-CSF barrier (BCSFB) prior to choroid plexus development (Parvas and Bueno, 2010; Parvas et al., 2008), suggesting a potential role for these channels during early CSF production. In rat and chick, AQP4 expression in the cerebellum coincides with the development of the BBB (Nico et al., 2001; Wen et al., 1999). Although aquaporins are expressed during embryonic development, the mechanisms that drive water movement in adults and embryos to promote CSF production require more attention.

Other mechanisms of CSF production

While a major driving force of CSF production is the generation of an osmotic gradient, other factors have also been identified that regulate this process. Brain ventricle inflation in the embryonic chick requires the secretion of proteoglycans such as chondroitin sulfate (Alonso et al., 1999). Application of beta-D-xyloside to inhibit chondroitin sulfate synthesis results in expanded brain ventricles due to disruption of the CSF osmolarity (Alonso et al., 1998; Alonso et al., 1999; Oohira et al., 1981), suggesting that proteoglycans affect brain ventricle inflation by regulating the osmotic gradient and thus CSF secretion.

CSF retention

Once CSF is produced, the brain ventricles retain and hold the CSF. The brain contains several barriers, (1) the CSF-brain barrier, which is created by tight junctions of the neuroepithelium, (2) the blood brain barrier (BBB), separating the endothelial blood vessels from brain cells and (3) the blood CSF barrier (BCSFB), which is the connection between the blood and choroid plexus (Figure 1.4A).

CSF-brain barrier

The CSF-brain barrier regulates mixing between the CSF and brain interstitial fluid (ISF). In the immature embryonic brain, intercellular junctions between the ependymal cells, which line the brain ventricles, provide an initial barrier between the CSF and the brain (Figure 1.4B) (Del Bigio, 1995; Fossan et al., 1985). However, in adults, exchange between CSF and ISF is thought to occur freely as ependymal cells do not contain intercellular junctions (Figure 1.4C) (Brightman and Reese, 1969). Adult ependymal cells also regulate transport of ions, small molecules, and water between the CSF and the rest of the brain tissue (Bruni, 1998). The disappearance of the CSF-brain barrier could be the result of development of a more effective epithelial BCSFB in adult mammals.

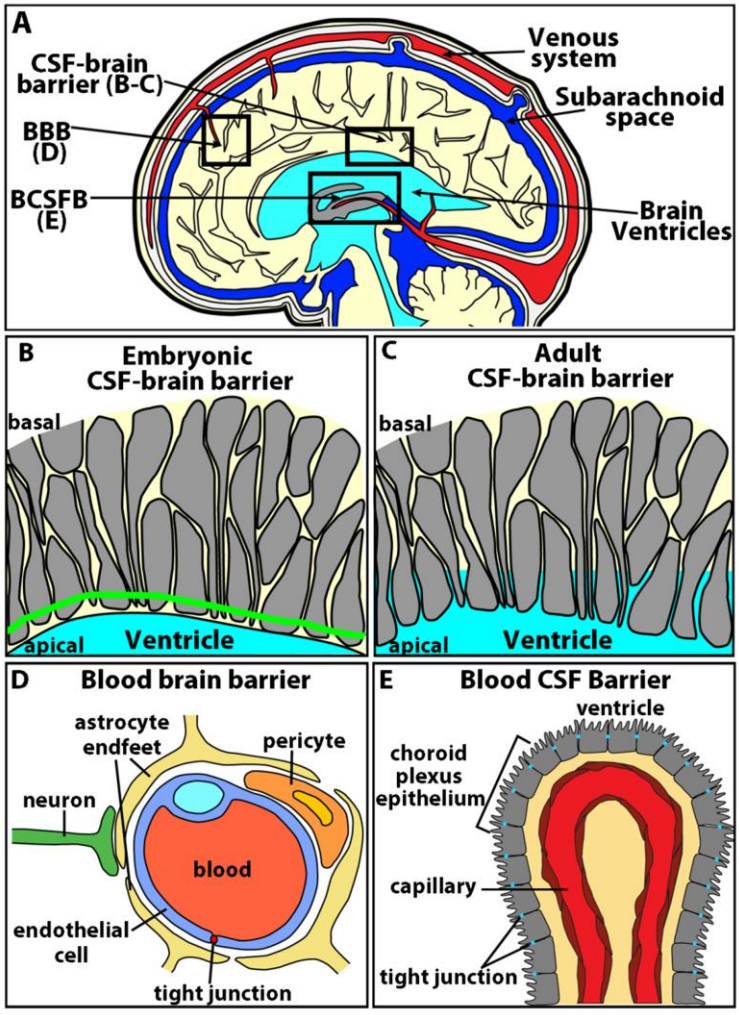

Figure 1.4 The brain barriers. (A) Diagram depicting barriers in the brain. (B-C) CSF-brain barrier in embryos (B) have apical junctions (green) compared to adults (C) which lack junctions. (D) Blood brain barrier. Communication between astrocytes and blood vessels. (E) Blood CSF barrier composed of the choroid plexus epithelium with tight junctions (blue) and capillaries (blood, red). Grey = brain/choroid plexus. Yellow = interstitial fluid (ISF), light blue = CSF.

In the embryonic zebrafish, we and others have identified a function for neuroepithelial tight junctions in the regulation of brain ventricle size (Chapter 2) (Zhang et al., 2010). Claudin 5a and the Na,K-ATPase regulate paracellular permeability of tight junctions, thereby creating a neuroepithelial-ventricular barrier equivalent to the CSF-brain barrier (Chapter 2) (Zhang et al., 2010). Further, we

identified that RhoA also regulates neuroepithelial permeability and acts downstream of the Na,K-ATPase (Chapter 2). While overexpression of RhoA does not alter brain ventricle size, overexpression of the Na,K-ATPase alpha subunit, *atp1a1*, increased brain ventricle size, suggesting a unique role for Atp1a1 during regulation of CSF dynamics and CSF-brain barrier formation (Chapter 2).

Blood brain barrier

The primary function of the BBB is to separate the blood and brain interstitial fluid, preventing free diffusion of polar molecules between the blood and brain. This barrier is composed of highly impermeable tight junctions between endothelial cells that form capillaries and venules in the brain (Nagy et al., 1984; Reese and Karnovsky, 1967). The endfeet of astrocytes are in contact with blood vessels in the brain and are thought to promote formation of endothelial tight junctions (Figure 1.4D) (Janzer and Raff, 1987). Additionally, the BBB protects the brain from changes in plasma composition and other circulating factors that could negatively affect neural function (Abbott and Romero, 1996). Formation of the BBB begins during embryonic brain development. However, prior to formation of a mature BBB, the blood vessels are observed to cover the entire surface of the neural tube in 2-day chick or 9-day rodent embryos likely facilitating transfer and communication between the blood and the brain (Bar, 1980; Dermietzel and Krause, 1991; Risau and Wolburg, 1990).

Blood CSF barrier

The blood-CSF barrier (BCSFB) is formed by the choroid plexus epithelium. As discussed above, this polarized epithelium differentially distributes channels to create an osmotic gradient necessary for CSF secretion. The choroid plexus epithelium is joined by tight junctions that are impermeable to the passage of molecules between the CSF and blood (Figure 1.4E) (Johansson et al., 2008b). Development of the choroid plexus occurs embryonically in zebrafish, chick, mouse, rat and humans (Garcia-Lecea et al., 2008; Keep and Jones, 1990; Korzhevskii, 2000; Stastny and Rychter, 1976; Sturrock, 1979). Further, in chick, a rudimentary BCSFB develops at the ventral midline of the mesencephalon and prosencephalon prior to choroid plexus development (Parvas and Bueno, 2010; Parvas et al., 2008). In the developing brain,

Dziegielewska et al., proposed that the choroid plexus epithelium is immature, since high levels of plasma proteins are detected within the CSF, and as the animal develops, this epithelium matures to prevents transfer between blood and CSF (Dziegielewska et al., 1980a; Dziegielewska et al., 1980b). An alternate hypothesis suggested by Johansson et al., proposes that the BCSFB is functional during development and high levels of transcellular permeability allows for transfer of proteins between the blood and CSF during development, again leading to elevated levels of plasma proteins in the CSF (Johansson et al., 2008b). As the animal ages, transcellular permeability decreases reducing levels of plasma proteins present in the CSF (Johansson et al., 2008b). This suggests that the BCSFB is dynamic and can adapt to specific requirements or environments of the developing nervous system.

CSF circulation

CSF flow

Movement of the CSF is required for recycling, absorbing and transporting substances throughout the brain. Adult CSF flows from the lateral ventricles, to the third and fourth ventricle and then into the subarachnoid spaces surrounding the brain or spinal cord (Figure 1.5A) (Czosnyka et al., 2004). CSF circulation is important for the clearance of waste and metabolites, movement of signaling molecules, and maintenance of CSF volume and pressure.

Several studies suggest that cilia and the pulsatile heartbeat drive CSF flow. Yamadori and Nara demonstrate that the ependymal cilia, which line the brain ventricles, beat in a directed manner. This action moves particles in the same direction, which was interpreted as bulk CSF flow (Yamadori and Nara, 1979). In addition, adult CSF movement is pulsatile and is generated by pulsations from the blood flow being transmitted across the choroid plexus to the CSF (Bering et al 1962). Disruptions of ependymal cilia or CSF pulsations are correlated with hydrocephalus, suggesting that CSF flow is necessary for maintenance of proper brain ventricle size (Brody et al., 2000; Kobayashi et al., 2002; Linninger et al., 2007; Madsen et al., 2006; Taulman et al., 2001).

Consistent with the observations in the adult, movement of eCSF likely requires cilia as inhibition of cilia function leads to an accumulation of fluid that results in hydrocephalus (Banizs et al., 2005; Fogelgren et al., 2011; Kramer-Zucker et al., 2005; Sun et al., 2004; Wodarczyk et al., 2009). Additional work in *Xenopus* also identified a role for the heartbeat in generating the majority of pulsatile CSF flow (Miskevich, 2010). Thus, it seems that mechanisms governing embryonic CSF flow are similar to those in adults.

CSF reabsorption

Researchers have long thought that the arachnoid granules are the main passage for CSF drainage and reabsorption. These granules are in direct contact with the venous system and allow for passage of fluid from the subarachnoid space into the venous system (Figure 1.5B) (Pollay, 2010). However, a recent body of work has demonstrated that CSF can also drain via

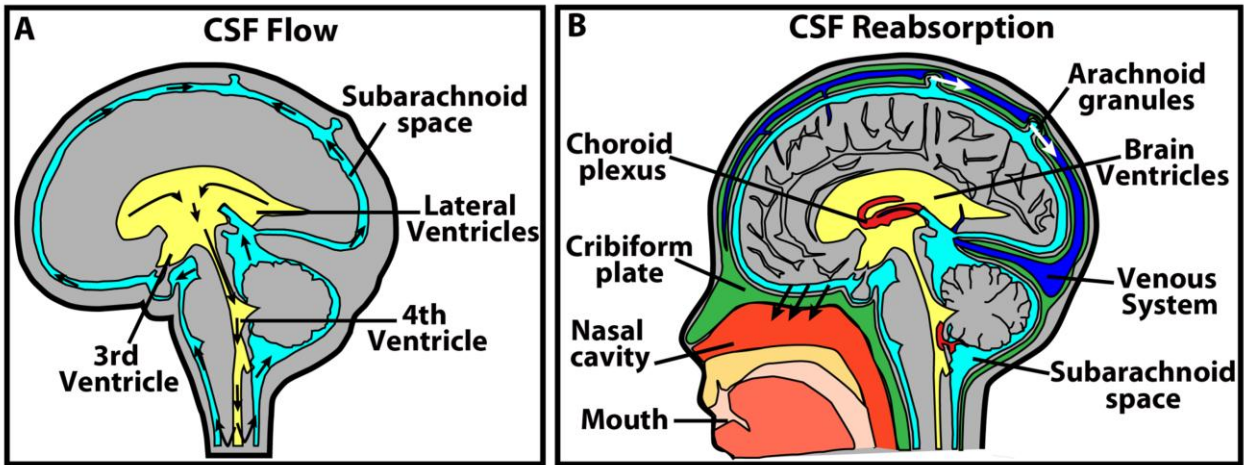

Figure 1.5 CSF circulation. (A) CSF flows from the lateral ventricles to the 3rd ventricle and 4th ventricle out into the spinal cord and subarachnoid space. Arrows indicate flow. (B). CSF is reabsorbed by the lymphatic system (black arrows) in the cribriform plate (green) and in higher pressure situations by the arachnoid granules (white arrows) into the venous system. Grey = brain, yellow = CSF.

the lymphatic system (Boulton et al., 1999; Johnston, 2003; Johnston et al., 2005; Koh et al., 2006; Ludemann et al., 2005; Papaiconomou et al., 2002; Zakharov et al., 2003). Although the lymphatic system does not directly connect to the brain, CSF in the subarachnoid space drains through the cranial and spinal nerves (Johnston, 2003; Johnston et al., 2005). In particular, CSF has been shown to exit the subarachnoid space near the olfactory neurons and through the cribiform plate, contributing to the nasal mucosa and being reabsorbed into the lymphatic system (Figure 1.5B) (Johnston et al., 2005; Mollanji et al., 2001a; Papaiconomou et al., 2002).

The current hypothesis suggests that the majority of CSF is drained via the lymphatic system under normal pressure, while in situations with elevated pressure, such as hydrocephalus, the brain engages the arachnoid granules to remove excess fluid into the venous system to relieve intercranial pressure (Mollanji et al., 2001a).

The connection of the subarachnoid space and the lymphatic system develops around birth (Koh et al., 2006; Mollanji et al., 2001b; Papaiconomou et al., 2002), and is correlated with a significant increase in CSF production to adult levels. Presumably, this increased CSF production creates demand for a constant drainage system to facilitate the removal of metabolites and other small molecules that are potentially dangerous to the brain tissue. In contrast to the adult, it is still unclear how CSF is drained or recycled in the embryo. One hypothesis is that the brain interstitial fluid is more contiguous with the CSF at this stage and is drained via the blood brain barrier (Kapoor et al., 2008). Several studies also demonstrate that blood vessels cover the surface of the embryonic neural tube (Bar, 1980; Dermietzel and Krause, 1991; Risau and Wolburg, 1990), suggesting an alternate route of CSF reabsorption. Thus, CSF drainage likely occurs through the blood vasculature, interstitial fluid or diffusion between the CSF and the neuroepithelium or spinal canal.

CSF function

Adult CSF is found both within brain ventricles and in the subarachnoid space between the skull and the brain. By filling this space, the CSF provides mechanical support for the brain and increases its buoyancy, reducing the brain's "effective weight" by more than 60% (Segal, 1993). Reabsorption and production of CSF provides a "sink", promoting CSF flow and facilitating the removal of waste, metabolites, and other small molecules and circulating nutrients and signaling molecules (Sawamoto et al., 2006; Segal, 1993). Consistent with this function, Sawamoto et al., identified that CSF flow generates a gradient of Slit 2 which guides olfactory neuron migration in adult mice (Sawamoto et al., 2006).

In the embryo, a number of studies have identified that eCSF is required for gene expression, cell proliferation, survival, and neurogenesis during embryonic brain development (Alonso et al., 2011; Gato et al., 2005; Lehtinen et al., 2011; Martin et al., 2009; Martin et al., 2006;

Mashayekhi, 2008; Mashayekhi and Salehi, 2006b; Miyan et al., 2006; Parada et al., 2008a; Parada et al., 2008b; Parada et al., 2005; Salehi and Mashayekhi, 2006; Salehi et al., 2009). Additionally, CSF dynamics regulate the composition of the fluid within the brain ventricles. In H-Tx hydrocephalic rats, which have reduced CSF flow due to an obstruction of the cerebral aquaduct, CSF composition is different from wild type and inhibits cell proliferation and neurogenesis (Mashayekhi et al., 2001; Mashayekhi et al., 2002). Similarly, patients with congenital hydrocephalus have abnormal CSF composition with elevated levels of nerve growth factor (Mashayekhi and Salehi, 2005). These studies indicate that normal composition of eCSF is crucial for proper neural development.

As animals age, CSF production and flow are reduced, altering CSF composition (May et al., 1990; Preston, 2001; Stoquart-ElSankari et al., 2007). CSF from patients with hydrocephalus and neurodegenerative disorders have elevated levels of growth factors and metabolites, and this CSF abnormally regulates the proliferation and neurogenesis of the surrounding brain tissue (Mashayekhi et al., 2010a; Mashayekhi et al., 2010b; Mashayekhi and Salehi, 2005; Mashayekhi and Salehi, 2006a). These studies suggest that in age-related disorders, a disruption of CSF dynamics likely results in an excess of metabolites, possibly leading to neurological disorders. Thus, the brain is very sensitive to changes in CSF composition both during development and adulthood.

Conclusions

Identification of the molecular processes that regulate CSF dynamics is still an ongoing area of research. In order for proper formation and maintenance of the brain ventricular system and surrounding brain tissue, CSF production, retention, flow, reabsorption and composition must be carefully coordinated to regulate brain development and maintain homeostasis. Therefore, understanding the physiological and molecular processes governing CSF dynamics is an important area to pursue.

Research Approach

In the following chapters, we examine eCSF production, retention, function, and flow during embryonic zebrafish brain development.

Brain ventricle development is a multi-step process that requires formation of a cohesive neuroepithelium, regulation of neuroepithelial permeability and production of CSF. In Chapter 2, we identified that the Na,K-ATPase subunits, Atp1a1 and Fxyd1 are required during brain ventricle development. Formation of a cohesive neuroepithelium with continuous apical junctions and apical-basal polarity requires both Atp1a1 and Fxyd1 while only Atp1a1 regulates neuroepithelial permeability and CSF production. To quantify permeability of the neuroepithelium, we developed a dye retention assay, which is described in Chapter 5. Further, we determined that RhoA acts downstream of the Na,K-ATPase to regulate neuroepithelial formation and permeability. Additionally, we determined that the Na,K-ATPase beta subunit, Atp1b3a, is required for CSF production independent of RhoA and this work is described in Appendix 1.

In the embryonic zebrafish, I identified a requirement for the eCSF during brain development, which is described in Chapter 3. To investigate the role of eCSF during brain development, I created a system to drain eCSF from the brain ventricles of zebrafish embryos (Chapter 6). Using this technique, I determined that eCSF is required for cell survival within the neuroepithelium and in particular, a subset of diencephalic cells are sensitive to the loss of eCSF. Further, retinoic acid (RA) synthesis and signaling through PPARγ (peroxisome proliferative activating gamma) nuclear receptors promote cell survival. In this work, we propose that eCSF delivers the precursor retinol (bound to retinol binding protein 4) to the neuroepithelium where RA is produced and activates PPARγ, which likely promotes transcription of anti-apoptotic genes.

Finally, in Chapter 4, I describe a novel Kaede activation technique to visualize eCSF flow in embryonic zebrafish. Kaede protein is injected into the brain ventricles, photoactivated in a region of interest, and its localization is followed as a function of time. We identified that (1)

CSF flow occurs in the hindbrain or midbrain/forebrain compartments, (2) initiation of the heartbeat increases CSF flow between the hindbrain and the midbrain/forebrain compartments, and (3) the midbrain-hindbrain tissue folds act as a physical barrier between the two compartments to restrict CSF flow. Furthermore, we show that some hydrocephalic conditions have increased CSF flow while others have abnormalities in CSF production or retention, demonstrating that hydrocephalus can result due to the disruption of multiple different aspects of CSF dynamics.

Together, this work demonstrates that careful regulation of CSF dynamics is crucial during normal brain development. While this work begins to dissect the mechanisms and requirements of CSF dynamics during embryonic zebrafish development, many aspects of CSF production, retention, flow, drainage and function still remain unknown. In Chapter 7 I outline some of the questions and hypotheses which remain to be tested to fully understand CSF dynamics during development and adulthood.

REFERENCES

Abbott, N. J., Romero, I. A., 1996. Transporting therapeutics across the blood-brain barrier. Mol Med Today. 2**,** 106-13.

Alonso, M. I., Gato, A., Moro, J. A., Barbosa, E., 1998. Disruption of proteoglycans in neural tube fluid by beta-D-xyloside alters brain enlargement in chick embryos. Anat Rec. 252**,** 499-508.

Alonso, M. I., Gato, A., Moro, J. A., Martin, P., Barbosa, E., 1999. Involvement of sulfated proteoglycans in embryonic brain expansion at earliest stages of development in rat embryos. Cells Tissues Organs. 165**,** 1-9.

Alonso, M. I., Martin, C., Carnicero, E., Bueno, D., Gato, A., 2011. Cerebrospinal fluid control of neurogenesis induced by retinoic acid during early brain development. Dev Dyn. 240**,** 1650-9.

Amiry-Moghaddam, M., Otsuka, T., Hurn, P. D., Traystman, R. J., Haug, F. M., Froehner, S. C., Adams, M. E., Neely, J. D., Agre, P., Ottersen, O. P., Bhardwaj, A., 2003. An alpha-

syntrophin-dependent pool of AQP4 in astroglial end-feet confers bidirectional water flow between blood and brain. Proc Natl Acad Sci U S A. 100**,** 2106-11.

Amiry-Moghaddam, M., Ottersen, O. P., 2003. The molecular basis of water transport in the brain. Nat Rev Neurosci. 4**,** 991-1001.

Banizs, B., Komlosi, P., Bevensee, M. O., Schwiebert, E. M., Bell, P. D., Yoder, B. K., 2007. Altered pH(i) regulation and Na(+)/HCO3(-) transporter activity in choroid plexus of cilia-defective Tg737(orpk) mutant mouse. Am J Physiol Cell Physiol. 292**,** C1409-16.

Banizs, B., Pike, M. M., Millican, C. L., Ferguson, W. B., Komlosi, P., Sheetz, J., Bell, P. D., Schwiebert, E. M., Yoder, B. K., 2005. Dysfunctional cilia lead to altered ependyma and choroid plexus function, and result in the formation of hydrocephalus. Development. 132**,** 5329-39.

Bar, T., 1980. The vascular system of the cerebral cortex. Adv Anat Embryol Cell Biol. 59**,** I-VI,1-62.

Bara, M., Guiet-Bara, A., Durlach, J., 1990. Comparative study of effects of magnesium and taurine on electrical parameters of natural and artificial membranes. VII. Effects on cellular and paracellular ionic transfer through isolated human amnion. Magnes Res. 3**,** 249-54.

Boassa, D., Stamer, W. D., Yool, A. J., 2006. Ion channel function of aquaporin-1 natively expressed in choroid plexus. J Neurosci. 26**,** 7811-9.

Boulton, M., Flessner, M., Armstrong, D., Mohamed, R., Hay, J., Johnston, M., 1999. Contribution of extracranial lymphatics and arachnoid villi to the clearance of a CSF tracer in the rat. Am J Physiol. 276**,** R818-23.

Brightman, M. W., Reese, T. S., 1969. Junctions between intimately apposed cell membranes in the vertebrate brain. J Cell Biol. 40**,** 648-77.

Brody, S. L., Yan, X. H., Wuerffel, M. K., Song, S. K., Shapiro, S. D., 2000. Ciliogenesis and left-right axis defects in forkhead factor HFH-4-null mice. Am J Respir Cell Mol Biol. 23**,** 45-51.

Brown, P. D., Davies, S. L., Speake, T., Millar, I. D., 2004. Molecular mechanisms of cerebrospinal fluid production. Neuroscience. 129**,** 957-70.

Bruni, J. E., 1998. Ependymal development, proliferation, and functions: a review. Microsc Res Tech. 41**,** 2-13.

Cabernard, C., Doe, C. Q., 2009. Apical/basal spindle orientation is required for neuroblast homeostasis and neuronal differentiation in Drosophila. Dev Cell. 17**,** 134-41.

Cereijido, M., Contreras, R. G., Shoshani, L., 2004. Cell adhesion, polarity, and epithelia in the dawn of metazoans. Physiol Rev. 84**,** 1229-62.

Chen, L., Liao, G., Yang, L., Campbell, K., Nakafuku, M., Kuan, C. Y., Zheng, Y., 2006. Cdc42 deficiency causes Sonic hedgehog-independent holoprosencephaly. Proc Natl Acad Sci U S A. 103**,** 16520-5.

Choi, I., Aalkjaer, C., Boulpaep, E. L., Boron, W. F., 2000. An electroneutral sodium/bicarbonate cotransporter NBCn1 and associated sodium channel. Nature. 405**,** 571-5.

Colas, J. F., Schoenwolf, G. C., 2001. Towards a cellular and molecular understanding of neurulation. Dev Dyn. 221**,** 117-45.

Cowan, F., Whitelaw, A., 1991. Acute effects of acetazolamide on cerebral blood flow velocity and pCO2 in the newborn infant. Acta Paediatr Scand. 80**,** 22-7.

Czosnyka, M., Czosnyka, Z., Momjian, S., Pickard, J. D., 2004. Cerebrospinal fluid dynamics. Physiol Meas. 25**,** R51-76.

Damkier, H. H., Brown, P. D., Praetorius, J., 2010. Epithelial pathways in choroid plexus electrolyte transport. Physiology (Bethesda). 25**,** 239-49.

Davidson, L. A., Keller, R. E., 1999. Neural tube closure in Xenopus laevis involves medial migration, directed protrusive activity, cell intercalation and convergent extension. Development. 126**,** 4547-56.

Davson, H., Segal, M. B., 1970. The effects of some inhibitors and accelerators of sodium transport on the turnover of 22Na in the cerebrospinal fluid and the brain. J Physiol. 209**,** 131-53.

De Vitry, F., Gomes, D., Rataboul, P., Dumas, S., Hillion, J., Catelon, J., Delaunoy, J. P., Tixier-Vidal, A., Dupouey, P., 1989. Expression of carbonic anhydrase II gene in early brain cells as revealed by in situ hybridization and immunohistochemistry. J Neurosci Res. 22**,** 120-9.

Del Bigio, M. R., 1995. The ependyma: a protective barrier between brain and cerebrospinal fluid. Glia. 14**,** 1-13.

Deng, Q. S., Johanson, C. E., 1989. Stilbenes inhibit exchange of chloride between blood, choroid plexus and cerebrospinal fluid. Brain Res. 501**,** 183-7.

Dermietzel, R., Krause, D., 1991. Molecular anatomy of the blood-brain barrier as defined by immunocytochemistry. Int Rev Cytol. 127**,** 57-109.

Drubin, D. G., Nelson, W. J., 1996. Origins of cell polarity. Cell. 84**,** 335-44.

Dziegielewska, K. M., Evans, C. A., Fossan, G., Lorscheider, F. L., Malinowska, D. H., Mollgard, K., Reynolds, M. L., Saunders, N. R., Wilkinson, S., 1980a. Proteins in cerebrospinal fluid and plasma of fetal sheep during development. J Physiol. 300**,** 441-55.

Dziegielewska, K. M., Evans, C. A., Malinowska, D. H., Mollgard, K., Reynolds, M. L., Saunders, N. R., 1980b. Blood-cerebrospinal fluid transfer of plasma proteins during fetal development in the sheep. J Physiol. 300**,** 457-65.

Fogelgren, B., Lin, S. Y., Zuo, X., Jaffe, K. M., Park, K. M., Reichert, R. J., Bell, P. D., Burdine, R. D., Lipschutz, J. H., 2011. The exocyst protein Sec10 interacts with Polycystin-2 and knockdown causes PKD-phenotypes. PLoS Genet. 7**,** e1001361.

Fossan, G., Cavanagh, M. E., Evans, C. A., Malinowska, D. H., Mollgard, K., Reynolds, M. L., Saunders, N. R., 1985. CSF-brain permeability in the immature sheep fetus: a CSF-brain barrier. Brain Res. 350**,** 113-24.

Frankel, H., Kazemi, H., 1983. Regulation of CSF composition--blocking chloride-bicarbonate exchange. J Appl Physiol. 55**,** 177-82.

Garcia-Lecea, M., Kondrychyn, I., Fong, S. H., Ye, Z. R., Korzh, V., 2008. In vivo analysis of choroid plexus morphogenesis in zebrafish. PLoS One. 3**,** e3090.

Gato, A., Moro, J. A., Alonso, M. I., Bueno, D., De La Mano, A., Martin, C., 2005. Embryonic cerebrospinal fluid regulates neuroepithelial survival, proliferation, and neurogenesis in chick embryos. Anat Rec A Discov Mol Cell Evol Biol. 284**,** 475-84.

Gilmour, K. M., Perry, S. F., 2009. Carbonic anhydrase and acid-base regulation in fish. J Exp Biol. 212**,** 1647-61.

Golden, J. A., Chernoff, G. F., 1993. Intermittent pattern of neural tube closure in two strains of mice. Teratology. 47**,** 73-80.

Gunnarson, E., Zelenina, M., Aperia, A., 2004. Regulation of brain aquaporins. Neuroscience. 129**,** 947-55.

Gutzman, J. H., Graeden, E. G., Lowery, L. A., Holley, H. S., Sive, H., 2008. Formation of the zebrafish midbrain-hindbrain boundary constriction requires laminin-dependent basal constriction. Mech Dev. 125**,** 974-83.

Gutzman, J. H., Sive, H., 2010. Epithelial relaxation mediated by the myosin phosphatase regulator Mypt1 is required for brain ventricle lumen expansion and hindbrain morphogenesis. Development. 137**,** 795-804.

Harrington, M. J., Hong, E., Brewster, R., 2009. Comparative analysis of neurulation: first impressions do not count. Mol Reprod Dev. 76**,** 954-65.

Hong, E., Brewster, R., 2006. N-cadherin is required for the polarized cell behaviors that drive neurulation in the zebrafish. Development. 133**,** 3895-905.

Jacobs, S., Ruusuvuori, E., Sipila, S. T., Haapanen, A., Damkier, H. H., Kurth, I., Hentschke, M., Schweizer, M., Rudhard, Y., Laatikainen, L. M., Tyynela, J., Praetorius, J., Voipio, J., Hubner, C. A., 2008. Mice with targeted Slc4a10 gene disruption have small brain ventricles and show reduced neuronal excitability. Proc Natl Acad Sci U S A. 105**,** 311-6.

Janzer, R. C., Raff, M. C., 1987. Astrocytes induce blood-brain barrier properties in endothelial cells. Nature. 325**,** 253-7.

Johanson, C. E., Duncan, J. A., 3rd, Klinge, P. M., Brinker, T., Stopa, E. G., Silverberg, G. D., 2008. Multiplicity of cerebrospinal fluid functions: New challenges in health and disease. Cerebrospinal Fluid Res. 5**,** 10.

Johansson, P., Dziegielewska, K., Saunders, N., 2008a. Low levels of Na, K-ATPase and carbonic anhydrase II during choroid plexus development suggest limited involvement in early CSF secretion. Neurosci Lett. 442**,** 77-80.

Johansson, P. A., Dziegielewska, K. M., Ek, C. J., Habgood, M. D., Mollgard, K., Potter, A., Schuliga, M., Saunders, N. R., 2005. Aquaporin-1 in the choroid plexuses of developing mammalian brain. Cell Tissue Res. 322**,** 353-64.

Johansson, P. A., Dziegielewska, K. M., Liddelow, S. A., Saunders, N. R., 2008b. The blood–CSF barrier explained: when development is not immaturity. Bioessays. 30**,** 237-248.

Johnston, M., 2003. The importance of lymphatics in cerebrospinal fluid transport. Lymphat Res Biol. 1**,** 41-4; discussion 45.

Johnston, M., Zakharov, A., Koh, L., Armstrong, D., 2005. Subarachnoid injection of Microfil reveals connections between cerebrospinal fluid and nasal lymphatics in the non-human primate. Neuropathol Appl Neurobiol. 31**,** 632-40.

Kapoor, K. G., Katz, S. E., Grzybowski, D. M., Lubow, M., 2008. Cerebrospinal fluid outflow: an evolving perspective. Brain Research Bulletin. 77**,** 327-34.

Keep, R. F., Jones, H. C., 1990. A morphometric study on the development of the lateral ventricle choroid plexus, choroid plexus capillaries and ventricular ependyma in the rat. Developmental Brain Research. 56**,** 47-53.

Keep, R. F., Xiang, J., Betz, A. L., 1994. Potassium cotransport at the rat choroid plexus. Am J Physiol. 267**,** C1616-22.

Kobayashi, Y., Watanabe, M., Okada, Y., Sawa, H., Takai, H., Nakanishi, M., Kawase, Y., Suzuki, H., Nagashima, K., Ikeda, K., Motoyama, N., 2002. Hydrocephalus, situs inversus, chronic sinusitis, and male infertility in DNA polymerase lambda-deficient mice: possible implication for the pathogenesis of immotile cilia syndrome. Mol Cell Biol. 22**,** 2769-76.

Koh, L., Zakharov, A., Nagra, G., Armstrong, D., Friendship, R., Johnston, M., 2006. Development of cerebrospinal fluid absorption sites in the pig and rat: connections between the subarachnoid space and lymphatic vessels in the olfactory turbinates. Anat Embryol (Berl). 211**,** 335-44.

Korzhevskii, D. E., 2000. Proliferative zones in the epithelium of the choroid plexuses of the human embryo brain. Neurosci Behav Physiol. 30**,** 509-12.

Kramer-Zucker, A. G., Olale, F., Haycraft, C. J., Yoder, B. K., Schier, A. F., Drummond, I. A., 2005. Cilia-driven fluid flow in the zebrafish pronephros, brain and Kupffer's vesicle is required for normal organogenesis. Development. 132**,** 1907-21.

Lehtinen, M. K., Zappaterra, M. W., Chen, X., Yang, Y. J., Hill, A. D., Lun, M., Maynard, T., Gonzalez, D., Kim, S., Ye, P., D'Ercole, A. J., Wong, E. T., LaMantia, A. S., Walsh, C. A.,

2011. The cerebrospinal fluid provides a proliferative niche for neural progenitor cells. Neuron. 69**,** 893-905.

Lindsey, A. E., Schneider, K., Simmons, D. M., Baron, R., Lee, B. S., Kopito, R. R., 1990. Functional expression and subcellular localization of an anion exchanger cloned from choroid plexus. Proc Natl Acad Sci U S A. 87**,** 5278-82.

Linninger, A. A., Xenos, M., Zhu, D. C., Somayaji, M. R., Kondapalli, S., Penn, R. D., 2007. Cerebrospinal fluid flow in the normal and hydrocephalic human brain. IEEE Trans Biomed Eng. 54**,** 291-302.

Lowery, L. A., De Rienzo, G., Gutzman, J. H., Sive, H., 2009. Characterization and classification of zebrafish brain morphology mutants. Anat Rec (Hoboken). 292**,** 94-106.

Lowery, L. A., Sive, H., 2004. Strategies of vertebrate neurulation and a re-evaluation of teleost neural tube formation. Mech Dev. 121**,** 1189-97.

Lowery, L. A., Sive, H., 2005. Initial formation of zebrafish brain ventricles occurs independently of circulation and requires the nagie oko and snakehead/atp1a1a.1 gene products. Development. 132**,** 2057-67.

Ludemann, W., Berens von Rautenfeld, D., Samii, M., Brinker, T., 2005. Ultrastructure of the cerebrospinal fluid outflow along the optic nerve into the lymphatic system. Childs Nerv Syst. 21**,** 96-103.

Lumsden, A., 2004. Segmentation and compartition in the early avian hindbrain. Mech Dev. 121**,** 1081-8.

Madsen, J. R., Egnor, M., Zou, R., 2006. Cerebrospinal fluid pulsatility and hydrocephalus: the fourth circulation. Clin Neurosurg. 53**,** 48-52.

Manley, G. T., Fujimura, M., Ma, T., Noshita, N., Filiz, F., Bollen, A. W., Chan, P., Verkman, A. S., 2000. Aquaporin-4 deletion in mice reduces brain edema after acute water intoxication and ischemic stroke. Nat Med. 6**,** 159-63.

Maren, T. H., 1988. The kinetics of HCO3- synthesis related to fluid secretion, pH control, and CO2 elimination. Annu Rev Physiol. 50**,** 695-717.

Martin, C., Alonso, M. I., Santiago, C., Moro, J. A., De la Mano, A., Carretero, R., Gato, A., 2009. Early embryonic brain development in rats requires the trophic influence of cerebrospinal fluid. Int J Dev Neurosci. 27**,** 733-40.

Martin, C., Bueno, D., Alonso, M. I., Moro, J. A., Callejo, S., Parada, C., Martin, P., Carnicero, E., Gato, A., 2006. FGF2 plays a key role in embryonic cerebrospinal fluid trophic properties over chick embryo neuroepithelial stem cells. Dev Biol. 297**,** 402-16.

Mashayekhi, F., 2008. Neural cell death is induced by neutralizing antibody to nerve growth factor: an in vivo study. Brain Dev. 30**,** 112-7.

Mashayekhi, F., Bannister, C. M., Miyan, J. A., 2001. Failure in cell proliferation in the germinal epithelium of the HTx rats. Eur J Pediatr Surg. 11 Suppl 1**,** S57-9.

Mashayekhi, F., Draper, C. E., Bannister, C. M., Pourghasem, M., Owen-Lynch, P. J., Miyan, J. A., 2002. Deficient cortical development in the hydrocephalic Texas (H-Tx) rat: a role for CSF. Brain. 125**,** 1859-74.

Mashayekhi, F., Hadavi, M., Vaziri, H. R., Naji, M., 2010a. Increased acidic fibroblast growth factor concentrations in the serum and cerebrospinal fluid of patients with Alzheimer's disease. J Clin Neurosci. 17**,** 357-9.

Mashayekhi, F., Mirzajani, E., Naji, M., Azari, M., 2010b. Expression of insulin-like growth factor-1 and insulin-like growth factor binding proteins in the serum and cerebrospinal fluid of patients with Parkinson's disease. J Clin Neurosci. 17**,** 623-7.

Mashayekhi, F., Salehi, Z., 2005. Expression of nerve growth factor in cerebrospinal fluid of congenital hydrocephalic and normal children. Eur J Neurol. 12**,** 632-7.

Mashayekhi, F., Salehi, Z., 2006a. Cerebrospinal fluid nerve growth factor levels in patients with Alzheimer's disease. Ann Saudi Med. 26**,** 278-82.

Mashayekhi, F., Salehi, Z., 2006b. The importance of cerebrospinal fluid on neural cell proliferation in developing chick cerebral cortex. Eur J Neurol. 13**,** 266-72.

May, C., Kaye, J. A., Atack, J. R., Schapiro, M. B., Friedland, R. P., Rapoport, S. I., 1990. Cerebrospinal fluid production is reduced in healthy aging. Neurology. 40**,** 500-3.

Miskevich, F., 2010. Imaging fluid flow and cilia beating pattern in Xenopus brain ventricles. J Neurosci Methods. 189**,** 1-4.

Miyan, J. A., Zendah, M., Mashayekhi, F., Owen-Lynch, P. J., 2006. Cerebrospinal fluid supports viability and proliferation of cortical cells in vitro, mirroring in vivo development. Cerebrospinal Fluid Res. 3**,** 2.

Mollanji, R., Bozanovic-Sosic, R., Silver, I., Li, B., Kim, C., Midha, R., Johnston, M., 2001a. Intracranial pressure accommodation is impaired by blocking pathways leading to extracranial lymphatics. Am J Physiol Regul Integr Comp Physiol. 280**,** R1573-81.

Mollanji, R., Papaiconomou, C., Boulton, M., Midha, R., Johnston, M., 2001b. Comparison of cerebrospinal fluid transport in fetal and adult sheep. Am J Physiol Regul Integr Comp Physiol. 281**,** R1215-23.

Murphy, V. A., Johanson, C. E., 1989. Alteration of sodium transport by the choroid plexus with amiloride. Biochim Biophys Acta. 979**,** 187-92.

Nagy, Z., Peters, H., Huttner, I., 1984. Fracture faces of cell junctions in cerebral endothelium during normal and hyperosmotic conditions. Lab Invest. 50**,** 313-22.

Nelson, W. J., 2003. Adaptation of core mechanisms to generate cell polarity. Nature. 422**,** 766-74.

Nico, B., Frigeri, A., Nicchia, G. P., Quondamatteo, F., Herken, R., Errede, M., Ribatti, D., Svelto, M., Roncali, L., 2001. Role of aquaporin-4 water channel in the development and integrity of the blood-brain barrier. J Cell Sci. 114**,** 1297-307.

Niessen, C. M., 2007. Tight junctions/adherens junctions: basic structure and function. J Invest Dermatol. 127**,** 2525-32.

Nyholm, M. K., Abdelilah-Seyfried, S., Grinblat, Y., 2009. A novel genetic mechanism regulates dorsolateral hinge-point formation during zebrafish cranial neurulation. J Cell Sci. 122**,** 2137-48.

Ohata, S., Aoki, R., Kinoshita, S., Yamaguchi, M., Tsuruoka-Kinoshita, S., Tanaka, H., Wada, H., Watabe, S., Tsuboi, T., Masai, I., Okamoto, H., 2011. Dual roles of Notch in regulation of apically restricted mitosis and apicobasal polarity of neuroepithelial cells. Neuron. 69**,** 215-30.

Oohira, A., Nogami, H., Nakanishi, Y., 1981. Abnormal overgrowth of chick embryos treated with p-nitrophenyl beta-D-xyloside at early stages of development. J Embryol Exp Morphol. 61**,** 221-32.

Orlowski, J., Grinstein, S., 2004. Diversity of the mammalian sodium/proton exchanger SLC9 gene family. Pflugers Arch. 447**,** 549-65.

Oshio, K., Song, Y., Verkman, A. S., Manley, G. T., 2003. Aquaporin-1 deletion reduces osmotic water permeability and cerebrospinal fluid production. Acta Neurochir Suppl. 86**,** 525-8.

Papaiconomou, C., Bozanovic-Sosic, R., Zakharov, A., Johnston, M., 2002. Does neonatal cerebrospinal fluid absorption occur via arachnoid projections or extracranial lymphatics? Am J Physiol Regul Integr Comp Physiol. 283**,** R869-76.

Parada, C., Escola-Gil, J. C., Bueno, D., 2008a. Low-density lipoproteins from embryonic cerebrospinal fluid are required for neural differentiation. J Neurosci Res. 86**,** 2674-84.

Parada, C., Gato, A., Bueno, D., 2008b. All-trans retinol and retinol-binding protein from embryonic cerebrospinal fluid exhibit dynamic behaviour during early central nervous system development. Neuroreport. 19**,** 945-50.

Parada, C., Martin, C., Alonso, M. I., Moro, J. A., Bueno, D., Gato, A., 2005. Embryonic cerebrospinal fluid collaborates with the isthmic organizer to regulate mesencephalic gene expression. J Neurosci Res. 82**,** 333-45.

Parvas, M., Bueno, D., 2010. The embryonic blood-CSF barrier has molecular elements to control E-CSF osmolarity during early CNS development. J Neurosci Res. 88**,** 1205-12.

Parvas, M., Parada, C., Bueno, D., 2008. A blood-CSF barrier function controls embryonic CSF protein composition and homeostasis during early CNS development. Dev Biol. 321**,** 51-63.

Plotkin, M. D., Kaplan, M. R., Peterson, L. N., Gullans, S. R., Hebert, S. C., Delpire, E., 1997. Expression of the Na(+)-K(+)-2Cl- cotransporter BSC2 in the nervous system. Am J Physiol. 272**,** C173-83.

Pollay, M., 2010. The function and structure of the cerebrospinal fluid outflow system. Cerebrospinal Fluid Res. 7**,** 9.

Pollay, M., Curl, F., 1967. Secretion of cerebrospinal fluid by the ventricular ependyma of the rabbit. Am J Physiol. 213**,** 1031-8.

Pollay, M., Hisey, B., Reynolds, E., Tomkins, P., Stevens, F. A., Smith, R., 1985. Choroid plexus Na+/K+-activated adenosine triphosphatase and cerebrospinal fluid formation. Neurosurgery. 17**,** 768-72.

Praetorius, J., Kim, Y. H., Bouzinova, E. V., Frische, S., Rojek, A., Aalkjaer, C., Nielsen, S., 2004. NBCn1 is a basolateral Na+-HCO3- cotransporter in rat kidney inner medullary collecting ducts. Am J Physiol Renal Physiol. 286**,** F903-12.

Preston, J. E., 2001. Ageing choroid plexus-cerebrospinal fluid system. Microsc Res Tech. 52**,** 31-7.

Reese, T. S., Karnovsky, M. J., 1967. Fine structural localization of a blood-brain barrier to exogenous peroxidase. J Cell Biol. 34**,** 207-17.

Risau, W., Wolburg, H., 1990. Development of the blood-brain barrier. Trends in Neurosciences. 13**,** 174-8.

Saito, Y., Wright, E. M., 1983. Bicarbonate transport across the frog choroid plexus and its control by cyclic nucleotides. J Physiol. 336**,** 635-48.

Saito, Y., Wright, E. M., 1984. Regulation of bicarbonate transport across the brush border membrane of the bull-frog choroid plexus. J Physiol. 350**,** 327-42.

Salehi, Z., Mashayekhi, F., 2006. The role of cerebrospinal fluid on neural cell survival in the developing chick cerebral cortex: an in vivo study. Eur J Neurol. 13**,** 760-4.

Salehi, Z., Mashayekhi, F., Naji, M., Pandamooz, S., 2009. Insulin-like growth factor-1 and insulin-like growth factor binding proteins in cerebrospinal fluid during the development of mouse embryos. J Clin Neurosci. 16**,** 950-3.

Sawamoto, K., Wichterle, H., Gonzalez-Perez, O., Cholfin, J. A., Yamada, M., Spassky, N., Murcia, N. S., Garcia-Verdugo, J. M., Marin, O., Rubenstein, J. L., Tessier-Lavigne, M., Okano, H., Alvarez-Buylla, A., 2006. New neurons follow the flow of cerebrospinal fluid in the adult brain. Science. 311**,** 629-32.

Sawyer, J. M., Harrell, J. R., Shemer, G., Sullivan-Brown, J., Roh-Johnson, M., Goldstein, B., 2010. Apical constriction: a cell shape change that can drive morphogenesis. Dev Biol. 341**,** 5-19.

Segal, M. B., 1993. Extracellular and cerebrospinal fluids. J Inherit Metab Dis. 16**,** 617-38.

Speake, T., Freeman, L. J., Brown, P. D., 2003. Expression of aquaporin 1 and aquaporin 4 water channels in rat choroid plexus. Biochim Biophys Acta. 1609**,** 80-6.

Speake, T., Whitwell, C., Kajita, H., Majid, A., Brown, P. D., 2001. Mechanisms of CSF secretion by the choroid plexus. Microsc Res Tech. 52**,** 49-59.

Stastny, F., Rychter, Z., 1976. Quantitative development of choroid plexuses in chick embryo cerebral ventricles. Acta Neurol Scand. 53**,** 251-9.

Stoquart-ElSankari, S., Baledent, O., Gondry-Jouet, C., Makki, M., Godefroy, O., Meyer, M. E., 2007. Aging effects on cerebral blood and cerebrospinal fluid flows. J Cereb Blood Flow Metab. 27**,** 1563-72.

Sturrock, R. R., 1979. A morphological study of the development of the mouse choroid plexus. J Anat. 129**,** 777-93.

Sun, Z., Amsterdam, A., Pazour, G. J., Cole, D. G., Miller, M. S., Hopkins, N., 2004. A genetic screen in zebrafish identifies cilia genes as a principal cause of cystic kidney. Development. 131**,** 4085-93.

Taulman, P. D., Haycraft, C. J., Balkovetz, D. F., Yoder, B. K., 2001. Polaris, a protein involved in left-right axis patterning, localizes to basal bodies and cilia. Mol Biol Cell. 12**,** 589-99.

Vajda, Z., Pedersen, M., Fuchtbauer, E. M., Wertz, K., Stodkilde-Jorgensen, H., Sulyok, E., Doczi, T., Neely, J. D., Agre, P., Frokiaer, J., Nielsen, S., 2002. Delayed onset of brain edema and mislocalization of aquaporin-4 in dystrophin-null transgenic mice. Proc Natl Acad Sci U S A. 99**,** 13131-6.

Van Allen, M. I., Kalousek, D. K., Chernoff, G. F., Juriloff, D., Harris, M., McGillivray, B. C., Yong, S. L., Langlois, S., MacLeod, P. M., Chitayat, D., et al., 1993. Evidence for multi-site closure of the neural tube in humans. Am J Med Genet. 47**,** 723-43.

Van Straaten, H. W., Janssen, H. C., Peeters, M. C., Copp, A. J., Hekking, J. W., 1996. Neural tube closure in the chick embryo is multiphasic. Dev Dyn. 207**,** 309-18.

Vanden Heuvel, G. B., Payne, J. A., Igarashi, P., Forbush, B., 3rd, 2006. Expression of the basolateral Na-K-Cl cotransporter during mouse nephrogenesis and embryonic development. Gene Expr Patterns. 6**,** 1000-6.

Verkman, A. S., Mitra, A. K., 2000. Structure and function of aquaporin water channels. Am J Physiol Renal Physiol. 278**,** F13-28.

Vogh, B. P., Godman, D. R., Maren, T. H., 1987. Effect of AlCl3 and other acids on cerebrospinal fluid production: a correction. J Pharmacol Exp Ther. 243**,** 35-9.

Welss, P., 1934. Secretory activity of the inner layer of the embryonic mid-brain of the chick, as revealed by tissue culture. The Anatomical Record. 58**,** 299-302.

Wen, H., Nagelhus, E. A., Amiry-Moghaddam, M., Agre, P., Ottersen, O. P., Nielsen, S., 1999. Ontogeny of water transport in rat brain: postnatal expression of the aquaporin-4 water channel. Eur J Neurosci. 11**,** 935-45.

Wodarczyk, C., Rowe, I., Chiaravalli, M., Pema, M., Qian, F., Boletta, A., 2009. A novel mouse model reveals that polycystin-1 deficiency in ependyma and choroid plexus results in dysfunctional cilia and hydrocephalus. PLoS One. 4**,** e7137.

Wright, E. M., Wiedner, G., Rumrich, G., 1977. Fluid secretion by the frog choroid plexus. Exp Eye Res. 25 Suppl**,** 149-55.

Wu, Q., Delpire, E., Hebert, S. C., Strange, K., 1998. Functional demonstration of Na+-K+-2Cl- cotransporter activity in isolated, polarized choroid plexus cells. Am J Physiol. 275**,** C1565-72.

Yamadori, T., Nara, K., 1979. The directions of ciliary beat on the wall of the lateral ventricle and the currents of the cerebrospinal fluid in the brain ventricles. Scan Electron Microsc. 335-40.

Ybot-Gonzalez, P., Gaston-Massuet, C., Girdler, G., Klingensmith, J., Arkell, R., Greene, N. D., Copp, A. J., 2007. Neural plate morphogenesis during mouse neurulation is regulated by antagonism of Bmp signalling. Development. 134**,** 3203-11.

Yingling, J., Youn, Y. H., Darling, D., Toyo-Oka, K., Pramparo, T., Hirotsune, S., Wynshaw-Boris, A., 2008. Neuroepithelial stem cell proliferation requires LIS1 for precise spindle orientation and symmetric division. Cell. 132**,** 474-86.

Zakharov, A., Papaiconomou, C., Djenic, J., Midha, R., Johnston, M., 2003. Lymphatic cerebrospinal fluid absorption pathways in neonatal sheep revealed by subarachnoid injection of Microfil. Neuropathol Appl Neurobiol. 29**,** 563-73.

Zhang, J., Piontek, J., Wolburg, H., Piehl, C., Liss, M., Otten, C., Christ, A., Willnow, T. E., Blasig, I. E., Abdelilah-Seyfried, S., 2010. Establishment of a neuroepithelial barrier by Claudin5a is essential for zebrafish brain ventricular lumen expansion. Proc Natl Acad Sci U S A. 107**,** 1425-30.

Zheng, W., Chodobski, A., 2005. The blood-cerebrospinal fluid barrier. Taylor and Francis Boca Raton, Fl.

CHAPTER TWO

Multiple roles for the Na,K-ATPase subunits, Atp1a1 and Fxyd1, during brain ventricle development.

Modified from:

Jessica T. Chang, Laura Anne Lowery, and Hazel Sive. Multiple roles for the Na,K-ATPase subunits, Atp1a1 and Fxyd1, during brain ventricle development. Submitted to *Developmental Biology*.

Contributions: Laura Anne performed initial characterization of *atp1a1* brain and junction phenotype. I performed all other experiments (*fxyd1* loss of function phenotype, permeability, $[Na^+]_i$, synergy and subunit interaction, and RhoA analysis). Hazel and I wrote the manuscript/Chapter.

ABSTRACT

Formation of the vertebrate brain ventricles requires both production of cerebrospinal fluid (CSF), and its retention in the ventricles. The Na,K-ATPase is required for brain ventricle development, and we show here that this protein complex impacts three associated processes. The first requires both the alpha subunit (Atp1a1) and the regulatory subunit, Fxyd1, and leads to formation of a cohesive neuroepithelium, with continuous apical junctions. The second process leads to modulation of neuroepithelial permeability, and requires Atp1a1, which increases permeability with partial loss of function and decreases it with overexpression. In contrast, *fxyd1* overexpression does not alter neuroepithelial permeability, suggesting that its activity is limited to neuroepithelium formation. RhoA regulates both neuroepithelium formation and permeability, downstream of the Na,K-ATPase. A third process, likely to be CSF production, is RhoA-independent, requiring Atp1a1, but not Fxyd1. Consistent with a role for Na,K-ATPase pump function, the inhibitor ouabain prevents neuroepithelium formation, while intracellular Na^+ increases after Atp1a1 and Fxyd1 loss of function. These data include the first reported role for Fxyd1 in the developing brain, and indicate that the Na,K-ATPase regulates three aspects of brain ventricle development essential for normal function - formation of a cohesive neuroepithelium, restriction of neuroepithelial permeability, and production of CSF.

INTRODUCTION

The vertebrate brain ventricular system comprises an essential set of interconnected cavities, filled with cerebrospinal fluid (CSF). Initially, CSF is produced by the neuroepithelium lining the ventricles (Welss, 1934), and later also by the choroid plexus, a series of vascularized secretory organs (Brown et al., 2004; Speake et al., 2001). Brain ventricle development requires a cohesive neuroepithelium with apical and basal polarity that can retain fluid, a correctly shaped epithelium, production of CSF, and expansion of the epithelium to accommodate the CSF (Ciruna et al., 2006; Gutzman and Sive, 2010; Hong and Brewster, 2006; Lowery and Sive, 2005; Lowery and Sive, 2009; Zhang et al., 2010). We previously demonstrated a requirement for the Na,K-ATPase during zebrafish brain ventricle development. Specifically, the *snakehead* (*snk* ^{to273a}) mutant, corresponding to a point mutation in the alpha subunit (*atp1a1*) of the Na,K-ATPase, fails to inflate its brain ventricles (Lowery and Sive, 2005). This led to the hypothesis that *snk* ^{to273a} ventricles fail to inflate because CSF is not produced (Lowery and Sive, 2005; Zhang et al., 2010).

The Na,K-ATPase is a protein complex composed of an alpha, beta, and FXYD subunit. Alpha and beta subunits form a heterodimer that is the minimal functional unit for catalytic activity and ion transport. FXYD subunits differentially regulate the stability of the alpha subunit, maximum catalytic activity, and apparent affinity for Na^+, K^+, and ATP in a tissue specific manner (Mishra et al., 2011). FXYD1, also called phospholemman, decreases the apparent K^+ and Na^+ affinity of Na,K-ATPase (Crambert et al., 2002). However, in both adult mouse cardiac myocytes and in *Xenopus* oocyte systems, phosphorylation of FXYD1 at Ser^{68} by PKA can increase apparent Na^+ affinity and pump current (Bibert et al., 2008; Pavlovic et al., 2007). FXYD and alpha subunit proteins co-localize (Bossuyt et al., 2006; Feschenko et al., 2003; Lansbery et al., 2006), and the crystal structure of Na,K-ATPases further demonstrates that alpha and FXYD subunits physically interact (Morth et al., 2007; Shinoda et al., 2009). In rats, FXYD1 is enriched in the adult brain, specifically in the cerebellum, choroid plexus, and ependymal lining of the ventricles (Feschenko et al., 2003).

Several studies, in tissues outside the nervous system, suggest that one function of the Na,K-ATPase is to direct formation of a normal epithelium. Analysis of *Drosophila* septate junction formation suggested that regulation of these junctions by the Na,K-ATPase occurs in a pump-independent manner (Paul et al., 2007). Conversely, tissue culture assays in MDCK cells show that levels of intracellular $[Na^+]$ ($[Na^+]_i$), regulated by the Na,K-ATPase alpha subunit, are correlated with the amount of RhoA-GTP and epithelial junction integrity (Rajasekaran et al., 2001). The Na,K-ATPase has been implicated in regulation of tight junction proteins such as occludins and claudins, and thereby, regulation of paracellular permeability (Rajasekaran et al., 2007; Zhang et al., 2010).

In this study, we clarify the mechanisms by which the Na,K-ATPase alpha subunit, Atp1a1, regulates brain ventricle development and show for the first time a role for Fxyd1 during brain development. The data demonstrate that the Na,K-ATPase acts as a key regulator of brain ventricle formation by impacting three processes: neuroepithelium formation, neuroepithelial permeability and CSF production.

MATERIALS AND METHODS

Fish lines and maintenance

Danio rerio fish were raised and bred according to standard methods (Westerfield et al., 2001). Embryos were kept at 28.5^{o}C and staged accordingly (Kimmel et al., 1995). Lines used: wild type AB, *snakehead* (*snk* ^{to273a}) (Jiang et al., 1996), and *heart and mind* (*had*^{m883}) (Ellertsdottir et al., 2006).

Antisense morpholino oligonucleotide (MO) injection

Start site or splice-site blocking morpholino (MO) antisense oligonucleotides (Gene Tools, LLC) (Draper et al., 2001; Nasevicius and Ekker, 2000) were injected into one cell stage embryos as previously described (Graeden and Sive, 2009). The translational start site MO targets bases -11 to +14 of *atp1a1* (5'-TCTCCTCGTCCATTTTGCTGCTTT-3') (Yuan and Joseph, 2004). Splice-site blocking MOs include, *atp1a1* (exon5-intron6), 5'- AATATAATATCAATAAGTACCTGGG-3', and *fxyd1* (intron4-exon5) 5'-CTGTGATAATCTAGAGAGAGAGACA-3'. Concentrations used were 0.5

ng or 1 ng *atp1a1* start site MO, 2.5 ng or 7.5 ng *atp1a1* splice site MO, and 0.5 ng or 1 ng *fxyd1* splice site MO. Standard control MO used is 5'-CCTCTTACCTCAGTTACAATTTATA-3 ' and *p53* morpholino 5'-GCGCCATTGCTTTGCAAGAATTG-3' (Gene Tools, LLC).

cDNA constructs

Full-length *atp1a1* cDNA constructs in pCS2+ were obtained from the Chen lab (Shu et al., 2003). The Quik Change II XL site directed mutagenesis kit (Stratagene) was used to modify wild type *atp1a1,* to correspond to the mutation associated with *snk* ^{to273a}, which would lead to a G to A substitution at nucleotide 812 of the coding sequence (with the resulting clone called *atp1a1GA)* (Lowery and Sive, 2005). Primers used for mutagenesis: *snkma*, 5'-CCGCACAGTCATGGATCGTATGCCACTCTCG-3' and *snkmb*, 5'-CGAGAGTGGCAATACGATCCATGACTGTGCGG-3'. For rescue of the *atp1a1* start site morphants, the translational start site of *atp1a1-pCS2+* was mutated from 5'-AAAAGCAGCAAAATGGGACGAGGAGAA-3' to 5'-AAGAGTAGTAAGATGGGTCGGGGCGAA-3' resulting in six mismatches within MO target sequence thus preventing MO binding.

The full-length *fxyd1* was obtained from an EST clone (ID 6894873, Open Biosystems) and subcloned into Stu1 site in pCS2+ with a minimal Kozak consensus sequence adjacent to the initiating ATG. This cDNA clone corresponds to a clone previously identified by Sweadner and Rael (Sweadner and Rael, 2000), who suggested the provisional terminology *FXYD9dr*. However, there is no *FXYD9* in any mammalian species, and since this *FXYD* gene is most closely related to human FXYD1 (Phospholemman), we have more accurately named the zebrafish gene *fxyd1*.

C-terminal FLAG tagged Fxyd1 were generated using PCR. Briefly, primers were designed to add a linker (S-G-G-G-G-S) followed by the FLAG tag (DYKDDDDK) between the last codon and stop codon using full length *fxyd1* in pCS2+ as template. Primers used were: *fxyd1FLAGCtermF*, 5'-GTCCTTGTAGTCAGAGCCGCCTCCACCAGAGCATTCACTCGCCCTCGCTGTGTC -3', *fxyd1FLAGCtermR* 5'-GACGATGACAAGTAAAAACCTGCTGACCTGAACCAATCAGAGGAG-3'.

pCS2+RhoAV14 and *pCS2+RhoAN19* were kindly provided by R. Winklbauer (University of Toronto) and K. Symes (Boston University).

Capped *atp1a1*, *atp1a1GA*, *fxyd1*, *RhoAV14*, *RhoAN19, mGFP* and *fxyd1-FLAG* were transcribed in vitro using the SP6 mMessage mMachine kit (Ambion) after linearization. Embryos were injected at the one-cell stage with 50-250 pg mRNA.

RT-PCR

RNA was extracted from morphant and control embryos using Trizol reagent (Invitrogen), followed by chloroform extraction and isopropanol precipitation. RNA was pelleted by centrifugation, re-suspended in water and precipitated with $LiCl_2$. cDNA synthesis was performed using Super Script III Reverse Transcriptase (Invitrogen) plus random hexamers. PCR was then performed using primers which amplified the exonic and intronic sequence surrounding the splice MO target. Primers used include: *atp1a1 test F* 5'-CTCTTTCAAGAATTTGGTTCCC-3', *atp1a1 test R* 5'-CTCAATAGAGATGGGGGTGC-3', *fxyd1L* 5'-CACAACCACGCATCAAACTT-3', *fxyd1R* 5'-CCGTCTCCTCTGATTGGTTC-3'. Primers used for detection of *fxyd1* reverse transcript include: *fxyd1oppL* 5'-CGGGTCGTTTATAAGCATTGA-3' and *fxyd1oppR* 5'-TACGGTGGATCCTCCACAAC-3'.

In situ hybridization

Standard methods for RNA probe synthesis containing digoxigenin (DIG)-11-UTP, hybridization and single color labeling were used as described (Sagerstrom et al., 1996). After staining, embryos were fixed in 4% paraformaldehyde overnight at $4^{o}C$, and washed in PBT. Embryos were either imaged right away or dehydrated in methanol and cleared in a 3:1 benzyl benzoate/benzyl alcohol (BB/BA) solution before mounting and imaging with a Nikon compound microscope or Zeiss dissecting scope.

Brain ventricle injections, dye retention assay, and ventricle size quantification

Brain ventricle injection and imaging have been described previously (Gutzman and Sive, 2009; Lowery and Sive, 2005).

For assaying permeability, 70 kDa MW dextran conjugated to FITC (Invitrogen; 2.5ng/ml in water) was injected into the brain ventricles at 22 hpf and imaged at various time-points as

noted in the text. Neuroepithelial permeability was quantified using ImageJ software to measure the distance of the dye front from the forebrain ventricle hinge-point. In Image J, the line tool was used to draw a line from the forebrain hinge-point to dye front at a 10-20^{o} angle from neuroepithelium. This region was chosen because it is the first and most noticeable site of dye leaking out of the wild type neuroepithelium. The net distance the dye front moved over time was calculated by subtracting distance at t=0 from other time points. Statistics were performed with GraphPad InStat software.

Forebrain ventricle area was calculated by measuring pixels per cm^2 of forebrain ventricle with ImageJ software. Scanning confocal stacks of the full depth of the forebrain ventricle were taken and analyzed using 3D doctor (Able Software) to reconstruct the forebrain ventricle and calculate volume in μm^3.

Immunohistochemistry and Western Blots

Embryos were fixed in 4% PFA or 2% TCA and blocked in 2%NGS/1%Triton-X/1%BSA or 5%NGS/1%Triton-X. 50μm transverse sections were obtained as described previously (Gutzman and Sive, 2010). Na,K-ATPase levels in whole embryos or brains (50 μg of protein) were analyzed via western blot as previously described (Gutzman and Sive, 2010). Antibodies used: Phalloidin-Texas Red/TRITC or Alexa-Fluor 633 (Molecular Probes), aPKC (Santa Cruz), Zo-1 (Invitrogen), FLAG (Sigma), propidium iodide (Invitrogen), and Na,K-ATPase (alpha) (Cell Signaling Technology) and GAPDH (Abcam).

Inhibitor treatments

Dechorionated embryos were incubated in 5 mM ouabain (Sigma) diluted in embryo medium. Not all embryos responded to ouabain soaking at 16 hpf, likely due to difficulty penetrating the embryonic epidermis at this stage. 50 μM ROCK inhibitor (Calbiochem) was injected between the yolk and the brain under the midbrain and hindbrain at 14 hpf or into the brain ventricles at 22 hpf.

Intracellular Na^+ Measurement

Dechorionated and deyolked embryos were collected at 24-28 hpf in 300 μl of nuclease free water. Embryos were dounce homogenized, spun at 1000 rpm, and supernatant collected. CoroNa Green (Invitrogen 10 μM) was added to the supernatant and fluorescence readings obtained using a Tecan Safire II microplate reader. A hemocytometer was used to determine number of cells per embryo (Westerfield et al., 2001).

RESULTS

Na,K-ATPase subunits, Atp1a1 and Fxyd1, are required for brain ventricle development.

In order to investigate the mechanisms by which the Na,K-ATPase alpha subunit, Atp1a1, regulates brain ventricle development (Lowery and Sive, 2005), we tested the effect of partial loss of *atp1a1* using either a second *atp1a1* mutant allele, *had*^{m883} (*heart and mind*) (Ellertsdottir et al., 2006), or a morpholino-modified antisense oligonucleotide (MO) to inhibit zygotic pre-mRNA splicing (splice site MO) (Draper et al., 2001). In all cases, brain ventricle inflation was reduced at 24 hours post fertilization (hpf) and all images shown are representative of the phenotype observed (Figure 2.1A-D; *snk* ^{to273a} - 65% normal ventricles (n=39), *had*^{m883} - 70% normal ventricles (n=55), *atp1a1* splice - 20% normal ventricles (n=31)). After more extensive loss of *atp1a1,* using a previously published MO (Yuan and Joseph, 2004) targeted to the translational start site (start site MO), no brain ventricle lumen was visible (Figure 2.1E; 0% normal ventricles (n=60)) (Nasevicius and Ekker, 2000). The effect of the *atp1a1* splice site MO, as identified by RT-PCR and sequencing of the resulting products, was to generate an early stop codon in the 4th extracellular loop of *atp1a1* due to the retention of intron 5 (Figure 2.2A). This intron inclusion was predicted to ablate Atp1a1 pumping function. Specificity of the MO phenotypes was shown by phenotypic rescue after co-injection of the MO with the corresponding zebrafish mRNA that does not bind the MO sequence (*atp1a1* splice rescue- 100% normal ventricles (n=31), *atp1a1* start rescue - 100% normal ventricles (n=35), Figure 2.2B). The cDNA injected for rescue of the splice site MO had a partial, non-functional target present, while the start site MO cDNA was mutated to prevent MO binding. The amount

of *atp1a1* mRNA used for rescue was the highest level that could be added into the embryo without adverse effects. Additionally, dose response assays demonstrated a correlation between brain ventricle inflation and the amount of *atp1a1* RNA (Figure 2.2C-H).

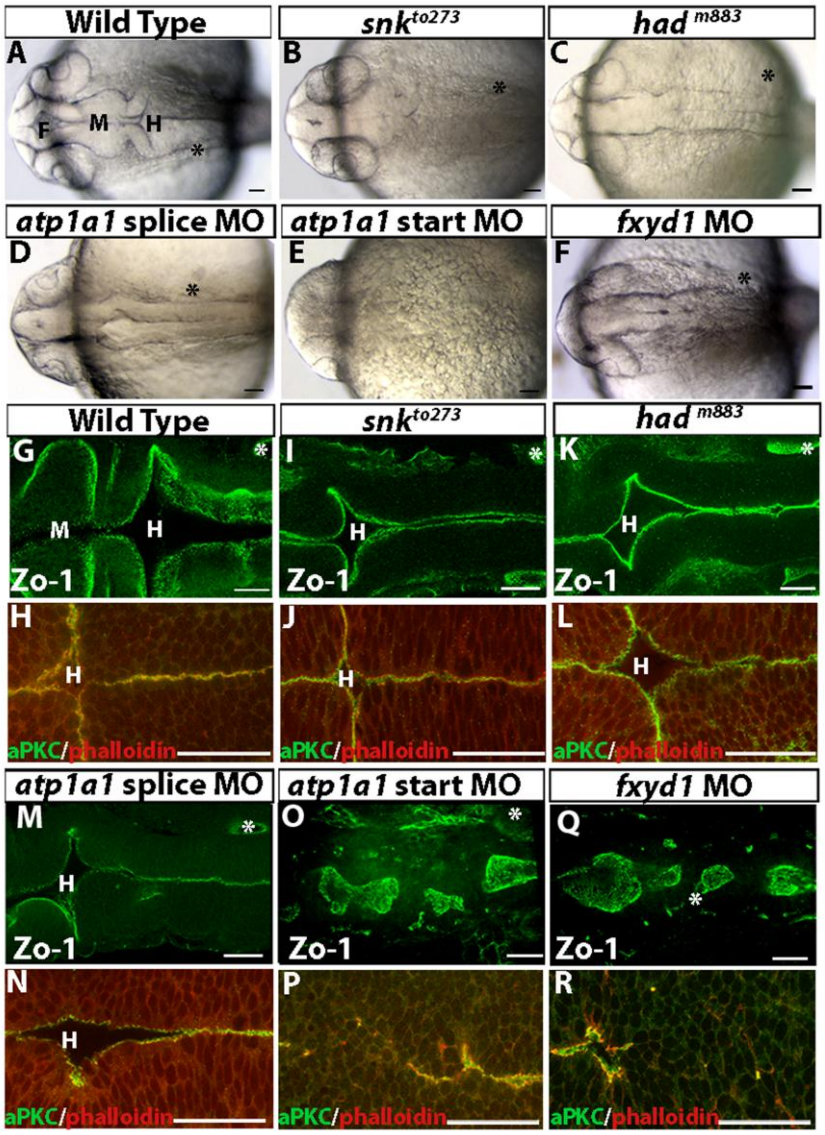

Figure 2.1: The Na,K-ATPase is required for brain ventricle development. (A-F) Loss of function Na,K-ATPase embryos brightfield dorsal view images wild type (A), partial loss of *atp1a1* with mutants *snk*^{to273} (B) and *had*^{m883} (C) and splice site MO (D) or complete loss of *atp1a1* with start site MO (E) and loss of function *fxyd1* splice site MO (F). (G-R) Neuroepithelial formation in Na,K-ATPase morphants/mutants labeled with Zo-1 (G,I,K,M,O,Q) or aPKC (green) and actin (phalloidin; red) (H,J,L,N,P,R). Images taken at 24 hpf with anterior to the left, asterisk = ear, F = forebrain, M = midbrain, H = hindbrain. Scale bars = 50μm.

The function of zebrafish *fxyd1* has not previously been described. *fxyd1* is expressed zygotically, and in the embryonic brain from 10 hpf (Figure 2.2I-L). In addition to the transcript encoding *fxyd1*, an antisense non-protein coding transcript was reproducibly detected by in situ hybridization and RT-PCR (Figure 2.2I-P). Further analysis was done on the *fxyd1* protein coding transcript, while activity of the non-coding transcript is not known. Loss of function, using a splice site MO targeting the *fxyd1* protein coding strand, resulted in absence of brain ventricle inflation in 24 hpf embryos (Figure 2.1F, 0% normal ventricles (n=114)), demonstrating a requirement for Fxyd1 during brain ventricle development. As measured by RT-PCR and sequencing of the resulting products, *fxyd1*

splice site morphants have a deletion of the FXYD and transmembrane domains, due to an excision of exon 5, with no remaining wild type *fxyd1* mRNA detectable (Figure 2.2A). Specificity was confirmed since the phenotype could be prevented by co-injection of the corresponding zebrafish mRNA that does not bind the MO (Figure 2.2B; 86% normal ventricles (n=21)). The amount of *fxyd1* mRNA used was the highest level that could be added into the embryo without adverse effects.

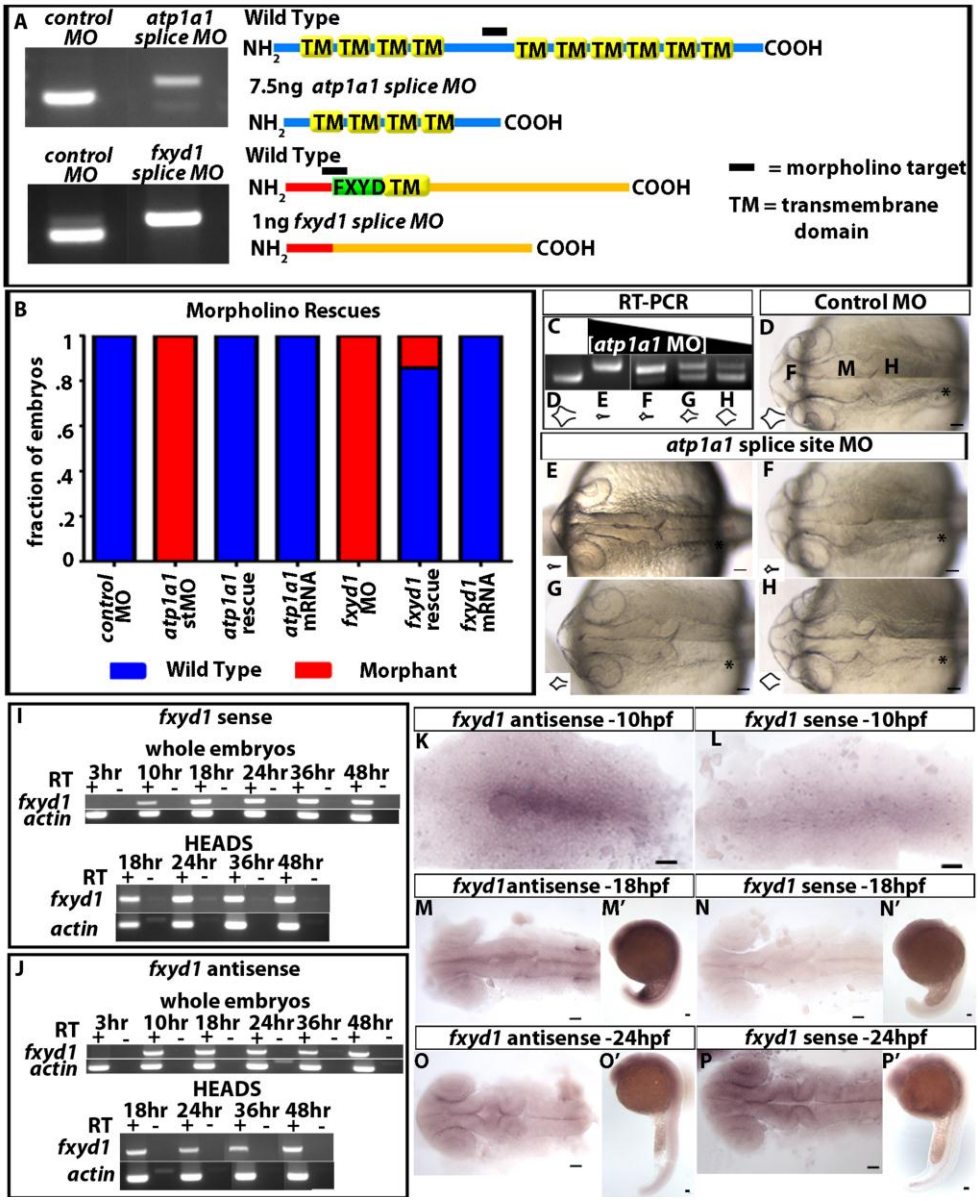

Figure 2.2: Characterization of Na,K-ATPase phenotypes. (A) Na,K-ATPase MO disrupt wild type splicing. TM= transmembrane domain. Black line = MO target. (B) Quantification for rescue of morphant phenotypes in control MO (C) RT-PCR of differing levels of *atp1a1* splice site MO and the corresponding forebrain ventricle tracings of embryos in D-H. (D-H) Dose dependent regulation of brain ventricle inflation by *atp1a1* splice site MO. (I-J) RT-PCR analysis of *fxyd1* sense (non-protein coding) (I) and antisense (protein coding) (J) expression from 3-48 hpf in whole embryos or dissected heads. (K-P) Dorsal (K-P) and lateral (M'-P') views of in situ hybridization of *fxyd1* antisense (K,M,O) and sense (L,N,P) expression from 10-24 hpf. All images taken at 24 hpf with anterior to left, asterisk = ear, F = forebrain, M = midbrain, H = hindbrain. Scale bar = 50μm.

The severity of the *atp1a1* start site morphants led us to examine apical polarity, marked by aPKC, and the apical junction complex using phalloidin

(actin) or Zo-1 (Figure 2.1G-R). In wild type embryos, junction and polarity proteins form a continuous apical band lining the ventricles (Figure 2.1G-H). Partial loss of *atp1a1* does not change localization or continuity of the apical junctions (Figure 2.1I-N) likely due to maternal contribution of Atp1a1. However, after greater loss of function elicited by an *atp1a1* start site MO, or by *fxyd1* MO, apical junction and polarity proteins are discontinuous, with non-polarized cells crossing the midline and multiple small lumens forming (Figure 2.1O-R).

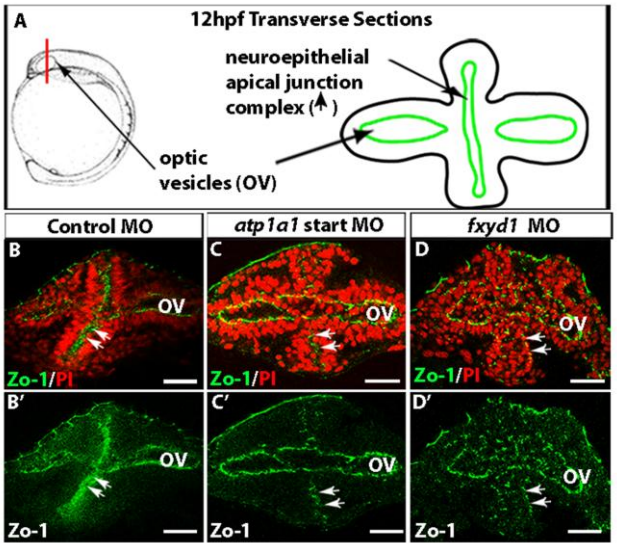

Figure 2.3: Atp1a1 and Fxyd1 regulate neuroepithelial junction formation. (A) Experimental design. Red line indicates region of transverse section in 12 hpf embryo. Transverse section model with apically localized junctions (green lines). (B-D) Transverse vibratome sections of 12 hpf embryos stained with Zo-1 (green) and propidium iodide (red) in control (B) *atp1a1* start site MO (C), and *fxyd1* MO (D,). (B'-D') Zo-1 only. Arrow indicates neuroepithelial apical junction complex. OV = optic vesicle. Scale bars = 50μm.

In order to determine whether apical junctions initially form, localization of Zo-1 was examined at 12 hpf, when apico-basal polarity and junctions are first established (Figure 2.3A). In control embryos, Zo-1 is expressed continuously at the apical surface of the neural tube (Figure 2.3B; n=8). Conversely, in *atp1a1* start site and *fxyd1* morphants, Zo-1 expression is patchy and scattered throughout the neuroepithelium (Figure 2.3C-D; n=9, n=10 respectively). Therefore, Atp1a1 and Fxyd1 are required during initial neuroepithelial formation.

These data show that Fxyd1 is required for formation of a correctly polarized, continuous neuroepithelium, and are the first demonstration of a function for this gene during brain development. The data also show that partial loss of *atp1a1* function leads to failure of ventricle inflation, and that more complete loss of function leads to absence of a polarized and continuous epithelium.

Atp1a1 regulates neuroepithelial permeability.

Reduced brain ventricle inflation in *atp1a1* partial loss-of-function embryos may be due to either abnormal CSF production or inability of the neuroepithelium to retain fluid. Therefore, we tested whether *atp1a1* loss of function increases epithelial permeability, using a dye retention assay. In this assay, FITC-Dextran was injected into the brain ventricles at 22 hpf, and leakage of the dye out of the ventricles was monitored. A 70 kDa FITC-Dextran was chosen as it leaks out of the brain slowly, thereby allowing for identification of conditions that increase or decrease permeability. The distance traveled by the dye over time, was measured from the

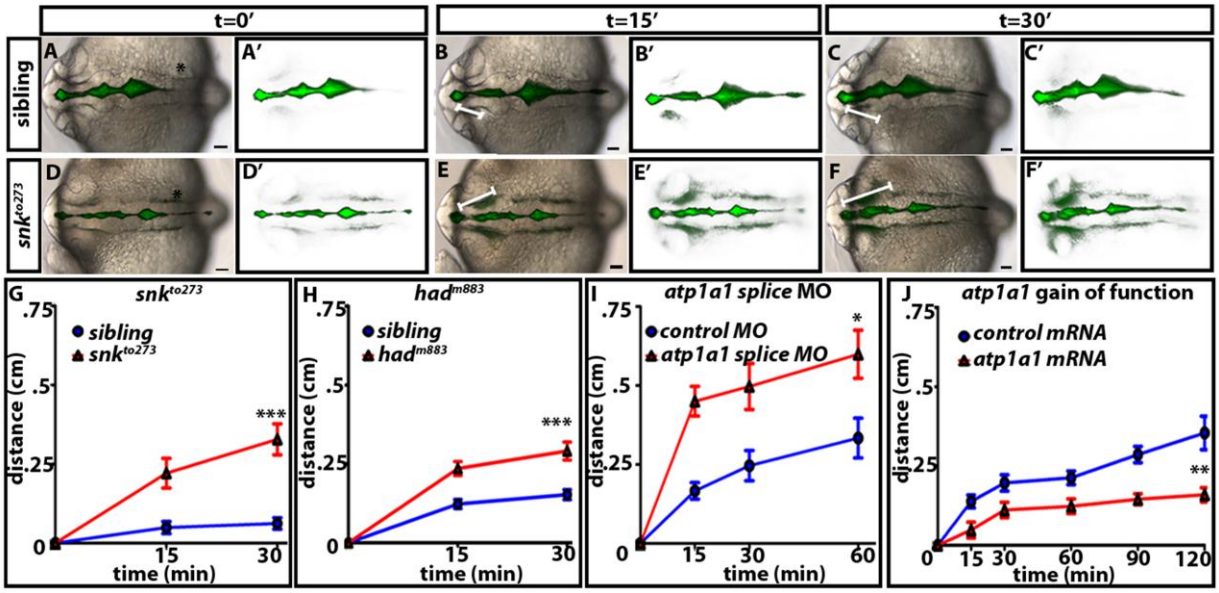

Figure 2.4: Atp1a1 regulates neuroepithelial permeability. (A-F) Dye retention assay in sibling embryos (A-C) vs. *snk*^{to273} mutants (D-F). Brightfield dorsal views of embryos ventricle injected with a 70 kDa FITC Dextran (A-F) and corresponding dye only images (A'-F') over time. The distance the dye front moves measured at each time point indicated by white line. (G-J) Quantification of permeability in *snk*^{to273} mutants (G), *had*^{m883} (H) *atp1a1* splice site morphants (I), and *atp1a1* gain-of-function embryos (J) compared to control injected. Average taken from 3-6 independent experiments and represented by mean +/- SEM. ***= p<0.0001, ** = p<0.005, *=p<0.05 All images taken at 22-24 hpf with anterior to left. Asterisk = ear. Scale bars = 50μm.

forebrain hinge-point to the furthest dye front, indicated by the white bar (Figure 2.4A-F). This region was chosen because it is the first and most noticeable site of dye leaking out of the wild type brain (Figure 2.4B). In *snk*^{to273a} sibling embryos (wild type and heterozygotes), very little dye movement was observed (Figure 2.4A-C,G). However, in *snk*^{to273a} or *had*^{m883} mutant embryos, or after injection of *atp1a1* splice site MO, dye begins to leak out of the brain

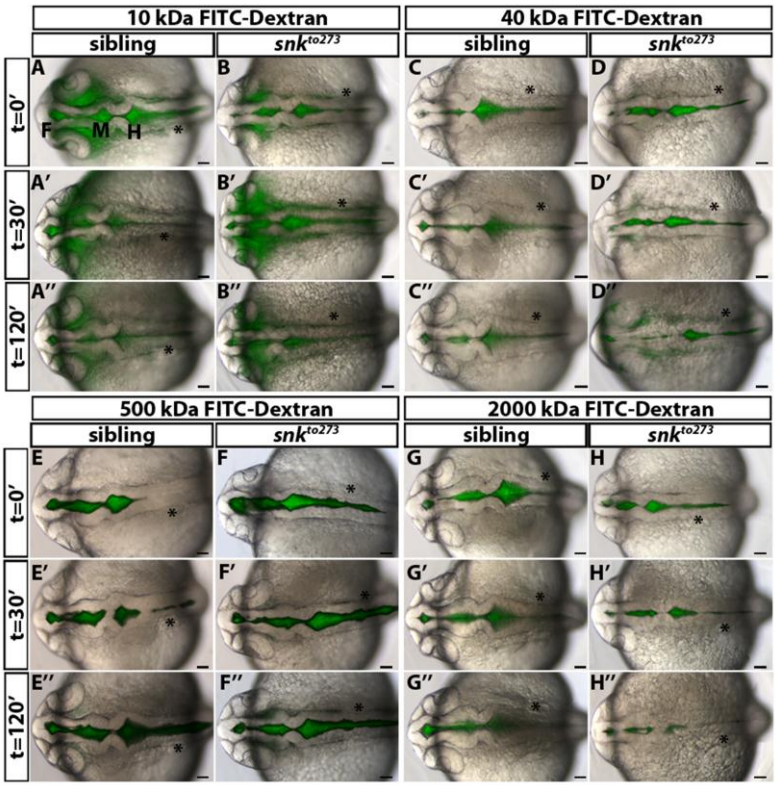

Figure 2.5: Selective permeability of the neuroepithelium. (A-H) Neuroepithelial permeability in sibling (A,C,E,G) and *snk*^{to273} (B,D,F,H) embryos. Brain ventricle injection of FITC-Dextran dye of molecular weight 10 (A-B), 40 (C-D), 500 (E-F) or 2000 kDa (G-H) at t = 0 (A-H), 30 (A'-H') and 120 minutes (A''-H''). All images 22-24 hpf with anterior to left. Asterisk = ear. F = forebrain, M = midbrain, H = hindbrain. Scale bars = 50μm.

immediately after injection (Figure 2.4D-I; *snk* ^{to273a} n=13 p<.0001; *had*^{m883} n=15, p<.001; *atp1a1* splice MO n=10, p<.05). Thus, although apical junction proteins properly localize, junctions do not function like wild type. Consistently, the *snk* ^{to273a} brain does not retain a 500 kDa FITC-Dextran whereas the wild type brain does demonstrating that these neuroepithelia are selectively permeable to dyes of different molecular weights (Figure 2.5).

These data suggested that *atp1a1* overexpression in wild type

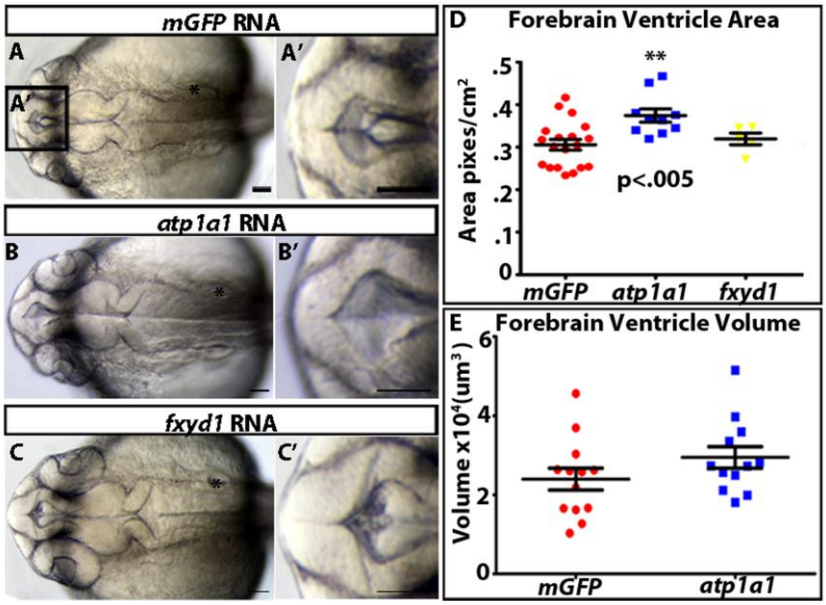

Figure 2.6: Atp1a1 regulates brain ventricle size. (A-C) Dorsal brightfield views (A-C) and magnified forebrain ventricles (A'-C') of control mRNA (*mGFP*) (A) *atp1a1* mRNA (B) and *fxyd1* mRNA (C). (D-E) Quantification of forebrain ventricle area (D) and volume (E). Taken from 5-7 independent experiments and represented as mean +/- SEM. All images taken at 24 hpf with anterior to left, asterisk= ear. Scale bar = 50μm

embryos would increase CSF retention relative to controls, and we obtained consistent results (Figure 2.4J, n=10, p<.005). Additionally, forebrain ventricle area and volume increased in embryos overexpressing *atp1a1* (n=10), compared to control injected embryos (Figure 2.6A-B, D-E). In contrast, overexpression of *fxyd1* did not alter neuroepithelial permeability (Figure 2.10M) or brain ventricle size (Figure 2.6C-D; n=5). We conclude that Atp1a1 regulates neuroepithelial permeability, and correlated with this, controls brain ventricle volume. Thus, part of the *snk* ^{to273a} mutant and *atp1a1* splice site morphant phenotypes is likely due to the inability of the neuroepithelium to retain CSF. However, Fxyd1 is not able to regulate neuroepithelial permeability, in the assays performed.

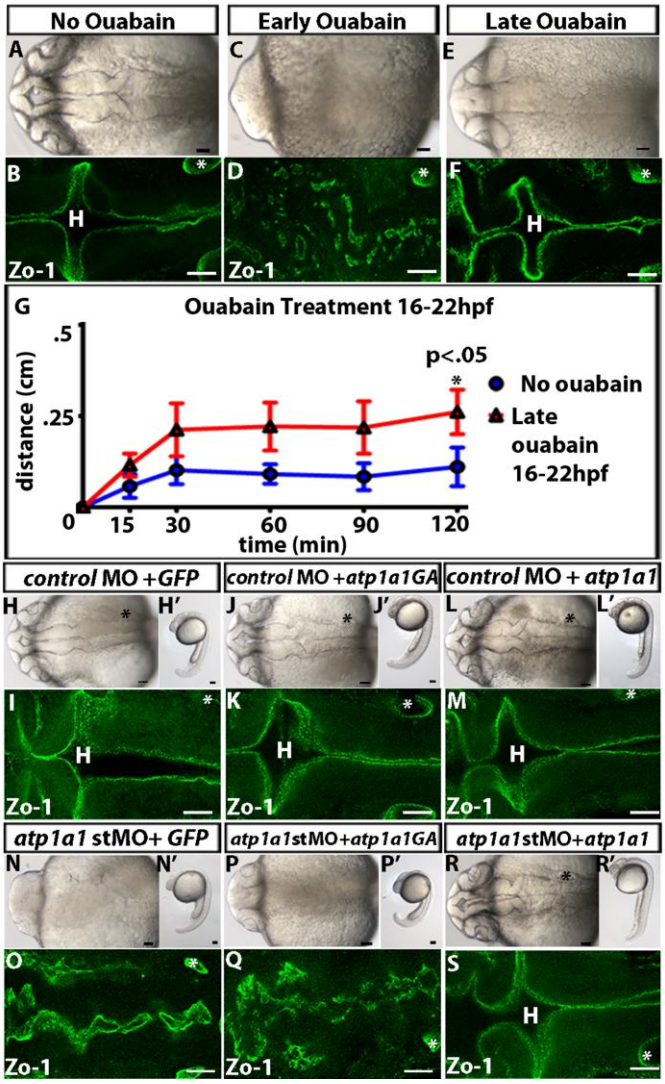

Figure 2.7: Na,K-ATPase pumping is required for brain ventricle development. (A-F) Wild type embryos either untreated (A-B) or ouabain treated early (5-24 hpf; C-D) or late (16-24 hpf; E-F). (G) Dye retention assay in untreated (red) vs. late ouabain treated (blue) embryos. Data represented as mean+/- SEM. (H-S) *atp1a1GA* mutant mRNA does not rescue *atp1a1* start site morphants. Control MO plus control (*GFP)* (H-I), *atp1a1GA* (J-K) or wild type *atp1a1* (L-M) mRNA or *atp1a1* start site MO plus mRNA expression of *GFP* (N-O) *atp1a1GA* (P-Q) or wild type *atp1a1* (R-S). Brightfield dorsal (A-S) and lateral (H'-S') images or Zo-1 staining (B,D,F,I,K,M,O,Q,S). All embryos at 24 hpf, anterior to left; Asterisk = ear, H = hindbrain. Scale bars = 50μm.

Na,K-ATPase pumping is required for brain ventricle development.

The Na,K-ATPase is proposed to be a scaffolding complex as well as a pump (Krupinski and Beitel, 2009). Thus, we asked whether pumping is required for brain ventricle development. Treatment with the pump inhibitor, ouabain (Linask and Gui, 1995), at 5 hpf (mid-gastrula stage) resulted in embryos with severely

disrupted apical junctions (Figure 2.7A-D; 0% normal ventricles (n=50)), similar to the effects of injecting an *atp1a1* start site MO. Ouabain treatment at 16 hpf, after neuroepithelium formation, resulted in embryos with reduced ventricle inflation, correctly localized apical junctions (Figure 2.7E-F; 25% normal ventricles (n=67)), but increased permeability (Figure 2.7G; n=12, p<.05). Consistently, injection of mRNA encoding the putative pump-deficient *snk ^{to273a}* mutant *atp1a1* (*atp1a1GA*) (Lowery and Sive, 2005) did not rescue brain ventricle development after *atp1a1* loss of function (Figure 2.7H-Q) where wild type *atp1a1* mRNA rescued both neuroepithelial formation and brain ventricle inflation (Figure 2.2B, 2.7R-S). These data show that the pump activity of zebrafish Atp1a1 is essential during brain ventricle development.

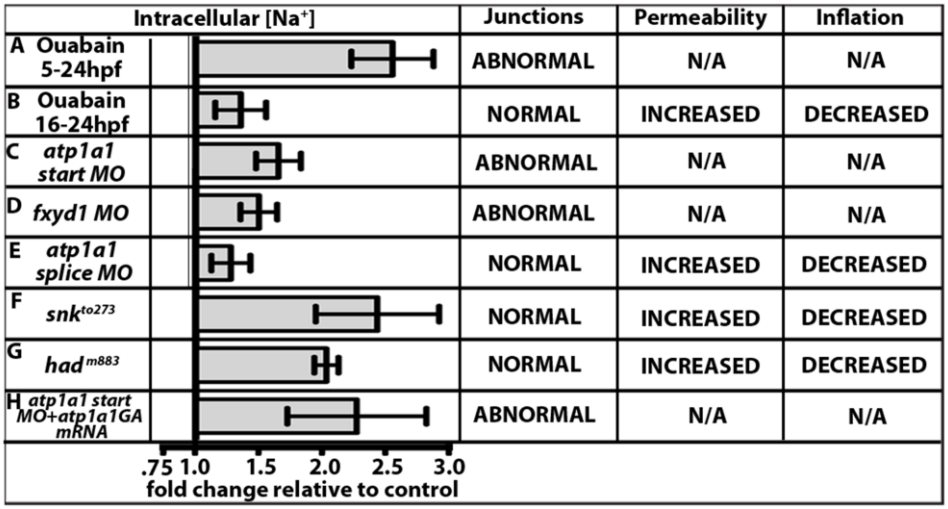

Figure 2.8: $[Na+]_i$ correlates with Na,K-ATPase activity and brain ventricle development. (A-H) Quantification of fold changes in $[Na^+]_i$ and corresponding brain ventricle phenotype. Data from 3-8 independent experiments represented as fold change compared to control MO (equal to 1) plotted as a mean +/- SEM.

Additionally, we predicted that loss of Atp1a1 function would lead to increased intracellular Na^+ concentration ($[Na^+]_i$) in the brain, and if Fxyd1 modulates pump function, $[Na^+]_i$ would also increase in *fxyd1* loss-of-function embryos. Therefore, we measured $[Na^+]_i$ in whole embryos after loss of function of the Na,K-ATPase. Since inhibiting the Na,K-ATPase using ouabain treatment or morpholinos affects the whole body and *atp1a1* and *fxyd1* are expressed ubiquitously (Figure 2.2O-P) (Canfield et al., 2002; Ellertsdottir et al., 2006), we assume that changes in whole embryo $[Na^+]_i$ are representative of differences within the brain. As predicted, we observed a 2.5 fold increase in $[Na^+]_i$ in embryos treated with ouabain from 5-24 hpf compared to controls (Figure 2.8A, p<.005), and a smaller increase in those treated with

ouabain from 16-24 hpf (1.3 fold; Figure 2.8B). Relative to controls, $[Na^+]_i$ also increased in embryos injected with high levels of *atp1a1* start site MO (1.7 fold; p<.05, Figure 2.8C), with *fxyd1* MO (1.5 fold; p<.05, Figure 2.8D), and after partial loss of *atp1a1* via the splice site MO (1.2 fold; Figure 2.8E). Additionally, we found that neuroepithelium abnormality was generally correlated with the highest $[Na^+]_i$, (Figure 2.8A,C-D).

Interestingly, while both ouabain treatment from 5-24 hpf, and *atp1a1* start site MO led to similar phenotypes with regard to development of the neuroepithelium, levels of $[Na^+]_i$ in ouabain-treated embryos were higher than after injection of the *atp1a1* start site MO. This difference is likely due to inhibition of maternal Atp1a1 protein function and that of other alpha subunits by ouabain, whereas the start site MO would not inhibit maternal protein, nor affect other subunits. Consistently, levels of $[Na^+]_i$ in both *snk* ^{to273a} and *had* ^{m883} mutant embryos, were higher than controls (Figure 2.8F-G; *snk* ^{to273a} = 2.4 fold increase, p<.05; *had* ^{m883} = 2.0 fold increase, p<.001). The *atp1a1* missense mutant, *snk* ^{to273a} also showed somewhat higher $[Na^+]_i$ (Figure 2.8F) relative to *atp1a1* start site MO (Figure 2.8C) (2.4 fold for *snk* ^{to273a} versus 1.7 fold for *atp1a1* start site MO relative to controls). We hypothesized that the protein produced in *snk* ^{to273a}, retained some activity affecting $[Na^+]_i$ but not neuroepithelium formation. Consistently, injection of *atp1a1GA* mRNA into *atp1a1* start site morphants, led to elevated $[Na^+]_i$ compared to *atp1a1* start site MO alone (Figure 2.8H, p<.05).

Thus, $[Na^+]_i$ increases after inhibition of Na,K-ATPase with ouabain or after knockdown of Atp1a1 or Fxyd1 subunits. Moreover, this suggests that Fxyd1 promotes Atp1a1 function, however, we cannot rule out another independent role for Fxyd1.

Atp1a1 and Fxyd1 co-regulate brain ventricle development.

Data from other tissues and in vitro systems, suggest that Atp1a1 and Fxyd1 physically and functionally interact (Bibert et al., 2008; Bossuyt et al., 2006; Crambert et al., 2002; Lansbery et al., 2006; Mishra et al., 2011; Morth et al., 2007; Pavlovic et al., 2007; Shinoda et al., 2009). To determine whether Atp1a1 and Fxyd1 functionally interact, we injected embryos with low, sub-effective concentrations of *atp1a1* splice site MO and *fxyd1* MO together, which resulted in a non-cohesive neuroepithelium (0% normal ventricles (n=17)), whereas the individual MOs do

not give a phenotype (Figure 2.9A-D; *atp1a1* splice site MO = 100% normal ventricles (n=14); *fxyd1* MO = 100% normal ventricles (n=19)) suggesting these subunits functionally interact. Consistently, whereas embryos injected with low *atp1a1* or *fxyd1* MOs had wild type levels of $[Na^+]_i$, the combination of MOs was associated with increased $[Na^+]_i$ (Figure 2.9E-G).

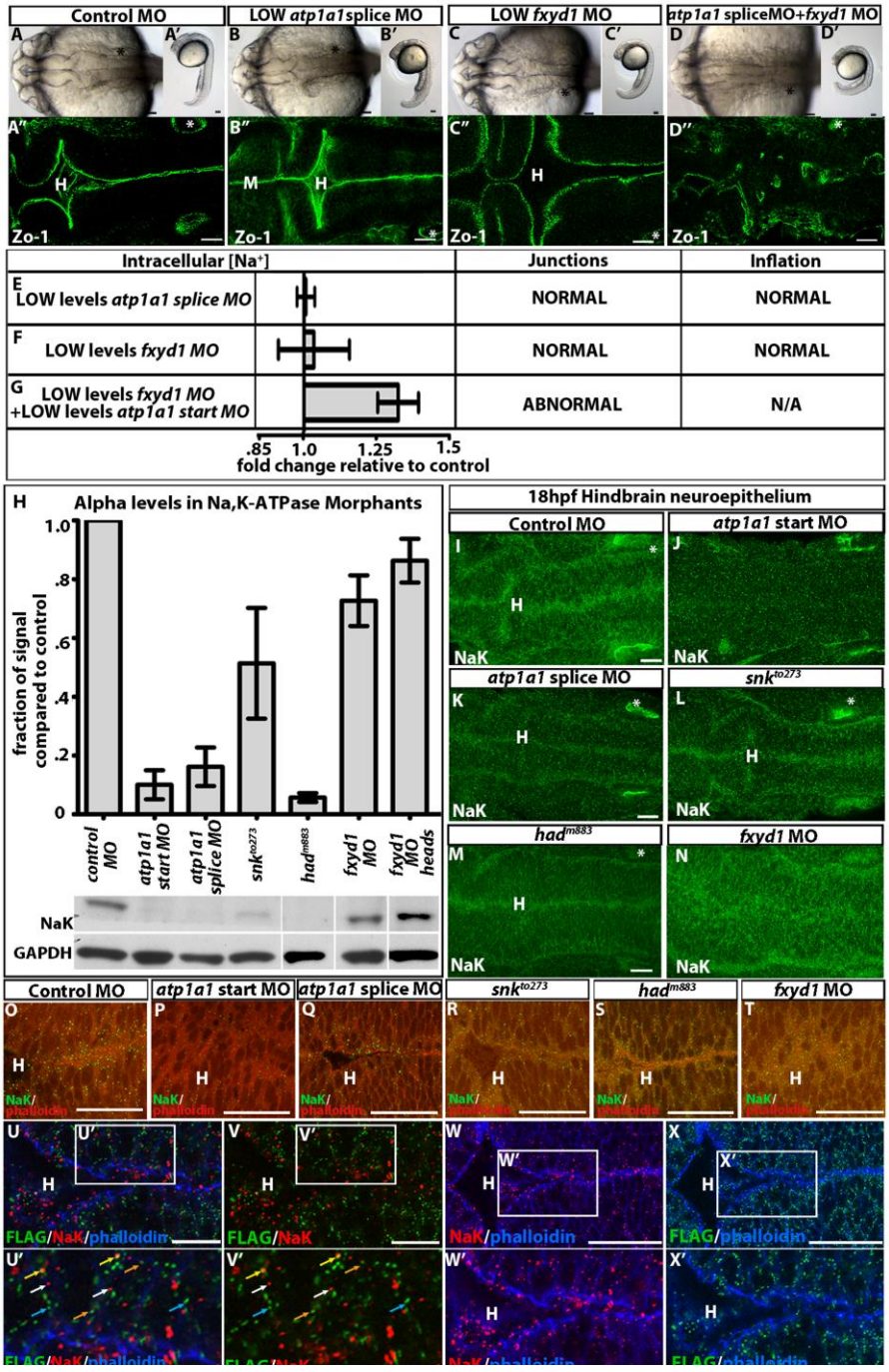

Figure 2.9: Atp1a1 and Fxyd1 synergy, interaction, and co-localization. (A-G) Na,K-ATPase synergy. Brightfield dorsal (A-D), lateral (A'-D') Zo-1 staining (A''-D''- different embryos imaged than A-D) and measurement of $[Na^+]_i$ and corresponding brain ventricle phenotype (E-G), in controls (A), low *atp1a1* splice MO (B,E), low *fxyd1* MO (C,F) or together (D,G) at 24 hpf. Data representative of 3-6 experiments as fold change relative to control = 1; mean +/- SEM. (H) Western quantification of Atp1a1 (NaK) in 24 hpf whole embryos normalized to GAPDH. Representative of 3-4 independent experiments; mean +/- SEM. (I-T) Atp1a1 (NaK) in 18 hpf control MO (H,N), *atp1a1* start site MO (I,O), *atp1a1* splice site MO (J,P), snk^{to273} (K,Q), had^{m883} (L,R) and *fxyd1* MO (M,S). NaK alone (I-N, green) or with phalloidin (O-T, actin, red). (U-X) Localization of Atp1a1 (NaK; red) and Fxyd1-FLAG (green), phalloidin (blue) in *fxyd 1* MO rescue embryos at 24 hpf. (U'-X') Higher magnification indicated by box in (U-X). Co-localization (yellow arrow), adjacent (orange arrow), Atp1a1 alone (white arrow) and Fxyd1 alone (blue arrow). Anterior to left. Asterisk = ear. H = hindbrain. Scale bars = 10μm (U-X), 50μm (A-T).

Studies in cell culture suggest that FXYD subunits localize, stabilize and prevent degradation of alpha subunit protein (Mishra et al., 2011). In order to ask whether similar functions for Fxyd1 were present in the developing brain, we examined Atp1a1 levels and localization in loss-of-function embryos by Western blot and immunohistochemisty. As expected, levels of Atp1a1 in *atp1a1* loss-of-function embryos were lower than controls and the protein remaining appeared as puncta enriched along the apical surface (Figure 2.9H-M,O-S). In *fxyd1* morphants, levels of Atp1a1 did not decrease, in either whole embryos or dissected heads (Figure 2.9H) indicating that Fxyd1 does not stabilize Atp1a1. However, Atp1a1 expression was dispersed in the *fxyd1* morphant neuroepithelium (Figure 2.9N,T) demonstrating the necessity for Fxyd1 in correct localization of Atp1a1.

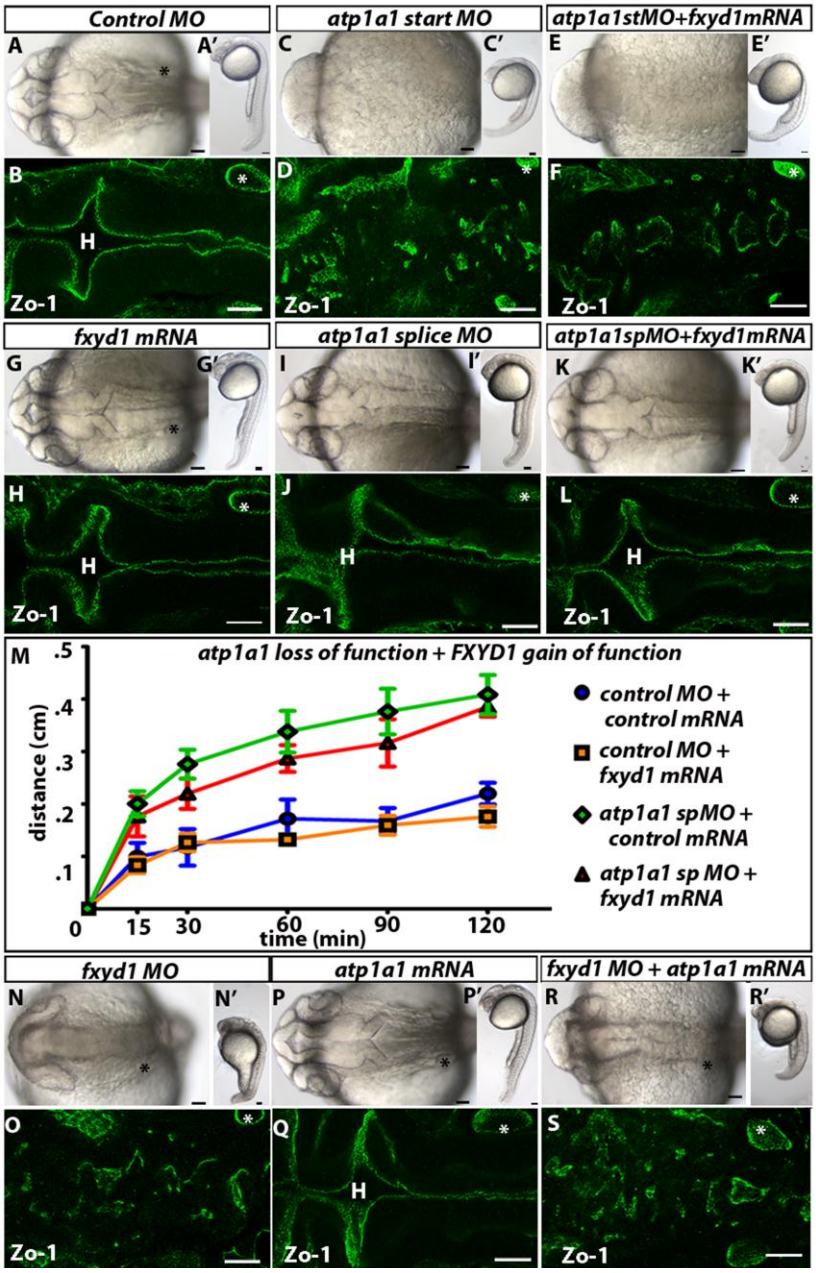

Figure 2.10: Atp1a1 and Fxyd1 do not substitute for one another. (A-L) Overexpression of *fxyd1* in *atp1a1* loss-of-function embryos. Control (A-B), *atp1a1* site start MO (C-D), *atp1a1* start site MO + *fxyd1* mRNA (E-F), *fxyd1* mRNA (G-H), *atp1a1* splice site MO (I-J), and *fxyd1* mRNA + *atp1a1* splice site MO (K-L). (M) Neuroepithelial permeability in control MO (blue), *fxyd1* gain of function (orange), *atp1a1* splice site MO (red), and *fxyd1* mRNA + *atp1a1* splice site MO (green). Data represented as mean +/- SEM. (N-S) *atp1a1* mRNA+ *fxyd1* MO (T-U), *fxyd1* MO (V-W) and *atp1a1* mRNA (P-Q). Brightfield dorsal (A-R) and lateral (A'-R') views. Zo-1 junction staining (B,D,F,H,J,L,O,Q,S). All images taken at 24 hpf with anterior to left. Asterisk = ear. H = hindbrain. Scale bars = 50μm.

Consistently, co-localization of Atp1a1 and Fxyd1 was observed as overlapping or adjacent protein staining of FLAG tagged Fxyd1 and endogenous Atp1a1 (Figure 2.9U-V). In addition, Atp1a1 is enriched apically while Fxyd1 is present at higher levels laterally (Figure 2.9W-X) suggesting some independent activity.

Consistent with independent functions for these subunits, overexpression of *fxyd1* mRNA in *atp1a1* start site morphants does not rescue junction formation suggesting that Fxyd1 cannot substitute for Atp1a1 function during neuroepithelial formation (Figure 2.10A-H). Additionally, Fxyd1 could not restore inflation or alter neuroepithelial permeability when overexpressed after partial loss of Atp1a1 function (Figure 2.10G-M) supporting the conclusion that Fxyd1 does not normally regulate neuroepithelial permeability or brain ventricle inflation. Further, overexpression of *atp1a1* could not substitute for loss of Fxyd1 function in *fxyd1* morphants (Figure 2.10N-S). The amount of *atp1a1* and *fxyd1* mRNA used in these assays was the same as was used to rescue the phenotypes caused by *atp1a1* or *fxyd1* MOs respectively.

Together, the data demonstrate functional interaction, co-localization and regulation of $[Na^+]_i$ by zebrafish Fxyd1 and Atp1a1 in the developing neuroepithelium, and show that these proteins have non-redundant functions during ventricle formation.

Constitutively active RhoA rescues neuroepithelial cohesiveness but not brain ventricle inflation.

Based on experiments in cell culture (Rajasekaran et al., 2001), we hypothesized that RhoA acts downstream of the Na,K-ATPase during brain ventricle development. Injection of mRNA encoding a constitutively active human RhoA, *RhoAV14,* resulted in formation of a continuous neuroepithelium in control, *atp1a1* start site, and *fxyd1* morphants (Figure 2.11A-F, J-K; *atp1a1* start site = 80% normal ventricles (n=12); *fxyd1* MO = 80% normal ventricles (n=20)). However, *RhoAV14* expression in *atp1a1* start site morphants (Figure 2.11C-D) or in *snk* ^{to273a} mutants (Figure 2.11G-H) did not lead to brain ventricle inflation. In contrast, expression of *RhoAV14* in *fxyd1* morphants not only restored a continuous neuroepithelium, but also led to fully inflated brain ventricles (Figure 2.11E-F) further supporting the hypothesis that Fxyd1 is not required for brain ventricle inflation. Expression of a dominant negative RhoA (*RhoAN19*) or incubation in an

inhibitor of ROCK (Y27632), a target of active RhoA (Amano et al., 2000), resulted in a discontinuous neuroepithelium (Figure 2.11I-O), supporting a normal requirement for RhoA during brain development. These results suggest that Fxyd1 and Atp1a1 act through RhoA during neuroepithelium formation.

One explanation for the inability of *RhoAV14* to restore brain ventricle inflation to *snk* ^{to273a}

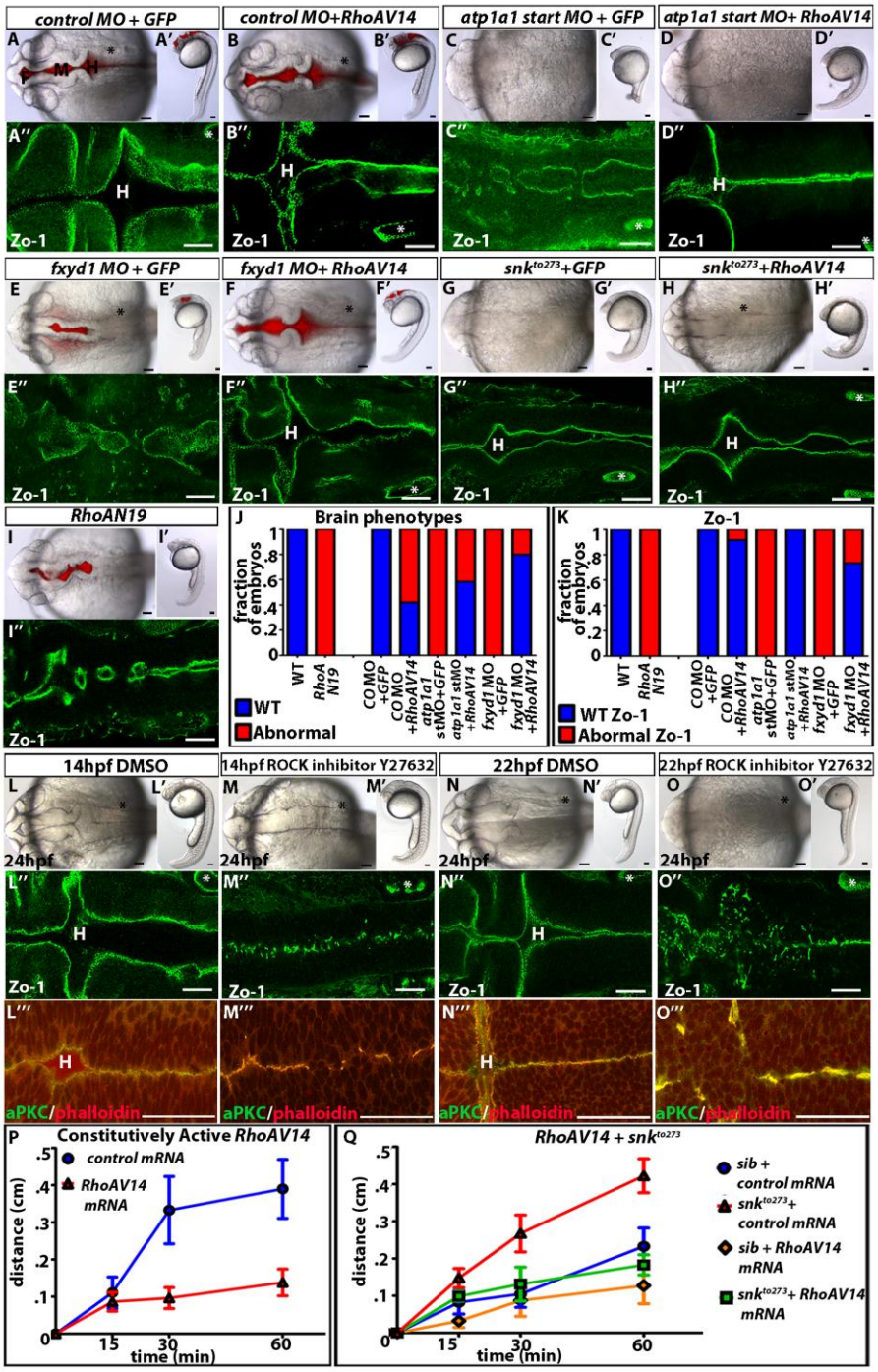

Figure 2.11: Constitutively active RhoA rescues neuroepithelial formation. (A-H) Constitutively active *RhoAV14* (B,D,F,H,), or control *mRNA* (*GFP*; A,C,E,G) in control MO (A-B), *atp1a1* start site MO (C-D), *fxyd1* MO (E-F), and *snk*^{to273} (G-H). (I) Overexpression of dominant negative *RhoAN19*. (J-K) Quantification of wild type vs. abnormal embryo brain ventricle phenotype (J), and Zo-1 (K). (L-O) Treatment with ROCK inhibitor (Y27632; M,O) or DMSO (L,N) at 14 hpf (L-M) or 22 hpf (N-O) wild type embryos. (P-Q) Dye retention assay in wild type embryos expressing control *mRNA* (blue), or *RhoAV14* (red) (P) and sibling (sib) + control *mRNA* (red), *snk* ^{to273} + control *mRNA* (blue), sib + *RhoAV14* (orange), and *snk* ^{to273} + *RhoAV14* (green) (Q). Brightfield dorsal (A-I, L-O) and lateral (A'-O') views. Ventricle injection of 2000 kDa Rhodamine Dextran dye (A,B,E,F). Zo -1 (A''-O''), aPKC (green), phalloidin (red; actin) (L'''-O''') All images taken at 24 hpf with anterior to left. F = forebrain, M = midbrain, H = hindbrain. Asterisk = ear. Scale bars = 50μm.

mutants, despite a continuous neuroepithelium, is that the neuroepithelium was leaky and could not retain CSF. In wild type embryos, expression of *RhoAV14* increased dye retention, and therefore decreased permeability (Figure 2.11P; $p<.05$). Significantly, *RhoAV14* expression also decreased permeability of *snk* ^{to273a} neuroepithelium, into the wild type range (Figure 2.11Q; $p<.05$), indicating that a RhoA is required for regulation of neuroepithelial permeability. Further, although *RhoA* overexpression in *snk* ^{to273a} embryos rescued neuroepithelial permeability, brain ventricle inflation remained reduced suggesting that a RhoA-insensitive process is necessary for brain ventricle inflation.

These results indicate that RhoA signaling acts downstream of Atp1a1 and Fxyd1 to regulate neuroepithelium formation and permeability. The data also delineate a RhoA-insensitive step in brain ventricle inflation, likely CSF production, which is dependent on Atp1a1, but not on Fxyd1 function.

DISCUSSION

The Na,K-ATPase has a well-known role as a modulator of membrane potential in neurons and is essential for generating an action potential. However, this protein complex has additional activities, and this study uncovers three processes in the developing brain that are regulated by Na,K-ATPase function to culminate in the formation of the brain ventricular system (Figure 2.12A). The ability of a single protein complex to regulate multiple aspects of brain ventricle formation and inflation suggests that the Na,K-ATPase is a pivotal regulator of ventricle volume.

Dissecting the activities of the Na,K-ATPase during brain ventricle formation.

Several experimental approaches allowed division of the Na,K-ATPase function into activities relevant for brain ventricle inflation, occurring sequentially and coordinately after neural tube closure. Formation of continuous apical neuroepithelial polarity and junctions requires RhoA activity downstream of both Atp1a1 and Fxyd1 (Figure 2.12B). Na,K-ATPase pumping appears to be important in establishing rather than maintaining junctions since adding the pump inhibitor, ouabain, after initial junctions had formed, did not disrupt the neuroepithelium.

By further exploring the interface with RhoA signaling, we showed that Atp1a1 had two additional activities. RhoA could substitute for one of these functions, modulation of neuroepithelial permeability (Figure 2.12C), however, the other was a RhoA-independent role uncovered by failure of RhoA to substitute for Atp1a1 during ventricle inflation, despite promoting wild type neuroepithelial permeability. This activity is likely to be CSF production (Figure 2.12D). Once the neuroepithelium has formed, equilibrium between drainage from the ventricles and CSF production would maintain a normal ventricular volume. The amount of active Atp1a1 may regulate the equilibrium, since different levels of this protein can increase or decrease permeability and ventricle size. Thus, the strong phenotypes observed in Atp1a1 mutants, are likely a composite of both impaired CSF production and retention.

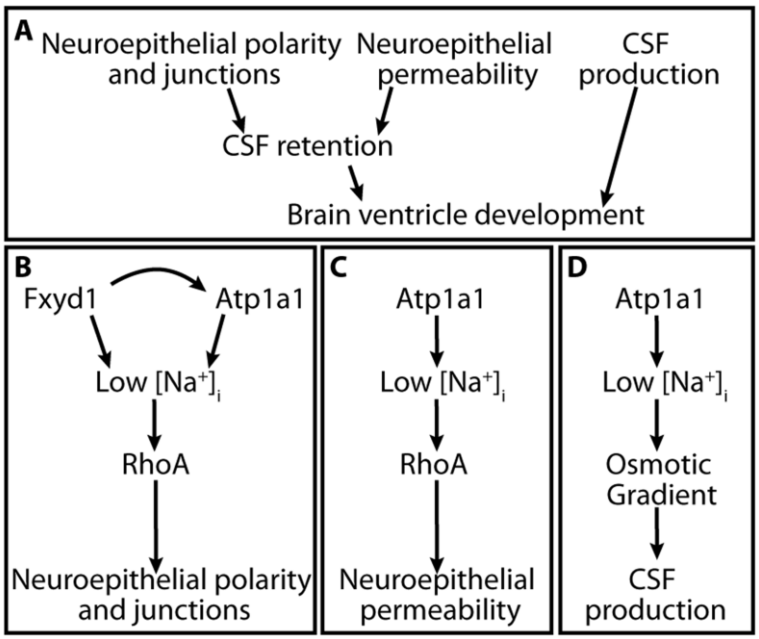

Figure 2.12: Model for requirement of Na,K-ATPase during brain ventricle development. (A) Brain ventricle development is a three step process that requires establishment of neuroepithelial polarity and junctions and regulation of neuroepithelial permeability allowing for CSF retention, in addition to CSF production. Brain ventricle inflation occurs via CSF retention and CSF production. (B) Neuroepithelial formation requires RhoA which acts downstream of Fxyd1 and Atp1a1. (C) Neuroepithelial permeability requires RhoA which acts downstream of only Atp1a1. (D) CSF production is RhoA – insensitive and requires Atp1a1.

The role of Fxyd1 during brain ventricle development.

This is the first report of a requirement for Fxyd1 function in the developing brain. FXYD1 knockout mice show no apparent brain phenotype, suggesting functional redundancy not present in zebrafish. *FXYD1* adult null mice had increased cardiac mass, larger cardiac myocytes and, consistent with results in zebrafish, show 50% reduced Na,K-ATPase activity in mutant hearts relative to wild type (Jia et al., 2005). Fxyd1 appears to have a distinct role during brain

ventricle formation, since it is required for neuroepithelium formation but, unlike Atp1a1, not for subsequent steps that lead to ventricle inflation. Consistently, overexpression of Atp1a1 does not substitute for Fxyd1, and *vice versa*. While synergy between *atp1a1* and *fxyd1* loss of function supports a major role for Fxyd1 as a regulator of Atp1a1 pumping, Fxyd1 may also have additional activity, that could modulate $[Na^+]_I$, for example, by inhibiting the Na^+/Ca^{2+} exchanger (Zhang et al., 2003).

Connection between Na,K-ATPase function, RhoA signaling, neuroepithelium formation and permeability.

How does the Na,K-ATPase modulate RhoA function, which impacts both neuroepithelial polarity and permeability? One possibility is that depolarization of the cell by the Na,K-ATPase leads to RhoA activation. In cell culture, depolarization of epithelial cells activates the Ras/MEK/ERK pathway (Waheed et al., 2010), by promoting GEF activity and increasing RhoA-GTP levels. In kidney tubular cells (LLC-PK1) and MDCK cells, depolarization activates RhoA and ROCK leading to Myosin Light Chain phosphorylation (Szaszi et al., 2005). However, in no case is the mechanism connecting depolarization and RhoA activation understood.

Unlike the case in *Drosophila* trachea formation (Paul et al., 2007), our data indicate a requirement for Na,K-ATPase pump function in epithelium formation. Multiple differences between fly and vertebrate junctions (Knust and Bossinger, 2002) likely explain these different requirements for the Na,K-ATPase. Consistent with our study, Na,K-ATPase pumping is required for formation of continuous junctions and lumens in the zebrafish heart and gut (Bagnat et al., 2007; Cibrian-Uhalte et al., 2007).

We propose that RhoA regulates paracellular permeability in the zebrafish neuroepithelium, based on the size selectivity of our dye retention assay. However, we cannot rule out some contribution of vesicular transcellular pathways. Consistently, Claudin5, a barrier claudin, and component of the tight junction complex responsible for paracellular ion transport and selectivity, is required for brain ventricle inflation and permeability (Terry et al., 2010; Zhang et al., 2010). In cell culture, RhoA activation promotes claudin phosphorylation and regulates permeability by modulating claudin-claudin interactions or recycling tight junction components

(Yamamoto et al., 2008). Thus, there are plausible connections between the Na,K-ATPase, RhoA and claudins.

Modulation of CSF production by the Na,K-ATPase.

Ventricle "inflation" is a scorable phenotype, but not a discrete process, as it includes formation of a non-leaky epithelium as well as CSF production, which appears to be a RhoA-insensitive process. This is likely to be mediated by the osmotic gradient formed as a result of a membrane potential difference, under control of the Na,K-ATPase and other pumps and channels (Figure 2.12D) (Brown et al., 2004; Pollay et al., 1985). Production of CSF requires both movement of water into the ventricular lumen, as well as secretion of proteins and other factors. The role of the Na,K-ATPase in water movement may occur either via Aquaporins in the plasma membrane or through the paracellular pathway. Although Aquaporin 1 is strongly expressed in the choroid plexus and knockout mice have abnormal CSF production (Oshio et al., 2003), analysis of Aquaporin activity during initial ventricle inflation has not been explored. Further, there is little data to suggest whether Na,K-ATPase regulates protein secretion into the ventricular lumen, although one report implicates Na,K-ATPase during FGF2 secretion in primate cells (Dahl et al., 2000). Analysis of the role of Na,K-ATPase during protein secretion and water movement that results in brain ventricle inflation will be a future direction of this study.

Significance of Na,K-ATPase activity during brain ventricle volume control.

Either an increase or decrease in CSF volume can be pathological throughout life (Lowery and Sive, 2009), due to either changes in pressure and CSF composition (Desmond et al., 2005; Gato et al., 2005). Since the amount of functional Na,K-ATPase can regulate brain ventricle size in a graded manner, this pump may play a "volume sensor" and homeostatic role. For example, the molecular basis for non-obstructive hydrocephalus is not clear, and our data suggest possible input from Na,K-ATPase function. In addition to the regulation described in this study, Na,K-ATPase activity can be fine-tuned by differential expression of beta and FXYD subunits which modulate pump activity, expression level and correct cellular localization (Geering, 2001; Geering, 2006; Wilson et al., 2000). Therefore a slight disruption of Na,K-ATPase subunits could lead to drastic changes in activity and abnormal CSF levels.

ACKNOWLEDGEMENTS

This work was supported by the National Institute for Mental Health, and National Science Foundation. Special thanks to Dr. Jen Gutzman, Dr. Iain Cheeseman and Sive lab members for many useful discussions and constructive criticism, and to Olivier Paugois for expert fish husbandry.

REFERENCES

Amano, M., Fukata, Y., Kaibuchi, K., 2000. Regulation and functions of Rho-associated kinase. Exp Cell Res. 261**,** 44-51.

Bagnat, M., Cheung, I. D., Mostov, K. E., Stainier, D. Y., 2007. Genetic control of single lumen formation in the zebrafish gut. Nat Cell Biol. 9**,** 954-60.

Bibert, S., Roy, S., Schaer, D., Horisberger, J. D., Geering, K., 2008. Phosphorylation of phospholemman (FXYD1) by protein kinases A and C modulates distinct Na,K-ATPase isozymes. J Biol Chem. 283**,** 476-86.

Bossuyt, J., Despa, S., Martin, J. L., Bers, D. M., 2006. Phospholemman phosphorylation alters its fluorescence resonance energy transfer with the Na/K-ATPase pump. J Biol Chem. 281**,** 32765-73.

Brown, P. D., Davies, S. L., Speake, T., Millar, I. D., 2004. Molecular mechanisms of cerebrospinal fluid production. Neuroscience. 129**,** 957-70.

Canfield, V. A., Loppin, B., Thisse, B., Thisse, C., Postlethwait, J. H., Mohideen, M. A., Rajarao, S. J., Levenson, R., 2002. Na,K-ATPase alpha and beta subunit genes exhibit unique expression patterns during zebrafish embryogenesis. Mech Dev. 116**,** 51-9.

Cibrian-Uhalte, E., Langenbacher, A., Shu, X., Chen, J. N., Abdelilah-Seyfried, S., 2007. Involvement of zebrafish Na+,K+ ATPase in myocardial cell junction maintenance. J Cell Biol. 176**,** 223-30.

Ciruna, B., Jenny, A., Lee, D., Mlodzik, M., Schier, A. F., 2006. Planar cell polarity signalling couples cell division and morphogenesis during neurulation. Nature. 439**,** 220-4.

Crambert, G., Fuzesi, M., Garty, H., Karlish, S., Geering, K., 2002. Phospholemman (FXYD1) associates with Na,K-ATPase and regulates its transport properties. Proc Natl Acad Sci U S A. 99**,** 11476-81.

Dahl, J. P., Binda, A., Canfield, V. A., Levenson, R., 2000. Participation of Na,K-ATPase in FGF-2 secretion: rescue of ouabain-inhibitable FGF-2 secretion by ouabain-resistant Na,K-ATPase alpha subunits. Biochemistry. 39**,** 14877-83.

Desmond, M. E., Levitan, M. L., Haas, A. R., 2005. Internal luminal pressure during early chick embryonic brain growth: descriptive and empirical observations. Anat Rec A Discov Mol Cell Evol Biol. 285**,** 737-47.

Draper, B. W., Morcos, P. A., Kimmel, C. B., 2001. Inhibition of zebrafish fgf8 pre-mRNA splicing with morpholino oligos: a quantifiable method for gene knockdown. Genesis. 30**,** 154-6.

Ellertsdottir, E., Ganz, J., Durr, K., Loges, N., Biemar, F., Seifert, F., Ettl, A. K., Kramer-Zucker, A. K., Nitschke, R., Driever, W., 2006. A mutation in the zebrafish Na,K-ATPase subunit atp1a1a.1 provides genetic evidence that the sodium potassium pump contributes to left-right asymmetry downstream or in parallel to nodal flow. Dev Dyn. 235**,** 1794-808.

Feschenko, M. S., Donnet, C., Wetzel, R. K., Asinovski, N. K., Jones, L. R., Sweadner, K. J., 2003. Phospholemman, a single-span membrane protein, is an accessory protein of Na,K-ATPase in cerebellum and choroid plexus. J Neurosci. 23**,** 2161-9.

Gato, A., Moro, J. A., Alonso, M. I., Bueno, D., De La Mano, A., Martin, C., 2005. Embryonic cerebrospinal fluid regulates neuroepithelial survival, proliferation, and neurogenesis in chick embryos. Anat Rec A Discov Mol Cell Evol Biol. 284**,** 475-84.

Geering, K., 2001. The functional role of beta subunits in oligomeric P-type ATPases. J Bioenerg Biomembr. 33**,** 425-38.

Geering, K., 2006. FXYD proteins: new regulators of Na-K-ATPase. Am J Physiol Renal Physiol. 290**,** F241-50.

Graeden, E., Sive, H., 2009. Live imaging of the zebrafish embryonic brain by confocal microscopy. J Vis Exp.

Gutzman, J. H., Sive, H., 2009. Zebrafish brain ventricle injection. J Vis Exp.

Gutzman, J. H., Sive, H., 2010. Epithelial relaxation mediated by the myosin phosphatase regulator Mypt1 is required for brain ventricle lumen expansion and hindbrain morphogenesis. Development. 137**,** 795-804.

Hong, E., Brewster, R., 2006. N-cadherin is required for the polarized cell behaviors that drive neurulation in the zebrafish. Development. 133**,** 3895-905.

Jia, L. G., Donnet, C., Bogaev, R. C., Blatt, R. J., McKinney, C. E., Day, K. H., Berr, S. S., Jones, L. R., Moorman, J. R., Sweadner, K. J., Tucker, A. L., 2005. Hypertrophy, increased ejection fraction, and reduced Na-K-ATPase activity in phospholemman-deficient mice. Am J Physiol Heart Circ Physiol. 288**,** H1982-8.

Jiang, Y. J., Brand, M., Heisenberg, C. P., Beuchle, D., Furutani-Seiki, M., Kelsh, R. N., Warga, R. M., Granato, M., Haffter, P., Hammerschmidt, M., Kane, D. A., Mullins, M. C., Odenthal, J., van Eeden, F. J., Nusslein-Volhard, C., 1996. Mutations affecting neurogenesis and brain morphology in the zebrafish, Danio rerio. Development. 123**,** 205-16.

Kimmel, C. B., Ballard, W. W., Kimmel, S. R., Ullmann, B., Schilling, T. F., 1995. Stages of embryonic development of the zebrafish. Dev Dyn. 203**,** 253-310.

Knust, E., Bossinger, O., 2002. Composition and formation of intercellular junctions in epithelial cells. Science. 298**,** 1955-9.

Krupinski, T., Beitel, G. J., 2009. Unexpected roles of the Na-K-ATPase and other ion transporters in cell junctions and tubulogenesis. Physiology (Bethesda). 24**,** 192-201.

Lansbery, K. L., Burcea, L. C., Mendenhall, M. L., Mercer, R. W., 2006. Cytoplasmic targeting signals mediate delivery of phospholemman to the plasma membrane. Am J Physiol Cell Physiol. 290**,** C1275-86.

Linask, K. K., Gui, Y. H., 1995. Inhibitory effects of ouabain on early heart development and cardiomyogenesis in the chick embryo. Dev Dyn. 203**,** 93-105.

Lowery, L. A., Sive, H., 2005. Initial formation of zebrafish brain ventricles occurs independently of circulation and requires the nagie oko and snakehead/atp1a1a.1 gene products. Development. 132**,** 2057-67.

Lowery, L. A., Sive, H., 2009. Totally tubular: the mystery behind function and origin of the brain ventricular system. Bioessays. 31**,** 446-58.

Mishra, N. K., Peleg, Y., Cirri, E., Belogus, T., Lifshitz, Y., Voelker, D. R., Apell, H. J., Garty, H., Karlish, S. J., 2011. FXYD proteins stabilize Na,K-ATPase: amplification of specific phosphatidylserine-protein interactions. J Biol Chem. 286**,** 9699-712.

Morth, J. P., Pedersen, B. P., Toustrup-Jensen, M. S., Sorensen, T. L., Petersen, J., Andersen, J. P., Vilsen, B., Nissen, P., 2007. Crystal structure of the sodium-potassium pump. Nature. 450**,** 1043-9.

Nasevicius, A., Ekker, S. C., 2000. Effective targeted gene 'knockdown' in zebrafish. Nat Genet. 26**,** 216-20.

Oshio, K., Song, Y., Verkman, A. S., Manley, G. T., 2003. Aquaporin-1 deletion reduces osmotic water permeability and cerebrospinal fluid production. Acta Neurochir Suppl. 86**,** 525-8.

Paul, S. M., Palladino, M. J., Beitel, G. J., 2007. A pump-independent function of the Na,K-ATPase is required for epithelial junction function and tracheal tube-size control. Development. 134**,** 147-55.

Pavlovic, D., Fuller, W., Shattock, M. J., 2007. The intracellular region of FXYD1 is sufficient to regulate cardiac Na/K ATPase. FASEB J. 21**,** 1539-46.

Pollay, M., Hisey, B., Reynolds, E., Tomkins, P., Stevens, F. A., Smith, R., 1985. Choroid plexus Na+/K+-activated adenosine triphosphatase and cerebrospinal fluid formation. Neurosurgery. 17**,** 768-72.

Rajasekaran, S. A., Barwe, S. P., Gopal, J., Ryazantsev, S., Schneeberger, E. E., Rajasekaran, A. K., 2007. Na-K-ATPase regulates tight junction permeability through occludin phosphorylation in pancreatic epithelial cells. Am J Physiol Gastrointest Liver Physiol. 292**,** G124-33.

Rajasekaran, S. A., Palmer, L. G., Moon, S. Y., Peralta Soler, A., Apodaca, G. L., Harper, J. F., Zheng, Y., Rajasekaran, A. K., 2001. Na,K-ATPase activity is required for formation of tight junctions, desmosomes, and induction of polarity in epithelial cells. Mol Biol Cell. 12**,** 3717-32.

Sagerstrom, C. G., Grinbalt, Y., Sive, H., 1996. Anteroposterior patterning in the zebrafish, Danio rerio: an explant assay reveals inductive and suppressive cell interactions. Development. 122**,** 1873-83.

Shinoda, T., Ogawa, H., Cornelius, F., Toyoshima, C., 2009. Crystal structure of the sodium-potassium pump at 2.4 A resolution. Nature. 459**,** 446-50.

Shu, X., Cheng, K., Patel, N., Chen, F., Joseph, E., Tsai, H. J., Chen, J. N., 2003. Na,K-ATPase is essential for embryonic heart development in the zebrafish. Development. 130**,** 6165-73.

Speake, T., Whitwell, C., Kajita, H., Majid, A., Brown, P. D., 2001. Mechanisms of CSF secretion by the choroid plexus. Microsc Res Tech. 52**,** 49-59.

Sweadner, K. J., Rael, E., 2000. The FXYD gene family of small ion transport regulators or channels: cDNA sequence, protein signature sequence, and expression. Genomics. 68**,** 41-56.

Szaszi, K., Sirokmany, G., Di Ciano-Oliveira, C., Rotstein, O. D., Kapus, A., 2005. Depolarization induces Rho-Rho kinase-mediated myosin light chain phosphorylation in kidney tubular cells. Am J Physiol Cell Physiol. 289**,** C673-85.

Terry, S., Nie, M., Matter, K., Balda, M. S., 2010. Rho signaling and tight junction functions. Physiology (Bethesda). 25**,** 16-26.

Waheed, F., Speight, P., Kawai, G., Dan, Q., Kapus, A., Szaszi, K., 2010. Extracellular signal-regulated kinase and GEF-H1 mediate depolarization-induced Rho activation and paracellular permeability increase. Am J Physiol Cell Physiol. 298**,** C1376-87.

Welss, P., 1934. Secretory activity of the inner layer of the embryonic mid-brain of the chick, as revealed by tissue culture. The Anatomical Record. 58**,** 299-302.

Westerfield, M., Sprague, J., Doerry, E., Douglas, S., Grp, Z., 2001. The Zebrafish Information Network (ZFIN): a resource for genetic, genomic and developmental research. Nucleic Acids Research. 29**,** 87-90.

Wilson, P. D., Devuyst, O., Li, X., Gatti, L., Falkenstein, D., Robinson, S., Fambrough, D., Burrow, C. R., 2000. Apical plasma membrane mispolarization of NaK-ATPase in polycystic kidney disease epithelia is associated with aberrant expression of the beta2 isoform. Am J Pathol. 156**,** 253-68.

Yamamoto, M., Ramirez, S. H., Sato, S., Kiyota, T., Cerny, R. L., Kaibuchi, K., Persidsky, Y., Ikezu, T., 2008. Phosphorylation of claudin-5 and occludin by rho kinase in brain endothelial cells. Am J Pathol. 172**,** 521-33.

Yuan, S., Joseph, E. M., 2004. The small heart mutation reveals novel roles of Na+/K+-ATPase in maintaining ventricular cardiomyocyte morphology and viability in zebrafish. Circ Res. 95**,** 595-603.

Zhang, J., Piontek, J., Wolburg, H., Piehl, C., Liss, M., Otten, C., Christ, A., Willnow, T. E., Blasig, I. E., Abdelilah-Seyfried, S., 2010. Establishment of a neuroepithelial barrier by Claudin5a is essential for zebrafish brain ventricular lumen expansion. Proc Natl Acad Sci U S A. 107**,** 1425-30.

Zhang, X. Q., Qureshi, A., Song, J., Carl, L. L., Tian, Q., Stahl, R. C., Carey, D. J., Rothblum, L. I., Cheung, J. Y., 2003. Phospholemman modulates Na+/Ca2+ exchange in adult rat cardiac myocytes. Am J Physiol Heart Circ Physiol. 284**,** H225-33.

CHAPTER THREE

Zebrafish embryonic cerebrospinal fluid is required for retinoic acid synthesis and neuroepithelial cell survival

To be submitted as:

Jessica T. Chang and Hazel Sive. Zebrafish embryonic cerebrospinal fluid is required for retinoic acid synthesis and neuroepithelial cell survival.

Contributions: I performed all the work for this Chapter.

ABSTRACT

The brain ventricular system is composed of a highly conserved set of cavities that contain cerebrospinal fluid (CSF), a protein-rich fluid essential for brain function. Although the embryonic brain ventricles contain large quantities of embryonic CSF (eCSF) little is known about the function of the fluid or the mechanisms that drive fluid production. Here, we developed a method to manually drain eCSF from zebrafish brain ventricles and showed that eCSF is necessary for cell survival within the neuroepithelium. Increased cell death in manually drained embryos is rescued by exogenous retinoic acid (RA) but not growth factors IGF2 or FGF2, suggesting a possible role for RA in cell survival. Our mass spectrometry analysis identified retinol binding protein 4 (Rbp4) within the CSF. Inhibition of Rbp4, RA synthesis and signaling via the PPARγ (peroxisome proliferator-activated receptor gamma) receptors increased neuroepithelial cell death. Conversely, exogenous Rbp4 and retinol or a PPARγ agonist, rescued cell death in manually drained embryos. We propose that Rbp4, present within the eCSF, is required for RA synthesis which promotes cell survival through PPARγ signaling.

INTRODUCTION

Deep within the vertebrate brain lie a series of connected cavities called brain ventricles, which form from the central lumen of the neural tube and are maintained into adulthood. The brain ventricles hold and retain cerebrospinal fluid (CSF), which is secreted into the ventricles by the choroid plexus, a specialized type of ependymal cell present in a series of highly vascularized secretory regions at the blood/CSF barrier (Brown et al., 2004; Johanson et al., 2011; Praetorius, 2007; Speake et al., 2001). In humans, 50-70% of adult CSF is produced by the choroid plexus with some contribution from the ependymal epithelium lining the brain ventricles (Pollay and Curl, 1967; Praetorius, 2007; Speake et al., 2001). Although the choroid plexus is the major producer of CSF, CSF exists prior to choroid plexus development suggesting that the neuroepithelium contributes to initial embryonic CSF (eCSF) production. Consistent with this hypothesis, explanted chick neuroepithelium was shown to be secretory (Welss, 1934).

eCSF contains three times more protein than adult CSF suggesting a potentially important role during development (Zheng et al., 2005). In humans, adult CSF is thought to cushion the brain, remove waste and transport secreted molecules (Chodobski and Szmydynger-Chodobska, 2001; Redzic et al., 2005). While in embryonic chick neuroepithelial explants and mouse embryos, secreted factors within the eCSF, hydrostatic pressure or a combination of the two are required for gene expression, cell proliferation, survival, and neurogenesis (Alonso et al., 1998; Alonso et al., 1999; Alonso et al., 2011; Desmond et al., 2005; Gato et al., 2005; Lehtinen et al., 2011; Martin et al., 2009; Martin et al., 2006; Mashayekhi, 2008; Mashayekhi et al., 2011; Mashayekhi and Salehi, 2006b; Miyan et al., 2006; Parada et al., 2008a; Parada et al., 2008b; Parada et al., 2005b; Salehi and Mashayekhi, 2006; Salehi et al., 2009). Similarly, in mice with hydrocephalus, an excess of CSF within the ventricles, there is a corresponding decrease in neurogenesis (Mashayekhi et al., 2001; Mashayekhi et al., 2002). Additionally, analysis of eCSF composition in mice, rat, chick, and humans has identified a variety of proteins including extracellular matrix components, ion carriers, hormone-binding factors, osmotic pressure regulating proteins, as well as proteins involved in cell death and proliferation (Gato et al., 2004; Parada et al., 2006;

Parada et al., 2005a; Zappaterra et al., 2007). Further studies have identified that insulin-like growth factor 2 (IGF2), retinoic acid (RA), fibroblast growth factor 2 (FGF2), and apolipoproteins within the eCSF are required for neurogenesis and cell proliferation (Alonso et al., 2011; Lehtinen et al., 2011; Martin et al., 2006; Mashayekhi et al., 2011; Parada et al., 2008a; Parada et al., 2008b; Salehi et al., 2009). These studies indicate that normal pressure and/or normal composition of eCSF are crucial for proper neural development. Our data complements these studies demonstrating a role for RA during neuroepithelial cell survival.

RA, a lipophilic vitamin A metabolite, is essential for proper embryonic development. The RA precursor, retinol, is first solubilized by binding to retinol binding protein 4 (RBP4) (Blomhoff et al., 1990). Retinol is then converted to retinaldehyde and eventually to RA by a series of dehydrogenases (Duester, 1998). In the classical RA signaling pathway, RA is then transported into the nucleus by CRABP (cellular retinoic acid binding protein) which delivers it to the retinoic acid receptors (RARs) (Budhu and Noy, 2002). This complex then binds to retinoic acid response elements (RAREs) located in regulatory regions of target genes, which results in differentiation, cell-cycle arrest and apoptosis (Noy, 2010). An alternate RA signaling pathway was recently identified in which fatty acid binding proteins (FABP) transport RA into the cell nucleus, resulting in survival and proliferation by the activation of peroxisome proliferator-activated receptors (PPAR) (Schug et al., 2007). In keratinocytes, PPAR β/δ promotes differentiation and anti-apoptotic signaling via the PDK-1/Akt signaling pathway (Di-Poi et al., 2002). Pathway selection appears to depend on the ratio of FABP to CRABP (Schug et al., 2007).

RA plays an important role within the vertebrate brain. Abnormal RA signaling disrupts embryonic patterning, neuronal plasticity, differentiation, regeneration, learning, and memory (Maden, 2007). Several studies have suggested a role for RA signaling in promoting both survival and differentiation of neurons. In adult mice, RA is required for survival of olfactory sensory neurons (Hagglund et al., 2006) and promotes neurogenesis in the dentate gyrus and hippocampus, (Bonnet et al., 2008; Jacobs et al., 2006). Disruption of RA signaling has also been associated with schizophrenia and depression (Goodman, 1998; Wysowski et al., 2001a; Wysowski et al., 2001b).

We are using the zebrafish to define the mechanisms underlying eCSF function and ventricle inflation. Although analysis of eCSF function and factors were performed on mouse, rat, and chick embryos, these studies focused on eCSF produced after choroid plexus formation. For the first time, we characterize the function of eCSF prior to choroid plexus formation in embryonic zebrafish. We have developed a method to remove eCSF from zebrafish brain ventricles and have found that eCSF is necessary for cell survival in the embryonic brain. In addition, we identified factors within zebrafish eCSF using mass spectrometry and determined that retinol binding protein 4 and subsequent downstream RA signaling via the PPARγ receptors is required for neuroepithelial cell survival.

MATERIALS AND METHODS

Fish lines and maintenance

Wild tpe (AB) *Danio rerio* fish were raised and bred according to standard methods (Westerfield et al., 2001). Embryos were kept at 28.5^{o}C and staged accordingly (Kimmel et al., 1995). Stages of development are expressed as hours post-fertilization (hpf).

Brightfield brain imaging

During imaging, embryos were anesthetized in 0.1 mg/mL Tricaine (Sigma) dissolved in embryo medium (E3) made according to (Westerfield et al., 2001). Images were taken using a Leica dissecting scope and KT Spot digital camera (RT KE Diagnostic instruments). Images were adjusted for brightness, contrast and coloring in Photoshop CS5 (Adobe).

Manual drainage and brain ventricle injection

Manual drainage technique was previously described (Chapter 6). Briefly, a micropipette needle was inserted through the roof plate of the hindbrain ventricle and was positioned either in the hindbrain, midbrain, or forebrain. eCSF was removed from all three brain ventricles, using an Eppendorf CellTram oil microinjector apparatus, every one to two hours from 22-36 hpf (six times total). After each drain, the needle was removed and embryos stored at 32^{o}C. As a control, the micropipette needle was inserted into embryos without removing any eCSF to rule out potential effects of insertion of a micropipette needle on the manually drained phenotype

(referred to as punctured). To reintroduce factors into drained embryos, 1-2 nl of factors listed in Table 1 or physiological saline (118 mM NaCl, 2 mM KCl, 10 mM $MgCl_2$, 10 mM HEPES, 10 mM glucose) were injected every two hours from 30-36 hpf (3 times total) into the brain ventricles as described previously (Gutzman and Sive, 2009). DMSO diluted 1:10-1:1000 in E3 or E3 alone were used as negative control injections.

Table 1: List of recombinant proteins, small molecules, and chemical inhibitors.

Factors	Catalog Number	Stock Concentration	Concentration injected
InSolution™ Caspase-3 Inhibitor I, cell permeable	Calbiochem 235427	5 mM in DMSO	500 μM in E3
Insulin like growth factor 2 (IGF2) Recombinant Human	US Biological I7661-12P	200 ng/ml in dH_2O + 0.01%BSA	25 ng/ml in E3
Fibroblast growth factor 2 (FGF2) human recombinant	Sigma SRP4037	600 ng/mL in dH_2O + 0.01%BSA	300 μg/ml in E3
All trans Retinoic Acid	Sigma R2625	10^{-6} M in DMSO	10^{-8} M in E3
All-trans Retinol	Sigma M6191	174 mM in EtOH and further to 348 μM in 50%DMSO/50%EtOH	348 nM in E3
Recombinant human Retinol Binding protein 4 (RBP4)	R&D systems 3378-LC	500 ng/μl in dH2O	2 ng/ μl in E3
A1120	Sigma A3111	30 mM in DMSO	$30x10^{-8}$ M
Citral	Sigma W230316	5.83 M in DMSO	250 μM in E3
BADGE	Sigma D3415	25 mM in DMSO	25 μM in E3
4-Diethylaminobenzaldehyde (DEAB)	Sigma D86256	1 M in DMSO	10 μM in E3
GW9662	Sigma M6191	15 mM in DMSO	0.5 μM in E3
Rosiglitazone	Sigma R2408	30 mM (10mg/ml) in DMSO	43 nM in E3

Immunohistochemistry

Whole mount immunohistochemistry was performed with propidium iodide (Invitrogen; 1:1000), PH3 (Millipore 06-570; 1:800), acetylated tubulin (Sigma, T6793; 1:1000), GABA (Sigma

2052; 1:500), tyrosine hydroxylase (TH, Millipore MAB318; 1:100) and 5-HT (Sigma, S5545; 1:100). Embryos were fixed with 4% PFA or 2% TCA for two hours at room temperature or overnight at 4^{o}C and blocked overnight at 4^{o}C or blocked for two hours at room temperature. Blocking solutions used were: 2% NGS+1% Triton+2% BSA+1%DMSO (PH3), 10%NGS+0.1% BSA1%+1%Triton (acetylated tubulin), 10%NGS+1% Triton (TH, 5HT) and 10% NGS+3% BSA+1% Triton (GABA). For TH, 5-HT and GABA, embryos were dehydrated into 100% EtOH and acetone treated at -20^{o}C for one hour before proceeding to blocking step. For TUNEL (Apoptag®, Millipore), embryos were fixed overnight in 4% PFA and dehydrated into 100% EtOH. After rehydration, embryos were treated in Proteinase K (2.5 μg/mL, Invitrogen) for 2 minutes and rinsed well. Embryos were subsequently treated using recommended Apoptag® protocol. TUNEL blocking solution used was 10% BMB (Boehringer Mannheim Blocking reagent) +10% lamb serum + 80% MAB (maleic acid buffer) and primary antibody anti-DIG-Fluorescein (Roche; 1:100). Propidium iodide was diluted in 1x PBT (PBS + 0.01% Tween) and incubated at room temperature for 45 minutes. Secondary antibodies goat anti-mouse Alexa Fluor 488, goat anti-rabbit Alexa Fluor 488 (Sigma), or goat anti-rabbit Cy5 (Jackson ImmunoResearch) were used at 1:500.

Antisense oligonucleotide morpholinos (MO)

A splice-site blocking MO (*rbp4sp:* 5' GTTGACTTACCCTCGTTCTGTTAAA 3', Gene Tools, LLC) was used to target *rbp4* exon2/intron3 as previously described (Li et al., 2007; Nasevicius and Ekker, 2000). Standard control MO used 5'-CCTCTTACCTCAGTTACAATTTATA-3 ' and *p53* morpholino 5'-GCGCCATTGCTTTGCAAGAATTG-3' (Gene Tools, LLC). MO were injected at the single cell stage and embryos were analyzed at 24 hpf.

Mass Spectrometry

SAMPLE PREPARATION: eCSF was collected from 1500 embryos, divided into three tubes, and stored at -80^{o}C in PBS + protease inhibitors (Roche cOmplete Mini tablets EDTA free). Proteins were initially separated on a 10-20% SDS-PAGE gel, and each gel lane to be analyzed was excised and cut into six segments of approximately equal length. Each gel fragment was further

cut into smaller pieces, typically 1mm^2 in order to facilitate de-staining, and SDS removal. In-gel reduction, alkylation and trypsin digestion were performed following published procedures (Shevchenko et al., 2007). Trypsin digestion was carried out overnight at room temperature.

MASS SPECTROMETRY: Extracted proteolytic peptides were analyzed by LC-MS. Peptide separation was carried out with gradient elution (water-acetonitrile-0.1% formic acid) from a 75μm ID capillary reversed phase C18 column (New Objective) using an Agilent 1100 nano HPLC system (Agilent Technologies); the flow rate was 280 nl/min. In order to optimize peptide separation, a three hour long gradient was used. Peptide molecular weight data as well as peptide fragment ion mass spectra were acquired with an LTQ ion trap mass spectrometer (ThermoFischer Scientific).

DATABASE SEARCHING: Tandem mass spectra were extracted by BioworksBrowser Version 3.3 (ThermoFisher) and submitted to the Mascot database search software version 2.2 (Matrix Science). Charge state deconvolution and deisotoping were not performed. All MS/MS samples were analyzed using Mascot (Matrix Science, London, UK; version Mascot). Mascot was set up to search the NCBInr_081410 database (selected for *Danio rerio*, unknown version, 44358 entries) assuming the digestion enzyme trypsin. Mascot was searched with a fragment ion mass tolerance of 0.60 Da and a parent ion tolerance of 2.0 Da. Iodoacetamide derivative of cysteine was specified in Mascot as a fixed modification. Deamidation of asparagine and glutamine and oxidation of methionine were specified in Mascot as variable modifications.

CRITERIA FOR PROTEIN IDENTIFICATION: Scaffold (version Scaffold_3.3.1, Proteome Software Inc., Portland, OR) was used to validate MS/MS based peptide and protein identifications. Peptide identifications were accepted if they exceeded specific database search engine thresholds. Mascot identifications required at least ion scores must be greater than both the associated identity scores and 20, 30, 40 and 40 for singly, doubly, triply and quadruply charged peptides. Protein identifications were accepted if they contained at least 1 identified peptide. Proteins that contained similar peptides and could not be differentiated based on MS/MS analysis alone were grouped to satisfy the principles of parsimony.

RESULTS

eCSF is required for cell survival and tail extension.

To determine whether zebrafish eCSF is necessary during embryonic brain development, we developed an in vivo technique to manually drain eCSF from the brain ventricles (Chapter 6). These studies found that newly produced eCSF refills the brain ventricles roughly two hours after draining (Chapter 6). To maintain an eCSF-depleted embryo, we removed eCSF by manually draining every 1-2 hours from 22 hpf (hours post fertilization) to 36 hpf, a crucial time for neurogenesis. We then analyzed cell proliferation, cell death, and neurogenesis in this depleted system. To ensure that the needle itself was not causing abnormal brain development, we inserted a needle into the embryonic brain being careful not to remove any eCSF (punctured). Although

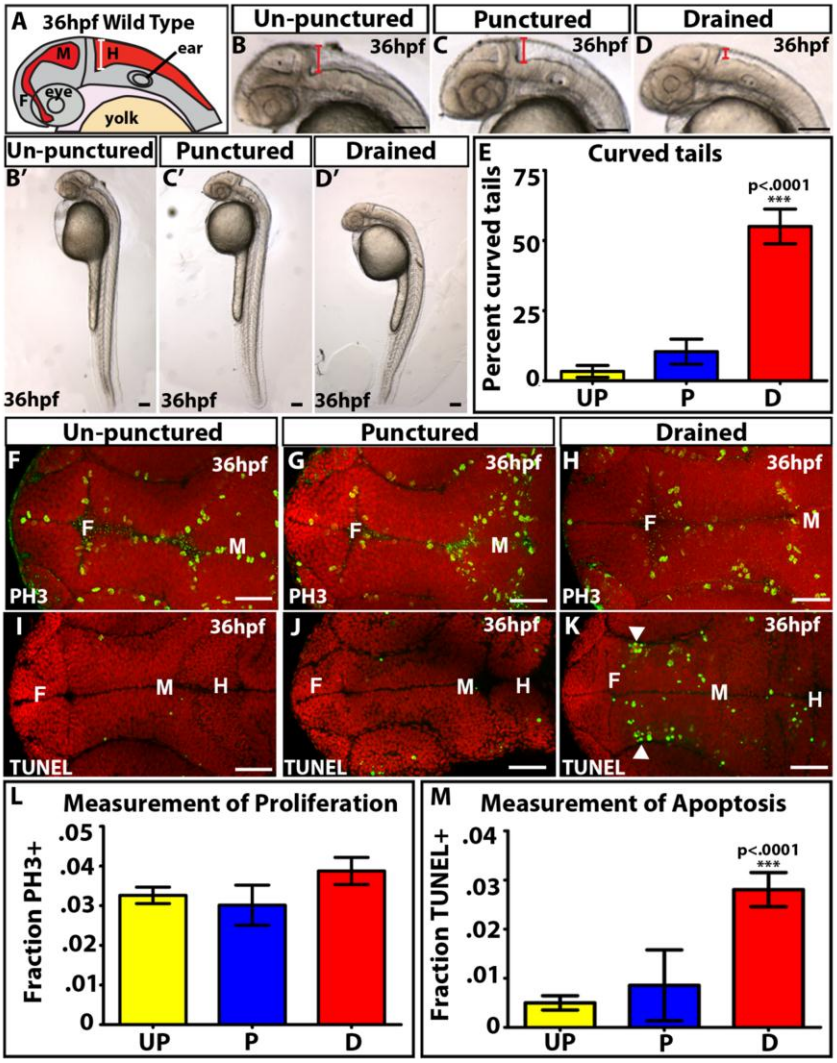

Figure 3.1: eCSF is required for cell survival and tail extension. (A) Lateral schematic of 36 hpf wild type embryo. (B-D) Brightfield lateral views of un-punctured (B), punctured (C), and drained (D) embryos. (B'-D') Whole embryo phenotype. (E) Percent of embryos with curved tails. (F-H) PH3 (green) and (I-K) TUNEL (green). Propidium iodide in red. (L-M) Quantification of proliferation (L) and apoptosis (M). Data represented as mean+/-SEM. F = forebrain, M = midbrain, H = hindbrain, UP = un-punctured, P = punctured, D = drained. Scale bars = 50μm.

some eCSF does leak out of the needle hole in our punctured embryos, we did not observe any difference in gross morphology or brain ventricle size compared to un-punctured embryos (Figure 3.1A-C). However, manual drainage from 22-36 hpf, reduces brain ventricle size compared to un-punctured and punctured (Figure 3.1D). Additionally, 55% of drained embryos had curved tails (n=60, p<.0001) compared to 4% in un-punctured (n=60), and 11% in punctured (n=62) embryos (Figure 3.1E) demonstrating that eCSF is necessary for proper elongation of the tail.

To determine whether eCSF is necessary for neuroepithelial cell proliferation we labeled dividing cells using phospho-histone H3 (PH3) and quantified the fraction of proliferating cells. Drained embryos did not exhibit a significant change in PH3 staining (n=15) compared to un-punctured (n=15) or punctured embryos (n=9) (Figure 3.1F-H, L), suggesting that eCSF is not required for proliferation at this developmental stage. Next, we asked whether eCSF was required for cell survival by marking cells undergoing apoptosis with TUNEL. We observed a five-fold increase in apoptosis in drained embryos (n=8) compared to un-punctured (n=9) and punctured brains (n=7) (Figure 3.1I-K, M) demonstrating that removal of eCSF, and not the insertion of the needle into the brain ventricles, leads to cell death. Interestingly, although apoptosis was observed sporadically throughout the whole neuroepithelium, we consistently noted two clusters of TUNEL positive cells localized basally within the diencephalon (Figure 3.1K, arrowheads).

Together, the data demonstrate that zebrafish eCSF is required for cell survival but not cell proliferation. Moreover, we have identified a population of diencephalic cells that are sensitive to removal of eCSF.

eCSF is not required for neurogenesis.

Neuroepithelial cells lining the apical (ventricular) surface are typically proliferating neural progenitors, while post-mitotic differentiated neurons line the basal surface of the neuroepithelium (Mueller and Wullimann, 2002a; Mueller and Wullimann, 2002b; Mueller and Wullimann, 2003) similar to the observed location of the dying cluster of cells. Therefore, we asked whether the dying cells were neurons. Neurogenesis in the whole embryo was assayed

by immunohistochemistry using the marker acetylated tubulin to label axon tracts. We did not observe any gross abnormalities in axonal projections (Figure 3.2A-C; un-punctured, n=10; punctured, n=14; drained, n=14). Similarly, using a NeuroD-GFP transgenic fish to label differentiating neurons (Ulitsky et al., 2011), we did not observe a difference in drained (n=11) embryos compared to un-punctured (n=9) or punctured brains (n=13) (Figure 3.2D-I) suggesting that during this time of development, eCSF does not grossly affect neurogenesis.

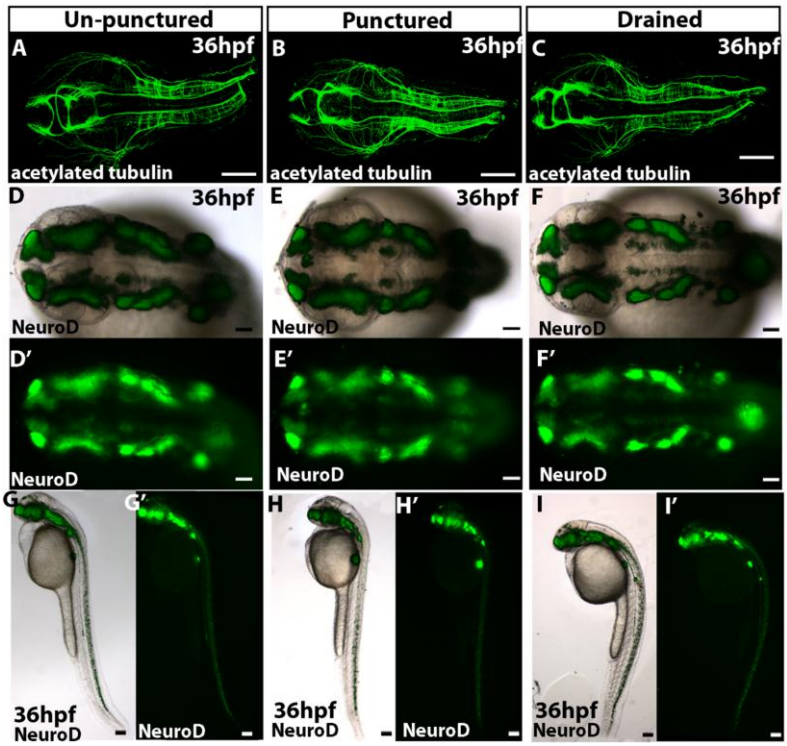

Figure 3.2: eCSF is not required for neurogenesis. (A-C) Acetylated tubulin and (D-I) NeuroD expression (NeuroD-GFP, green) in un-punctured (A,D,G), punctured (B,E,H) and drained (C,F,I). Scale bars = 50μm.

These assays, however, do not rule out the possibility that smaller populations of neurons could be affected by lack of eCSF but the effects are masked by an abundance of unaffected neurons. Therefore we asked whether dopaminergic and serotonergic neurons in the hypothalamus and posterior tuberculum, two ventral diencephalic structures, specifically require eCSF. There were no detectable differences in dopaminergic neurons (labeled with anti-tyrosine hydroxylase (TH)) or serotonergic neurons (labeled with anti-serotonin (5-HT)), in un-punctured (n=14), punctured (n=17) or drained embryos (n=17) suggesting that these neuronal populations are not sensitive to eCSF (Figure 3.3A-C). Additionally, we noticed that the clusters of dying diencephalic cells are more dorsal within the diencephalon than the hypothalamus and posterior tuberculum. From dorsal to ventral, the diencephalon gives rise to the habenula, thalamus (dorsal and ventral), posterior tuberculum, and hypothalamus (Wullimann and Rink, 2001). Therefore, we asked whether GABA (anti-GABA), a marker for the ventral thalamus, was abnormal in drained embryos and whether these cells co-localized with dying, TUNEL-positive

cells. We did not observe any difference in GABAergic neurons in drained (n=28) embryos compared to un-punctured (n=23) or punctured (n=25) (Figure 3.3D-F). Further we found that most TUNEL-positive cells in drained embryos did not co-localize with GABAergic neurons, and

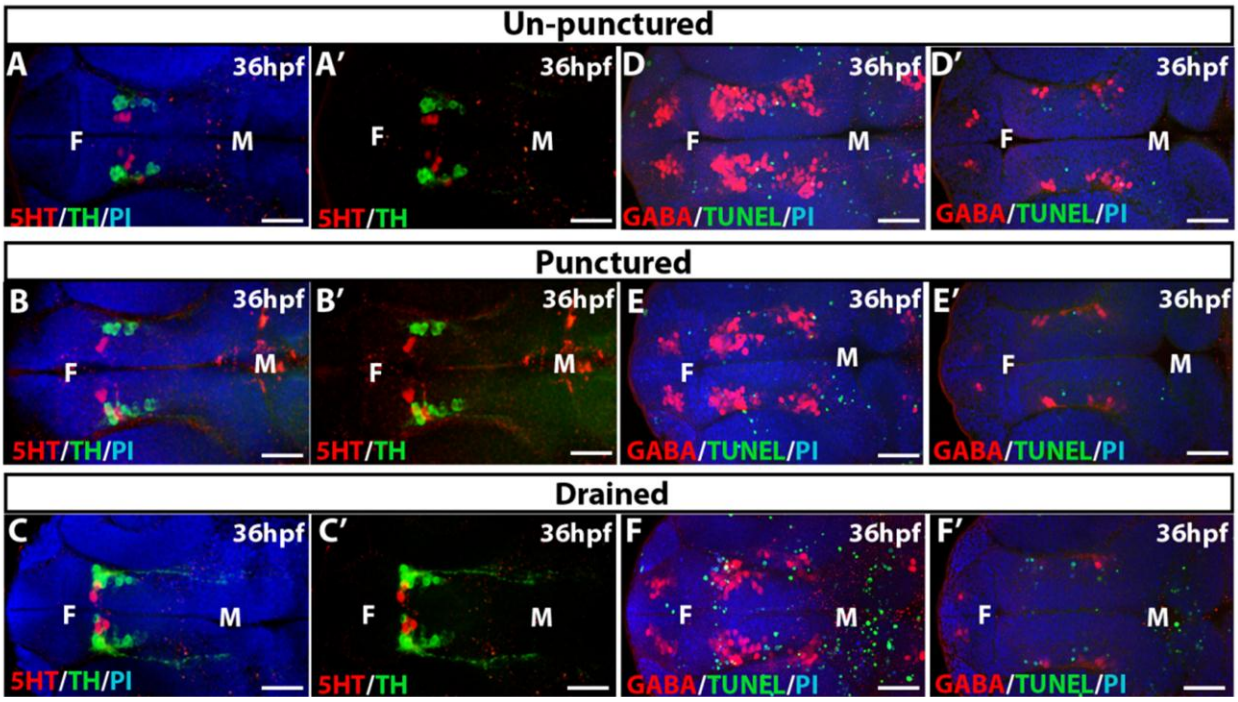

Figure 3.3: eCSF drainage does not disrupt dopaminergic, serotonergic or GABAergic neurons. (A-F) Dorsal projection of confocal stacks. Dopaminergic (tyrosine hydroxylase (TH), green) and serotonergic (5HT, red) neurons and propidum iodide (nuclei, blue, PI) (A'-C') 5HT and TH only. (D-F) GABA (red), TUNEL (green) and propidum iodide (blue). (D'-F') Single slice at dorsal/ventral level off dying cluster of cells. Un-punctured (A,D), punctured (B,E) and drained (C,F). F = forebrain, M = midbrain. Scale bars= 50μm.

these neurons slightly overlapped, but were mostly localized ventral to the dying cluster of cells (Figure 3.3D'-F'). This suggests that the diencephalic cluster of TUNEL-positive cells is likely localized within the dorsal thalamus or habenula and further experiments to identify these populations are underway.

eCSF promotes cell survival from 25-30 hpf.

To identify developmental periods that require eCSF to promote cell survival, we removed fluid for differing lengths of time. Embryos that were drained only once at 22 hpf (n=10), or twice from 22-24 hpf (n=8), and allowed to recover until 36 hpf, did not significantly differ in apoptosis compared to controls (Figure 3.4A-B; un-punctured (n=7), punctured 22 hpf (n=7) punctured 22-24 hpf (n=6)). Draining from 22-26 hpf with subsequent recovery until 36 hpf

(n=10), slightly increased apoptosis (Figure 3.4C; punctured 22-26 hpf (n=9)) whereas removal of eCSF from 22-28 (n=9) or 22-30 hpf (n=6) with recovery until 36 hpf, significantly increased levels of cell death compared to un-punctured (n=9) or punctured embryos (22-28 hpf (n=6), 22-30 hpf (n=5)) (Figure 3.4D-F, H-I). Furthermore, we observed a significant increase in cell death in embryos drained from 22-30 hpf (n=8) and immediately assayed at 30 hpf (Figure 3.4G, J; punctured (n=8), unpunctured (n=6)). This suggests that eCSF must be present from 25 hpf to 30 hpf to promote cell survival and that eCSF must be drained continuously from 22-30 hpf to induce cell death.

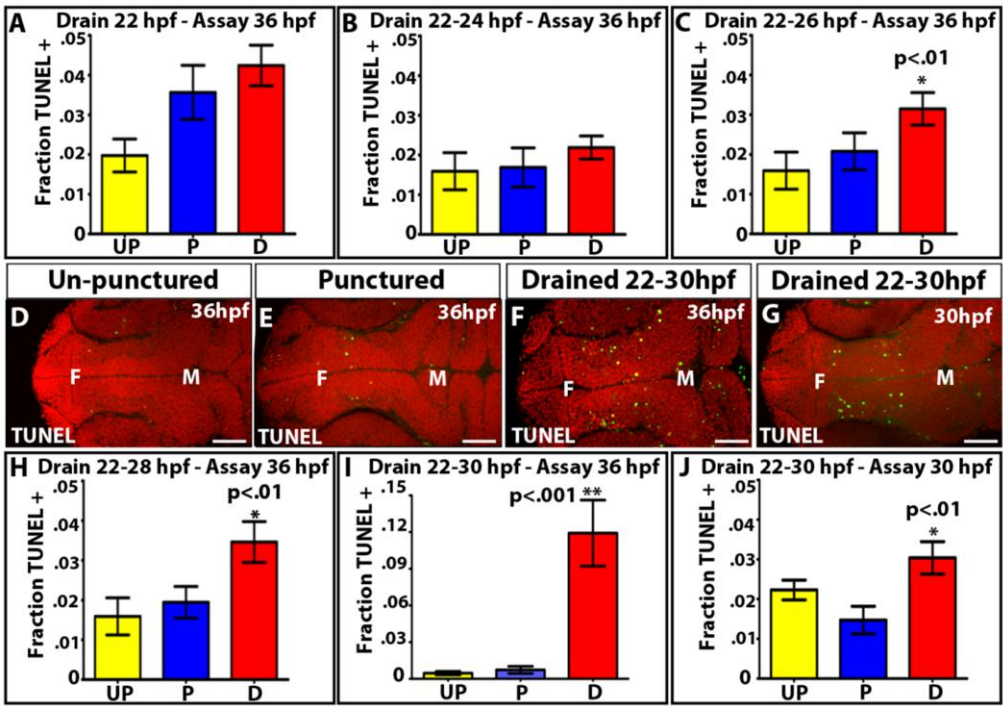

Figure 3.4: eCSF is required form 25-30 hpf. (A-C) Fraction of TUNEL + cells after drain at 22 hpf (A), 22-24 hpf (B) or 22-26 hpf (C). (D-G) Dorsal view of TUNEL (green) and propidium iodide (nuclei, red) in un-punctured (D), punctured (E), drain from 22-30 hpf, assay at 36 hpf (F), or from 22-30 hpf and assay at 30 hpf (G). Time of assay indicated. (H-J) Quantification of cell death after drain from 22-28 hpf (H) or 22-30 hpf assay at 36 hpf (I), or 22-30 hpf with assay at 30 hpf (J). Data represented as mean +/- SEM. F = forebrain, M = midbrain, UP = un-punctured, P = punctured, D = drained. Scale bars= 50μm.

Cell survival is not dependent on ionic concentration or hydrostatic pressure.

To identify potential eCSF candidate factors which promote cell survival of the embryonic brain, we asked whether factors could be reintroduced into the brain ventricles of drained embryos to rescue neuroepithelial cell death. To test this, we injected a cell permeable Caspase 3 inhibitor into the brain ventricles of un-punctured, punctured, or drained embryos (drained/punctured

from 22-36 hpf). From 30-36 hpf, all conditions were injected with either DMSO or the Caspase 3 inhibitor (Figure 3.5A). An increase in apoptosis was observed in drained embryos injected with DMSO (n=7) compared to un-punctured (n=7) or punctured brains (n=8) plus DMSO (Figure 3.5B-D,K). However, injection of the Caspase 3 inhibitor significantly reduced levels of cell death in drained embryos (n=9) (Figure 3.5E-G, K) demonstrating that injection of a factor into the brain ventricle can rescue neuroepithelial cell death. Interestingly injection of the Caspase 3 inhibitor increases cell death in un-punctured (n=9) and punctured embryos (n=8) suggesting it causes cell death. Thus, rescue of cell death in drained embryos is significant despite toxicity of the inhibitor.

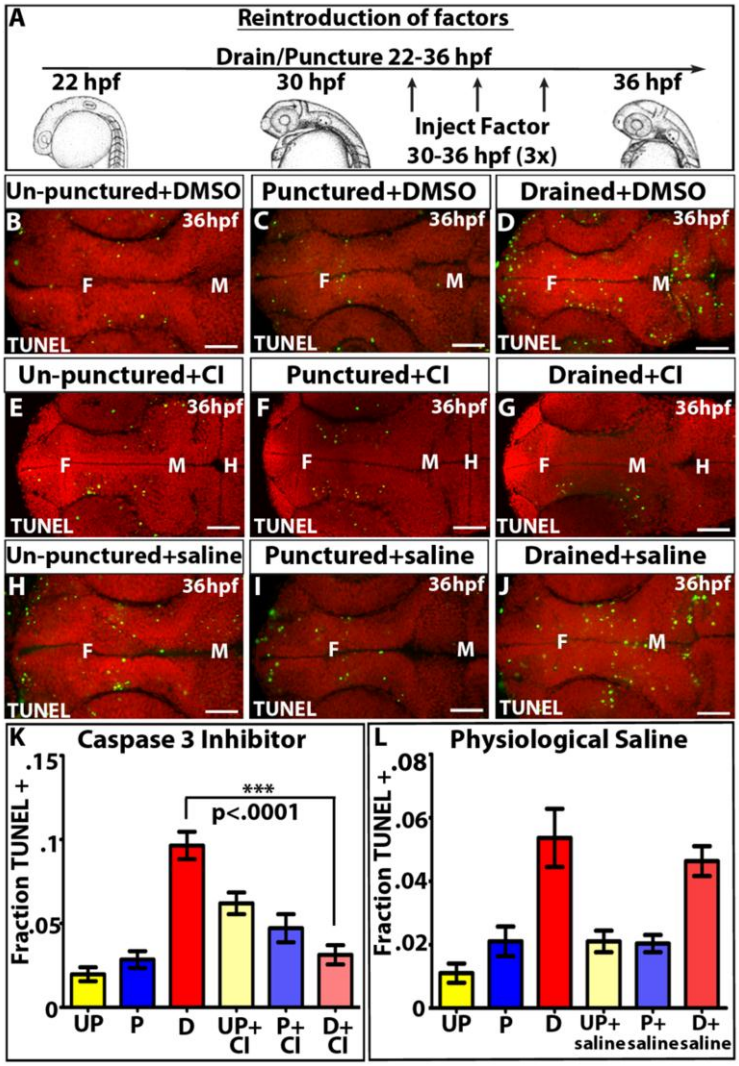

Figure 3.5: Neuroepithelial cell death can be rescued and is not pressure/ion dependent. (A) Experimental design. (B-J) Dorsal view of TUNEL (green) and propidium iodide (red) in un-punctured (B,E,H), punctured (C,F,I), or drained embryos (D,G,J) injected with DMSO (B-D), Caspase 3 inhibitor (E-G), or saline (H-J). (K-L) Quantification of cell death after Caspase 3 inhibitor (K), or saline treatments (K). Data represented as mean +/- SEM. F = forebrain, M= midbrain, H = hindbrain, UP = un-punctured, P = punctured, D = drained, CI = Caspase 3 inhibitor. Scale bars = 50μm.

The Desmond lab previously demonstrated that hydrostatic pressure generated by the eCSF can promote cell proliferation in chick embryos (Desmond and Jacobson, 1977; Desmond et al., 2005). To determine whether cell survival also requires proper ventricular pressure or is dependent on the ionic concentration within the eCSF, we asked whether injection of physiological saline could rescue neuroepithelial cell death. Embryos were manually drained or punctured from 22-36 hpf and

physiological saline was injected three times from 30-36 hpf making sure the brain ventricles were inflated to a size comparable levels to wild type (Figure 3.5A). We did not observe any change between embryos injected with saline and controls (Figure 3.5H-J,L; un-punctured (n=5), punctured (n=5), drained (n=6), un-punctured + saline (n=5), punctured + saline (n=8), drained + saline (n=7)) suggesting that pressure and ionic concentration are not sufficient to rescue cell survival. Therefore, eCSF must contain some small molecule or protein required for cell survival.

Retinoic acid but not IGF2 or FGF2 is required for neuroepithelial cell survival.

Studies in chick neuroepithelial explants and mouse embryos have previously identified insulin like growth factor 2 (IGF2), fibroblast growth factor 2 (FGF2) and retinoic acid (RA) as important components of the eCSF required for neurogenesis and cell proliferation (Alonso et al., 2011; Lehtinen et al., 2011; Martin et al., 2006; Mashayekhi et al., 2011; Salehi et al., 2009). Therefore, we asked whether injection of IGF2, FGF2, or RA into the brain ventricles could promote cell survival after eCSF drainage. Embryos were drained or punctured from 22-36 hpf and injected from 30-36 hpf, with DMSO, IGF2, FGF2 or RA (Figure 3.5A, Figure 3.6). Injection of IGF2 or FGF2 did not rescue neuroepithelial cell death in drained embryos compared to controls, demonstrating that IGF2 and FGF2 are not required within the eCSF to promote cell survival at this time of development (Figure 3.6A-I, M; un-punctured + DMSO (n=27), punctured + DMSO (n=23), drained + DMSO (n=25), un-punctured + IGF2 (n=17), punctured + IGF2 (n=15), drained + IGF2 (n=15), un-punctured + FGF2 (n=11), punctured + FGF2 (n=14), drained + FGF2 (n=13)). In contrast, injection of RA into the brain ventricles of drained embryos (n=16) rescued cell death compared to drained embryos injected with DMSO (n=19) (Figure 3.6J-L, N). Injection of RA reduced cell death to levels comparable to punctured or un-punctured embryos injected with either DMSO or RA (Figure 3.6N; un-punctured + DMSO (n=14), punctured + DMSO (n=15), un-punctured + RA (n=16), punctured + RA (n=18)). Exogenous RA injected into un-punctured or punctured embryos did not change cell death levels compared to DMSO injection demonstrating that RA does not generally block cell death (Figure 3.6 J-K, N). Interestingly, we found that neither IGF2 nor RA rescued the tail phenotype observed in drained embryos (Figure

3.6O, un-punctured =97% (n=40), punctured = 95% wild type (n=42), drained + DMSO = 47% wild type (n=40), drained + RA = 40% wild type (n=20), drained + IGF2 = 55% wild type (n=20)) suggesting a separate function of eCSF in the regulation of this phenotype.

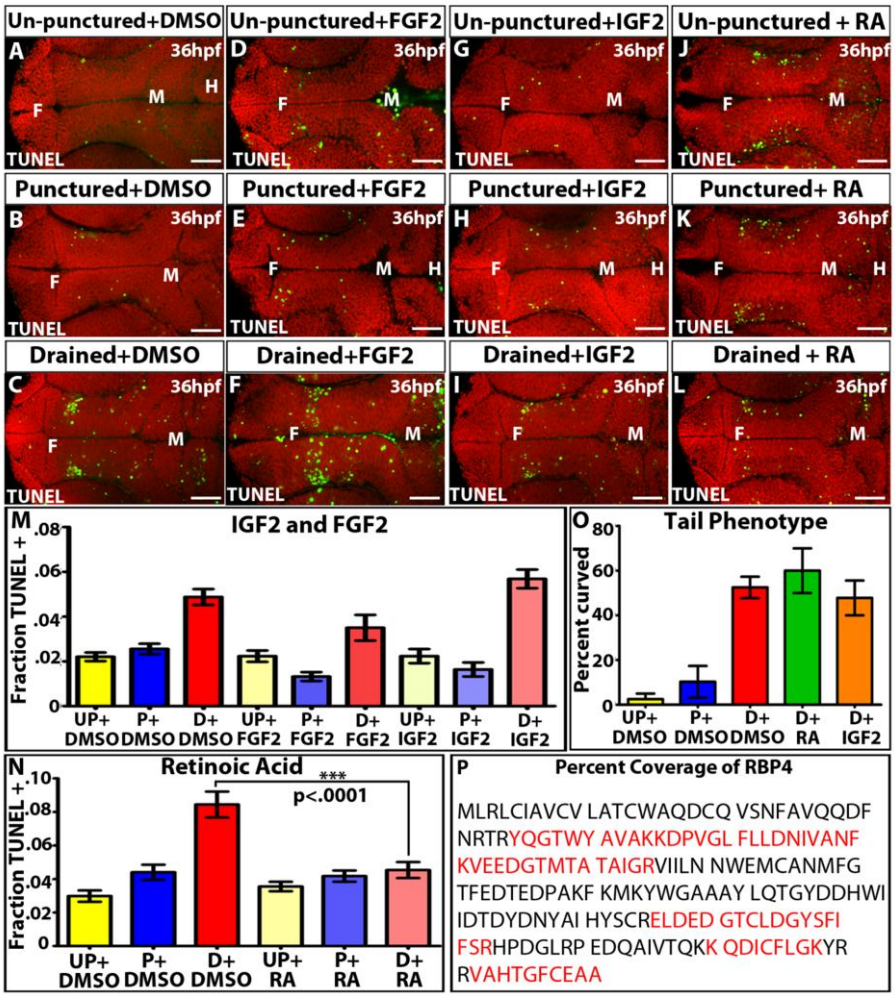

Figure 3.6: RA rescues neuroepithelial cell death. (A-I) Dorsal view of TUNEL (green) and propidum iodide (red) of un-punctured (A,D,G,J), punctured (B,E,H,K) or drained (C,F,I,L) embryos injected with DMSO (A-C), FGF2 (D-F), IGF2(G-I), or RA (J-L). (M-N) Quantification of cell death after FG2, IGF2 (M), or RA (N). (P) Quantification of curved tails of at least 20 embryos. (P) RBP4 sequence coverage from mass spectrometry. Data represented as mean +/- SEM. F = forebrain, M = midbrain, H = hindbrain, UP = un-punctured, P = punctured, D = drained. Scale bars = 50μm.

Furthermore, we performed mass spectrometry analysis of eCSF collected from 500 zebrafish embryos at 25-30 hpf. Collected fractions of eCSF were subjected to trypsin digestion and subsequent LC-MS/MS analysis. Tandem mass spectra were extracted by BioworksBrowser Version 3.3 (ThermoFisher) and submitted to the Mascot database search software version 2.2 (Matrix Science) to search the NCBInr_081410 database selected for *Danio rerio* proteins. We identified factors similar to those previously found in chick, mouse, rat and human. Factors identified included apolipoproteins, metabolic enzymes, and extracellular matrix components. Interestingly, we identified retinol binding protein 4 (Rbp4), a plasma protein which transports retinol, the precursor for RA with about 40% coverage (Figure 3.6P) supporting a role for RA during cell survival at this time during development.

Together, the data suggest that in zebrafish embryos prior to choroid plexus development, RA but not IGF2 or FGF2 is required for neuroepithelial cell survival.

Rbp4 and retinol are required for neuroepithelial cell survival.

To dissect the mechanism by which Rbp4 and RA promote cell survival, we asked whether components of RA signaling are required for cell survival. RT-PCR analysis showed *rbp4* expression from 3 hpf to 48 hpf in whole embryos (Figure 3.7A) confirming previous expression patterns (Li et al., 2007). Further, we found that *rbp4* was specifically expressed in the head tissue however, this includes the brain, eyes and all organs between the brain and yolk thus we cannot definitively conclude whether *rbp4* is expressed in the neuroepithelium (Figure 3.7B). Next, we asked whether Rbp4 is required for cell survival during embryonic brain development. To inhibit Rbp4, we used the A1120 inhibitor, which competes with retinol for binding to Rbp4 (Motani et al., 2009). A1120 was injected into the brain ventricles every two hours from 22-36 hpf. We

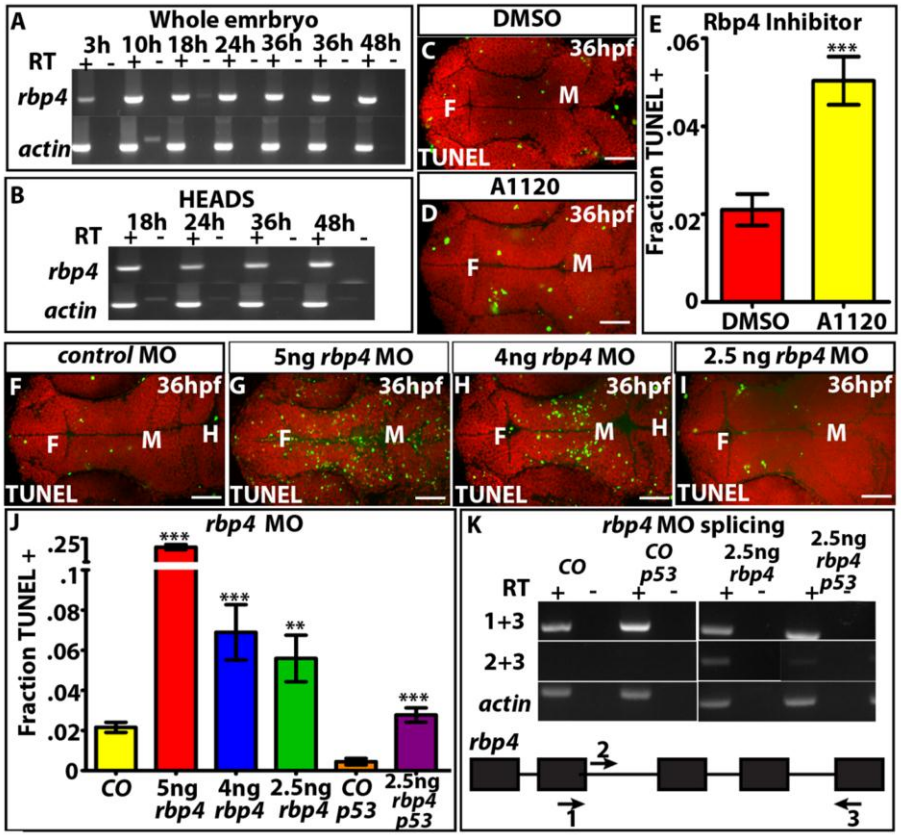

Figure 3.7: Rbp4 is required for cell survival. (A-B) RT-PCR in whole embryos (A) or heads (B) to detect *rbp4* expression. (C-E) Dorsal view of TUNEL (green) in A1120 treatment (D) vs. DMSO (C) and quantification of cell death (E). (F-J) Dorsal view of TUNEL (green) in control (CO; F) or *rbp4* MO at specific concentrations noted (G-I) with quantification of cell death (J). (K) RT-PCR analysis of splicing in *rbp4* MO. 1,2,3, and arrows indicate primers and direction. Data represented as mean+/- SEM. ***= p<.0001, **= p<.005 compared to control. Propidium iodide (nuclei) in red. F = forebrain, M = midbrain, H = hindbrain. Scale bars = 50μm.

observed a significant ($p<.0001$) increase in cell death compared to DMSO injected embryos (Figure 3.7C-E). To confirm this result, we knocked down *rbp4* expression in vivo using morpholinos (modified antisense oligonucleotides; MO), which targets the exon 2/intron 3 splice site of *rbp4* (Figure 3.7F-J) (Li et al., 2007). RT-PCR analysis identified that the *rbp4* MO causes an intron inclusion (Figure 3.7K). In *rbp4* loss-of-function embryos, we observed a significant dose-dependent increase in cell death (Figure 3.7F-J; control = 100% wild type (n=108), 5ng *rbp4* MO= 0% wild type (n=54), 4ng *rbp4* MO = 0% wild type (n=17), 2.5ng *rbp4* MO = 20% wild type (n=67)). *p53* MO is commonly co-injected with a target MO to prevent non-specific MO-mediated cell death and reveal the specific loss of function phenotype (Robu et al., 2007). Thus, co-injection of *p53* MO with *rbp4* MO reduced cell death, however, *rbp4* morphants still had significantly elevated levels of cell death compared to controls (Figure 3.7J orange vs. purple; *control + p53* = 100% wild type (n=116), 2.5ng *rbp4* MO + *p53* = 45% wild type (n=55)). Experiments are ongoing to further identify the specificity of the *rbp4* MO phenotype. Together, these data support the hypothesis that Rbp4 is required for neuroepithelial cell survival.

Next, we asked whether injection of exogenous human RBP4 and/or retinol (RE) into the brain ventricles was sufficient to prevent neuroepithelial cell death in drained embryos. Exogenous human RBP4, RE or a combination was injected every two hours from 30-36 hpf, into un-punctured, embryos or those that were punctured or drained from 22-36 hpf (Figure 3.5A). Injection of human RBP4, RE, or both RE and RBP4 did not significantly affect cell death in un-punctured or punctured embryos compared to DMSO treatment (Figure 3.8A-H, M; un-punctured + DMSO (n=10), punctured + DMSO (n=14), un-punctured + RE (n=18), punctured + RE (11), un-punctured + RBP4 (n=8), punctured + RBP4 (n=14), un-punctured + RBP4 + RE (n=12), punctured + RBP4 + RE (n=17)) while increased cell death was observed in drained embryos injected with DMSO (n=14) (Figure 3.8I, M). Drained embryos injected with RE alone slightly reduced levels of cell death relative to drained embryos injected with DMSO (Figure 3.8J, M, n=14, $p<.05$). In contrast, drained embryos injected with RBP4 alone did not affect cell death compared to the DMSO control (n=18, $p>.05$), suggesting that Rbp4 alone is not sufficient to produce RA at levels required for cell survival (Figure 3.8K, M). Critically, we found that the

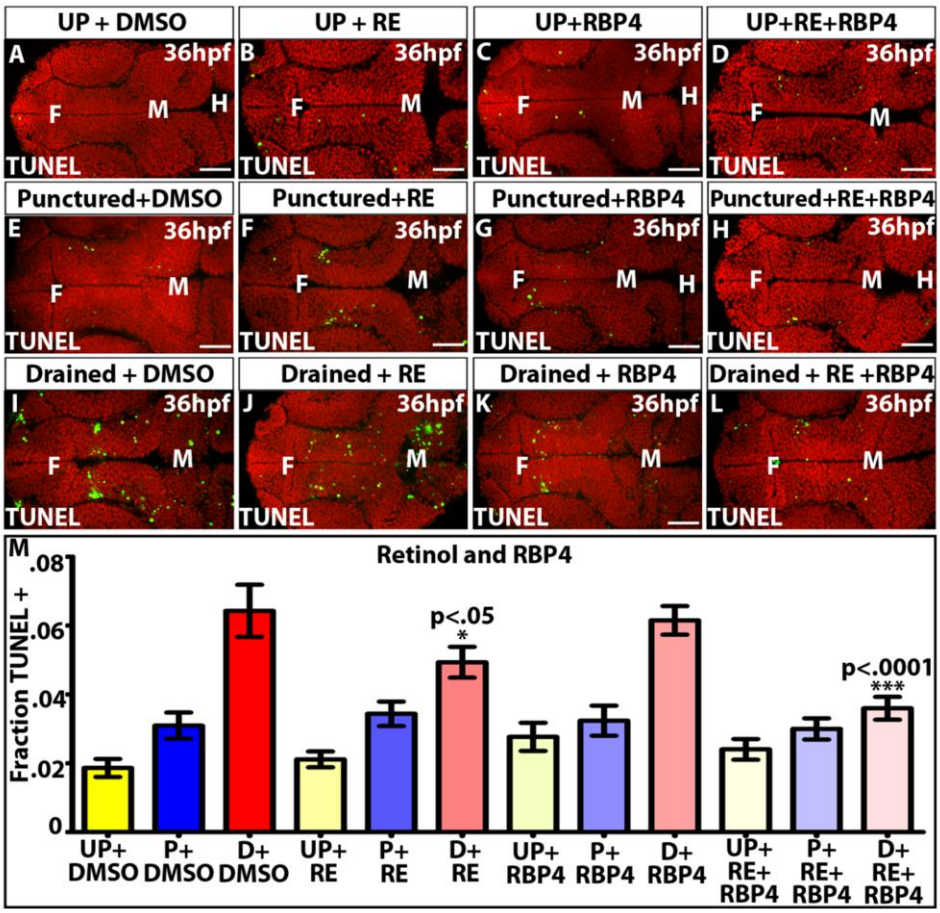

Figure 3.8: RBP4 and retinol can rescue neuroepithelial cell death. (A-L) Dorsal view of TUNEL (green) and propidium iodide (red) in un-punctured (UP; A-D), punctured (E-H) and drained (I-L) after injection of DMSO, (A,E,I), retinol (RE; B,F,J) RBP4 (C,G,K) or RE+RBP4 (D,H,L). (M) Quantification of cell death. Data represented as mean +/- SEM. F = forebrain, M = midbrain, H = hindbrain, UP= un-punctured, P = punctured, D = drained. Scale bars= 50μm.

combined injection of RBP4 and RE into drained embryos decreased cell death to levels comparable to punctured embryos treated with DMSO (Figure 3.8L, M, n=15, p<.0001). Together, the data suggest that RE, the precursor to RA, is required for neuroepithelial cell survival and Rbp4 likely promotes RE solubility within the eCSF to facilitate delivery to target cells. Furthermore, these data support the hypothesis that Rbp4 and RE within the eCSF are required for neuroepithelial cell survival.

RA synthesis is required for neuroepithelial cell survival.

Our data suggest that RE is delivered to the neuroepithelium via Rbp4 in the eCSF. Thus, we hypothesize that RE is converted to RA by neuroepithelial cells. To test this hypothesis, we asked whether inhibition of RA synthesis affects neuroepithelial cell survival. In order to test this hypothesis, we used two drugs, Citral and 4-Diethylaminobenzaldehyde (DEAB) to inhibit retinaldehyde dehydrogenase (RALDH), the enzyme necessary for converting retinaldehyde to RA (Marsh-Armstrong et al., 1994; Perz-Edwards et al., 2001). DMSO, DEAB or Citral were

injected into the wild-type brain ventricles every 2 hours from 22-36 hpf (Figure 3.9A-D). Injection of DEAB (Figure 3.9B) or Citral (Figure 3.9C) into the brain ventricles significantly increased neuroepithelial cell death (Figure 3.9D; n=11, n=9 respectively, p<.001) compared to DMSO treated embryos (Figure 3.9A; n=11). Thus, inhibiting the production of RA corresponds to an increase in cell death and suggests that RA synthesis is required for cell survival.

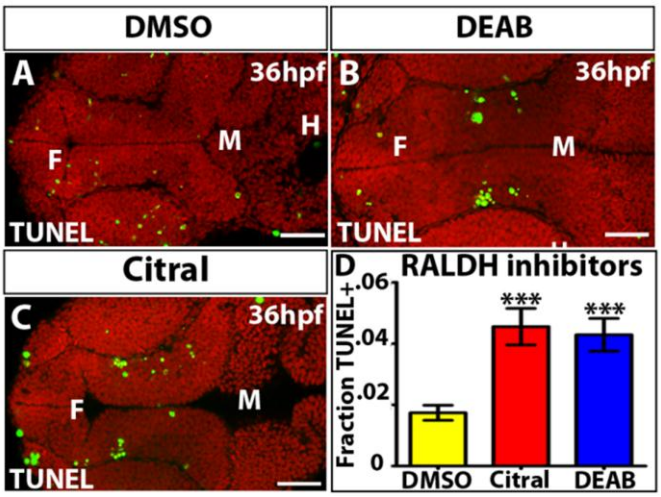

Figure 3.9: RA synthesis is required for cell survival. (A-C) Dorsal view of TUNEL (green) and propidium iodide after injection of DMSO (A), DEAB (B) or Citral (C). (D) Quantification of cell death. F = forebrain, M = midbrain. ***= p<.001. Scale bars = 50μm.

RA signaling via PPARγ receptors promotes neuroepithelial cell survival.

Previous work demonstrates that PPAR receptors activate cell proliferation and survival genes (Noy, 2010; Schug et al., 2007). Furthermore, in situ hybridization of PPARγ or PPARγ co-activator 1α (PGC-1α) showed that these genes are expressed specifically in diencephalic nuclei within the neuroepithelium (Thisse and Thisse, 2008). Thus we hypothesized that RA signals via PPARγ receptors to promote cell survival of the diencephalic cluster of cells. To test this hypothesis we asked whether inhibition of the PPARγ receptors increases cell death. We used two drugs, BADGE and GW9662, which specifically inhibit PPARγ receptors (Song et al., 2009; Tiefenbach et al., 2010). The drugs were injected into brain ventricles of wild-type embryos every two hours from 22-36 hpf. Injection of BADGE (n=9) or GW9662 (n=11) significantly increased levels of cell death compared to DMSO (n=14) injection (Figure 3.10A-C, J, p<.0001, p<.0005 respectively) suggesting that PPARγ signaling prevents neuroepithelial cell death.

Conversely, we asked whether a PPARγ agonist could rescue the increase in cell death observed in drained embryos. Embryos were punctured or drained from 22-36 hpf and the PPARγ agonist, Rosiglitazone (Tiefenbach et al., 2010), or DMSO was injected every 2 hours into the

brain ventricles from 30-36 hpf (Figure 3.5A, Figure 3.10D-I). We observed that un-punctured (n=10) and punctured (n=13) embryos injected with Rosiglitazone did not differ in levels of cell death compared to DMSO injected embryos (Figure 3.10 D-E, G-H, K; un-punctured+DMSO (n=9), punctured + DMSO (n=15)). However, drained embryos treated with Rosiglitazone had significantly rescued cell death (n=11, p<.0001) compared to DMSO treated embryos (n=13) (Figure 3.10 F,I,K).

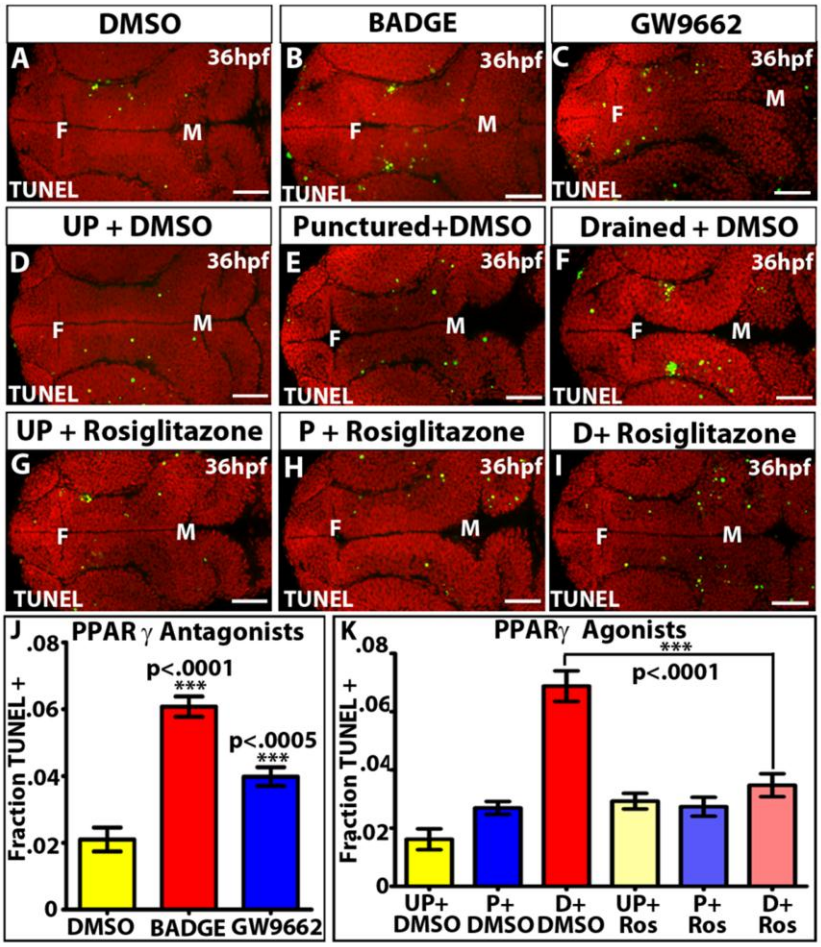

Figure 3.10: PPARγ signaling is required for cell survival. (A-C) Inhibition of PPARγ with BADGE (B) or GW9662 (C) compared to DMSO (A). (D-I) Injection of PPARγ agonist Rosiglitazone (Ros; G-I) vs. DMSO (D-F) in UP (D,G), P (E,H) and D (F,I). (J-K) Quantification cell death after PPARγ antagonists (J) or PPARγ agonist (K). Data represented as mean +/- SEM. F= Forebrain, M = midbrain, UP = un-punctured, P = punctured, D = drained. Scale bars= 50μm.

Together, the data suggest that RA signals via the PPARγ receptors to promote cell death in the diencephalic cells.

DISCUSSION

eCSF is required for RA synthesis and neuroepithelial cell survival.

Our data suggest a novel role for eCSF and RA signaling in embryonic neuroepithelial cell survival prior to choroid plexus development. Consistent with our study, experiments in chick embryos and human neural progenitor cell cultures demonstrate a requirement of eCSF during neuroepithelial cell survival (Buddensiek et al., 2009; Mashayekhi, 2008). Our data further

suggest that RA exerts its effect on cell survival through the activation of PPARγ receptors. Additionally, we identified two diencephalic populations of cells that are extremely sensitive to loss of eCSF. We propose that Rbp4 binds to retinols and transports them to the eCSF where retinol is metabolized into retinoic acid. Once metabolized, we propose that RA binds to PPARγ receptors and promotes transcription of cell survival genes (Figure 3.11).

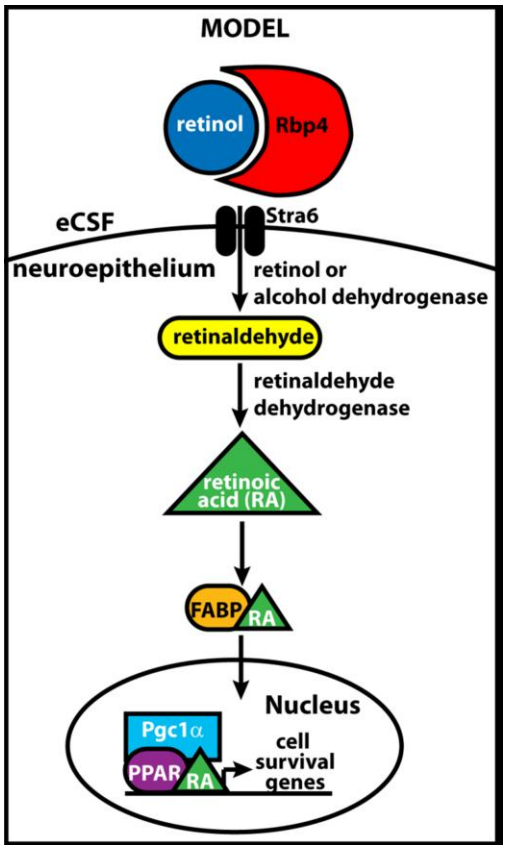

Figure 3.11: Mechanism of RA signaling during neuroepithelial cell survival. Rbp4 binds retinol in the CSF, is then taken up by the cell, oxidized into retinoic acid and bind to PPAR to promote transcription.

Generation of an eCSF depleted zebrafish embryo.

We describe a novel technique to study the role of eCSF during embryonic development and identified that draining the eCSF every 2 hours from 22-36 hpf increases cell death and results in a curved tail. This demonstrates that despite the continuous production of eCSF in between each drain, removal of the fluid every two hours sufficiently disrupts normal eCSF content and function. Further, we determined that exogenous RA or IGF2 does not rescue the curvature of the tail. Thus additional studies are required to identify the mechanism by which the presence or content of eCSF regulates tail elongation.

Role of IGF2 and FGF2 within the eCSF.

IGF2 and FGF2 were previously identified as important components of the eCSF required for proper cell proliferation and neurogenesis (Lehtinen et al., 2011; Martin et al., 2006; Mashayekhi et al., 2011; Salehi et al., 2009). These studies were all performed using eCSF produced after choroid plexus development. In contrast, we examined eCSF function prior to choroid plexus development and found that IGF2 and FGF2 do not promote neuroepithelial cell

survival in zebrafish embryos suggesting that IGF2 and FGF2 are not required for cell survival during this stage of development. Moreover, we did not observe any changes in cell proliferation or neurogenesis in drained embryos suggesting that either eCSF is not required for these processes at this stage, or eCSF produced between each drain is sufficient for cell division and neurogenesis, but not cell survival.

Given that eCSF composition changes throughout development (Cavanagh et al., 1983; Zappaterra et al., 2007), IGF2 or FGF2 may be required to promote cell division and neurogenesis later in zebrafish development. Indeed, Blum and Begemann investigated the role of RA during adult zebrafish tail regeneration. They show that RA promotes cell survival and cell proliferation and suggest that IGF, FGF, and canonical Wnt signaling are regulated by RA (Blum and Begemann, 2012). Therefore, we propose that RA signaling occurs early (22-30 hpf) to promote cell survival and induce IGF2 or FGF2 signaling to regulate cell proliferation and neurogenesis later in development.

Identifying the source of Rbp4 and RA synthesis.

Currently, we have not identified the source of Rbp4 within the eCSF. In humans, RBP4 is secreted by the liver and helps solubilize retinol in the plasma (Blomhoff et al., 1990). In zebrafish, Rbp4 is expressed at 24 hpf in the yolk syncytial layer, a transient extra-embryonic syncytial tissue (Li et al., 2007), however it is not known whether it is expressed at lower levels in the neuroepithelium. Because the yolk contains carotenoids and maternally-deposited retinaldehydes (Lampert et al., 2003) which can both be converted into retinol, it is possible that Rbp4 binds to retinol in the yolk, is transported to the eCSF and is the source of RA which activates PPAR induced transcription of cell survival genes. Experiments to test this hypothesis and to determine whether Rbp4 is expressed in the neuroepithelium are crucial to identifying the source of Rbp4.

Once Rbp4 and retinol arrive in the eCSF, which cells synthesize RA? STRA6 has previously been identified as the receptor that binds RBP4 and transports retinol into the cell (Figure 3.11) (Kawaguchi et al., 2007). However, it is not known whether there are other receptors that can also perform this function or whether retinol alone can enter certain cells. In zebrafish, *stra6* is

expressed in the pineal gland, a potential site of RA production (Isken et al., 2008). Additionally, many retinol, alcohol and retinaldehyde dehydrogenases are expressed in the brain and retina and could provide a source of RA. Therefore, it is likely that RA synthesizing cells are apically localized as they are in direct contact with the eCSF but it is also possible that Rbp4/retinol complex can diffuse between these cells. Indeed, Rbp4/retinol complex is only 21 KDa (Newcomer et al., 1984) and is below the size restriction of neuroepithelial cell junctions at this stage (Chapter 2) and thus may be able to freely diffuse deeper into the neuroepithelium.

Identifying the diencephalic cluster of eCSF and RA sensitive cells.

We are the first to describe specific regions of the neuroepithelium that are susceptible to the removal of eCSF. Here, we identified two clusters of diencephalic tissue that are sensitive to loss of eCSF and RA signaling. At this stage of development, the embryonic zebrafish diencephalon is composed of the habenulae, the most dorsal tissue, thalamus (dorsal and ventral), posterior tuberculum and hypothalamus (Wullimann and Rink, 2001). We have identified that the serotonergic, dopaminergic and GABAergic neurons of the posterior tuberculum, hypothalamus, and ventral thalamus are not disrupted by lack of eCSF. Additionally, the population of dying cells is more dorsal than the ventral thalamus neurons suggesting that these cells are part of the dorsal thalamus or habenula. Further investigation into the identity of these cells will include determining the requirement of eCSF for glutamatergic neuron, glycinergic neuron and glial cell differentiation or survival.

We propose that in order to prevent cell death, this diencephalic cluster of cells express both a FABP and PPARγ. Thus, once the RA signal reaches these cells, it is transported into the nucleus by FABP and promotes transcription activation of PPARγ targets and cell survival. In zebrafish, PPARγ and FABP3 are expressed throughout the embryonic brain, while FABP11 is localized in the diencephalic tissue between the eyes, the region where the population of dying cells is localized (Thisse and Thisse, 2008). In support of PPARγ promoting neuronal cell survival, studies in mice demonstrate that PPARγ is expressed in hypothalamic neurons and neuronal specific knock out of PPARγ, resulted in abnormal food intake, energy expenditure and insulin sensitivity (Lu et al., 2011; Sarruf et al., 2009). Additionally, several studies have demonstrated

a protective role for PPARγ in promoting recovery and preventing neuronal injury or death (Glatz et al., 2010; Zhao et al., 2009). Thus, PPARγ does act within the brain to promote neuronal survival and likely promotes neuroepithelial cell survival in embryonic zebrafish through regulation of energy metabolism. Experiments to validate this hypothesis are necessary to provide a connection between RA signaling, energy metabolism, and cell survival.

Interestingly, in zebrafish, PGC-1α, a co-activator of PPARγ (Figure 3.11), is expressed in two diencephalic nuclei of similar size and location to the dying cluster of cells in drained embryos (Thisse and Thisse, 2008). Therefore, the presence of PGC-1α may increase the sensitivity of these cells to the presence of RA whereas other neuroepithelial cells which lack PGC-1α are more resistant. Thus, the spatially restricted expression of PGC-1α, may lead to heightened activation of target genes in the diencephalic cluster of cells in response to RA.

Altered eCSF composition and RA signaling in nervous system disorders

eCSF composition changes throughout development and is different within each brain ventricle (Cavanagh et al., 1983). Abnormal CSF content is also associated with hydrocephalus, amyotrophic lateral sclerosis (ALS), and neurodegenerative disorders (Johanson et al., 2004; Mashayekhi et al., 2002; Mashayekhi and Salehi, 2006a; Parada et al., 2005a; Pratico et al., 2004; Shuvaev et al., 2001). Furthermore, several lines of evidence suggest that levels of RBP and RA signaling are disrupted in neurodegenerative diseases (Corcoran et al., 2002; Maury and Teppo, 1987). These data suggest that CSF and RA signaling play a crucial role not only during embryonic development but also into adulthood. Therefore, determining the role of eCSF and its contribution to RA synthesis and signaling will prove to be an interesting avenue to pursue in understanding embryonic development and diseases of the nervous system.

ACKNOWLEDGEMENTS

This work was supported by the National Institute for Mental Health, and National Science Foundation. Special thanks to Dr. Jen Gutzman, Dr. Amanda Dickinson and other Sive lab members for many useful discussions and constructive criticism, Dr. Joey Davis for excellent comments on the manuscript, Ioannis Papayannopolous (Koch Institute Biopolymers and

Proteomics) and Eric Spooner for help with mass spectrometry and analysis, and to Olivier Paugois for expert fish husbandry.

REFERENCES

Alonso, M. I., Gato, A., Moro, J. A., Barbosa, E., 1998. Disruption of proteoglycans in neural tube fluid by beta-D-xyloside alters brain enlargement in chick embryos. Anat Rec. 252**,** 499-508.

Alonso, M. I., Gato, A., Moro, J. A., Martin, P., Barbosa, E., 1999. Involvement of sulfated proteoglycans in embryonic brain expansion at earliest stages of development in rat embryos. Cells Tissues Organs. 165**,** 1-9.

Alonso, M. I., Martin, C., Carnicero, E., Bueno, D., Gato, A., 2011. Cerebrospinal fluid control of neurogenesis induced by retinoic acid during early brain development. Dev Dyn. 240**,** 1650-9.

Blomhoff, R., Green, M. H., Berg, T., Norum, K. R., 1990. Transport and storage of vitamin A. Science. 250**,** 399-404.

Blum, N., Begemann, G., 2012. Retinoic acid signaling controls the formation, proliferation and survival of the blastema during adult zebrafish fin regeneration. Development. 139**,** 107-16.

Bonnet, E., Touyarot, K., Alfos, S., Pallet, V., Higueret, P., Abrous, D. N., 2008. Retinoic acid restores adult hippocampal neurogenesis and reverses spatial memory deficit in vitamin A deprived rats. PLoS One. 3**,** e3487.

Brown, P. D., Davies, S. L., Speake, T., Millar, I. D., 2004. Molecular mechanisms of cerebrospinal fluid production. Neuroscience. 129**,** 957-70.

Buddensiek, J., Dressel, A., Kowalski, M., Storch, A., Sabolek, M., 2009. Adult cerebrospinal fluid inhibits neurogenesis but facilitates gliogenesis from fetal rat neural stem cells. J Neurosci Res. 87**,** 3054-66.

Budhu, A. S., Noy, N., 2002. Direct channeling of retinoic acid between cellular retinoic acid-binding protein II and retinoic acid receptor sensitizes mammary carcinoma cells to retinoic acid-induced growth arrest. Mol Cell Biol. 22**,** 2632-41.

Cavanagh, M. E., Cornelis, M. E., Dziegielewska, K. M., Evans, C. A., Lorscheider, F. L., Mollgard, K., Reynolds, M. L., Saunders, N. R., 1983. Comparison of proteins in CSF of lateral and IVth ventricles during early development of fetal sheep. Brain Res. 313**,** 159-67.

Chodobski, A., Szmydynger-Chodobska, J., 2001. Choroid plexus: target for polypeptides and site of their synthesis. Microsc Res Tech. 52**,** 65-82.

Corcoran, J., So, P. L., Maden, M., 2002. Absence of retinoids can induce motoneuron disease in the adult rat and a retinoid defect is present in motoneuron disease patients. Journal of Cell Science. 115**,** 4735-4741.

Desmond, M. E., Jacobson, A. G., 1977. Embryonic brain enlargement requires cerebrospinal fluid pressure. Dev Biol. 57**,** 188-98.

Desmond, M. E., Levitan, M. L., Haas, A. R., 2005. Internal luminal pressure during early chick embryonic brain growth: descriptive and empirical observations. Anat Rec A Discov Mol Cell Evol Biol. 285**,** 737-47.

Di-Poi, N., Tan, N. S., Michalik, L., Wahli, W., Desvergne, B., 2002. Antiapoptotic role of PPARbeta in keratinocytes via transcriptional control of the Akt1 signaling pathway. Mol Cell. 10**,** 721-33.

Duester, G., 1998. Alcohol dehydrogenase as a critical mediator of retinoic acid synthesis from vitamin A in the mouse embryo. J Nutr. 128**,** 459S-462S.

Gato, A., Martin, P., Alonso, M. I., Martin, C., Pulgar, M. A., Moro, J. A., 2004. Analysis of cerebro-spinal fluid protein composition in early developmental stages in chick embryos. J Exp Zool A Comp Exp Biol. 301**,** 280-9.

Gato, A., Moro, J. A., Alonso, M. I., Bueno, D., De La Mano, A., Martin, C., 2005. Embryonic cerebrospinal fluid regulates neuroepithelial survival, proliferation, and neurogenesis in chick embryos. Anat Rec A Discov Mol Cell Evol Biol. 284**,** 475-84.

Glatz, T., Stock, I., Nguyen-Ngoc, M., Gohlke, P., Herdegen, T., Culman, J., Zhao, Y., 2010. Peroxisome-proliferator-activated receptors gamma and peroxisome-proliferator-activated receptors beta/delta and the regulation of interleukin 1 receptor antagonist expression by pioglitazone in ischaemic brain. J Hypertens. 28**,** 1488-97.

Goodman, A. B., 1998. Three independent lines of evidence suggest retinoids as causal to schizophrenia. Proc Natl Acad Sci U S A. 95**,** 7240-4.

Gutzman, J. H., Sive, H., 2009. Zebrafish brain ventricle injection. J Vis Exp.

Hagglund, M., Berghard, A., Strotmann, J., Bohm, S., 2006. Retinoic acid receptor-dependent survival of olfactory sensory neurons in postnatal and adult mice. J Neurosci. 26**,** 3281-91.

Isken, A., Golczak, M., Oberhauser, V., Hunzelmann, S., Driever, W., Imanishi, Y., Palczewski, K., von Lintig, J., 2008. RBP4 disrupts vitamin A uptake homeostasis in a STRA6-deficient animal model for Matthew-Wood syndrome. Cell Metab. 7**,** 258-68.

Jacobs, S., Lie, D. C., DeCicco, K. L., Shi, Y., DeLuca, L. M., Gage, F. H., Evans, R. M., 2006. Retinoic acid is required early during adult neurogenesis in the dentate gyrus. Proc Natl Acad Sci U S A. 103**,** 3902-7.

Johanson, C., McMillan, P., Tavares, R., Spangenberger, A., Duncan, J., Silverberg, G., Stopa, E., 2004. Homeostatic capabilities of the choroid plexus epithelium in Alzheimer's disease. Cerebrospinal Fluid Res. 1**,** 3.

Johanson, C. E., Stopa, E. G., McMillan, P. N., 2011. The blood-cerebrospinal fluid barrier: structure and functional significance. Methods Mol Biol. 686**,** 101-31.

Kawaguchi, R., Yu, J., Honda, J., Hu, J., Whitelegge, J., Ping, P., Wiita, P., Bok, D., Sun, H., 2007. A membrane receptor for retinol binding protein mediates cellular uptake of vitamin A. Science. 315**,** 820-5.

Kimmel, C. B., Ballard, W. W., Kimmel, S. R., Ullmann, B., Schilling, T. F., 1995. Stages of embryonic development of the zebrafish. Dev Dyn. 203**,** 253-310.

Lampert, J. M., Holzschuh, J., Hessel, S., Driever, W., Vogt, K., von Lintig, J., 2003. Provitamin A conversion to retinal via the beta,beta-carotene-15,15'-oxygenase (bcox) is essential for pattern formation and differentiation during zebrafish embryogenesis. Development. 130**,** 2173-86.

Lehtinen, M. K., Zappaterra, M. W., Chen, X., Yang, Y. J., Hill, A. D., Lun, M., Maynard, T., Gonzalez, D., Kim, S., Ye, P., D'Ercole, A. J., Wong, E. T., LaMantia, A. S., Walsh, C. A.,

2011. The cerebrospinal fluid provides a proliferative niche for neural progenitor cells. Neuron. 69**,** 893-905.

Li, Z., Korzh, V., Gong, Z., 2007. Localized rbp4 expression in the yolk syncytial layer plays a role in yolk cell extension and early liver development. BMC Dev Biol. 7**,** 117.

Lu, M., Sarruf, D. A., Talukdar, S., Sharma, S., Li, P., Bandyopadhyay, G., Nalbandian, S., Fan, W., Gayen, J. R., Mahata, S. K., Webster, N. J., Schwartz, M. W., Olefsky, J. M., 2011. Brain PPAR-gamma promotes obesity and is required for the insulin-sensitizing effect of thiazolidinediones. Nat Med. 17**,** 618-22.

Maden, M., 2007. Retinoic acid in the development, regeneration and maintenance of the nervous system. Nat Rev Neurosci. 8**,** 755-65.

Marsh-Armstrong, N., McCaffery, P., Gilbert, W., Dowling, J. E., Drager, U. C., 1994. Retinoic acid is necessary for development of the ventral retina in zebrafish. Proc Natl Acad Sci U S A. 91**,** 7286-90.

Martin, C., Alonso, M. I., Santiago, C., Moro, J. A., De la Mano, A., Carretero, R., Gato, A., 2009. Early embryonic brain development in rats requires the trophic influence of cerebrospinal fluid. Int J Dev Neurosci. 27**,** 733-40.

Martin, C., Bueno, D., Alonso, M. I., Moro, J. A., Callejo, S., Parada, C., Martin, P., Carnicero, E., Gato, A., 2006. FGF2 plays a key role in embryonic cerebrospinal fluid trophic properties over chick embryo neuroepithelial stem cells. Dev Biol. 297**,** 402-16.

Mashayekhi, F., 2008. Neural cell death is induced by neutralizing antibody to nerve growth factor: an in vivo study. Brain Dev. 30**,** 112-7.

Mashayekhi, F., Bannister, C. M., Miyan, J. A., 2001. Failure in cell proliferation in the germinal epithelium of the HTx rats. Eur J Pediatr Surg. 11 Suppl 1**,** S57-9.

Mashayekhi, F., Draper, C. E., Bannister, C. M., Pourghasem, M., Owen-Lynch, P. J., Miyan, J. A., 2002. Deficient cortical development in the hydrocephalic Texas (H-Tx) rat: a role for CSF. Brain. 125**,** 1859-74.

Mashayekhi, F., Sadeghi, M., Rajaei, F., 2011. Induction of perlecan expression and neural cell proliferation by fgf-2 in the developing cerebral cortex: an in vivo study. J Mol Neurosci. 45**,** 87-93.

Mashayekhi, F., Salehi, Z., 2006a. Cerebrospinal fluid nerve growth factor levels in patients with Alzheimer's disease. Ann Saudi Med. 26**,** 278-82.

Mashayekhi, F., Salehi, Z., 2006b. The importance of cerebrospinal fluid on neural cell proliferation in developing chick cerebral cortex. Eur J Neurol. 13**,** 266-72.

Maury, C. P., Teppo, A. M., 1987. Immunodetection of protein composition in cerebral amyloid extracts in Alzheimer's disease: enrichment of retinol-binding protein. J Neurol Sci. 80**,** 221-8.

Miyan, J. A., Zendah, M., Mashayekhi, F., Owen-Lynch, P. J., 2006. Cerebrospinal fluid supports viability and proliferation of cortical cells in vitro, mirroring in vivo development. Cerebrospinal Fluid Res. 3**,** 2.

Motani, A., Wang, Z., Conn, M., Siegler, K., Zhang, Y., Liu, Q., Johnstone, S., Xu, H., Thibault, S., Wang, Y., Fan, P., Connors, R., Le, H., Xu, G., Walker, N., Shan, B., Coward, P., 2009. Identification and characterization of a non-retinoid ligand for retinol-binding protein 4 which lowers serum retinol-binding protein 4 levels in vivo. J Biol Chem. 284**,** 7673-80.

Mueller, T., Wullimann, M. F., 2002a. BrdU-, neuroD (nrd)- and Hu-studies reveal unusual non-ventricular neurogenesis in the postembryonic zebrafish forebrain. Mech Dev. 117**,** 123-35.

Mueller, T., Wullimann, M. F., 2002b. Expression domains of neuroD (nrd) in the early postembryonic zebrafish brain. Brain Research Bulletin. 57**,** 377-9.

Mueller, T., Wullimann, M. F., 2003. Anatomy of neurogenesis in the early zebrafish brain. Brain Res Dev Brain Res. 140**,** 137-55.

Nasevicius, A., Ekker, S. C., 2000. Effective targeted gene 'knockdown' in zebrafish. Nat Genet. 26**,** 216-20.

Newcomer, M. E., Jones, T. A., Aqvist, J., Sundelin, J., Eriksson, U., Rask, L., Peterson, P. A., 1984. The three-dimensional structure of retinol-binding protein. EMBO J. 3**,** 1451-4.

Noy, N., 2010. Between death and survival: retinoic acid in regulation of apoptosis. Annu Rev Nutr. 30**,** 201-17.

Parada, C., Escola-Gil, J. C., Bueno, D., 2008a. Low-density lipoproteins from embryonic cerebrospinal fluid are required for neural differentiation. J Neurosci Res. 86**,** 2674-84.

Parada, C., Gato, A., Aparicio, M., Bueno, D., 2006. Proteome analysis of chick embryonic cerebrospinal fluid. Proteomics. 6**,** 312-20.

Parada, C., Gato, A., Bueno, D., 2005a. Mammalian embryonic cerebrospinal fluid proteome has greater apolipoprotein and enzyme pattern complexity than the avian proteome. J Proteome Res. 4**,** 2420-8.

Parada, C., Gato, A., Bueno, D., 2008b. All-trans retinol and retinol-binding protein from embryonic cerebrospinal fluid exhibit dynamic behaviour during early central nervous system development. Neuroreport. 19**,** 945-50.

Parada, C., Martin, C., Alonso, M. I., Moro, J. A., Bueno, D., Gato, A., 2005b. Embryonic cerebrospinal fluid collaborates with the isthmic organizer to regulate mesencephalic gene expression. J Neurosci Res. 82**,** 333-45.

Perz-Edwards, A., Hardison, N. L., Linney, E., 2001. Retinoic acid-mediated gene expression in transgenic reporter zebrafish. Dev Biol. 229**,** 89-101.

Pollay, M., Curl, F., 1967. Secretion of cerebrospinal fluid by the ventricular ependyma of the rabbit. Am J Physiol. 213**,** 1031-8.

Praetorius, J., 2007. Water and solute secretion by the choroid plexus. Pflugers Arch. 454**,** 1-18.

Pratico, D., Yao, Y., Rokach, J., Mayo, M., Silverberg, G. G., McGuire, D., 2004. Reduction of brain lipid peroxidation by CSF drainage in Alzheimer's disease patients. J Alzheimers Dis. 6**,** 385-9; discussion 443-9.

Redzic, Z. B., Preston, J. E., Duncan, J. A., Chodobski, A., Szmydynger-Chodobska, J., 2005. The choroid plexus-cerebrospinal fluid system: from development to aging. Curr Top Dev Biol. 71**,** 1-52.

Robu, M. E., Larson, J. D., Nasevicius, A., Beiraghi, S., Brenner, C., Farber, S. A., Ekker, S. C., 2007. p53 Activation by Knockdown Technologies. PLoS Genet. 3**,** e78.

Salehi, Z., Mashayekhi, F., 2006. The role of cerebrospinal fluid on neural cell survival in the developing chick cerebral cortex: an in vivo study. Eur J Neurol. 13**,** 760-4.

Salehi, Z., Mashayekhi, F., Naji, M., Pandamooz, S., 2009. Insulin-like growth factor-1 and insulin-like growth factor binding proteins in cerebrospinal fluid during the development of mouse embryos. J Clin Neurosci. 16**,** 950-3.

Sarruf, D. A., Yu, F., Nguyen, H. T., Williams, D. L., Printz, R. L., Niswender, K. D., Schwartz, M. W., 2009. Expression of peroxisome proliferator-activated receptor-gamma in key neuronal subsets regulating glucose metabolism and energy homeostasis. Endocrinology. 150**,** 707-12.

Schug, T. T., Berry, D. C., Shaw, N. S., Travis, S. N., Noy, N., 2007. Opposing effects of retinoic acid on cell growth result from alternate activation of two different nuclear receptors. Cell. 129**,** 723-33.

Shevchenko, A., Tomas, H., Havlis, J., Olsen, J. V., Mann, M., 2007. In-gel digestion for mass spectrometric characterization of proteins and proteomes. Nat. Protocols. 1**,** 2856-2860.

Shuvaev, V. V., Laffont, I., Serot, J. M., Fujii, J., Taniguchi, N., Siest, G., 2001. Increased protein glycation in cerebrospinal fluid of Alzheimer's disease. Neurobiol Aging. 22**,** 397-402.

Song, Y., Selak, M. A., Watson, C. T., Coutts, C., Scherer, P. C., Panzer, J. A., Gibbs, S., Scott, M. O., Willer, G., Gregg, R. G., Ali, D. W., Bennett, M. J., Balice-Gordon, R. J., 2009. Mechanisms underlying metabolic and neural defects in zebrafish and human multiple acyl-CoA dehydrogenase deficiency (MADD). PLoS One. 4**,** e8329.

Speake, T., Whitwell, C., Kajita, H., Majid, A., Brown, P. D., 2001. Mechanisms of CSF secretion by the choroid plexus. Microsc Res Tech. 52**,** 49-59.

Thisse, C., Thisse, B., 2008. Expression from: Unexpected Novel Relational Links Uncovered by Extensive Developmental Profiling of Nuclear Receptor Expression.

Tiefenbach, J., Moll, P. R., Nelson, M. R., Hu, C., Baev, L., Kislinger, T., Krause, H. M., 2010. A live zebrafish-based screening system for human nuclear receptor ligand and cofactor discovery. PLoS One. 5**,** e9797.

Ulitsky, I., Shkumatava, A., Jan, C. H., Sive, H., Bartel, D. P., 2011. Conserved function of lincRNAs in vertebrate embryonic development despite rapid sequence evolution. Cell. 147**,** 1537-50.

Welss, P., 1934. Secretory activity of the inner layer of the embryonic mid-brain of the chick, as revealed by tissue culture. The Anatomical Record. 58**,** 299-302.

Westerfield, M., Sprague, J., Doerry, E., Douglas, S., Grp, Z., 2001. The Zebrafish Information Network (ZFIN): a resource for genetic, genomic and developmental research. Nucleic Acids Research. 29**,** 87-90.

Wullimann, M. F., Rink, E., 2001. Detailed immunohistology of Pax6 protein and tyrosine hydroxylase in the early zebrafish brain suggests role of Pax6 gene in development of dopaminergic diencephalic neurons. Brain Res Dev Brain Res. 131**,** 173-91.

Wysowski, D. K., Pitts, M., Beitz, J., 2001a. An analysis of reports of depression and suicide in patients treated with isotretinoin. J Am Acad Dermatol. 45**,** 515-9.

Wysowski, D. K., Pitts, M., Beitz, J., 2001b. Depression and suicide in patients treated with isotretinoin. N Engl J Med. 344**,** 460.

Zappaterra, M. D., Lisgo, S. N., Lindsay, S., Gygi, S. P., Walsh, C. A., Ballif, B. A., 2007. A comparative proteomic analysis of human and rat embryonic cerebrospinal fluid. J Proteome Res. 6**,** 3537-48.

Zhao, X., Strong, R., Zhang, J., Sun, G., Tsien, J. Z., Cui, Z., Grotta, J. C., Aronowski, J., 2009. Neuronal PPARgamma deficiency increases susceptibility to brain damage after cerebral ischemia. J Neurosci. 29**,** 6186-95.

Zheng, W., Chodobski, A., . 2005. The blood-cerebrospinal fluid barrier. Taylor and Francis, Boca Raton Fl.

CHAPTER FOUR

Embryonic zebrafish cerebrospinal fluid circulation in wild type and hydrocephalic models

Contributions: I supervised a summer undergraduate researcher, Nicole Ann Aponte-Santiago, who performed all injections and together we imaged CSF flow. Dr. Alicia Blaker-Lee contributed ventricle injection images of *gdpd3* gain of function morphants and analysis of morpholino splicing defects.

ABSTRACT

The cerebrospinal fluid (CSF) is a protein rich fluid contained within the brain ventricles, which, in adult humans, has a directional flow. Here, we demonstrate a new technique to directly visualize CSF movement using a photoconvertible protein, Kaede. We specifically labeled an area of CSF by photoactivating Kaede and subsequently followed the converted protein within the embryonic zebrafish brain ventricles. We found that zebrafish embryonic CSF moved freely between the midbrain and forebrain but not between the midbrain and hindbrain, and was separated by the midbrain-hindbrain boundary which acted as a physical barrier. After the heartbeat starts, CSF flow changed slightly and increased mixing between the midbrain and hindbrain ventricles. Surprisingly, CSF flow increased in one zebrafish model of hydrocephalus, while another, had no change in CSF flow. Together, these data demonstrate the importance of CSF flow during development and further suggest that disruption of CSF production, flow or retention can all result in hydrocephalus.

INTRODUCTION

Cerebrospinal fluid (CSF) volume and pressure are maintained by finely balancing CSF production, circulation and drainage. In humans CSF production occurs at a rate of 0.4 ml/min/g (May et al., 1990; Silverberg et al., 2001) and CSF is turned over 3-4 times a day. Flow in mouse, the smallest animal in which CSF flow rate has been examined, is 3.3 $x10^{-4}$ ml/min (Rudick, 1982). Adult human CSF flows from the lateral ventricles (forebrain), to the third ventricle, through the cerebral aqueduct (midbrain), into the 4th ventricle (hindbrain) and finally to the spinal cord and subdural spaces (Czosnyka et al., 2004). CSF flow is important for circulation of waste, metabolites and signaling molecules and for maintenance of CSF volume and pressure. Studies in adult mice demonstrate that CSF flow is also responsible for proper olfactory bulb neuron migration by setting up concentration gradients of a guidance cue (Sawamoto et al., 2006).

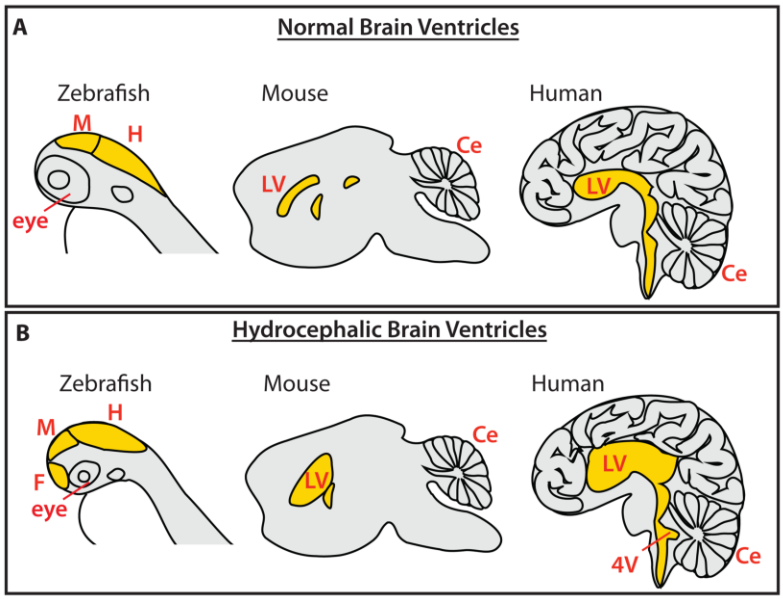

Figure 4.1: Hydrocephalic brain ventricles. (A-B) Lateral tracings of zebrafish, mouse and human normal (A) or hydrocephalic brains (B). Brain ventricles shown in yellow. F = forebrain, M = midbrain, H = hindbrain, LV = lateral ventricle, Ce = cerebellum, 4V = 4th ventricle.

Excess CSF accumulation results in hydrocephalus, a disorder that has been observed in all vertebrates, develops by mid-gestation, and persists after birth (Figure 4.1A-B). Congenital hydrocephalus is present in ~1/500 live births and requires the surgical insertion of a shunt to alleviate symptoms. Over-drainage, however, can lead to subdural hematomas, slit ventricles, misshapen heads, low pressure headaches, and brain stem shifting (Faulhauer and Schmitz, 1978). This suggests that correct CSF pressure or composition is essential for normal brain development. In patients with communicating or non-obstructive hydrocephalus, there is no physical obstruction to CSF drainage making it unclear

why excess CSF accumulates and whether CSF composition, flow, or function are altered. A disruption of CSF flow, for example, may disturb distribution of regulatory factors, nutrients or wastes, as well as change the signaling properties of the CSF. Indeed, the hydrocephalic Texas (H-Tx) rat has abnormal CSF composition and exhibits reduced neurogenesis (Mashayekhi et al., 2002) while children with congenital hydrocephalus have elevated levels of NGF within the CSF (Mashayekhi and Salehi, 2005).

Within the vertebrate kidney, lung, brain, oviduct and gut, beating cilia are thought to generate fluid movement, (Fliegauf et al., 2007; Francis et al., 2009; Kramer-Zucker et al., 2005; Miskevich, 2010; Shi et al., 2011) and inhibition of cilia movement and signaling results in increased fluid accumulation in the brain and kidney (Banizs et al., 2005; Fogelgren et al., 2011; Kramer-Zucker et al., 2005; Sun et al., 2004; Wodarczyk et al., 2009). Thus, cilia are hypothesized to generate CSF flow. Alternatively, Miskevich suggests that in *Xenopus,* cilia beating contribute minimally to CSF flow and instead, that the pulsatile heartbeat is the major driving force of CSF movement (Miskevich, 2010). Further, in adults, CSF movement is pulsatile and is generated by pulsations from the blood flow being transmitted across the choroid plexus to the CSF (Bering et al 1962). Abnormalities in CSF pulsations and movement are thought to result in hydrocephalus (Linninger et al., 2007; Madsen et al., 2006).

In this work, we use zebrafish to study CSF flow in wild type and hydrocephalus models. We developed an assay to visualize CSF flow in the living zebrafish embryo by following the movement of photocoverted Kaede within the brain ventricles. These experiments provide the first characterization of the direction of CSF flow within adult or embryonic zebrafish brain ventricles and demonstrate that the midbrain-hindbrain boundary can act as a physical barrier. Interestingly, we observed movement in wild-type embryos that differs in some, but not all hydrocephalic models. Taken together, our data suggests that CSF flow, production and retention all contribute to brain ventricle size.

MATERIALS AND METHODS

Fish lines and maintenance

Danio rerio fish were raised and bred according to standard methods (Westerfield et al., 2001). Embryos were kept at 28.5^{o}C and staged accordingly (Kimmel et al., 1995). Times of development are expressed as hours post-fertilization (hpf). Lines used were wild type AB.

Antisense morpholino oligonucleotide (MO) injection

A splice-site blocking morpholino (MO) antisense oligonucleotide (Gene Tools, LLC) was used to target *gdpd3* (intron 4 - exon 5): 5'-GTGGCCTGTGCAAAGAGAATTATTA-3'. The splice-site MO was injected into single-cell stage embryos (Nasevicius and Ekker, 2000) and phenotypes analyzed at 24 hpf. Standard control MO used was 5'-CCTCTTACCTCAGTTACAATTTATA-3 ' and *p53* morpholino 5'-GCGCCATTGCTTTGCAAGAATTG-3' (Gene Tools, LLC).

cDNA constructs and in vitro translation

Full-length *atp1a1* cDNA constructs in pCS2+ were obtained from the Chen lab (Shu et al., 2003) Capped *atp1a1*, was transcribed in vitro using the SP6 mMessage mMachine kit (Ambion) after linearization of the cDNA. Embryos were injected at the single-cell stage with 200-250 pg mRNA.

Purification of Kaede protein

pCS2+ Kaede was kindly provided by Atsushi Miyawaki (RIKEN) (Ando et al., 2002). BamHI and NheI sites were added to 5' and 3' ends of *Kaede* by PCR. A *6xHis-Kaede* was generated by inserting *Kaede* into the REST vector. Kaede protein was expressed in BL21 *E. coli* and purified on Ni-NTA beads (Qiagen). Beads were washed in WB1 (50mM sodium phosphate [pH 8.0], 500 mM NaCl, 40mM imidazole, 10 mM B-ME,0.1% Tween-20) and eluted into EB1 (50 mM sodium phosphate [pH 7.0], 500 mM NaCl, 250 mM imidazole and 10 mM B-ME at pH7). Elution was run on a superdex-200 gel filtration column (GE) into PBS and peak fractions were pooled and used for brain ventricle injection.

Mounting embryos for live imaging

Fluorescent Kaede protein was injected into ventricles of wild type or morphant embryos at 23, or 25 hpf as previously described (Gutzman and Sive, 2009). Embryos were then prepared for live imaging as described (Graeden and Sive, 2009). Briefly, 1% agarose was poured into the 1 cm diameter hole of special 2 mm thick plastic slide with a coverslip adhered to the bottom. Dechorionated embryos are then pushed head first into holes in 1% agarose, placing the desired brain ventricles as close to the coverslip as possible.

Live imaging – photoconversion and time-course

Photoconversion and time-course imaging were done using a Zeiss LSM 710 scanning confocal microscope. We set a circular region of interest within the desired ventricle to indicate the region to be photoconverted using the LSM software (representative regions of interest chosen for each ventricle shown in Figure 4.2-1). Using the time-course setting on the LSM software, we photoconverted our region of interest and then took a scan of red and green channels of the brain ventricles. Photoconversion, using the 405nm and 458nm lasers, began after the first two scans and continued prior to each scan for the remaining scans converting Kaede protein from green to red. For each embryo, 100 scans were obtained sequentially across the 7-10 minute time-course of the experiment.

Quantification of fluorescent intensity

Fluorescent intensity in the forebrain, midbrain, and hindbrain was quantified in Adobe Photoshop. Background levels of fluorescence (i.e. fluorescence within the neuroepithelial tissue) were subtracted from fluorescence in the brain ventricles. Increase in fluorescent intensity was plotted over five different time points using GraphPad InStat software. Statistical analysis was performed using GraphPad InStat software using the unpaired t-test. Linear regression analysis was used to calculate slope. Slope greater than zero indicated an increase in activated Kaede as a function of time.

RESULTS

Visualization of CSF flow within embryonic zebrafish.

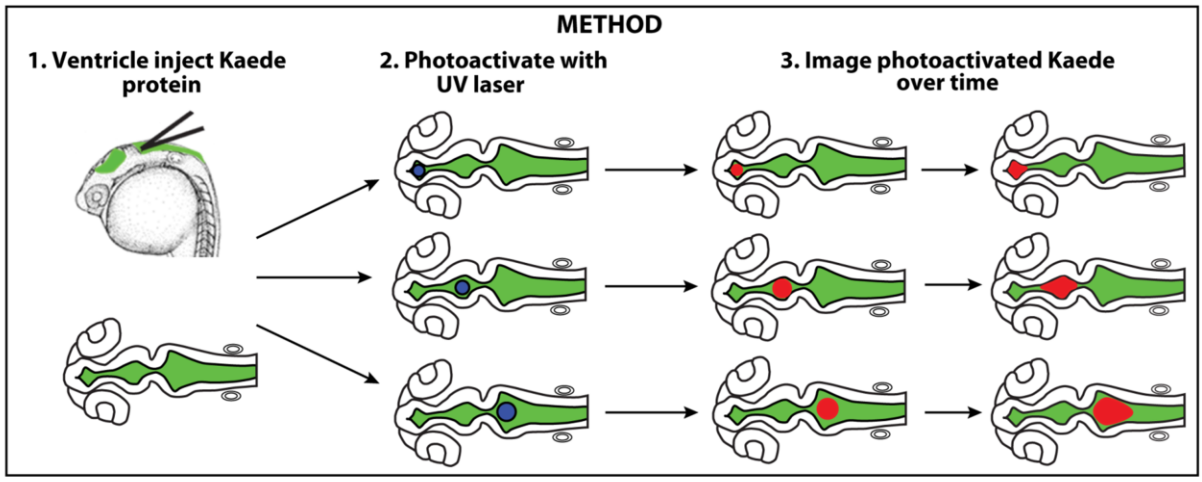

Figure 4.2: Method for detection of CSF flow. Step1: Kaede protein was injected into the brain ventricles. Top = lateral Bottom = dorsal. Step 2: Kaede was photoactivated using a UV laser in either the forebrain (top) midbrain, (middle) or hindbrain (bottom). Step 3: Photoactivated Kaede was imaged over time.

To determine whether there is CSF movement within embryonic zebrafish brain ventricles, we developed a novel technique to visualize fluid movement (Figure 4.2). We purified photoconvertible Kaede protein and injected it into the brain ventricles being careful to limit the exposure to light, which could prematurely activate the Kaede protein (Figure 4.2-1). Either the forebrain, midbrain, or hindbrain ventricles were photoactivated using a UV laser converting the Kaede protein from green to red (Figure 4.2-2). Using confocal microscopy, we observed movement of the photoactivated region as a function of time and we interpreted this movement as the directionality of CSF flow (Figure 4.2-3). Further, the fluorescent intensity was measured in each ventricle to determine (1) whether Kaede was converted in the appropriate brain ventricle and (2) whether photoactivated Kaede entered the other brain ventricles.

Embryonic zebrafish CSF flow.

To determine whether there is directional CSF flow in embryonic zebrafish, we injected Kaede into the brain ventricles at 23 hpf, a developmental time point during brain ventricle inflation but prior to the start of the heartbeat and blood flow (Figure 4.3A-F). Photoactivation occured continuously over the time course thus, significantly increased the intensity of photoactivated

Kaede in the ventricle activated. Thus, as confirmation of Kaede photoactivation, we observed a significant amount of activated Kaede in the ventricle which was targeted (Figure 4.3B,D,F). An increase in fluorescence intensity in the other brain ventricles was identified by determining whether the slope of the line differed from zero. When the forebrain ventricle was photoactivated, we observed a slight increase over time in the amount of photoactivated Kaede in the midbrain (slope =0.15 +/- 0.01) but no change in the hindbrain (slope = 0.01 +/- 0.01) (Figure 4.3A-B, n= 3). Similarly, photoactivated Kaede in the midbrain entered the forebrain (slope = 0.11 +/- 0.004) but not the hindbrain (slope = 0.01 +/- 0.07) (Figure 4.3C-D, n=2). After photoactivation of Kaede in the hindbrain, we did not observe movement of into the midbrain (slope = 0.04 +/- 0.02) or forebrain ventricle (slope = 0.0006) although, there was movement within the hindbrain ventricle as determined by increasing amounts of photoactivated Kaede outside of the photoactivated region (Figure 4.3E-F, n=3). Together, this suggests that there is CSF movement within each ventricle as well as exchange between the forebrain and midbrain ventricles exclusively.

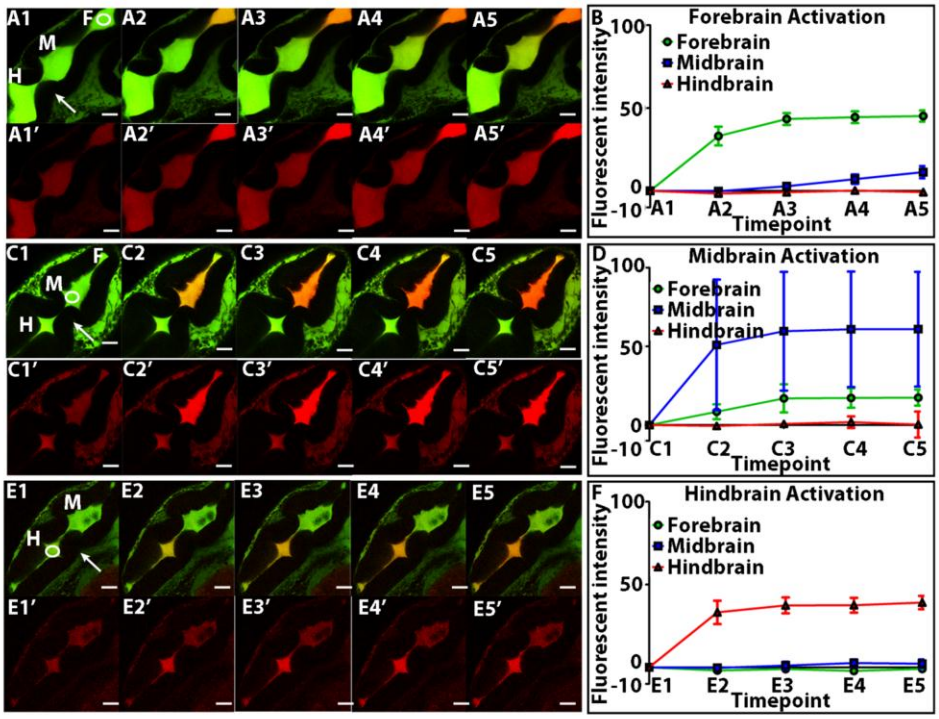

Figure 4.3: CSF flow at 23 hpf. (A-F) Kaede (green) and activated Kaede (red) in embryos at 23 hpf after UV activation in the forebrain (A-B), midbrain (C-D) and hindbrain (E-F) at 5 different time points (A,C,E 1-5). Timepoint 5 = 7-10 minutes. Quantification of fluorescent intensity in each brain ventricle (B,D,F). Data = mean +/- SEM. Circle indicates photoactivated region. Arrow = midbrain-hindbrain boundary. F = forebrain, M = midbrain, H = hindbrain. Scale bars = 50μm.

Contributions of the heartbeat to CSF flow.

CSF flow in brain ventricles of *Xenopus* tadpoles, is driven mainly by the pulsatile heartbeat (Miskevich, 2010). To determine whether the heartbeat alters CSF flow in zebrafish, we examined CSF flow at 25 hpf, a developmental time-point after which the heart has begun to beat. Similar to embryos at 23 hpf, Kaede was successfully photoactivated in the desired ventricle and intensity of activated Kaede in the other two brain ventricles identified as the difference in slope relative to zero. Photoactivated Kaede from the forebrain moved into the midbrain (slope = 0.12 +/- 0.06) but not the hindbrain (slope = -0.04 +/- 0.01) (Figure 4.4A-B, n=5). The decrease in activated Kaede over time observed in the hindbrain ventricle was likely due to photobleaching. However, after photoactivation in the midbrain (Figure 4.4C-D, n=4, slope forebrain = 0.12 +/- 0.03, slope hindbrain = 0.07 +/- 0.03) or hindbrain (Figure 4.4E-F, n=5, slope forebrain = 0.11 +/- 0.06, slope midbrain = 0.14 +/- 0.05), we observed increased fluorescence in all three ventricles. This demonstrates that at 25 hpf, CSF mixes between the forebrain and midbrain ventricles and to a lesser extent between the midbrain and hindbrain ventricles. Consistent with the data from *Xenopus*, we also observed that the heartbeat promoted an

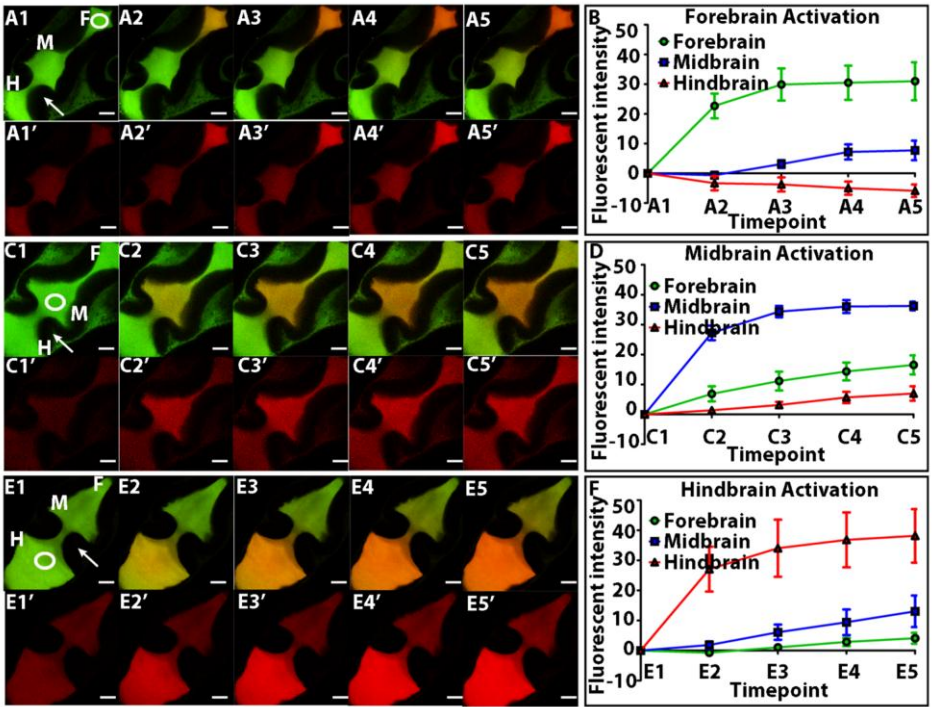

Figure 4.4: CSF flow at 25 hpf. (A-F) Kaede (green) and activated Kaede (red) in embryos at 25 hpf after UV activation in the forebrain (A-B), midbrain (C-D) and hindbrain (E-F) at 5 different time points (A,C,E 1-5). Timepoint 5 = 7-10 minutes. Quantification of fluorescent intensity in each brain ventricle (B,D,F). Data = mean +/- SEM. Circle indicates photoactivated region. Arrow = midbrain-hindbrain boundary. F = forebrain, M = midbrain, H = hindbrain. Scale bars = 50μm.

increase in CSF flow specifically between the midbrain and hindbrain ventricle compared to 23 hpf ($p<.05$).

CSF flow in hydrocephalus models.

Prior work has suggested that CSF volume may be regulated through a tightly controlled balance between CSF production, retention, and drainage (Chapter 2) (Johanson et al., 2008). Disruption of this balance can result in hydrocephalus which may alter embryonic brain development by affecting CSF signaling, flow and brain morphology. In order to determine whether an excess of CSF correlates with abnormal CSF movement, we examined CSF movement in embryos with hydrocephalus (Figure 4.5A-C). The Sive lab previously identified that *gdpd3* (Figure 4.5B) and *atp1a1* (Figure 4.5C) gain-of-function embryos have increased brain ventricle size as compared to wild-type embryos (Figure 4.5A). Increased brain ventricle size is indicated by the white bar (Figure 4.5A'-C') representing the increased height of the hindbrain ventricles. For this study, these hydrocephalic conditions were chosen for their penetrant non-obstructive hydrocephalus phenotype at 25 hpf. Furthermore, in zebrafish embryos, *gdpd3* and *atp1a1* are both expressed in the neuroepithelium lining the brain ventricles (Blaker-Lee et al., 2012 submitted; Canfield et al., 2002; Ellertsdottir et al., 2006). Since the brain ventricles are larger and the tissue further apart, we hypothesize that CSF flow will be abnormal in hydrocephalic embryos and will result in increased mixing of hindbrain and midbrain/forebrain CSF.

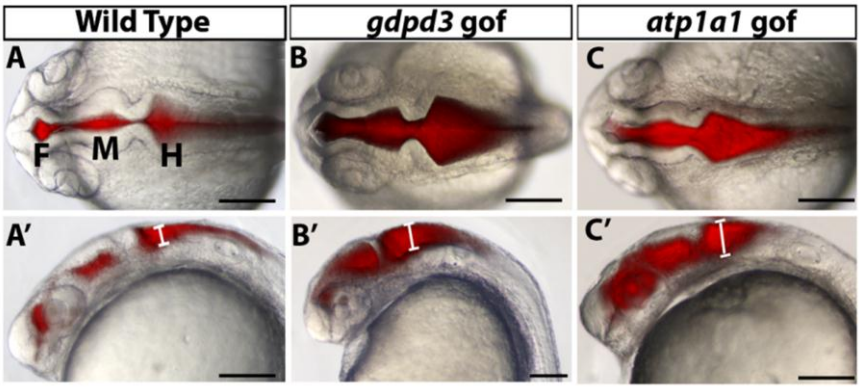

Figure 4.5: Hydrocephalic zebrafish at 25 hpf. (A-C) Brightfield dorsal and (A'-C') lateral views of wild type (A), *gdpd3* gain of function (gof) (B) and *atp1a1* gof (C) embryos ventricle injected with Rhodamine dextran dye. White bar indicates height of hindbrain ventricle. F = forebrain, M = midbrain, H = hindbrain. Scale bars = 50μm.

The *gdpd3* gene encodes an enzymatic subunit of glycerophosphodiester phosphodiesterase, an enzyme that also has phospholipase C activity (Corda et al., 2009). Using an antisense

oligonucleotide morpholino targeted to the *gdpd3* gene, we created a constitutively active version of the protein, which resulted in embryos with expanded, hydrocephalic ventricles compared to controls (Figure 4.5A-B). Upon examination of CSF flow in 25 hpf *gdpd3* gain-of-

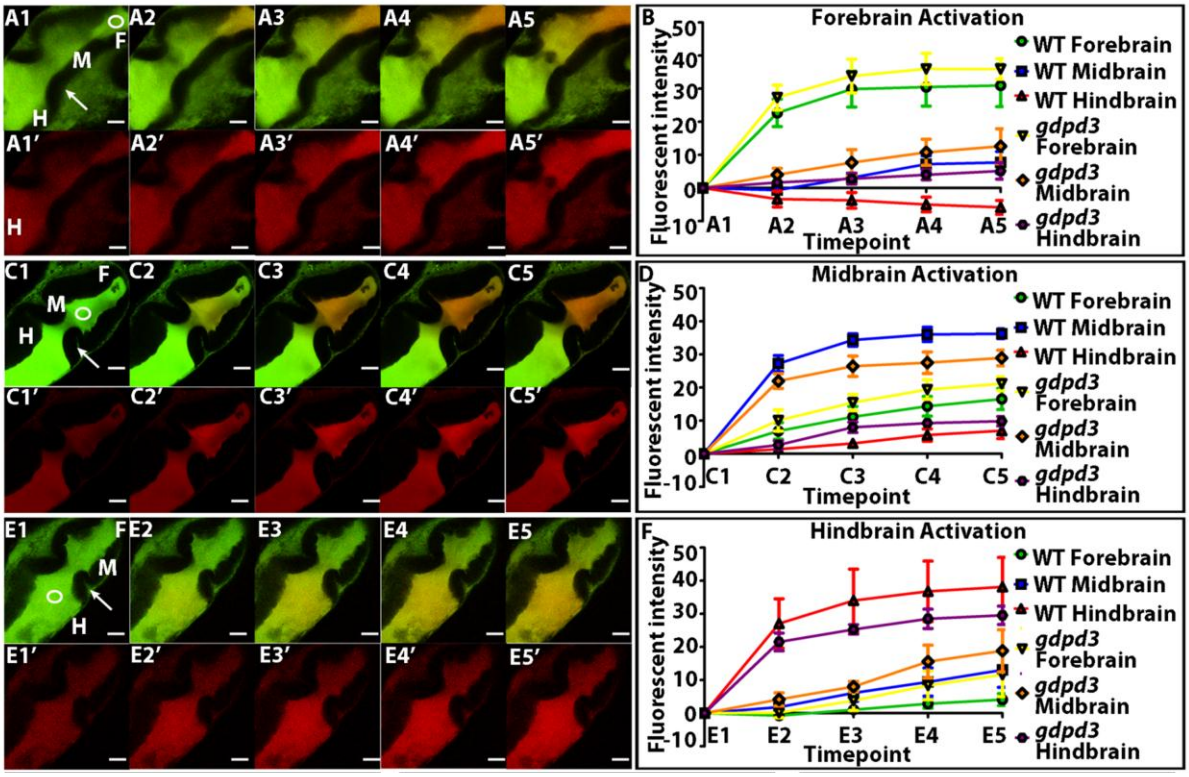

Figure 4.6: CSF flow in hydrocephalic *gdpd3* gain-of-function embryos. (A-F) Kaede (green) and activated Kaede (red) in *gdpd3* MO embryos at 25hpf after UV activation in the forebrain (A-B), midbrain, (C-D and hindbrain (E-F) at 5 different time points (A,C,E 1-5). Timepoint 5 = 7-10 minutes. Quantification of fluorescent intensity in each brain ventricle (B,D,F). Data represented as mean +/- SEM. Circle indicates photoactivated region. Arrow = midbrain hindbrain boundary. F= forebrain, M=midbrain, H= Hindbrain.

function embryos, we observed an increase in movement of photoactivated Kaede from the forebrain ventricle into the midbrain (slope = 0.12 +/- 0.05) and hindbrain ventricles (slope = 0.04 +/- 0.02) (Figure 4.6A-B, n=3). Photoactivated Kaede from the midbrain ventricle of *gdpd3* gain-of-function embryos spread into both the forebrain (slope = 0.10 +/- 0.09) and hindbrain (slope = 0.09 +/- 0.009) ventricle at a slightly increased rate compared to wild type (Figure 4.6C-D, n=4). Additionally, upon photoactivation of *gdpd3* gain-of-function hindbrain ventricles, we observed an increase in the amount of photoactivated Kaede in the midbrain (slope = 0.20 +/- 0.07) and forebrain ventricles (slope = 0.16 +/- 0.07) (Figure 4.6E-F, n=5). Although the observed increases in CSF flow after midbrain and hindbrain activation are not significantly different compared to wild type, there was a significant increase in CSF flow from the forebrain

to hindbrain ventricle (p<.01) in *gdpd3* gain-of-function embryos compared to controls. Thus, the hydrocephalic *gdpd3* gain-of-function embryos exhibit increased CSF mixing between all three brain ventricles.

atp1a1 encodes the alpha subunit of the Na,K-ATPase, which we previously demonstrated is a key regulator during brain ventricle formation (Chapter 2). Atp1a1 is essential for neuroepithelial permeability and brain ventricle inflation (Chapter 2). The increase in brain ventricle size observed in *atp1a1* gain-of-function embryos (Figure 4.5C) is likely due to decreased neuroepithelial permeability and increased CSF production. Based on our *gdpd3* experiments, we asked whether CSF flow also contributes to the increase in brain ventricle size in 25 hpf *atp1a1* gain-of-function embryos. Kaede activated in the forebrain ventricle of *atp1a1*

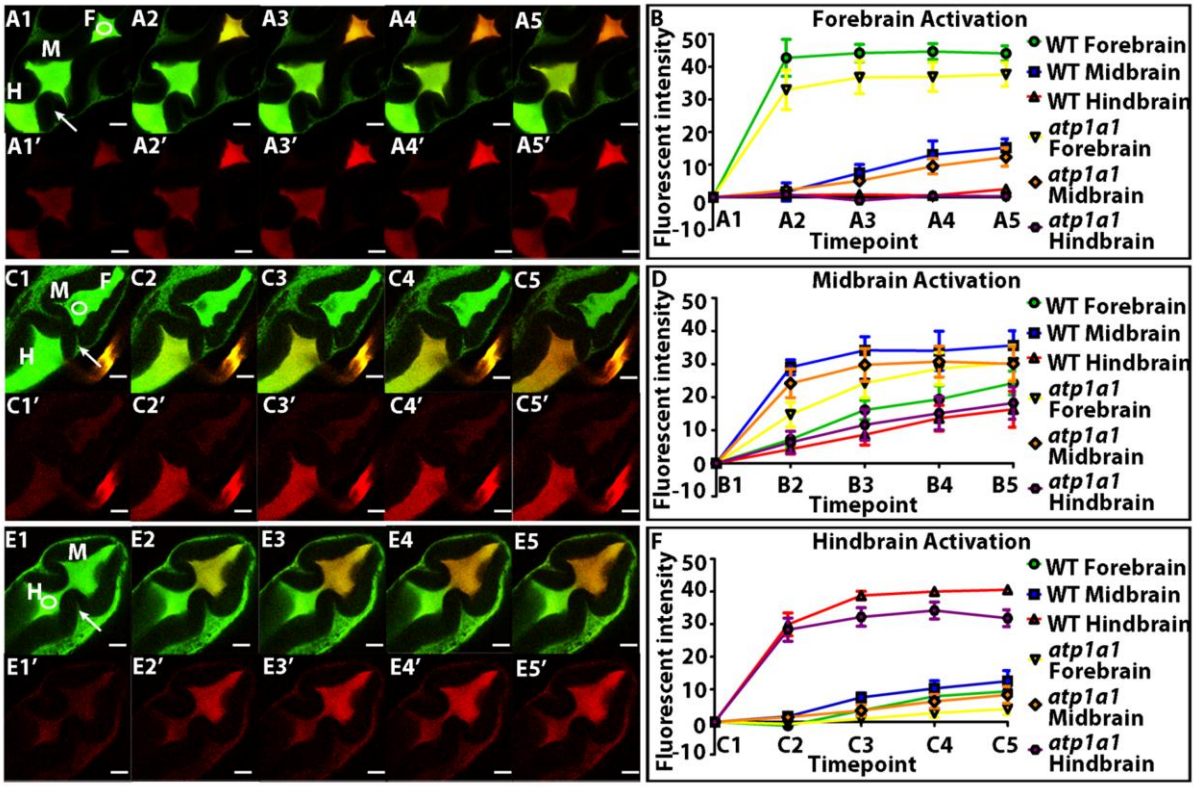

Figure 4.7: CSF flow in hydrocephalic *atp1a1* gain-of-function embryos. (A-F) Kaede (green) and activated Kaede (red) in *atp1a1* mRNA injected embryos at 25 hpf after UV activation in the forebrain (A-B), midbrain, (C-D and hindbrain (E-F) at 5 different time points (A,C,E 1-5). Timepoint 5 = 7-10 minutes. Quantification of fluorescent intensity in each brain ventricle (B,D,F). Data represented as mean +/- SEM. Circle indicates photoactivated region. Arrow = midbrain-hindbrain boundary. F = forebrain, M = midbrain, H = hindbrain. Scale bars = 50μm.

gain-of-function embryos, was later observed in the midbrain (slope = 0.14 +/- 0.04) but not the

hindbrain (slope = -0.002 +/- 0.01) (Figure 4.7A-B, n=5). Similarly, activation of Kaede in the midbrain ventricle was detected in all three ventricles (Figure 4.7C-D, n=8, slope forebrain = 0.22 +/- 0.06, slope hindbrain = 0.17 +/- 0.04). Finally, hindbrain Kaede activation resulted in a slight increase in midbrain (slope = 0.09 +/- 0.02) and forebrain (slope = 0.06 +/- 0.02) activated Kaede (Figure 4.7E-F, n=7). Overall, we did not observe a significant difference between *atp1a1* gain-of-function and wild-type embryos at 25 hpf (p>.05) suggesting that abnormal CSF flow does not significantly contribute to *atp1a1* gain of function increase in brain ventricle size.

Neuroepithelial morphology prevents CSF mixing.

The midbrain-hindbrain boundary (MHB) is one of the first bends within the embryonic brain and is an essential organizer within the brain (Joyner, 1996; Sato et al., 2004). We propose that the MHB can also act as a physical barrier to prevent mixing of CSF between the forebrain/midbrain and the hindbrain ventricle in wild type zebrafish. If this is true, then the increase in CSF flow observed in *gdpd3* gain-of-function embryos is due to an increased distance between the MHB folds. To test this hypothesis, we measured the distance between the MHB folds (Figure 4.8A, red bar) in wild type compared to embryos with hydrocephalus. Wild type embryos at 23 hpf and 25 hpf did not differ in the distance between MHB folds (Figure 4.8B-C, n=8 and 24 respectively) suggesting that the heartbeat, and not changes in tissue morphology, result in increased CSF flow at 25 hpf. However, *gdpd3* gain-of-function embryos had a significant increase in the distance observed between the MHB relative to wild type (Figure 4.8D,F n=11, p<.0005). Conversely, the

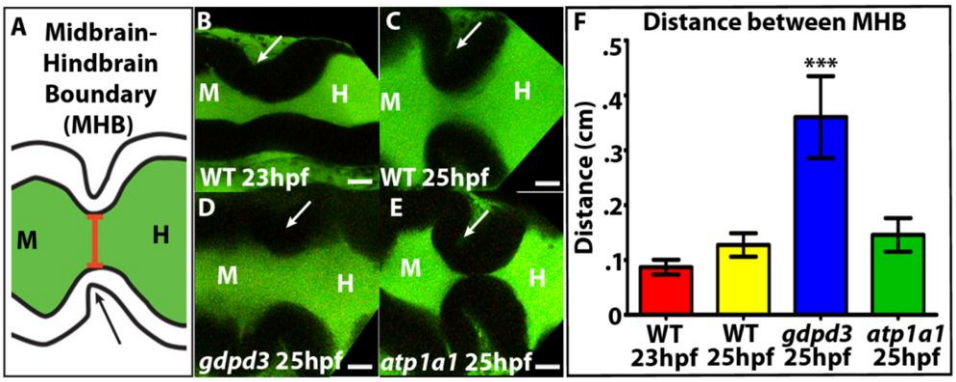

Figure 4.8: Distance between MHB tissue folds is increased in *gdpd3* gain-of-function embryos. (A) Midbrain-hindbrain boundary (MHB) diagram. Red bar indicates distance measured. (B-E) MHB in 23 hpf wild type (WT) (B), 25 hpf WT (C), 25 hpf *gdpd3* MO (D) or 25 hpf *atp1a1* mRNA (E). (F) Quantification of distance between MHB. Data represented as mean +/- SEM. *** = p<.0005 compared to control. Anterior to left. M = midbrain, H = hindbrain. Arrows indicate MHB. Scale bars = 50μm.

distance between the MHB folds in *atp1a1* gain-of-function embryos was not significantly different compared to wild type (Figure 4.8E-F, n=20). Thus, the difference observed in CSF flow between *gdpd3* and *atp1a1* gain-of-function embryos is correlated with differences in MHB morphology and is consistent with the hypothesis that the MHB acts as a physical barrier to prevent mixing between forebrain/midbrain and hindbrain ventricles.

DISCUSSION

This technique successfully identifies changes in CSF flow between the embryonic brain ventricles. We observed CSF movement between brain ventricles prior to the heartbeat and consistent with prior studies in *Xenopus*, we see increased inter-ventricle CSF movement once the heart begins to beat (Figure 4.9A-B). Additionally, we have identified that abnormalities in CSF flow occur in some, but not all, hydrocephalic conditions (Figure 4.9 C-D) and these differences correlate with the distance between the MHB tissue folds. These results suggest that multiple components are necessary for regulating proper brain ventricle size. We propose that at least three different

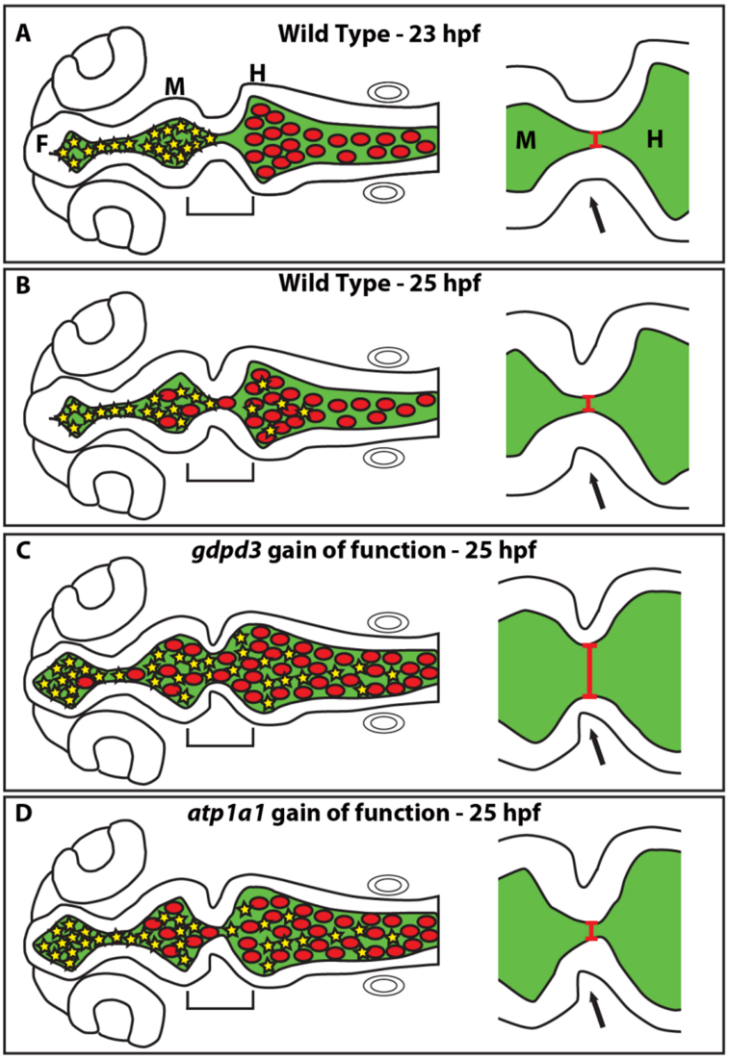

Figure 4.9: CSF flow model. (A) Wild type 23 hpf before heartbeat. CSF does not mix between F/M and H (left), and MHB folds close together (right) (B) after heartbeat (25 hpf) CSF mixing increases between F/M and H (left), but MHB folds close together (right). (C) *gdpd3* gain of function has increased CSF mixing (left), and MHB folds further apart (right). (D) *atp1a1* gain of function CSF flow (right) and MHB tissue (right) did not differ from wild type. Bracket indicates region magnified on the right. Yellow stars =F/M CSF, red circle = H CSF. Arrow indicates midbrain-hindbrain boundary (MHB), F = forebrain, M = midbrain, H = hindbrain.

processes regulate brain ventricle size: neuroepithelial permeability, CSF production, and CSF flow.

CSF flow method.

With this technique, we were able to observe CSF movement in zebrafish at different developmental stages and those exhibiting hydrocephalus. In contrast to traditional fluid flow assays, which use fluorescently labeled polystyrene beads, our CSF flow assay relies on the photoconvertible Kaede protein. We expect this approach will yield a more accurate representation of the CSF fluid flow, as the Kaede protein will behave and be transported more similarly to CSF proteins than traditional beads, which are much larger. However, we cannot rule out the possibility that proteins of larger or smaller molecular weights than Kaede behave differently or move in a different direction than observed in our assay. One limitation of our assays is that in order to photoactivate enough Kaede to observe movement, we must photoactivate after each image acquisition. As a result, we cannot determine the velocity of CSF flow between the brain ventricles. Shorter movies, faster acquisition or a more effective laser, may solve this problem. Notably, fluorescence intensity saturates within the photoactivated ventricle indicating the majority of Kaede is photoconverted. Finally, differentiation between generated flow and passive diffusion will need to be identified either by calculating Kaede diffusion *in vitro* or in fish with no cilia or heartbeat.

What generates CSF flow?

Although, we demonstrate that the heartbeat affects CSF flow, we have not identified the force that generates CSF flow prior to the heartbeat. Previous studies have identified a requirement for cilia in fluid movement within the kidney and brain and inhibition of cilia movement and signaling results in hydrocephalus (Banizs et al., 2005; Fogelgren et al., 2011; Kramer-Zucker et al., 2005; Sun et al., 2004; Wodarczyk et al., 2009). Therefore, cilia may be responsible for CSF flow prior to the heartbeat. Analysis of mutants that have no cilia, abnormal cilia movement or disrupted cilia signaling will identify whether cilia are required for CSF flow and give us further insight into the mechanism by which cilia are required for fluid flow.

Identifying the mechanism leading to hydrocephalus

Our *gdpd3* gain-of-function hydrocephalus model exhibits increased CSF flow between all three ventricles whereas CSF flow in *atp1a1* gain-of-function embryos does not differ from wild type. We propose that the observed difference is due to the increased distance between MHB tissue folds in *gdpd3* gain-of-function embryos. These data suggest that in addition to functioning as a critical signaling center, the MHB can act as a barrier between the forebrain/midbrain CSF and hindbrain CSF. This observation leads to the possibility that, in these hydrocephalic embryos, increased CSF mixing between the three ventricles may disrupt any local microenvironments present in the hindbrain or forebrain/midbrain CSF. Previous mass-spectrometry based studies in mammals have identified differential protein expression within each brain ventricle (Cavanagh et al., 1983; Zappaterra et al., 2007). Further analysis of CSF protein content in hydrocephalic models may identify whether these micro-environments are disturbed. Because zebrafish ventricles are extremely small, a larger vertebrate such as chick or mouse could be used to obtain sufficient CSF quantities for such an analysis.

Finally, the difference in CSF flow in zebrafish hydrocephalus models suggests that much like the human condition, there are multiple different causes of hydrocephalus. Here we have identified three processes that regulate the size of the brain ventricles: CSF production, retention, and flow. However, there may be other mechanisms by which CSF flow can be disrupted. Genes that impact cilia function are associated with hydrocephalus in fish, mouse and human (Banizs et al., 2005; Fogelgren et al., 2011; Kramer-Zucker et al., 2005; Wodarczyk et al., 2009). Recent data indicates that Polycystin 1+2 (Pkd1/2) form a TRP-type Ca^{2+} channel associated with the cilium, that is opened in response to mechanical forces generated by beating cilia (Kamura et al., 2011; Nauli et al., 2003). Opening of the Pkd1/2 channel leads to an influx of Ca^{2+} which activates CamKII and overexpression of activated CamKII can reverse hydrocephalus in the *pkd2* loss-of-function zebrafish (Rothschild et al., 2011). These data implicate abnormal intracellular Ca^{2+} levels in the etiology of hydrocephalus, either through a direct response to the Ca^{2+} gradient or to a downstream effect of CamKII activation.

Intriguingly, the Na,K-ATPase functionally and physically couples with the $Na^{+}Ca^{2+}$ exchanger (Dostanic et al., 2004), possibly connecting both $[Na^{+}]_i$ and $[Ca^{2+}]_i$ ion distribution to hydrocephalus.

Further investigation into the role of CSF production, retention, circulation and drainage will allow for the dissection of the mechanisms which regulate brain ventricle size and for development of new therapeutics and diagnostics.

ACKNOWLEDGEMENTS

This work was supported by the National Institute for Mental Health, and National Science Foundation. Special thanks to Dr. Alicia Blaker-Lee for the *gdpd3* data, David Kern, for help with Kaede protein purification, Tom DiCesare for re-drawing Figure 1, Dr. Joey Davis, Nicole Ann Aponte-Santiago, and Sive lab members for many useful discussions and constructive criticism, and to Olivier Paugois for expert fish husbandry.

REFERENCES

Ando, R., Hama, H., Yamamoto-Hino, M., Mizuno, H., Miyawaki, A., 2002. An optical marker based on the UV-induced green-to-red photoconversion of a fluorescent protein. Proc Natl Acad Sci U S A. 99**,** 12651-6.

Banizs, B., Pike, M. M., Millican, C. L., Ferguson, W. B., Komlosi, P., Sheetz, J., Bell, P. D., Schwiebert, E. M., Yoder, B. K., 2005. Dysfunctional cilia lead to altered ependyma and choroid plexus function, and result in the formation of hydrocephalus. Development. 132**,** 5329-39.

Blaker-Lee, A., Gupta, S., McCammon, J. M., Sive, H., 2012 submitted. Zebrafish 16p11.2 homologZebrafish 16p11.2 homologs are active during brain development, and include two deletion dosage sensor genes.s are highly active during brain development, and include at least two gene copy number sensors. Disease Models and Mechanisms.

Canfield, V. A., Loppin, B., Thisse, B., Thisse, C., Postlethwait, J. H., Mohideen, M. A., Rajarao, S. J., Levenson, R., 2002. Na,K-ATPase alpha and beta subunit genes exhibit unique expression patterns during zebrafish embryogenesis. Mech Dev. 116**,** 51-9.

Cavanagh, M. E., Cornelis, M. E., Dziegielewska, K. M., Evans, C. A., Lorscheider, F. L., Mollgard, K., Reynolds, M. L., Saunders, N. R., 1983. Comparison of proteins in CSF of lateral and IVth ventricles during early development of fetal sheep. Brain Res. 313**,** 159-67.

Corda, D., Kudo, T., Zizza, P., Iurisci, C., Kawai, E., Kato, N., Yanaka, N., Mariggio, S., 2009. The developmentally regulated osteoblast phosphodiesterase GDE3 is glycerophosphoinositol-specific and modulates cell growth. J Biol Chem. 284**,** 24848-56.

Czosnyka, M., Czosnyka, Z., Momjian, S., Pickard, J. D., 2004. Cerebrospinal fluid dynamics. Physiol Meas. 25**,** R51-76.

Dostanic, I., Schultz Jel, J., Lorenz, J. N., Lingrel, J. B., 2004. The alpha 1 isoform of Na,K-ATPase regulates cardiac contractility and functionally interacts and co-localizes with the Na/Ca exchanger in heart. J Biol Chem. 279**,** 54053-61.

Ellertsdottir, E., Ganz, J., Durr, K., Loges, N., Biemar, F., Seifert, F., Ettl, A. K., Kramer-Zucker, A. K., Nitschke, R., Driever, W., 2006. A mutation in the zebrafish Na,K-ATPase subunit atp1a1a.1 provides genetic evidence that the sodium potassium pump contributes to left-right asymmetry downstream or in parallel to nodal flow. Dev Dyn. 235**,** 1794-808.

Faulhauer, K., Schmitz, P., 1978. Overdrainage phenomena in shunt treated hydrocephalus. Acta Neurochir (Wien). 45**,** 89-101.

Fliegauf, M., Benzing, T., Omran, H., 2007. When cilia go bad: cilia defects and ciliopathies. Nat Rev Mol Cell Biol. 8**,** 880-93.

Fogelgren, B., Lin, S. Y., Zuo, X., Jaffe, K. M., Park, K. M., Reichert, R. J., Bell, P. D., Burdine, R. D., Lipschutz, J. H., 2011. The exocyst protein Sec10 interacts with Polycystin-2 and knockdown causes PKD-phenotypes. PLoS Genet. 7**,** e1001361.

Francis, R. J., Chatterjee, B., Loges, N. T., Zentgraf, H., Omran, H., Lo, C. W., 2009. Initiation and maturation of cilia-generated flow in newborn and postnatal mouse airway. Am J Physiol Lung Cell Mol Physiol. 296**,** L1067-75.

Graeden, E., Sive, H., 2009. Live imaging of the zebrafish embryonic brain by confocal microscopy. J Vis Exp.

Gutzman, J. H., Sive, H., 2009. Zebrafish brain ventricle injection. J Vis Exp.

Johanson, C. E., Duncan, J. A., 3rd, Klinge, P. M., Brinker, T., Stopa, E. G., Silverberg, G. D., 2008. Multiplicity of cerebrospinal fluid functions: New challenges in health and disease. Cerebrospinal Fluid Res. 5**,** 10.

Joyner, A. L., 1996. Engrailed, Wnt and Pax genes regulate midbrain--hindbrain development. Trends in Genetics. 12**,** 15-20.

Kamura, K., Kobayashi, D., Uehara, Y., Koshida, S., Iijima, N., Kudo, A., Yokoyama, T., Takeda, H., 2011. Pkd1l1 complexes with Pkd2 on motile cilia and functions to establish the left-right axis. Development. 138**,** 1121-9.

Kimmel, C. B., Ballard, W. W., Kimmel, S. R., Ullmann, B., Schilling, T. F., 1995. Stages of embryonic development of the zebrafish. Dev Dyn. 203**,** 253-310.

Kramer-Zucker, A. G., Olale, F., Haycraft, C. J., Yoder, B. K., Schier, A. F., Drummond, I. A., 2005. Cilia-driven fluid flow in the zebrafish pronephros, brain and Kupffer's vesicle is required for normal organogenesis. Development. 132**,** 1907-21.

Linninger, A. A., Xenos, M., Zhu, D. C., Somayaji, M. R., Kondapalli, S., Penn, R. D., 2007. Cerebrospinal fluid flow in the normal and hydrocephalic human brain. IEEE Trans Biomed Eng. 54**,** 291-302.

Madsen, J. R., Egnor, M., Zou, R., 2006. Cerebrospinal fluid pulsatility and hydrocephalus: the fourth circulation. Clin Neurosurg. 53**,** 48-52.

Mashayekhi, F., Draper, C. E., Bannister, C. M., Pourghasem, M., Owen-Lynch, P. J., Miyan, J. A., 2002. Deficient cortical development in the hydrocephalic Texas (H-Tx) rat: a role for CSF. Brain. 125**,** 1859-74.

Mashayekhi, F., Salehi, Z., 2005. Expression of nerve growth factor in cerebrospinal fluid of congenital hydrocephalic and normal children. Eur J Neurol. 12**,** 632-7.

May, C., Kaye, J. A., Atack, J. R., Schapiro, M. B., Friedland, R. P., Rapoport, S. I., 1990. Cerebrospinal fluid production is reduced in healthy aging. Neurology. 40**,** 500-3.

Miskevich, F., 2010. Imaging fluid flow and cilia beating pattern in Xenopus brain ventricles. J Neurosci Methods. 189**,** 1-4.

Nasevicius, A., Ekker, S. C., 2000. Effective targeted gene 'knockdown' in zebrafish. Nat Genet. 26**,** 216-20.

Nauli, S. M., Alenghat, F. J., Luo, Y., Williams, E., Vassilev, P., Li, X., Elia, A. E., Lu, W., Brown, E. M., Quinn, S. J., Ingber, D. E., Zhou, J., 2003. Polycystins 1 and 2 mediate mechanosensation in the primary cilium of kidney cells. Nat Genet. 33**,** 129-37.

Rothschild, S. C., Francescatto, L., Drummond, I. A., Tombes, R. M., 2011. CaMK-II is a PKD2 target that promotes pronephric kidney development and stabilizes cilia. Development. 138**,** 3387-97.

Rudick, R. A., Zirretta, D.K., Herndon, R.M., 1982. Clearance of albumin from mouse subarachnoid space: a measure of CSF bulk flow. Journal of Neuroscience Methods. 6**,** 253-259.

Sato, T., Joyner, A. L., Nakamura, H., 2004. How does Fgf signaling from the isthmic organizer induce midbrain and cerebellum development? Development Growth & Differentiation. 46**,** 487-94.

Sawamoto, K., Wichterle, H., Gonzalez-Perez, O., Cholfin, J. A., Yamada, M., Spassky, N., Murcia, N. S., Garcia-Verdugo, J. M., Marin, O., Rubenstein, J. L., Tessier-Lavigne, M., Okano, H., Alvarez-Buylla, A., 2006. New neurons follow the flow of cerebrospinal fluid in the adult brain. Science. 311**,** 629-32.

Shi, D., Komatsu, K., Uemura, T., Fujimori, T., 2011. Analysis of ciliary beat frequency and ovum transport ability in the mouse oviduct. Genes Cells. 16**,** 282-90.

Shu, X., Cheng, K., Patel, N., Chen, F., Joseph, E., Tsai, H. J., Chen, J. N., 2003. Na,K-ATPase is essential for embryonic heart development in the zebrafish. Development. 130**,** 6165-73.

Silverberg, G. D., Heit, G., Huhn, S., Jaffe, R. A., Chang, S. D., Bronte-Stewart, H., Rubenstein, E., Possin, K., Saul, T. A., 2001. The cerebrospinal fluid production rate is reduced in dementia of the Alzheimer's type. Neurology. 57**,** 1763-6.

Sun, Z., Amsterdam, A., Pazour, G. J., Cole, D. G., Miller, M. S., Hopkins, N., 2004. A genetic screen in zebrafish identifies cilia genes as a principal cause of cystic kidney. Development. 131**,** 4085-93.

Westerfield, M., Sprague, J., Doerry, E., Douglas, S., Grp, Z., 2001. The Zebrafish Information Network (ZFIN): a resource for genetic, genomic and developmental research. Nucleic Acids Research. 29**,** 87-90.

Wodarczyk, C., Rowe, I., Chiaravalli, M., Pema, M., Qian, F., Boletta, A., 2009. A novel mouse model reveals that polycystin-1 deficiency in ependyma and choroid plexus results in dysfunctional cilia and hydrocephalus. PLoS One. 4**,** e7137.

Zappaterra, M. D., Lisgo, S. N., Lindsay, S., Gygi, S. P., Walsh, C. A., Ballif, B. A., 2007. A comparative proteomic analysis of human and rat embryonic cerebrospinal fluid. J Proteome Res. 6**,** 3537-48.

CHAPTER FIVE

An assay for permeability of the zebrafish embryonic neuroepithelium

Modified from:

Jessica T. Chang and Hazel Sive. An assay for permeability of the zebrafish embryonic neuroepithelium. Submitted to JOVE 2012.

ABSTRACT

We describe a live whole animal quantitative measurement for permeability of the embryonic zebrafish neuroepithelium. The technique analyzes the ability to retain cerebrospinal fluid and molecules of different molecular weights within the neural tube lumen and quantifies their movement out of the ventricles. This method is useful for determining differences in epithelial permeability and maturation during development and disease.

INTRODUCTION

The brain ventricular system is conserved among vertebrates and is composed of a series of interconnected cavities called brain ventricles, which form during the earliest stages of brain development and are maintained throughout the animal's life. The brain ventricles are designed to hold and retain cerebrospinal fluid (CSF), a protein rich fluid that is essential for normal brain development and function (Gato et al., 2005; Lehtinen et al., 2011; Martin et al., 2009; Salehi and Mashayekhi, 2006). During vertebrate embryonic development, the central lumen of the neural tube gives rise to the brain ventricular system (Harrington et al., 2009; Lowery and Sive, 2004).

In zebrafish, brain ventricle inflation begins around 18 hours post fertilization (hpf) after the neural tube is closed. We previously demonstrated that brain ventricle inflation and expansion is driven by both CSF production and regulation of cell shape (Gutzman and Sive, 2010; Lowery and Sive, 2005). However, tight junction function is also required for proper brain ventricle inflation as loss of *claudin 5a* reduces lumen size consistent with the regulation of permeability during brain ventricle inflation (Zhang et al., 2010).

To further investigate the regulation of permeability during zebrafish brain ventricle inflation, we developed a ventricular dye retention assay. This method uses brain ventricle injection in a living zebrafish embryo, a previously described technique developed in our lab (Gutzman and Sive, 2009), to fluorescently label the cerebrospinal fluid. Embryos are then imaged over time as the fluorescent dye moves through the brain ventricles and neuroepithelium. The distance the dye front moves away from the basal side of the neuroepithelium over time is quantified

and is a measure of neuroepithelial permeability (Figure 5.1). We observe that dyes 70 kDa and smaller will move through the neuroepithelium and can be detected outside the embryonic zebrafish brain at 24 hpf (Figure 5.2).

The dye retention assay can be used to analyze neuroepithelial permeability in a variety of different genetic backgrounds, at different times during development, after environmental perturbations and to understand how permeability is affected in embryos with too much fluid (hydrocephalus) or too little fluid. Overall, this technique allows for identification of mechanisms regulating permeability and the role of permeability during development and disease.

MATERIALS AND METHODS

Fish lines and maintenance

Wild type (AB) *Danio rerio* fish were raised and bred according to standard methods (Westerfield et al., 2001). Embryos were kept at 28.5^{o}C and staged according to Kimmel et al., (Kimmel et al., 1995). Times of development are expressed as hours post-fertilization (hpf).

Brain ventricle injection

Microinjection needles were made using capillary tubes (FHC Inc.) and prepared using a Sutter instruments needle puller. An anionic, lysine fixable FITC-Dextran (Invitrogen) was loaded into the microinjection needle, the tip of the was broken using forceps and the drop size measured so that each injection was equal to 1 nl. Tricaine (Sigma, 0.1 mg/ml) was added to embryos at 18 hpf or older embryos stop moving to anesthetize them (made according to Westerfield (Westerfield et al., 2001). Holes were poked in an agarose plate and the plugs removed. After transferring embryos to agarose dish, embryos were oriented so that their tail was in the hole and posterior closest to micromanipulator allowing for a clear view of the dorsal side of the embryo. The needle was positioned at the widest point of the hindbrain ventricle and carefully pierced the roof plate of being sure not to go through the depth of the brain into the yolk (Figure 5.1A). One to two nl of fluorescent dye was injected into the ventricles making sure the dye fills the whole length of the brain ventricle, and imaged immediately.

Brain ventricle imaging

Injected embryos were transferred into a second agarose coated dish, anesthetized with Tricaine, and oriented with their tail in the hole and so the dorsal side of the embryo can be seen. A brightfield image is acquired using transmitted light and then without moving the embryo, microscope or dish, a corresponding fluorescent image was taken. This is repeated for each embryo at the desired time points.

Quantification of dye movement

Brightfield and fluorescent images were merged in Adobe Photoshop as previously described by Gutzman and Sive (Gutzman and Sive, 2009). Measurement of the distance the dye front moves was done in Image J. The merged file was opened in Image J and the line tool used to draw a line from forebrain hinge-point to dye front at a 10-20^{o} angle from neuroepithelium (Figure 5.1A, red line). Using the measurement tool the length of the line is calculated. This is repeated for each time-point. To calculate net distance the dye front moved over time, the distance at t=0 was subtract from other time points and plotted on graph using GraphPad InStat software.

RESULTS

An example of neuroepithelial permeability in wild type embryos is shown in Figure 5.1B-D. To accurately differentiate permeability, one must try different molecular weight dyes to identify a dye that is only slightly leaky in wild type or control embryos (Figure 5.2). This allows for identification of molecules that are necessary for either increasing or decreasing permeability (Figure 5.1D, green and red lines respectively). For the 24 hpf zebrafish neuroepithelium, 70 kDa FITC Dextran leaks slowly over 2 hours, whereas 2000 kDa does not and 10 kDa almost immediately leaks out (Figure 5.2). Therefore 70 kDa is the ideal molecular weight to identify conditions that both increase and decrease permeability.

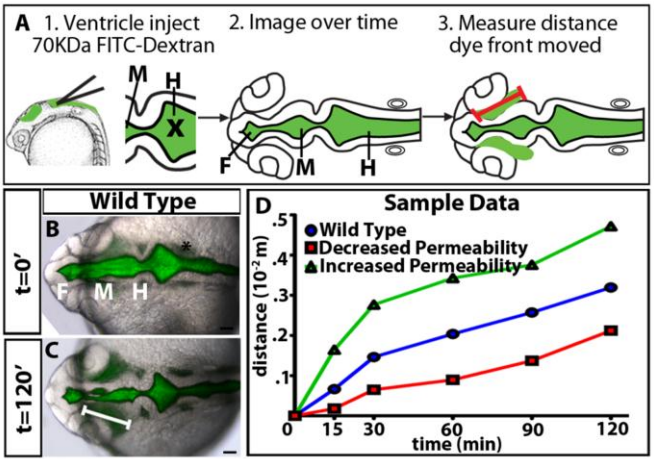

Figure 5.1: Dye retention assay. (A) Experimental Diagram. First, ventricle inject fluorescent dye (X = position of needle), next take dorsal images over time, and finally measure distance dye front moves from forebrain hinge-point represented by red line. (B-C) Merged brightfield and fluorescent dorsal images at 22 hpf (t= 0 minutes, B) and 24 hpf (t=120 minutes, C). White line indicates distance of the dye front from forebrain ventricle. (D) Hypothetical sample data. Blue = wild type or controls, red = decreased permeability relative to control, and green = increased permeability relative to control. F= forebrain, M= midbrain, H= hindbrain. Scale bars = 50μm.

If the needle misses the ventricular lumen, fluorescence will appear outside the brain at t=0 (for an example see Gutzman and Sive (Gutzman and Sive, 2009). These embryos should be discarded since the injected dye was not initially contained within the neuroepithelium and no clear conclusion regarding movement of the dye and permeability of the neuroepithelium can be made.

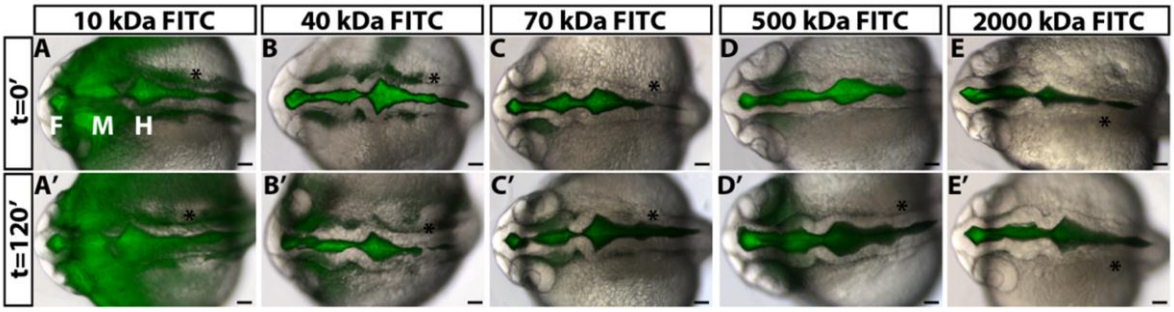

Figure 5.2: Neuroepithelial permeability to different molecular weight dyes. (A-E) Dorsal merged brightfield and fluorescent images of 22 hpf wild type embryos at t=0 minutes injected with 10 kDa (A), 40 kDa (B), 70 kDa (C), 500 kDa (D) and 2000 kDa (E). (A'-E') Same embryo as in (A-E) at t=120 minutes now 24 hpf. Anterior to left. F = forebrain, M = midbrain, H = hindbrain. Asterisk = ear. Scale bars = 50μm.

Finally, if embryos have small ventricles or un-inflated brain ventricles, pre-injection of ventricles with a saline solution can be done prior to injection of the fluorescent dye. This creates a hole and inflates the ventricles making it easier to puncture the roof plate and see the brain ventricles when injecting with the fluorescent dye.

DISCUSSION

We demonstrate the ability to quantify permeability of the living embryonic zebrafish neuroepithelium which is determined for an injected dye of a given molecular weight. Our

observation that the embryonic zebrafish neuroepithelium is differentially permeable to dyes of differing molecular weights suggests that the dye is moving via paracellular permeability. However, we cannot rule out the possibility of any transcellular contribution to the observed permeability. Additionally, this technique can be applied to any other tubular structure as long as both the inside and outside of the tube can be seen and the lumen can be injected.

This assay for permeability will enable further investigation into the role of epithelial permeability during lumen inflation and the regulation of lumen size. In addition this technique will allow characterization of alterations in epithelial permeability associated with disorders such as hydrocephalus and polycystic kidney disease.

ACKNOWLEDGEMENTS

This work was supported by the National Institute for Mental Health, and National Science Foundation. Special thanks to Sive lab members for many useful discussions and constructive criticism, and to Olivier Paugois for expert fish husbandry.

REFERENCES

Gato, A., Moro, J. A., Alonso, M. I., Bueno, D., De La Mano, A., Martin, C., 2005. Embryonic cerebrospinal fluid regulates neuroepithelial survival, proliferation, and neurogenesis in chick embryos. Anat Rec A Discov Mol Cell Evol Biol. 284, 475-84.

Gutzman, J. H., Sive, H., 2009. Zebrafish brain ventricle injection. J Vis Exp.

Gutzman, J. H., Sive, H., 2010. Epithelial relaxation mediated by the myosin phosphatase regulator Mypt1 is required for brain ventricle lumen expansion and hindbrain morphogenesis. Development. 137, 795-804.

Harrington, M. J., Hong, E., Brewster, R., 2009. Comparative analysis of neurulation: first impressions do not count. Mol Reprod Dev. 76, 954-65.

Kimmel, C. B., Ballard, W. W., Kimmel, S. R., Ullmann, B., Schilling, T. F., 1995. Stages of embryonic development of the zebrafish. Dev Dyn. 203, 253-310.

Lehtinen, M. K., Zappaterra, M. W., Chen, X., Yang, Y. J., Hill, A. D., Lun, M., Maynard, T., Gonzalez, D., Kim, S., Ye, P., D'Ercole, A. J., Wong, E. T., LaMantia, A. S., Walsh, C. A.,

2011. The cerebrospinal fluid provides a proliferative niche for neural progenitor cells. Neuron. 69, 893-905.

Lowery, L. A., Sive, H., 2004. Strategies of vertebrate neurulation and a re-evaluation of teleost neural tube formation. Mech Dev. 121, 1189-97.

Lowery, L. A., Sive, H., 2005. Initial formation of zebrafish brain ventricles occurs independently of circulation and requires the nagie oko and snakehead/atp1a1a.1 gene products. Development. 132, 2057-67.

Martin, C., Alonso, M. I., Santiago, C., Moro, J. A., De la Mano, A., Carretero, R., Gato, A., 2009. Early embryonic brain development in rats requires the trophic influence of cerebrospinal fluid. Int J Dev Neurosci. 27, 733-40.

Salehi, Z., Mashayekhi, F., 2006. The role of cerebrospinal fluid on neural cell survival in the developing chick cerebral cortex: an in vivo study. Eur J Neurol. 13, 760-4.

Westerfield, M., Sprague, J., Doerry, E., Douglas, S., Grp, Z., 2001. The Zebrafish Information Network (ZFIN): a resource for genetic, genomic and developmental research. Nucleic Acids Research. 29, 87-90.

Zhang, J., Piontek, J., Wolburg, H., Piehl, C., Liss, M., Otten, C., Christ, A., Willnow, T. E., Blasig, I. E., Abdelilah-Seyfried, S., 2010. Establishment of a neuroepithelial barrier by Claudin5a is essential for zebrafish brain ventricular lumen expansion. Proc Natl Acad Sci U S A. 107, 1425-30.

CHAPTER SIX

Manual drainage of the zebrafish embryonic brain ventricles

Modified from:

Jessica T. Chang and Hazel Sive. Manual drainage of the zebrafish embryonic brain ventricles. Submitted to JOVE 2012.

ABSTRACT

We present a method to collect cerebrospinal fluid (CSF) and to create a system which lacks CSF within the embryonic zebrafish brain ventricular system. This allows for further examination of CSF composition and its requirement during embryonic brain development.

INTRODUCTION

Cerebrospinal fluid (CSF) is a protein rich fluid contained within the brain ventricles. It is present during early vertebrate embryonic development and persists throughout life. Adult CSF is thought to cushion the brain, remove waste, and carry secreted molecules (Chodobski and Szmydynger-Chodobska, 2001; Redzic et al., 2005). The majority of vertebrate adult CSF is made by the choroid plexus, a series of highly vascularized secretory regions located adjacent to the brain ventricles (Brown et al., 2004; Praetorius, 2007; Speake et al., 2001). In zebrafish, the choroid plexus is fully formed at 144 hours post fertilization (hpf) (Garcia-Lecea et al., 2008). Prior to choroid plexus formation, a significant amount of embryonic CSF (eCSF) is present in many vertebrates, including zebrafish. Studies in chick suggest that the neuroepithelium is secretory early in development and may be the major source of eCSF prior to choroid plexus development (Welss, 1934).

eCSF contains about three times more protein than adult CSF, suggesting that it may have an important role during development (Saunders et al., 1999; Zheng and Chodobski, 2005). Studies in chick and mouse demonstrate that secreted factors in the eCSF, fluid pressure, or a combination of these, are important for neurogenesis, gene expression, cell proliferation, and cell survival in the neuroepithelium (Alonso et al., 2011; Desmond et al., 2005; Gato et al., 2005; Lehtinen et al., 2011; Martin et al., 2009; Martin et al., 2006; Mashayekhi et al., 2001; Mashayekhi and Salehi, 2006; Miyan et al., 2006; Parada et al., 2005b; Salehi and Mashayekhi, 2006). Proteomic analyses of human, rat, mouse, and chick eCSF have identified many proteins that may be necessary for these processes. These include extracellular matrix components, apolipoproteins, osmotic pressure regulating proteins, and proteins involved in cell death and proliferation (Gato et al., 2004; Parada et al., 2005a; Parvas et al., 2008; Zappaterra et al., 2007). However, the complex functions of the eCSF are largely unknown.

We have developed a method for removing eCSF from zebrafish brain ventricles, thus allowing for identification of eCSF components and for analysis of eCSF requirement during development. Although more eCSF can be collected from other vertebrate systems with larger embryos, using the zebrafish, we can collect eCSF from the earliest stages, and under many genetic or environmental conditions that lead to abnormal brain ventricle volume or morphology. Removal and collection of eCSF allows for mass spectrometric analysis of eCSF composition, investigation of the role of eCSF, and reintroduction of select factors into the ventricles to identify their function during brain development. Thus the accessibility of the early zebrafish embryo allows for detailed analysis of eCSF function during development.

MATERIALS AND METHODS

Preparing microinjection needles and CellTram

Microinjection needles (FHC Inc.) were made by pulling capillary tubes using the Sutter Instruments needle puller. The Eppendorf CellTram oil microinjector apparatus was filled with mineral oil (Sigma) according to manufacturer's instructions and the needle mounted on the micromanipulator connected to CellTram. The tip of the needle was carefully broken and the needle filled with oil by turning the CellTram knob clockwise being careful to avoid creating bubbles.

Draining the eCSF

Using a 1-200 µl pipette tip, holes were poked into in a 1% agarose coated dish and agarose plugs removed. Dechorionated embryos are transferred into the agarose coated dish and Tricaine (Sigma, 0.1 mg/ml) added until embryos stop moving (made according to Westerfield (Westerfield et al., 2001)). Embryos are oriented with their tails in the hole of the agarose and their posterior side closest to the micromanipulator, allowing for visualization of the dorsal side of the brain. The needle is positioned at the r0/r1 (rhombomere boundary) hinge-point or the widest point of hindbrain ventricle (Figure 6.1A). The needle is carefully inserted into the hindbrain ventricle piercing the roof plate being sure not to go through the depth of the brain into the yolk. eCSF is drained, being careful to avoid any cells, using the CellTram, and fluid

collected in microinjection needle. The needle is further inserted into the midbrain and forebrain to drain eCSF in the whole brain (Figure 6.1A red arrows).

Collecting the eCSF for composition analysis

Once the CSF is collected in the needle, suction from the Cell Tram is carefully stopped. The dish is moved from under the needle and the needle is positioned in a tube with PBS or other buffer. Using the CellTram, collected eCSF is drained out of the needle into the buffer being careful to avoid oil contamination.

Reintroduction of selected factors

eCSF is drained every 1-2 hours during desired time interval. Between drains, embryos are stored at 28.5^{o}C. For reintroduction of fluid, a second micropipette needle is loaded with the desired factor. The needle is fixed to the micromanipulator attached to gas-powered microinjector, broken and injection volume adjusted to 1 nl. One to two nl of the factor is injected into the brain ventricles as previously described (Gutzman and Sive, 2009).

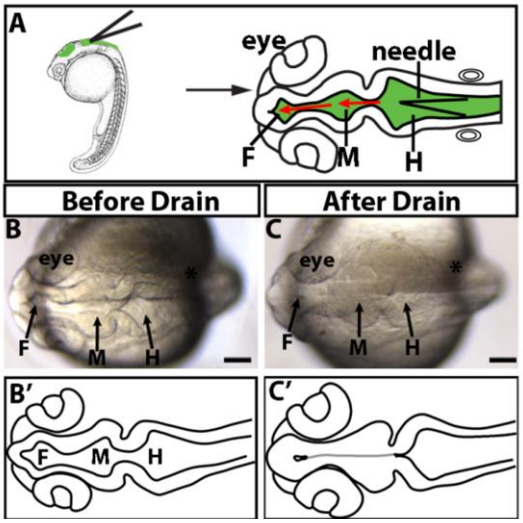

Figure 6.1: Manually drained brain ventricles. (A) Experimental design. Lateral (left) and dorsal (right) views indicating where needle (black triangle) is inserted into the roof plate of the hindbrain ventricle. The needle is then further inserted into the midbrain and forebrain ventricles as designated by the red arrows. (B-C) Examples of 24 hpf manually drained embryo. The same embryo imaged before draining (B) or after drain (C). (B'-C') Tracings of B-C. Grey line indicates morphology present but not visible. F = forebrain, M = midbrain, H = hindbrain. Scale bars = 50μm.

RESULTS

An example of a drained brain ventricle is shown in Figure 6.1B-C. Brain ventricles are collapsed and lack eCSF (Figure 6.1B vs. C). As seen in dorsal images (Figure 6.1B-C, 6.2A-B) the hindbrain neuroepithelium does retain its characteristic morphology and seems to be open despite lack of eCSF likely due to robust hindbrain hinge-points. However, lateral views (Figure 6.2A'-D') demonstrate that the hindbrain ventricle has been

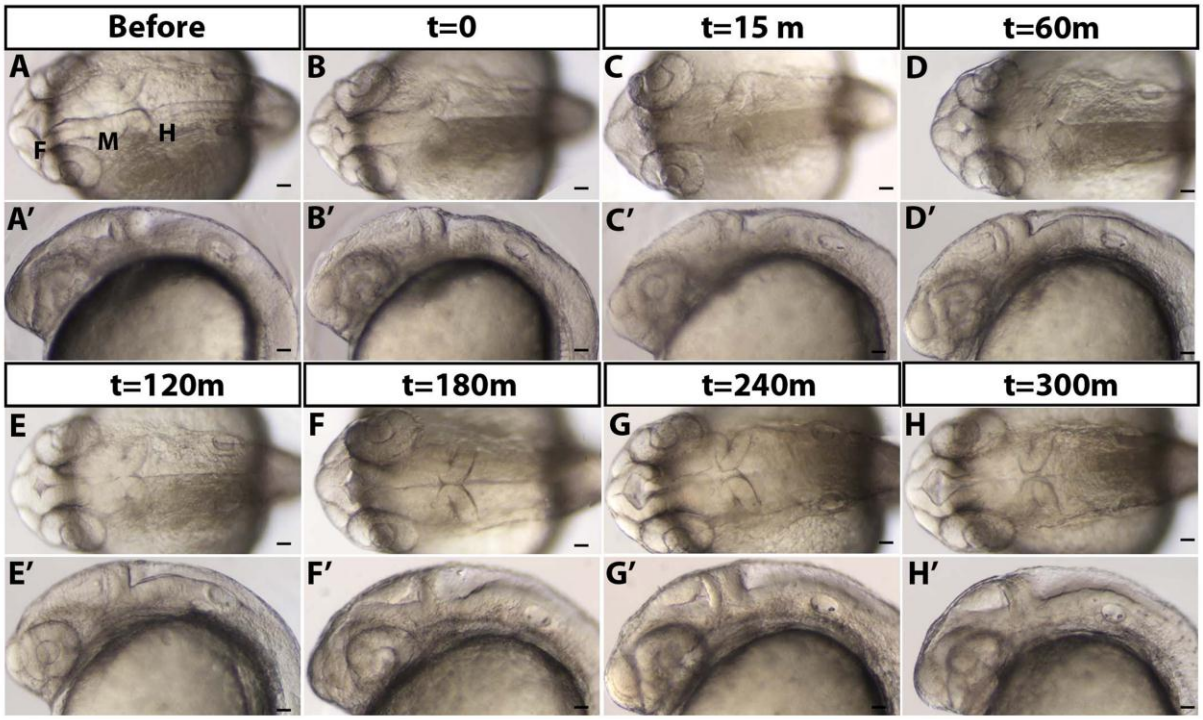

Figure 6.2: eCSF refills the brain ventricles over time. (A) 24 hpf embryo before draining (B) immediately after t = 0 minute (m) (C) 15 m, (D) 60 m, (E) 120 m, (F) 180 m, (G) 240 m, and (H) 300 m after draining. (A-H) Dorsal and (A'-H') lateral brightfield images with anterior to the left. F = forebrain, M = midbrain, H= hindbrain. Scale bars = 50μm.

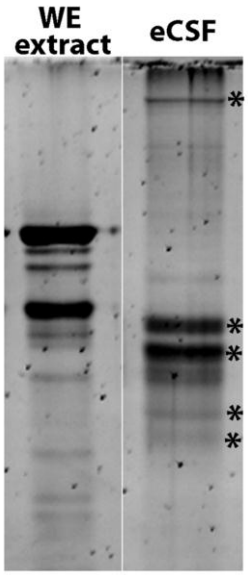

drained, consistent with the presence of a thin flexible roof plate epithelium which collapses ventrally. In wild type embryos, eCSF is continuously produced and refills the brain ventricles 2-3 hours post draining (Figure 6.2). Therefore, CSF needs to be continuously depleted over the time of interest. eCSF has a different protein profile than whole embryo extract, and analysis on a SDS-PAGE protein gel demonstrates that a detectable amount of protein can be collected from zebrafish eCSF (Figure 6.3).

Figure 6.3: eCSF protein content. Protein profile differs between 0.5 μg 24 hpf whole zebrafish embryo (WE) extract and 24 hpf eCSF from 50 embryos. SDS loading buffer added to collected eCSF to denature proteins, sample run on an 8% Tris-HCl PAGE gel, and detected with Sypro Ruby. * indicate bands unique to eCSF.

DISCUSSION

Use of this technique to manually drain eCSF from zebrafish brain ventricles will be useful for determining the requirement of eCSF during development in addition to describing the protein

profile of eCSF over the course of embryonic development. Identification of different proteins during this time will enable further investigation into the function of eCSF and its potential role during brain development. IGF2, FGF2, retinoic acid, and apolipoproteins have been identified as factors present in the eCSF that are necessary for neuroepithelial cell survival, proliferation and neurogenesis (Alonso et al., 2011; Lehtinen et al., 2011; Martin et al., 2006; Parada et al., 2008a; Parada et al., 2005a; Parada et al., 2008b). However, in these studies, the eCSF used was obtained after choroid plexus formation, later than the time-points demonstrated here. Additionally, our lab and others have identified many zebrafish mutants that have abnormal brain ventricle size or brain defects. This method allows for investigation into the effect of abnormal eCSF quantity or composition on embryonic brain development. One advantage of using zebrafish as a system for eCSF analysis is the ability to collect eCSF from many embryos during early development prior to choroid plexus formation.

The zebrafish system allows for replacement of selected factors via injection into the brain ventricles after removal of eCSF, allowing for functional analysis of specific factors during brain development. Small molecules, proteins, and eCSF obtained after genetic or chemical perturbation can therefore be tested for function during development. Reintroduction of eCSF from other species will allow for comparison of factors and functions across species and under different pathological conditions, such as hydrocephalus, complementing and interfacing with mammalian studies in a powerful fashion. Overall, use of the zebrafish to remove eCSF, analyze its composition and reintroduce eCSF or specific factors into the brain ventricles, will significantly contribute to understanding the role and regulation of eCSF function and that of the brain ventricular system.

ACKNOWLEDGEMENTS

This work was supported by the National Institute for Mental Health, and National Science Foundation. Special thanks to Dr. Jen Gutzman, Dr. Amanda Dickinson and other Sive lab members for many useful discussions and constructive criticism, and to Olivier Paugois for expert fish husbandry.

REFERENCES

Alonso, M. I., Martin, C., Carnicero, E., Bueno, D., Gato, A., 2011. Cerebrospinal fluid control of neurogenesis induced by retinoic acid during early brain development. Dev Dyn. 240**,** 1650-9.

Brown, P. D., Davies, S. L., Speake, T., Millar, I. D., 2004. Molecular mechanisms of cerebrospinal fluid production. Neuroscience. 129**,** 957-70.

Chodobski, A., Szmydynger-Chodobska, J., 2001. Choroid plexus: target for polypeptides and site of their synthesis. Microsc Res Tech. 52**,** 65-82.

Desmond, M. E., Levitan, M. L., Haas, A. R., 2005. Internal luminal pressure during early chick embryonic brain growth: descriptive and empirical observations. Anat Rec A Discov Mol Cell Evol Biol. 285**,** 737-47.

Garcia-Lecea, M., Kondrychyn, I., Fong, S. H., Ye, Z. R., Korzh, V., 2008. In vivo analysis of choroid plexus morphogenesis in zebrafish. PLoS One. 3**,** e3090.

Gato, A., Martin, P., Alonso, M. I., Martin, C., Pulgar, M. A., Moro, J. A., 2004. Analysis of cerebro-spinal fluid protein composition in early developmental stages in chick embryos. J Exp Zool A Comp Exp Biol. 301**,** 280-9.

Gato, A., Moro, J. A., Alonso, M. I., Bueno, D., De La Mano, A., Martin, C., 2005. Embryonic cerebrospinal fluid regulates neuroepithelial survival, proliferation, and neurogenesis in chick embryos. Anat Rec A Discov Mol Cell Evol Biol. 284**,** 475-84.

Gutzman, J. H., Sive, H., 2009. Zebrafish brain ventricle injection. J Vis Exp.

Lehtinen, M. K., Zappaterra, M. W., Chen, X., Yang, Y. J., Hill, A. D., Lun, M., Maynard, T., Gonzalez, D., Kim, S., Ye, P., D'Ercole, A. J., Wong, E. T., LaMantia, A. S., Walsh, C. A., 2011. The cerebrospinal fluid provides a proliferative niche for neural progenitor cells. Neuron. 69**,** 893-905.

Martin, C., Alonso, M. I., Santiago, C., Moro, J. A., De la Mano, A., Carretero, R., Gato, A., 2009. Early embryonic brain development in rats requires the trophic influence of cerebrospinal fluid. Int J Dev Neurosci. 27**,** 733-40.

Martin, C., Bueno, D., Alonso, M. I., Moro, J. A., Callejo, S., Parada, C., Martin, P., Carnicero, E., Gato, A., 2006. FGF2 plays a key role in embryonic cerebrospinal fluid trophic properties over chick embryo neuroepithelial stem cells. Dev Biol. 297**,** 402-16.

Mashayekhi, F., Bannister, C. M., Miyan, J. A., 2001. Failure in cell proliferation in the germinal epithelium of the HTx rats. Eur J Pediatr Surg. 11 Suppl 1**,** S57-9.

Mashayekhi, F., Salehi, Z., 2006. The importance of cerebrospinal fluid on neural cell proliferation in developing chick cerebral cortex. Eur J Neurol. 13**,** 266-72.

Miyan, J. A., Zendah, M., Mashayekhi, F., Owen-Lynch, P. J., 2006. Cerebrospinal fluid supports viability and proliferation of cortical cells in vitro, mirroring in vivo development. Cerebrospinal Fluid Res. 3**,** 2.

Parada, C., Escola-Gil, J. C., Bueno, D., 2008a. Low-density lipoproteins from embryonic cerebrospinal fluid are required for neural differentiation. J Neurosci Res. 86**,** 2674-84.

Parada, C., Gato, A., Bueno, D., 2005a. Mammalian embryonic cerebrospinal fluid proteome has greater apolipoprotein and enzyme pattern complexity than the avian proteome. J Proteome Res. 4**,** 2420-8.

Parada, C., Gato, A., Bueno, D., 2008b. All-trans retinol and retinol-binding protein from embryonic cerebrospinal fluid exhibit dynamic behaviour during early central nervous system development. Neuroreport. 19**,** 945-50.

Parada, C., Martin, C., Alonso, M. I., Moro, J. A., Bueno, D., Gato, A., 2005b. Embryonic cerebrospinal fluid collaborates with the isthmic organizer to regulate mesencephalic gene expression. J Neurosci Res. 82**,** 333-45.

Parvas, M., Parada, C., Bueno, D., 2008. A blood-CSF barrier function controls embryonic CSF protein composition and homeostasis during early CNS development. Dev Biol. 321**,** 51-63.

Praetorius, J., 2007. Water and solute secretion by the choroid plexus. Pflugers Arch. 454**,** 1-18.

Redzic, Z. B., Preston, J. E., Duncan, J. A., Chodobski, A., Szmydynger-Chodobska, J., 2005. The choroid plexus-cerebrospinal fluid system: from development to aging. Curr Top Dev Biol. 71**,** 1-52.

Salehi, Z., Mashayekhi, F., 2006. The role of cerebrospinal fluid on neural cell survival in the developing chick cerebral cortex: an in vivo study. Eur J Neurol. 13**,** 760-4.

Saunders, N. R., Habgood, M. D., Dziegielewska, K. M., 1999. Barrier mechanisms in the brain, II. Immature brain. Clin Exp Pharmacol Physiol. 26**,** 85-91.

Speake, T., Whitwell, C., Kajita, H., Majid, A., Brown, P. D., 2001. Mechanisms of CSF secretion by the choroid plexus. Microsc Res Tech. 52**,** 49-59.

Welss, P., 1934. Secretory activity of the inner layer of the embryonic mid-brain of the chick, as revealed by tissue culture. The Anatomical Record. 58**,** 299-302.

Westerfield, M., Sprague, J., Doerry, E., Douglas, S., Grp, Z., 2001. The Zebrafish Information Network (ZFIN): a resource for genetic, genomic and developmental research. Nucleic Acids Research. 29**,** 87-90.

Zappaterra, M. D., Lisgo, S. N., Lindsay, S., Gygi, S. P., Walsh, C. A., Ballif, B. A., 2007. A comparative proteomic analysis of human and rat embryonic cerebrospinal fluid. J Proteome Res. 6**,** 3537-48.

Zheng, W., Chodobski, A. Eds.), 2005. The blood-cerebrospinal fluid barrier. Taylor and Francis, Boca Raton, Fl.

CHAPTER 7

Conclusions and Future Directions

Contributions: I wrote this chapter.

Cerebrospinal fluid (CSF) dynamics plays a crucial role during brain development and homeostasis. However, many aspects of CSF production, retention, flow, drainage, and function still remain unknown. In previous chapters, we present data that begin to dissect the mechanisms governing CSF dynamics during zebrafish embryonic development. First, we identified a role for the Na,K-ATPase during CSF production and retention. Second, we determined that embryonic CSF (eCSF) is required for neuroepithelial survival through the promotion of retinoic acid synthesis and signaling. Finally, we found that zebrafish eCSF circulates and is contained within two distinct compartments separated by the midbrain-hindbrain boundary tissue folds. Further, we identified a requirement for CSF production, retention and flow in the regulation of brain ventricle size where disruption of these processes resulted in hydrocephalus. Many hypotheses remain to be tested in order to fully understand CSF dynamics, the differences between embryonic and adult CSF, and the process of CSF maturation during development. Here, I present some of the outstanding questions, hypotheses, and experiments that may help dissect the mechanisms of CSF dynamics.

Regulating CSF production.

The osmotic gradient drives CSF production and perturbations to this gradient can either increase or decrease production (Chapter 2). Therefore, several important questions to address are (1) what drives the establishment of the osmotic gradient, (2) how does water movement affect the gradient, and (3) what regulates protein secretion and/or movement of proteins into the CSF.

Establishment of the osmotic gradient.

The Na,K-ATPase is a protein complex required for regulation of cell volume, vectorial transport of salt and water, and establishment and maintenance of the membrane potential and osmotic gradient (Horisberger et al., 1991). We identified a role for Na,K-ATPase pumping during both CSF production and retention (Chapter 2). Thus, the regulation of Na^+ and K^+ within the embryonic zebrafish neuroepithelium must be tightly controlled for proper CSF production to occur. In the choroid plexus, a specialized ependymal cell required for CSF secretion, several ion transporters necessary for Na^+ and K^+ movement, including the Na^+-H^+ exchanger, the Na^+-K^+-

$2Cl^-$ co-transporter, and the Na^+-HCO_3^- co-transporter, are required for CSF production (Davson and Segal, 1970; Keep et al., 1994; Murphy and Johanson, 1989; Pollay et al., 1985). Because the neuroepithelium is responsible for CSF production prior to choroid plexus formation, (Welss, 1934), it will be interesting to determine whether these transporters are also required for CSF production within the embryonic zebrafish neuroepithelium.

Water influx into the brain ventricles.

Once the osmotic gradient is established, water must fill the embryonic brain ventricles. Currently, the source of this water is unknown. In embryonic zebrafish, water can enter the brain ventricles through transport from the blood, neuroepithelium or environment. At 24 hpf, the neuroepithelium consists of only a single layer of cells, therefore, expression of water channels (Aquaporins) within the neuroepithelium may facilitate movement of water from within the cells or transcellularly (across cells). Identification of where and when during development Aquaporin expression commences is the first step to identifying the source of brain ventricle water. Interestingly Aquaporin 3a is expressed in the epidermis of 24 hpf embryos while 6 others are expressed in the brain (Thisse and Thisse, 2008).

Alternatively, water may enter the embryonic brain through paracellular transport (between cells), which is regulated by tight junctions. We demonstrated that the embryonic brain is permeable to molecules under 70 kDa (Chapter 2). Additionally, a recent study identified Claudin 2, a component of the tight junctions, as a paracellular water channel in cell culture (Rosenthal et al., 2010), while another demonstrated a requirement for Claudin 5a during eCSF retention in zebrafish (Zhang et al., 2010). Therefore, it is possible that water influx is, in part, governed by the neuroepithelial tight junctions. Again, a combination of expression (location and timing) and loss of function studies may help elucidate the role of the tight junctions during water movement into the brain ventricles.

Protein secretion into the CSF.

We and others have identified numerous proteins within the embryonic CSF (Chapter 3) (Gato et al., 2004; Parada et al., 2006; Parada et al., 2005; Parvas et al., 2008; Zappaterra et al., 2007).

However, the source of these proteins is still unclear. In the simplest hypothesis, the neuroepithelium directly secretes proteins into the CSF. Indeed, Welss found that the chick neuroepithelium is secretory (Welss, 1934). Alternatively, or additionally, once the blood vasculature has developed, proteins can diffuse from the blood into the CSF thus allowing proteins from other parts of the body to enter the CSF. Given that we identified a number of proteins within the eCSF not natively expressed in the neuroepithelium, this mechanism seems likely. Additionally, in chick there is a large contribution of plasma proteins to the CSF and this exchange occurs through a rudimentary blood CSF barrier at the ventral midline of the mesencephalon and prosencephalon (Parvas and Bueno, 2010; Parvas et al., 2008). An interesting hypothesis to be tested is the possible link between ionic gradient and increased protein secretion. There is little data to suggest whether the ionic gradient regulates protein secretion into the ventricular lumen. Although, one report does demonstrate a requirement for the Na,K-ATPase during FGF2 secretion in primate cells (Dahl et al., 2000) suggesting a possible connection between ionic gradient or membrane potential and protein secretion. Additionally, we have performed preliminary experiments to determine whether the Na,K-ATPase mutant, *snakehead* (*snk*^{to273}), contains proteins within its ventricles despite lack of ventricle inflation. Thus, we injected saline into the brain ventricles to flush out any proteins, collected the fluid, and ran it on a SDS-PAGE gel. We did not observe any proteins within the "flushed" eCSF of *snk*^{to273} (Figure 7.1, right lane) compared to wild type (Figure 7.1, left lane) suggesting that Na,K-ATPase and the ionic gradient are required for protein secretion. However, more rigorous experiments are required to concretely establish a link between ionic gradient and protein secretion.

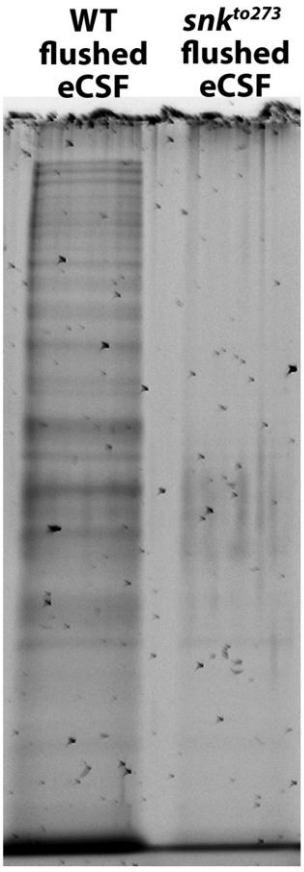

Figure 7.1: *snakehead* (*snk*^{to273}) lacks protein secretion. Saline was injected into wild type (left lane) or *snk*^{to273} (right lane) embryos and then collected and run on a 8% SDS-PAGE gel.

Pump-independent role of the Na,K-ATPase.

Studies in *Drosophila* and cell culture suggest that the Na,K-ATPase directly interacts with components of the junctions. Although we demonstrate that Na,K-ATPase plays a pump-dependent role during brain ventricle inflation, it is also possible that this protein complex physically interacts with the neuroepithelial junctions. Experiments in cell culture demonstrate that the Na,K-ATPase binds to protein phosphatase 2A (PP2A) and regulates phosphorylation of occludins, a component of the tight junction complex (Figure 7.2A) (Rajasekaran et al., 2007). Further, Na,K-ATPase binds to ankyrin an integral protein which links spectrin and actin to membrane proteins suggesting a connection between the Na,K-ATPase and the cytoskeleton (Figure 7.2B) (Devarajan et al., 1994). Identification of components that the alpha subunit, Atp1a1, binds to within the neuroepithelium would begin to identify the mechanism by which Atp1a1 regulates neuroepithelial junction formation and permeability.

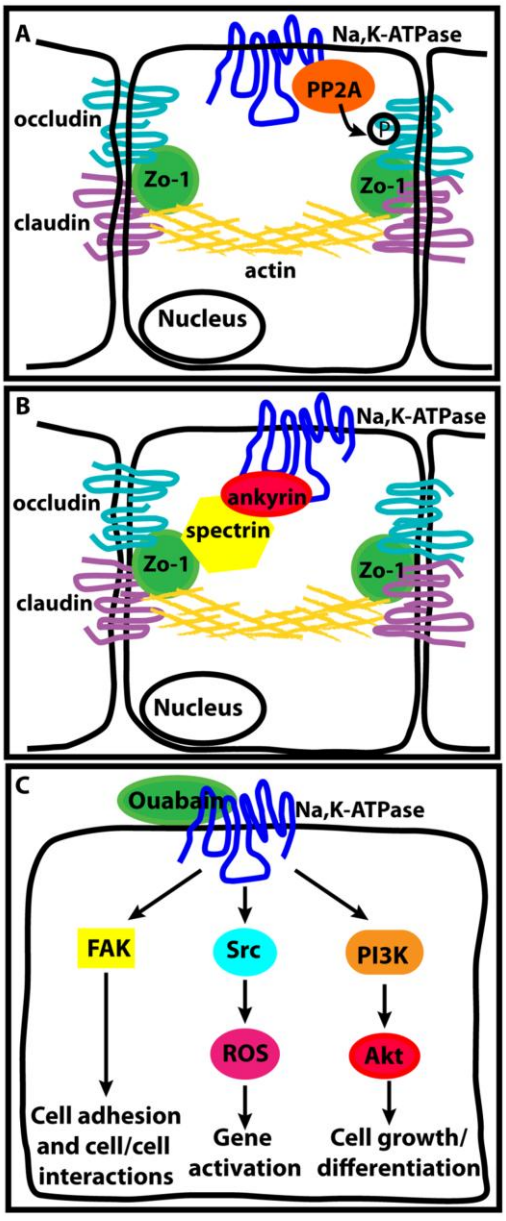

Figure 7.2: Pump-independent role of Na,K-ATPase. (A) Na,K-ATPase can interact with PP2A to regulate phosphorylation of tight junction protein occludin. (B) Na,K-ATPase binds to ankyrin/spectrin thus connecting to the actin cytoskeleton. (C) Ouabain induced signaling through the Na,K-ATPase can activate FAK, Src, and PI3K/Akt. ROS = reactive oxygen species.

Aside from the pumping function of the Na,K-ATPase, it can also participate in signal transduction through the binding of the endogenous cardiac glycoside, ouabain. Binding of ouabain to the Na,K-ATPase activates Src, FAK, and Akt signaling in cardiac myocytes (Figure 7.2C) (Liang et al., 2006; Xie, 2003). Furthermore, activation of Src leads to increased

levels of reactive oxygen species (ROS), which increases cell death. Consistent with the studies in cardiac myocytes, our data also suggest a pump-independent role of the Na,K-ATPase during brain ventricle development. First, measurement of intracellular Na^+ concentrations ($[Na^+]_i$) in the *snk*^{to273} mutant, which contains a point mutation in Atp1a1 abolishing pump function, revealed much higher $[Na^+]_i$ compared to *atp1a1* start site morphants suggesting a pump

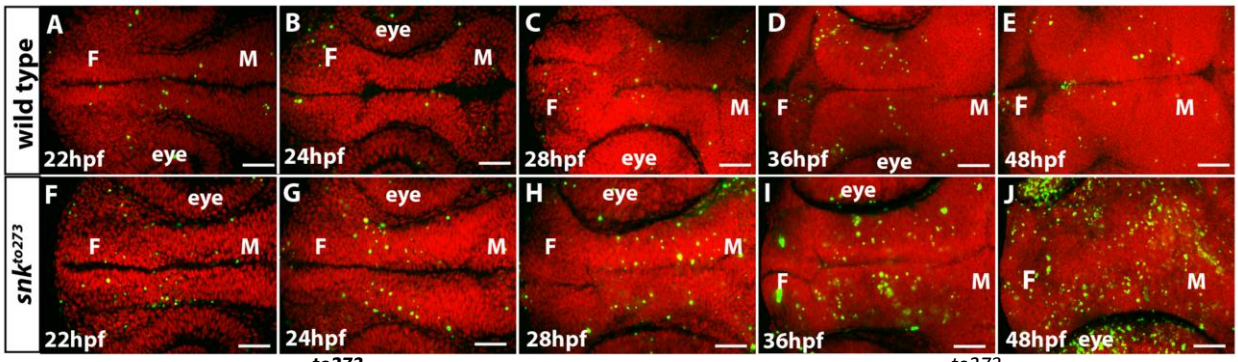

Figure 7.3: *snakehead* (*snk*^{to273}) mutant has elevated levels of cell death. (A-J) *snk*^{to273} cell death increases from 24-48 hpf (hours post fertilization) compared to wild type. Dorsal views of TUNEL (green; apoptosis) and all nuclei (red, propidium iodide) in wild type (A-E) and *snk*^{to273} (F-J) at 22 hpf (A,F), 24 hpf (B,G), 28 hpf (C,H), 36 hpf (D,I) and 48 hpf (E,J). Anterior to left. F = forebrain, M = midbrain. Scale bars =50 μm.

independent regulation of Na^+ (Chapter 2). Further, *snk*^{to273} mutants have extremely high levels of cell death (Figure 7.3) which is likely a combination of reduced eCSF signaling components such as retinoic acid (Chapter 3), in addition to possible Na,K-ATPase pump-independent increases in ROS.

<u>Regulating paracellular permeability and CSF retention.</u>

Once eCSF is produced, the brain ventricles must be able to retain it within the lumen. We identified that the Na,K-ATPase and RhoA regulate neuroepithelial permeability in embryonic zebrafish, however the mechanism of junction regulation remains unanswered. We propose that RhoA regulates paracellular permeability in the zebrafish neuroepithelium, based on the size selectivity of our dye retention assay. Consistent with these data, Claudin 5a, a component of the tight junction complex responsible for paracellular ion transport and selectivity, is required for brain ventricle inflation and permeability (Terry et al., 2010; Zhang et al., 2010). In cell culture, RhoA activation promotes claudin phosphorylation and regulates permeability by either modulating claudin-claudin interactions and/or recycling tight junction components (Yamamoto et al., 2008). Additionally, in endothelial barriers, ROCK, the downstream target of

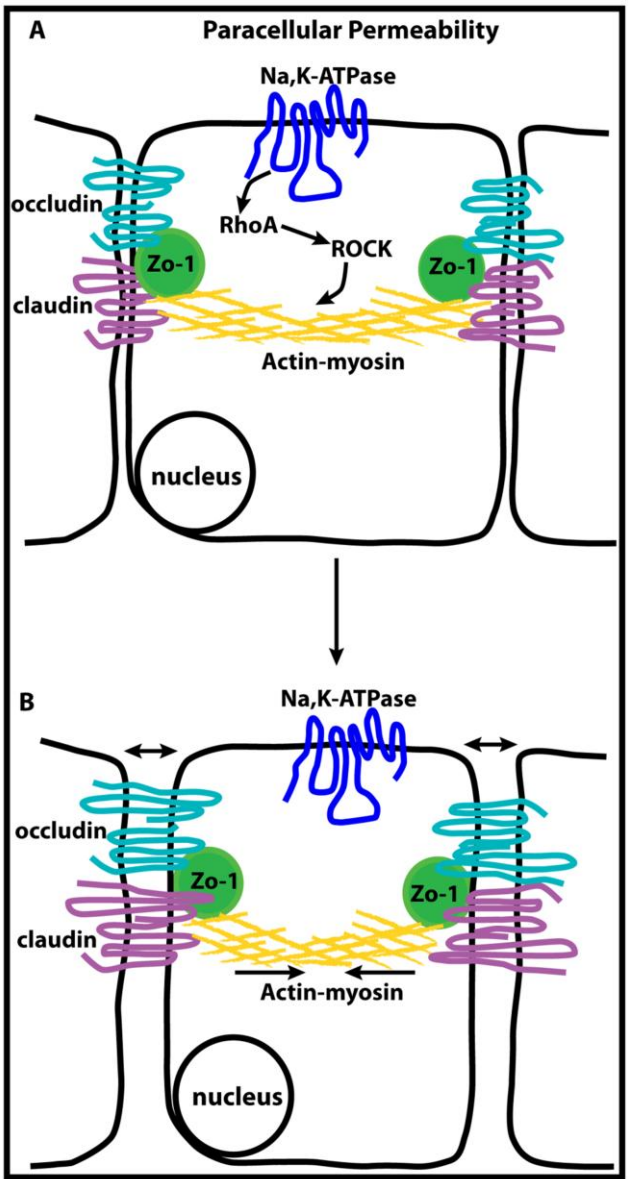

Figure 7.4: Paracellular permeability. (A) Na,K-ATPase activation of ROCK can promote actin myosin contraction and permeability (arrows in B).

activated RhoA, promotes paracellular transport by increasing actin-myosin contraction (Figure 7.4) (Shen et al., 2010). Thus, there are plausible connections between the Na,K-ATPase, RhoA and claudins.

Several other studies have identified a connection between Na^+ levels and RhoA activation (Rajasekaran and Rajasekaran, 2003). Although we did correlate abnormalities in brain ventricle development with elevated intracellular Na^+ concentration, we were not able to reliably detect activated RhoA (RhoA-GTP) in Na,K-ATPase loss-of-function embryos. Thus, identification of how Na,K-ATPase function can affect the activity of RhoA is still unknown. One hypothesis is that the absolute Na^+ concentration directly regulates RhoA activation. Alternatively, Na^+ levels may indirectly contribute to the membrane potential, which then regulates RhoA activity (Szaszi et al., 2005; Waheed et al., 2010). Further experiments to identify changes in RhoA-GTP, or a requirement for Rho-GEF and Rho-GAPs during brain ventricle development and the response to changes in membrane potential are needed to address these questions.

Mechanisms of eCSF and retinoic acid induced cell survival.

In Chapter 3, we demonstrated a requirement for eCSF and retinoic acid (RA) signaling during cell survival in the embryonic brain through activation of the PPARγ (peroxisome proliferator

activated receptor gamma) nuclear receptors. Further, we identified a subset of cells within the diencephalon which are more sensitive to the loss of eCSF and RA signaling. Currently, we are in the process of confirming specificity of the *rbp4* (retinol binding protein 4) morpholino, identifying the population of dying cells, and determining whether these cells express PPARγ receptors. However, there are many interesting questions which remain regarding the function of eCSF during embryonic zebrafish development.

Recent evidence suggests that RA regulates IGF (insulin like growth factor), FGF (fibroblast growth factor), Shh (Sonic hedgehog) and Wnt signaling (Blum and Begemann, 2012; Helms et al., 1994). IGF2 and FGF2 are also required within mouse and chick eCSF to promote cell proliferation and neurogenesis (Lehtinen et al., 2011; Martin et al., 2006; Salehi et al., 2009). However, our data demonstrate that IGF2 and FGF2 are not necessary for cell survival, and that removal of eCSF does not disrupt cell proliferation or neurogenesis at this stage of zebrafish development (Chapter 3). Therefore, we propose that RA is expressed early (25-30 hpf) to activate IGF and FGF signaling required later in development. In zebrafish, there are two waves of embryonic neurogenesis (Wullimann, 2009). The first occurs before 24 hpf (primary neurogenesis), is transitory, and allows for simple behaviors such as locomotion. The second occurs roughly around 48 hpf (secondary neurogenesis) when major brain structures begin to form and replace the early primary neurons. Therefore, it is possible that IGF2 and FGF2 are required at these later stages of development (36-48 hpf) in order to increase proliferation and promote secondary neurogenesis.

We identified that cell survival in the neuroepithelium requires Rbp4 and retinol. In zebrafish, *rbp4* is first (24 hpf) expressed in the yolk syncytial layer, a transient extra-embryonic syncytial tissue, and later expressed in the liver (Li et al., 2007). The yolk contains carotenoids and maternally deposited retinaldehydes both of which can be converted into the retinoic acid precursor, retinol (Lampert et al., 2003). Therefore, we propose that Rbp4 binds to retinol in the yolk, is transported to the eCSF, and is the source of retinoic acid. Alternatively, Rbp4 could be expressed at levels below the detection sensitivity of in situ hybridization within the neuroepithelium and directly secreted into the eCSF.

Our data demonstrate a requirement of RA and PPARγ signaling however, the downstream targets that are activated at this stage of development have yet to be determined. Previous work identified that RA signaling increases levels of Bcl2 which promotes anti-apoptotic signaling (Blum and Begemann, 2012). Additionally, PPARβ/δ receptors can stimulate cell survival and differentiation through the Akt signaling pathway (Di-Poi et al., 2002). However, the role of the γ isoform, PPARγ, during cell survival is largely unknown. Prior work has focused on PPARγ function during energy metabolism and has demonstrated that PPARγ is essential in brown adipose tissue for adipogenesis, differentiation, and lipid metabolism (Lowell, 1999; Rangwala and Lazar, 2004; Spiegelman, 1998). However, several studies suggest a role for PPARγ within the brain. Studies in mice demonstrate that PPARγ is expressed in hypothalamic neurons and a neuronal-specific knockout of PPARγ results in abnormal food intake, energy expenditure and insulin sensitivity (Lu et al., 2011; Sarruf et al., 2009). Additionally, several studies demonstrate a protective role for PPARγ in promoting recovery and preventing neuronal injury or death (Glatz et al., 2010; Zhao et al., 2009). Interestingly, in fish, increased glycolysis resulted in elevated levels of neuronal cell division, which is dependent on the PPARγ/ERK pathway (Song et al., 2009) suggesting a connection between PPARγ signaling, lipid metabolism and energy production in the brain.

Investigating the function of other eCSF components.

Our mass spectrometry analysis identified over 300 proteins in the embryonic zebrafish CSF. Encouragingly, many of these proteins are similar to those previously identified in mouse, rat, human and chick CSF (Gato et al., 2004; Parada et al., 2006; Parada et al., 2005; Parvas et al., 2008; Zappaterra et al., 2007). Of the proteins identified from zebrafish eCSF, a few stand out as particularly interesting candidates for future study.

Apolipoproteins and vitellogenins, two classes of proteins important for lipidogenesis were identified as some of the most abundant proteins in the embryonic zebrafish CSF. Surprisingly, apolipoproteins are mostly expressed in the yolk syncytial layer while vitellogenins, the precursor to yolk protein, are expressed in the whole body and excluded from the yolk (Thisse and Thisse, 2008). Lipid metabolism is crucial for embryonic brain development and for

neuronal migration in the embryonic cortex (Bock and Herz, 2003; Hiesberger et al., 1999; Trommsdorff et al., 1999). In fact, defects in lipid metabolism often result in craniofacial defects and holoprosencephaly (Willnow et al., 2007). Studies in embryonic chick have identified that apolipoproteins within the eCSF are required for neural progenitor differentiation (Parada et al., 2008). Further, lipoproteins have been implicated as essential transporters of sterols and morphogen signaling molecules (Willnow et al., 2007). Therefore, examination of lipids in embryonic zebrafish, its role within the eCSF, and its potential interaction with RA and other signaling pathways is of particular interest.

A second important class of proteins identified in our mass spectrometry analysis are involved in energy metabolism. In the mammalian brain around 50% of total energy consumption occurs in the brain and is required for neurotransmitter recycling, neural signaling, macromolecule turnover, and axonal transport (Attwell and Laughlin, 2001). However, the majority of energy produced is used to restore ion gradients and resting membrane potentials by the Na,K-ATPase (Astrup and Sorensen, 1981). Therefore, metabolism is an essential process required for normal brain function and abnormalities can lead to neurological disorders. For example, patients with hydrocephalus have elevated levels of lactate within the CSF suggesting a possible disruption in normal metabolism (Raisis et al., 1976). Consistent with these data, we identified lactate dehydrogenase within zebrafish eCSF suggesting that lactate production occurs within the eCSF. Additionally, work in the lab has identified a role for aldolase A, a glycolytic enzyme, during early embryonic brain development (Blaker-Lee et al., 2012 submitted). Given that energy regulation is clearly crucial to the brain, understanding the requirement for energy metabolism during early embryonic development, and identifying the metabolite profile in eCSF are avenues worth investigating.

CSF circulation in embryonic zebrafish.

We demonstrated that embryonic CSF circulates in the zebrafish, that this circulation is increased by the heartbeat, and that the CSF is separated into two compartments by the midbrain-hindbrain boundary, which acts as a physical barrier. However, what generates fluid flow prior to the heartbeat is unknown. Typically, cilia generate fluid movement and inhibition

of cilia movement and signaling results in increased fluid accumulation in the brain and kidney (Banizs et al., 2005; Fogelgren et al., 2011; Kramer-Zucker et al., 2005; Sun et al., 2004; Wodarczyk et al., 2009). Therefore, one hypothesis is that cilia physically generate CSF movement (Kramer-Zucker et al., 2005; Sullivan-Brown et al., 2008). Alternatively, cilia signaling may be required for CSF production, and CSF movement activates this signaling (Fogelgren et al., 2011; Schottenfeld et al., 2007; Sullivan-Brown et al., 2008). Analysis of eCSF flow using our Kaede assay in mutants that have no cilia, abnormal cilia movement or disrupted cilia signaling will identify whether the presence, movement, or signaling of cilia are required to regulate brain ventricle size, inflation and CSF flow.

In all vertebrates, CSF is continuously produced, moves through the brain ventricles and is eventually reabsorbed. CSF drainage in adult primates, sheep and rats occurs via the lymphatic system and, in conditions where there is elevated pressure, through the arachnoid granules as well (Boulton et al., 1999; Johnston, 2003; Johnston et al., 2005; Ludemann et al., 2005; Zakharov et al., 2003). Because the connection between the subarachnoid space and the lymphatic system develops around birth (Koh et al., 2006; Mollanji et al., 2001; Papaiconomou et al., 2002), the site of reabsorption in embryos is currently unknown.

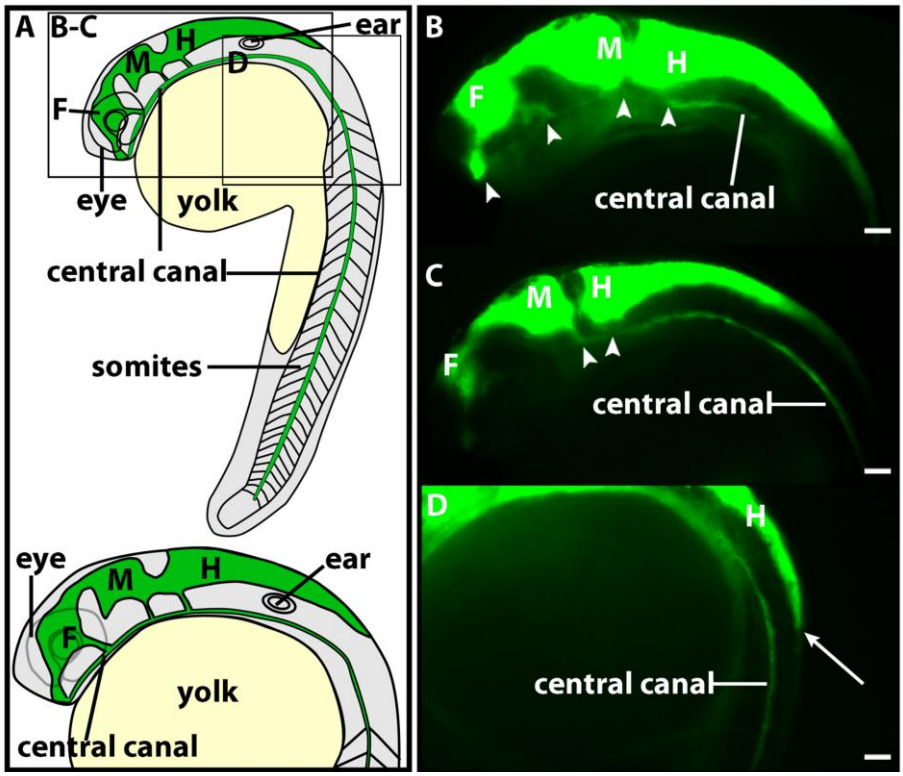

Figure 7.5: The zebrafish brain ventricular system. (A) Diagrams of the lateral view of the zebrafish brain ventricular system. Boxes indicate regions imaged in B-D. (B-D) Lateral views of 24 hpf embryos injected with 2000 kDa FITC-Dextran into the brain ventricles. Arrow heads = connections to central canal. Arrow = closure of hindbrain ventricle. Anterior to left, F = forebrain, M = midbrain, H = hindbrain. Scale bars = 50 μm.

Consistently, in the embryonic zebrafish,

lymphatic system is an unlikely CSF drainage route as it has not fully formed at this point during development. Therefore, embryonic CSF drainage likely occurs through the blood vasculature, interstitial fluid or diffusion between the CSF and the neuroepithelium or spinal canal.

The shape of the embryonic brain ventricles is highly conserved among vertebrates (Lowery et al., 2009). However in zebrafish, the hindbrain ventricle does not connect to the spinal cord at the most posterior end as is the case in other vertebrates (Figure 7.5, A, D arrow). Brain ventricle injection of a fluorescent FITC-dextran dye is visible in the central canal of the spinal cord indicating that the brain ventricles do connect to the spinal cord (Figure 7.5 A-D). We propose that in zebrafish, each ventricle has a ventral connection to the spinal cord allowing for fluid to drain directly into the central canal. In fact, connections with the spinal cord can be seen at the ventral-most region of the forebrain, midbrain and hindbrain (Figure 7.5 A-D, arrowheads). Further, we demonstrated that the zebrafish neuroepithelium is selectively permeable suggesting yet another route for CSF reabsorption (Chapter 2). Therefore, CSF is likely reabsorbed through diffusion in the neuroepithelium or spinal cord between the CSF and blood or interstitial fluid. Together, our data suggests that CSF produced in the ventricles, is circulated and eventually drains into the central canal of the spinal cord.

Abnormalities in CSF dynamics.

CSF production, retention, flow, and reabsorption are all finely balanced to regulate the pressure and volume of the brain ventricular system. Even a slight disturbance can affect the surrounding brain tissue. Moreover, CSF dynamics are crucial for the circulation of factors and removal of wastes and, when disrupted, can result in neurodegenerative disorders, mental health disorders and hydrocephalus (Johanson et al., 2004; Kay et al., 1987; Mashayekhi et al., 2002; Mashayekhi and Salehi, 2006; Rubenstein, 1998).

Interestingly, as animals age, CSF production and flow are reduced and this reduction may lead to age-related disorders (May et al., 1990; Preston, 2001; Stoquart-ElSankari et al., 2007). Indeed, CSF from patients with hydrocephalus and neurodegenerative disorders have elevated levels of growth factors and metabolites, and, moreover, this CSF abnormally regulates the proliferation and neurogenesis of the surrounding brain tissue (Mashayekhi et al., 2010a;

Mashayekhi et al., 2010b; Mashayekhi and Salehi, 2005; Mashayekhi and Salehi, 2006). Thus, in age-related disorders, a reduction of CSF production and flow likely leads to a build-up of metabolites that can lead to neurological disorders.

Understanding CSF dynamics is becoming an important area of research. The work we have done here demonstrate an intimate connection between the CSF and brain that is sensitive to disruption at multiple different levels. We contend that studying the development of the brain ventricular system will not only further our understanding of developmental disorders but may also lead to insight into adult pathologies and aging.

REFERENCES:

Astrup, J., Sorensen, H. R., 1981. Inhibition of cerebral metabolism by lidocaine. Eur Neurol. 20**,** 221-4.

Attwell, D., Laughlin, S. B., 2001. An energy budget for signaling in the grey matter of the brain. J Cereb Blood Flow Metab. 21**,** 1133-45.

Banizs, B., Pike, M. M., Millican, C. L., Ferguson, W. B., Komlosi, P., Sheetz, J., Bell, P. D., Schwiebert, E. M., Yoder, B. K., 2005. Dysfunctional cilia lead to altered ependyma and choroid plexus function, and result in the formation of hydrocephalus. Development. 132**,** 5329-39.

Blaker-Lee, A., Gupta, S., McCammon, J. M., Sive, H., 2012 submitted. Zebrafish 16p11.2 homologZebrafish 16p11.2 homologs are active during brain development, and include two deletion dosage sensor genes.s are highly active during brain development, and include at least two gene copy number sensors. Disease Models and Mechanisms.

Blum, N., Begemann, G., 2012. Retinoic acid signaling controls the formation, proliferation and survival of the blastema during adult zebrafish fin regeneration. Development. 139**,** 107-16.

Bock, H. H., Herz, J., 2003. Reelin activates SRC family tyrosine kinases in neurons. Curr Biol. 13**,** 18-26.

Boulton, M., Flessner, M., Armstrong, D., Mohamed, R., Hay, J., Johnston, M., 1999. Contribution of extracranial lymphatics and arachnoid villi to the clearance of a CSF tracer in the rat. Am J Physiol. 276**,** R818-23.

Dahl, J. P., Binda, A., Canfield, V. A., Levenson, R., 2000. Participation of Na,K-ATPase in FGF-2 secretion: rescue of ouabain-inhibitable FGF-2 secretion by ouabain-resistant Na,K-ATPase alpha subunits. Biochemistry. 39**,** 14877-83.

Davson, H., Segal, M. B., 1970. The effects of some inhibitors and accelerators of sodium transport on the turnover of 22Na in the cerebrospinal fluid and the brain. J Physiol. 209**,** 131-53.

Devarajan, P., Scaramuzzino, D. A., Morrow, J. S., 1994. Ankyrin binds to two distinct cytoplasmic domains of Na,K-ATPase alpha subunit. Proc Natl Acad Sci U S A. 91**,** 2965-9.

Di-Poi, N., Tan, N. S., Michalik, L., Wahli, W., Desvergne, B., 2002. Antiapoptotic role of PPARbeta in keratinocytes via transcriptional control of the Akt1 signaling pathway. Mol Cell. 10**,** 721-33.

Fogelgren, B., Lin, S. Y., Zuo, X., Jaffe, K. M., Park, K. M., Reichert, R. J., Bell, P. D., Burdine, R. D., Lipschutz, J. H., 2011. The exocyst protein Sec10 interacts with Polycystin-2 and knockdown causes PKD-phenotypes. PLoS Genet. 7**,** e1001361.

Gato, A., Martin, P., Alonso, M. I., Martin, C., Pulgar, M. A., Moro, J. A., 2004. Analysis of cerebro-spinal fluid protein composition in early developmental stages in chick embryos. J Exp Zool A Comp Exp Biol. 301**,** 280-9.

Glatz, T., Stock, I., Nguyen-Ngoc, M., Gohlke, P., Herdegen, T., Culman, J., Zhao, Y., 2010. Peroxisome-proliferator-activated receptors gamma and peroxisome-proliferator-activated receptors beta/delta and the regulation of interleukin 1 receptor antagonist expression by pioglitazone in ischaemic brain. J Hypertens. 28**,** 1488-97.

Helms, J., Thaller, C., Eichele, G., 1994. Relationship between retinoic acid and sonic hedgehog, two polarizing signals in the chick wing bud. Development. 120**,** 3267-74.

Hiesberger, T., Trommsdorff, M., Howell, B. W., Goffinet, A., Mumby, M. C., Cooper, J. A., Herz, J., 1999. Direct binding of Reelin to VLDL receptor and ApoE receptor 2 induces tyrosine phosphorylation of disabled-1 and modulates tau phosphorylation. Neuron. 24**,** 481-9.

Horisberger, J. D., Lemas, V., Kraehenbuhl, J. P., Rossier, B. C., 1991. Structure-function relationship of Na,K-ATPase. Annu Rev Physiol. 53**,** 565-84.

Johanson, C., McMillan, P., Tavares, R., Spangenberger, A., Duncan, J., Silverberg, G., Stopa, E., 2004. Homeostatic capabilities of the choroid plexus epithelium in Alzheimer's disease. Cerebrospinal Fluid Res. 1**,** 3.

Johnston, M., 2003. The importance of lymphatics in cerebrospinal fluid transport. Lymphat Res Biol. 1**,** 41-4; discussion 45.

Johnston, M., Zakharov, A., Koh, L., Armstrong, D., 2005. Subarachnoid injection of Microfil reveals connections between cerebrospinal fluid and nasal lymphatics in the non-human primate. Neuropathol Appl Neurobiol. 31**,** 632-40.

Kay, A. D., Schapiro, M. B., Riker, A. K., Haxby, J. V., Rapoport, S. I., Cutler, N. R., 1987. Cerebrospinal fluid monoaminergic metabolites are elevated in adults with Down's syndrome. Ann Neurol. 21**,** 408-11.

Keep, R. F., Xiang, J., Betz, A. L., 1994. Potassium cotransport at the rat choroid plexus. Am J Physiol. 267**,** C1616-22.

Koh, L., Zakharov, A., Nagra, G., Armstrong, D., Friendship, R., Johnston, M., 2006. Development of cerebrospinal fluid absorption sites in the pig and rat: connections between the subarachnoid space and lymphatic vessels in the olfactory turbinates. Anat Embryol (Berl). 211**,** 335-44.

Kramer-Zucker, A. G., Olale, F., Haycraft, C. J., Yoder, B. K., Schier, A. F., Drummond, I. A., 2005. Cilia-driven fluid flow in the zebrafish pronephros, brain and Kupffer's vesicle is required for normal organogenesis. Development. 132**,** 1907-21.

Lampert, J. M., Holzschuh, J., Hessel, S., Driever, W., Vogt, K., von Lintig, J., 2003. Provitamin A conversion to retinal via the beta,beta-carotene-15,15'-oxygenase (bcox) is essential for pattern formation and differentiation during zebrafish embryogenesis. Development. 130**,** 2173-86.

Lehtinen, M. K., Zappaterra, M. W., Chen, X., Yang, Y. J., Hill, A. D., Lun, M., Maynard, T., Gonzalez, D., Kim, S., Ye, P., D'Ercole, A. J., Wong, E. T., LaMantia, A. S., Walsh, C. A.,

2011. The cerebrospinal fluid provides a proliferative niche for neural progenitor cells. Neuron. 69**,** 893-905.

Li, Z., Korzh, V., Gong, Z., 2007. Localized rbp4 expression in the yolk syncytial layer plays a role in yolk cell extension and early liver development. BMC Dev Biol. 7**,** 117.

Liang, M., Cai, T., Tian, J., Qu, W., Xie, Z. J., 2006. Functional characterization of Src-interacting Na/K-ATPase using RNA interference assay. J Biol Chem. 281**,** 19709-19.

Lowell, B. B., 1999. PPARgamma: an essential regulator of adipogenesis and modulator of fat cell function. Cell. 99**,** 239-42.

Lowery, L. A., De Rienzo, G., Gutzman, J. H., Sive, H., 2009. Characterization and classification of zebrafish brain morphology mutants. Anat Rec (Hoboken). 292**,** 94-106.

Lu, M., Sarruf, D. A., Talukdar, S., Sharma, S., Li, P., Bandyopadhyay, G., Nalbandian, S., Fan, W., Gayen, J. R., Mahata, S. K., Webster, N. J., Schwartz, M. W., Olefsky, J. M., 2011. Brain PPAR-gamma promotes obesity and is required for the insulin-sensitizing effect of thiazolidinediones. Nat Med. 17**,** 618-22.

Ludemann, W., Berens von Rautenfeld, D., Samii, M., Brinker, T., 2005. Ultrastructure of the cerebrospinal fluid outflow along the optic nerve into the lymphatic system. Childs Nerv Syst. 21**,** 96-103.

Martin, C., Bueno, D., Alonso, M. I., Moro, J. A., Callejo, S., Parada, C., Martin, P., Carnicero, E., Gato, A., 2006. FGF2 plays a key role in embryonic cerebrospinal fluid trophic properties over chick embryo neuroepithelial stem cells. Dev Biol. 297**,** 402-16.

Mashayekhi, F., Draper, C. E., Bannister, C. M., Pourghasem, M., Owen-Lynch, P. J., Miyan, J. A., 2002. Deficient cortical development in the hydrocephalic Texas (H-Tx) rat: a role for CSF. Brain. 125**,** 1859-74.

Mashayekhi, F., Hadavi, M., Vaziri, H. R., Naji, M., 2010a. Increased acidic fibroblast growth factor concentrations in the serum and cerebrospinal fluid of patients with Alzheimer's disease. J Clin Neurosci. 17**,** 357-9.

Mashayekhi, F., Mirzajani, E., Naji, M., Azari, M., 2010b. Expression of insulin-like growth factor-1 and insulin-like growth factor binding proteins in the serum and cerebrospinal fluid of patients with Parkinson's disease. J Clin Neurosci. 17**,** 623-7.

Mashayekhi, F., Salehi, Z., 2005. Expression of nerve growth factor in cerebrospinal fluid of congenital hydrocephalic and normal children. Eur J Neurol. 12**,** 632-7.

Mashayekhi, F., Salehi, Z., 2006. Cerebrospinal fluid nerve growth factor levels in patients with Alzheimer's disease. Ann Saudi Med. 26**,** 278-82.

May, C., Kaye, J. A., Atack, J. R., Schapiro, M. B., Friedland, R. P., Rapoport, S. I., 1990. Cerebrospinal fluid production is reduced in healthy aging. Neurology. 40**,** 500-3.

Mollanji, R., Papaiconomou, C., Boulton, M., Midha, R., Johnston, M., 2001. Comparison of cerebrospinal fluid transport in fetal and adult sheep. Am J Physiol Regul Integr Comp Physiol. 281**,** R1215-23.

Murphy, V. A., Johanson, C. E., 1989. Alteration of sodium transport by the choroid plexus with amiloride. Biochim Biophys Acta. 979**,** 187-92.

Papaiconomou, C., Bozanovic-Sosic, R., Zakharov, A., Johnston, M., 2002. Does neonatal cerebrospinal fluid absorption occur via arachnoid projections or extracranial lymphatics? Am J Physiol Regul Integr Comp Physiol. 283**,** R869-76.

Parada, C., Gato, A., Aparicio, M., Bueno, D., 2006. Proteome analysis of chick embryonic cerebrospinal fluid. Proteomics. 6**,** 312-20.

Parada, C., Gato, A., Bueno, D., 2005. Mammalian embryonic cerebrospinal fluid proteome has greater apolipoprotein and enzyme pattern complexity than the avian proteome. J Proteome Res. 4**,** 2420-8.

Parvas, M., Bueno, D., 2010. The embryonic blood-CSF barrier has molecular elements to control E-CSF osmolarity during early CNS development. J Neurosci Res. 88**,** 1205-12.

Parvas, M., Parada, C., Bueno, D., 2008. A blood-CSF barrier function controls embryonic CSF protein composition and homeostasis during early CNS development. Dev Biol. 321**,** 51-63.

Pollay, M., Hisey, B., Reynolds, E., Tomkins, P., Stevens, F. A., Smith, R., 1985. Choroid plexus Na+/K+-activated adenosine triphosphatase and cerebrospinal fluid formation. Neurosurgery. 17**,** 768-72.

Preston, J. E., 2001. Ageing choroid plexus-cerebrospinal fluid system. Microsc Res Tech. 52**,** 31-7.

Raisis, J. E., Kindt, G. W., McGillicuddy, J. E., Miller, C. A., 1976. Cerebrospinal fluid lactate and lactate/pyruvate ratios in hydrocephalus. J Neurosurg. 44**,** 337-41.

Rajasekaran, A. K., Rajasekaran, S. A., 2003. Role of Na-K-ATPase in the assembly of tight junctions. Am J Physiol Renal Physiol. 285**,** F388-96.

Rajasekaran, S. A., Barwe, S. P., Gopal, J., Ryazantsev, S., Schneeberger, E. E., Rajasekaran, A. K., 2007. Na-K-ATPase regulates tight junction permeability through occludin phosphorylation in pancreatic epithelial cells. Am J Physiol Gastrointest Liver Physiol. 292**,** G124-33.

Rangwala, S. M., Lazar, M. A., 2004. Peroxisome proliferator-activated receptor gamma in diabetes and metabolism. Trends Pharmacol Sci. 25**,** 331-6.

Rosenthal, R., Milatz, S., Krug, S. M., Oelrich, B., Schulzke, J. D., Amasheh, S., Gunzel, D., Fromm, M., 2010. Claudin-2, a component of the tight junction, forms a paracellular water channel. J Cell Sci. 123**,** 1913-21.

Rubenstein, E., 1998. Relationship of senescence of cerebrospinal fluid circulatory system to dementias of the aged. Lancet. 351**,** 283-5.

Salehi, Z., Mashayekhi, F., Naji, M., Pandamooz, S., 2009. Insulin-like growth factor-1 and insulin-like growth factor binding proteins in cerebrospinal fluid during the development of mouse embryos. J Clin Neurosci. 16**,** 950-3.

Sarruf, D. A., Yu, F., Nguyen, H. T., Williams, D. L., Printz, R. L., Niswender, K. D., Schwartz, M. W., 2009. Expression of peroxisome proliferator-activated receptor-gamma in key neuronal subsets regulating glucose metabolism and energy homeostasis. Endocrinology. 150**,** 707-12.

Schottenfeld, J., Sullivan-Brown, J., Burdine, R. D., 2007. Zebrafish curly up encodes a Pkd2 ortholog that restricts left-side-specific expression of southpaw. Development. 134**,** 1605-15.

Shen, Q., Rigor, R. R., Pivetti, C. D., Wu, M. H., Yuan, S. Y., 2010. Myosin light chain kinase in microvascular endothelial barrier function. Cardiovasc Res. 87**,** 272-80.

Song, Y., Selak, M. A., Watson, C. T., Coutts, C., Scherer, P. C., Panzer, J. A., Gibbs, S., Scott, M. O., Willer, G., Gregg, R. G., Ali, D. W., Bennett, M. J., Balice-Gordon, R. J., 2009.

Mechanisms underlying metabolic and neural defects in zebrafish and human multiple acyl-CoA dehydrogenase deficiency (MADD). PLoS One. 4**,** e8329.

Spiegelman, B. M., 1998. PPAR-gamma: adipogenic regulator and thiazolidinedione receptor. Diabetes. 47**,** 507-14.

Stoquart-ElSankari, S., Baledent, O., Gondry-Jouet, C., Makki, M., Godefroy, O., Meyer, M. E., 2007. Aging effects on cerebral blood and cerebrospinal fluid flows. J Cereb Blood Flow Metab. 27**,** 1563-72.

Sullivan-Brown, J., Schottenfeld, J., Okabe, N., Hostetter, C. L., Serluca, F. C., Thiberge, S. Y., Burdine, R. D., 2008. Zebrafish mutations affecting cilia motility share similar cystic phenotypes and suggest a mechanism of cyst formation that differs from pkd2 morphants. Dev Biol. 314**,** 261-75.

Sun, Z., Amsterdam, A., Pazour, G. J., Cole, D. G., Miller, M. S., Hopkins, N., 2004. A genetic screen in zebrafish identifies cilia genes as a principal cause of cystic kidney. Development. 131**,** 4085-93.

Szaszi, K., Sirokmany, G., Di Ciano-Oliveira, C., Rotstein, O. D., Kapus, A., 2005. Depolarization induces Rho-Rho kinase-mediated myosin light chain phosphorylation in kidney tubular cells. Am J Physiol Cell Physiol. 289**,** C673-85.

Terry, S., Nie, M., Matter, K., Balda, M. S., 2010. Rho signaling and tight junction functions. Physiology (Bethesda). 25**,** 16-26.

Thisse, C., Thisse, B., 2008. Expression from: Unexpected Novel Relational Links Uncovered by Extensive Developmental Profiling of Nuclear Receptor Expression.

Trommsdorff, M., Gotthardt, M., Hiesberger, T., Shelton, J., Stockinger, W., Nimpf, J., Hammer, R. E., Richardson, J. A., Herz, J., 1999. Reeler/Disabled-like disruption of neuronal migration in knockout mice lacking the VLDL receptor and ApoE receptor 2. Cell. 97**,** 689-701.

Waheed, F., Speight, P., Kawai, G., Dan, Q., Kapus, A., Szaszi, K., 2010. Extracellular signal-regulated kinase and GEF-H1 mediate depolarization-induced Rho activation and paracellular permeability increase. Am J Physiol Cell Physiol. 298**,** C1376-87.

Welss, P., 1934. Secretory activity of the inner layer of the embryonic mid-brain of the chick, as revealed by tissue culture. The Anatomical Record. 58**,** 299-302.

Willnow, T. E., Hammes, A., Eaton, S., 2007. Lipoproteins and their receptors in embryonic development: more than cholesterol clearance. Development. 134**,** 3239-49.

Wodarczyk, C., Rowe, I., Chiaravalli, M., Pema, M., Qian, F., Boletta, A., 2009. A novel mouse model reveals that polycystin-1 deficiency in ependyma and choroid plexus results in dysfunctional cilia and hydrocephalus. PLoS One. 4**,** e7137.

Wullimann, M. F., 2009. Secondary neurogenesis and telencephalic organization in zebrafish and mice: a brief review. Integr Zool. 4**,** 123-33.

Xie, Z., 2003. Molecular mechanisms of Na/K-ATPase-mediated signal transduction. Ann N Y Acad Sci. 986**,** 497-503.

Yamamoto, M., Ramirez, S. H., Sato, S., Kiyota, T., Cerny, R. L., Kaibuchi, K., Persidsky, Y., Ikezu, T., 2008. Phosphorylation of claudin-5 and occludin by rho kinase in brain endothelial cells. Am J Pathol. 172**,** 521-33.

Zakharov, A., Papaiconomou, C., Djenic, J., Midha, R., Johnston, M., 2003. Lymphatic cerebrospinal fluid absorption pathways in neonatal sheep revealed by subarachnoid injection of Microfil. Neuropathol Appl Neurobiol. 29**,** 563-73.

Zappaterra, M. D., Lisgo, S. N., Lindsay, S., Gygi, S. P., Walsh, C. A., Ballif, B. A., 2007. A comparative proteomic analysis of human and rat embryonic cerebrospinal fluid. J Proteome Res. 6**,** 3537-48.

Zhang, J., Piontek, J., Wolburg, H., Piehl, C., Liss, M., Otten, C., Christ, A., Willnow, T. E., Blasig, I. E., Abdelilah-Seyfried, S., 2010. Establishment of a neuroepithelial barrier by Claudin5a is essential for zebrafish brain ventricular lumen expansion. Proc Natl Acad Sci U S A. 107**,** 1425-30.

Zhao, X., Strong, R., Zhang, J., Sun, G., Tsien, J. Z., Cui, Z., Grotta, J. C., Aronowski, J., 2009. Neuronal PPARgamma deficiency increases susceptibility to brain damage after cerebral ischemia. J Neurosci. 29**,** 6186-95.

APPENDIX ONE

The Na,K-ATPase beta subunit, Atp1b3a, is required for brain ventricle inflation

Contributions: Laura Anne Lowery (LAL) designed the Na,K-ATPase beta subunit morpholinos and performed initial dose-response experiments. LAL also supervised Jenny Ruan who performed Na,K-ATPase beta subunit in situ hybridizations shown in Figure A1.1B-G. I performed all other work for this Chapter.

ABSTRACT

Brain ventricle morphogenesis is a three step process requiring neuroepithelium formation, regulation of epithelial permeability and brain ventricle inflation. We previously demonstrated that the Na,K-ATPase subunits Atp1a1 and Fxyd1 are required for neuroepithelium formation whereas Atp1a1 alone regulates permeability and brain ventricle inflation (Chapter 2). Here, we investigated the role of the beta subunits in brain ventricle development. We found that *atp1b2a, atp1b3a,* and *atp1b3b* are all necessary for brain ventricle inflation but are not needed for neuroepithelial formation. Further we identified that loss of *atp1b3a* did not disrupt neuroepithelial permeability, brain ventricle size or intracellular sodium levels. Additionally, *atp1b3a* synergized with *fxyd1*, but not *atp1a1*, during neuroepithelial formation and this can be rescued with RhoA.

INTRODUCTION

The three dimensional development of the vertebrate central nervous system (CNS) is highly conserved throughout evolution. Deep within the brain lie a series of connected cavities called brain ventricles, which hold and retain the protein-rich cerebrospinal fluid (CSF). The brain ventricular system forms early during brain development, and is maintained into adulthood. This system is critical for proper development as abnormal formation of the brain ventricles can lead to devastating birth defects such as hydrocephalus and anencephaly.

During vertebrate embryonic development, the central lumen of the neural tube gives rise to the brain ventricular system. In zebrafish, the neural plate, a single sheet of cells, thickens and forms the neural keel. Next, cells intercalate and form apical-basal polarity and junctions resulting in a closed neural tube (Harrington et al., 2009; Hong and Brewster, 2006). The lumen of the neural tube then fills with CSF to open and inflate the brain ventricles (Lowery and Sive, 2005). Further expansion of the brain ventricles is driven by changes in cell morphology (Gutzman and Sive, 2010). Our previous study proposed that the Na,K-ATPase directs brain ventricle development by regulating three processes: formation of a cohesive neuroepithelium, regulation of epithelial permeability, and CSF production (Chapter 2).

The Na,K-ATPase is composed of three subunits, an alpha, a beta, and FXYD. The alpha subunit is required for ion pumping, whereas the beta subunit is obligatory for alpha subunit maturation, K^+ transport and correct cellular localization (Geering, 2001; Jaisser et al., 1994; Wilson et al., 2000; Wilson et al., 1991). Indeed, in the absence of beta, the alpha subunit remains in the ER, cannot integrate into the membrane, and is subsequently degraded (Geering, 2001). Further, studies in MDCK (Madin Darby canine kidney) cells demonstrated that the beta subunit promotes translation of the alpha subunit (Rajasekaran et al., 2003). Several lines of evidence support the hypothesis that the beta subunit can play a role in intracellular trafficking of the alpha subunit. Vagin et al. found that the extracellular N-terminus of the beta subunit is heavily glycosylated (Vagin et al., 2007a), and proposed that this modification specifically directs trafficking, membrane targeting and plasma membrane retention of the Na,K-ATPase (Lian et al., 2006; Vagin et al., 2007a). In related studies, Shoshani et al.

demonstrated that polycystic kidney disease epithelia have apically localized alpha subunits due to increased β2 subunit expression whereas in wild type β1 and the alpha are localized basolaterally. Furthermore, the polarized distribution of the alpha subunit is dependent on beta subunit association between cells (Shoshani et al., 2005). Finally, recent work demonstrates that beta subunits can mediate cell-cell adhesion, regulate epithelial permeability (Gloor et al., 1990; Shoshani et al., 2005; Vagin et al., 2007a; Vagin et al., 2006; Vagin et al., 2008; Vagin et al., 2007b), and are required for proper epithelial junction formation in MDCK cells, *Drosophila* trachea and mouse blastocysts (Madan et al., 2007; Paul et al., 2007; Paul et al., 2003; Rajasekaran et al., 2001).

We previously demonstrated that the zebrafish Na,K-ATPase alpha, Atp1a1, and Fxyd1 subunits are involved in neuroepithelial formation, whereas Atp1a1 also plays a role in neuroepithelial permeability and brain ventricle inflation (Chapter 2). Here we investigate the requirement for the beta subunit during zebrafish brain ventricle development and identify that Atp1b3a is required for brain ventricle inflation. Further, Atp1b3a synergizes with Fxyd1 but not Atp1a1.

MATERIALS AND METHODS

Fish lines and maintenance

Wild type (AB) *Danio rerio* fish were raised and bred according to standard methods (Westerfield et al., 2001). Embryos were kept at 28.5^{o}C and staged according to Kimmel et al., (Kimmel et al., 1995). Times of development are expressed as hours post-fertilization (hpf).

Antisense morpholino oligonucleotide (MO) injection

Start site or splice-site blocking morpholino (MO) antisense oligonucleotide (Gene Tools, LLC) were injected into once cell stage embryos (Draper et al., 2001; Nasevicius and Ekker, 2000)). MOs used included, 5ng *atp1b1a* start site 5'-ACCATCTTTATTTGCGGGCTTTTC-3', 5ng *atp1b2a* start site 5'-GCCATGTCTCCGGTAGATTCTCGGT-3', 5 ng or 2.5ng *atp1b3a* splice site (exon 2-intron 3) 5'-AACTGCACACTAACAAACTTACCTG-3', 5ng *atp1b3b* splice site (intron 2 –exon 3) 5'-CAGCCCTGTGGACAAAATAGGCCAA-3', and 0.5ng *FXYD1* (intron4-exon5) 5'-CTGTGATAATCTAGAGAGAGAGACA-3'. Standard control MO used is 5'-

CCTCTTACCTCAGTTACAATTTATA-3 ' and *p53* morpholino 5'-GCGCCATTGCTTTGCAAGAATTG-3' (Gene Tools, LLC).

cDNA constructs

The full-length *atp1b3a* construct was made with a minimal Kozak consensus sequence adjacent to the initiating ATG was generated by RT-PCR with primers *b3aF*, 5'-CACCATGTCTAAAAAGAGCGAAAAT-3' and *b3aR*, 5'-AGCACAAGTTCCCCTTCAGC-3'. The PCR fragments were subcloned into pGEM-T Easy Vector (Promega), and then subcloned into the EcoRI site in pCS2+.

C terminal FLAG tagged Atp1b3a was generated by PCR. Briefly, primers were designed to add a linker (S-G-G-G-G-S) followed by the FLAG tag (DYKDDDDK) between the last codon and stop codon using full length *atp1b3a* in pCS2+ as a template. Primers used were: *b3aFLAG2L* 5'-GACGATGACAAGTAAAGCCTCTAGAACTATAGTGAGTCGTATTAC-3' , *b3aFLAG2R* 5' – GTCCTTGTAGTCAGAGCCGCCTCCACCAGATTCGGTCACCAGGACCCGGAAGGT-3'.

pCS2+RhoAV14 were kindly provided by R. Winklbauer (University of Toronto) and K. Symes (Boston University).

Capped *atp1b3a, atp1b3a-FLAG, RhoAV14* and *mGFP* were transcribed in vitro using the SP6 mMessage mMachine kit (Ambion), after linearization by Not1. Embryos were injected at the one cell stage with 50-100 pg mRNA.

RT-PCR

RNA was extracted from morphant and control embryos using Trizol reagent (Invitrogen), followed by chloroform extraction and isopropanol precipitation. RNA was pelleted by centrifugation, resuspended in water and precipitated with $LiCl_2$. cDNA synthesis was performed using Super Script III Reverse Transcriptase (Invitrogen) plus random hexamers (Invitrogen). To determine changes in splicing, PCR was then performed using primers which amplified the exonic and intronic sequence surrounding the splice MO target. Primers used include: *b3atestF* 5'-GCAGTGATTTCAGCCTCCTC-3' and *b3atest R* 5'-GTATCCTCCATCCCAGAGCA-

3'. For beta expression, primers used include: *b1aF* 5'-ACACCACCAAAAAGGGAACT-3', *b1aR* 5'-GTGTTTTGAAATGGGCAGAA-3', *b1bF* 5'-GTCCTCAAGTGGACAAACA-3', *b1bR* 5'-GGCCTTAGTTTGCCTTTCAGT-3', *b2aF* 5'-GCGTTTATTCCAAGCGGTTA-3', *b2aR* 5'-GCGTTTATTCCAAGCGGTTA-3', *b2bF* 5'-CATATTCCTGGCTGGATTGTG-3', *b2bR* 5'-GGGTTTGCCTTCATCGTAAC-3', *b3aF* 5'-CACCATGTCTAAAAAGAGCGAAAAT-3', *b3aR* 5'-AGCACAAGTTCCCCTTCAGC-3', *b3bF* 5'-CATCCATCGCTCTCAAACTG-3', and *b3bR* 5'-ATGGACGTGATGGACATGAA-3'.

In situ hybridization

RNA probes, containing digoxigenin (DIG)-11-UTP, were synthesized from linearized plasmid DNA, as described (Harland, 1991). Standard methods for hybridization and single color labeling were used as described (Sagerstrom et al., 1996). After staining, embryos were fixed in 4% paraformaldehyde overnight at 4^{o}C, and washed in PBT (PBS + .01% Tween). Embryos were either imaged right away or dehydrated in methanol and cleared in a 3:1 benzyl benzoate/benzyl alcohol (BB/BA) solution before mounting and imaging with a Nikon compound microscope or Zeiss dissecting scope.

Brightfield brain imaging, ventricle injections, forebrain ventricle size and dye retention assay

Brightfield brain imaging: Embryos were anesthetized in 0.1 mg/mL Tricaine (Sigma) dissolved in embryo medium (Westerfield et al., 2001) during imaging. Images were taken using a Leica dissecting scope and KT Spot digital camera (RT KE Diagnostic instruments). Images were adjusted for brightness, contrast and coloring in Photoshop CS5 (Adobe). Line tracings of brain morphology were done using Xara Xtreme Pro (Xara Group Ltd).

Brain ventricle injections: Methods for brain ventricle imaging after ventricle injection have been described previously (Gutzman and Sive, 2009; Lowery and Sive, 2005). Briefly, 1 nL of 2000 kDa dextran conjugated to Rhodamine (Invitrogen, 2.5 mg/ml in water) was injected into the forebrain ventricle and between the midbrain and hindbrain ventricle.

Forebrain ventricle size quantification: The forebrain ventricle area was measured with Image J software using a dorsal brightfield image taken as described above. Statistical analysis was performed with GraphPad InStat software.

Dye retention Assay: 70 kDa dextran conjugated to FITC (Invitrogen, 2.5 mg/ml in water) was injected into the brain ventricles at 22 hpf and imaged at various time-points as noted in the text. Neuroepithelial permeability was quantified using Image J software to measure the distance of the dye front from the forebrain ventricle hinge-point. Statistics were performed with GraphPad InStat software.

Immunohistochemistry and Western Blots

Whole mount immunostaining was performed with phallodin-Texas Red/TRITC or FITC (Molecular probes 1:200), aPKC (santa cruz 1:1000), Zo-1 (Invitrogen, 1:100), FLAG (Sigma, 1:500) and Na,K-ATPase (alpha) (Cell Signaling Technology, 1:100). Embryos were fixed with 4% PFA or 2% TCA from either for 2 hours at room temperature or overnight at 4^{o}C and blocked overnight at 4^{o}C 4 hours at room temperature. Blocking solutions used were: 2% NGS+ 1% Triton+1% BSA (aPKC) and 5%NGS+ 1% Triton (Zo-1, NaKATPase, FLAG). Propidium iodide and phalloidin were diluted in PBT and incubated at room temperature for 45 minutes or overnight respectively. Secondary antibodies used were goat anti-mouse Alexa Fluor 488, goat anti-rabbit Alexa Fluor 488 (1:500, Invitrogen). Brains were flat-mounted in glycerol and imaged with Zeiss LSM scanning confocal microscope. For Western blots, soluble proteins were run on Tris-HCl SDS PAGE gel and detected using antibodies to Na,K-ATPase (alpha) (Cell Signaling Technology, 1:500).

Intracellular Na^{+} Measurement

Dechorionated and deyolked embryos were collected at 24-28 hpf in 300 μl of nuclease free water. Embryos were dounce homogenized, spun at 1000 rpm, and supernatant collected. CoroNa Green (Invitrogen 10 μM) added to supernatant and fluorescence readings obtained using a Tecan Safire II microplate reader. A hemocytometer was used to determine number of cells per embryo (Westerfield et al., 2001).

RESULTS

Na,K-ATPase beta subunits are expressed at the time of brain ventricle development.

The *Danio rerio g*enome contains seven beta subunits. We analyzed expression of six of these subunits (all beta subunits identified at the time of the study) at various points of development using RT-PCR. We found that at 10 hpf only *atp1b1a*, *atp1b2a, atp1b3b* and *atp1b3a* were expressed but by 24 hpf, all six were expressed (Figure A1.1A). This expression level was maintained at 36 hpf, confirming the results of Canfield et al., (Canfield et al., 2002).

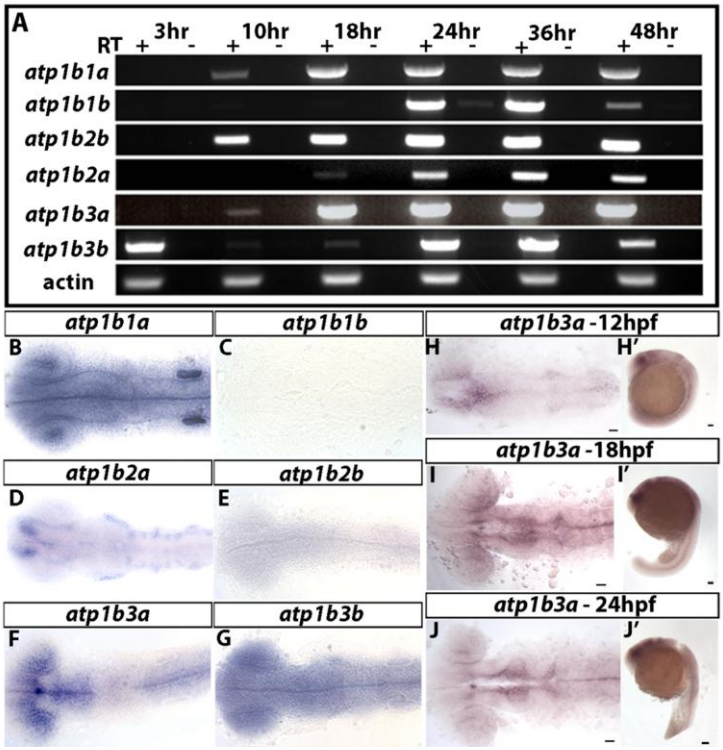

Figure A1.1: Expression of zebrafish Na,K-ATPase beta subunits. (A) RT-PCR analysis of whole embryos at 3, 10, 18, 24, 36, and 48 hpf. With RT (+) and without RT (-). (B-J) In situ hybridization of beta subunits at 18 hpf. (B-G) or *atp1b3a* at 12 (H), 18 (I) or 24 hpf (J). Dorsal (B-J) and lateral (H'-J') views. Anterior to left. Scale bars = 50 μm.

To localize beta expression within the brain, we performed in situ hybridization in 18 hpf embryos just prior to brain ventricle inflation. We found that *atp1b1a* and *atp1b3b* were expressed ubiquitously in the brain (Figure A1.1B, G), whereas *atp1b2a* is specific to known locations of neuronal differentiation (Figure A1.1D). Consistent with our RT-PCR experiments, we did not observe expression of *atp1b1b* or *atp1b2b* at this time point (Figure A1.1C, E). Interestingly, *atp1b3a* expression was anteriorly localized at 12 hpf (Figure A1.1H) and continued to be expressed from 18-24 hpf in the brain at higher levels in the midbrain and forebrain (Figure A1.1F,I-J), indicating that this particular subunit is expressed in the neural tissue at the time of neuroepithelial formation (12 hpf) and brain ventricle inflation (18-24 hpf) .

Na,K-ATPase beta subunits are required for brain ventricle inflation.

To identify whether the Na,K-ATPase beta subunit is required for brain ventricle inflation or neuroepithelial formation, we designed splice-site blocking morpholino antisense oligonucleotides (MO) against *atp1b1a, atp1b2a, atp1b3a,* and *atp1b3b*. We did not examine the effect of *atp1b1b* or *atp1b2a* loss of function as we could not detect their expression during the time of brain ventricle development. Loss of *atp1b1a* (23/28 wild type) did not affect brain ventricle inflation compared to wild type (16/16 wild type) (Figure A1.2A-B), whereas loss of

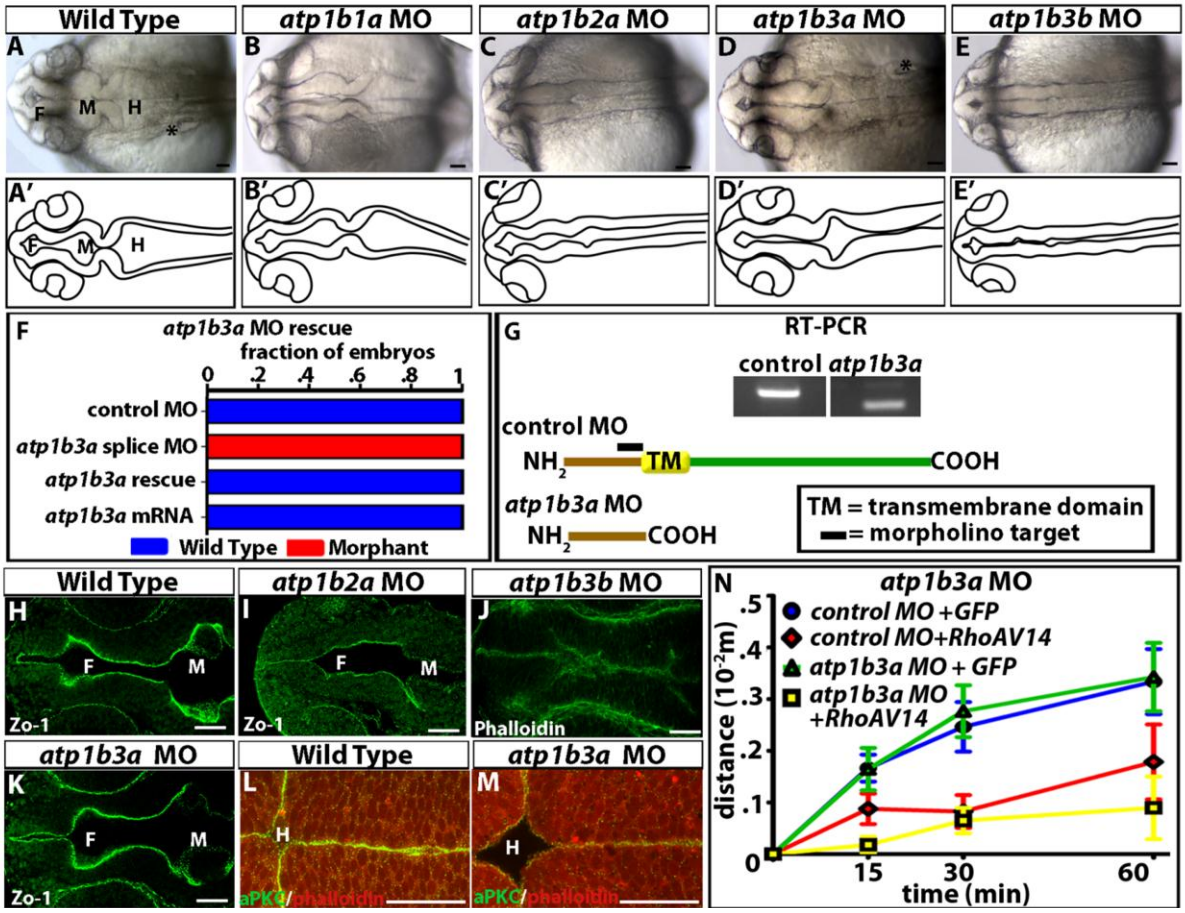

Figure A1.2: Beta subunits are necessary for brain ventricle inflation. (A-E) Dorsal brightfield images of (A) wild type, or MO loss of function of (B) *atp1b1a*, (C) *atp1b2a*, (D) *atp1b3a* and (E) *atp1b3b*. (A'-E') corresponding tracings of (A-E). (F) Quantification of *atp1b3a* MO rescue. (G) RT-PCR analysis of *atp1b3a* MO splicing. (H-K) Zo-1 or phallodin staining. (L-M) aPKC (green) and phalloidin (actin, red) staining in (L) wild type vs. (M) *atp1b3a* morphants. (N) Dye retention assay in control MO, *atp1b3a*MO, control MO + *RhoAV14* or *atp1b3a* MO + *RhoAV14*. Data represented as mean +/- SEM. All images of 24 hpf, anterior to the left. Asterisk = ear. F = forebrain, M = midbrain, H = hindbrain. Scale bars = 50 μm.

atp1b2a (4/17 wild type), *atp1b3a* (0/31 wild type), or *atp1b3b* (0/36 wild type) led to decreased brain ventricle inflation as identified by a reduction in brain ventricle size (Figure

A1.2C-E). Interestingly, inhibition of *atp1b3a* resulted in reduced forebrain and midbrain ventricles, consistent with in situ expression pattern (Figure A1.2D). Specificity of the *atp1b3a* loss-of-function phenotype was shown by phenotypic rescue with the cognate zebrafish mRNA that does not hybridize to the MO sequence (Figure A1.2F, fraction wild type in control MO=35/35, *atp1b3a* MO = 0/60, *control* MO + *atp1b3a* = 35/35, *atp1b3a* MO + *atp1b3a* = 32/32). RT-PCR analysis of *atp1b3a* morphants (i.e. embryos with loss of function by morpholino) revealed the generation of an early stop codon before the transmembrane domain (Figure A1.2G). Further experiments are needed to determine the specificity of the other beta morpholinos. Taken together, these data demonstrate a requirement for beta subunits during brain ventricle development.

To determine whether the Na,K-ATPase beta subunits play a role during neuroepithelial formation, we examined the apical junction and polarity complex in beta loss of function embryos. Apical junctions were labeled using Zo-1, which is a component of the adherens and tight junctions, or phalloidin which binds to actin. Additionally, aPKC was used as a marker of apical polarity. In wild type embryos, the apical junctions form a continuous apical band (Figure A1.2H, 5/5 wild type). *atp1b2b* (11/11 wild type), *atp1b3a* (10/10 wild type) *and atp1b3b* morphants (9/9 wild type) did not show a change in localization or continuity of the apical junctions (Figure A1.2I-K). Due to its interesting expression pattern and loss-of-function phenotype, we performed a more detailed analysis of Atp1b3a beta subunit function. Interestingly, in *atp1b3a* morphants, apical polarity is also normal as seen by continuously localized apical aPKC (Figure A1.2L-M). Together these data demonstrate that beta subunits individually do not disrupt the apical junction complex.

The decrease in brain ventricle inflation observed in *atp1b3a* morphants could be due to either abnormal CSF production or increased neuroepithelial permeability. Therefore, using our dye retention assay (Chapter 5), we quantified neuroepithelial permeability in either wild-type or *atp1b3a* morphant embryos at 22-24 hpf. We did not observe a difference in permeability in *atp1b3a* morphants (Figure A1.2N green, n=16) compared to controls (Figure A1.2N blue, n=23). This suggests that *atp1b3a* alone does not regulate neuroepithelial permeability. We

previously demonstrated that RhoA acts downstream of Atp1a1 to regulate neuroepithelial permeability. Therefore we asked whether RhoA could reduce permeability in *atp1b3a* morphants. To test this hypothesis, we injected a constitutively active human *RhoA* mRNA (*RhoAV14*), at a concentration which did not affect development in wild type embryos, into *atp1b3a* morphants or controls. Overexpression of *RhoAV14* decreased permeability in *atp1b3a* morphants (Figure A1.2N yellow, n=11, p<.01) comparable to overexpression of *RhoAV14* in controls (Figure A1.2N red, n=9, p<.01). Thus, although RhoA can regulate neuroepithelial permeability, it does not act downstream of *atp1b3a* and *atp1b3a* is not required for neuroepithelial permeability.

These data show that *atp1b3a*, *atp1b2a* and *atp1b3b* loss of function reduced brain ventricle inflation. As some of the beta functions may be redundant in individual genes, combinations of beta subunit loss of function may be required to completely identify a potential role in regulation of the apical junction complex formation and neuroepithelial permeability. Furthermore, experiments to address the specificity of the morphant phenotype and analyze the possible regulation of neuroepithelial formation and permeability should be undertaken.

Atp1b3a is required for CSF production.

Brain ventricle inflation requires both CSF retention and production. Since *atp1b3a* alone is not required for CSF retention, we hypothesized that the reduction in brain ventricle inflation observed in *atp1b3a* morphants is due to a reduction in CSF production. In order to further understand the mechanism by which *atp1b3a* regulates brain ventricle inflation, we asked whether an overexpression of *atp1b3a* changes brain ventricle size. We previously demonstrated that overexpression of *atp1a1* increases dye retention and CSF production (Chapter 2). However, *atp1b3a* gain of function (n=5) did not significantly alter the size of the brain ventricles compared to control mRNA (*mGFP*, n=19) injected embryos (Figure A1.3A-C) demonstrating that although Atp1b3a may be necessary for brain ventricle inflation, it is not sufficient. This suggests that Atp1b3a cannot act alone to promote brain ventricle inflation and that another factor, likely Atp1a1, is rate-limiting in Atp1b3a gain-of-function embryos.

We have identified that CSF production is a RhoA-independent process. Therefore, we hypothesize that if Atp1b3a directly regulates CSF production, it does so through modulation of the osmotic gradient. Thus, an important question arising from our data is whether intracellular Na^+ concentration ($[Na^+]_i$) would increase as a result of loss of *atp1b3a* function. We measured intracellular Na^+ ($[Na^+]_i$) levels at 24 hpf, using the CoroNa Green dye in wild-type or *atp1b3a* morphant embryos. Loss of *atp1b3a* did not significantly alter $[Na^+]_i$ compared to control levels (Figure A1.3D), suggesting that Atp1b3a affects CSF production independent of Na^+ concentration. We cannot, however, rule out the possibility that other beta subunits can compensate for the loss of *atp1b3a* in regulating $[Na^+]_i$ levels.

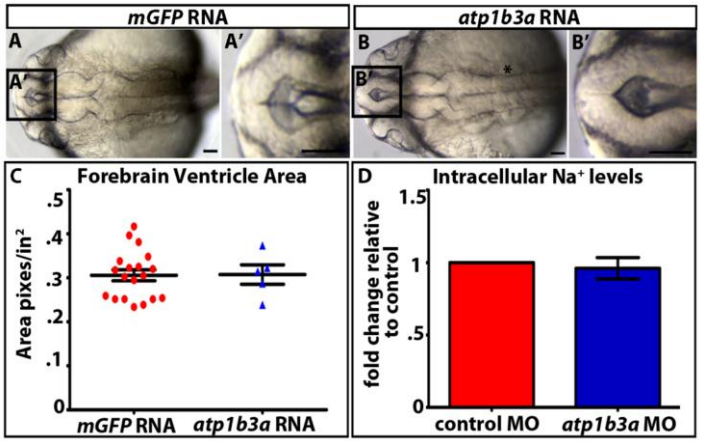

Figure A1.3: Atp1b3a does not regulate brain ventricle size or intracellular sodium. (A-B) Dorsal brightfield images of embryos expressing (A) control RNA (*mGFP*) or (B) *atp1b3a* mRNA gain of function (GOF). (A'-B') Magnified view of forebrain ventricle. (C) Quantification of forebrain ventricle area in *mGFP* (red) or *atp1b3a* GOF (blue). (D) Measurement of $[Na^+]_i$ in control MO (red) vs. *atp1b3a* MO (blue). Data = mean+/-SEM from 3 experiments. All images 24 hpf, anterior to the left. Asterisk = ear. Scale bars = 50 μm.

These data further support the hypothesis that the beta subunits are functionally redundant and Atp1b3a does not function alone during brain ventricle inflation.

Atp1a1, Atp1b3a and Fxyd1 function together to regulate brain ventricle development.

Experiments in other systems indicate that the Na,K-ATPase subunits interact both physically and functionally. To investigate whether Atp1b3a physically interacts with Atp1a1 in zebrafish, we performed fluorescence co-localization experiments. We expressed a FLAG tagged version of Atp1b3a and performed immunohistochemistry to detect endogenous Atp1a1 using an anti-Na,K-ATPase antibody, and Atp1b3a using an anti-FLAG antibody. At 24 hpf, we observed that zebrafish Atp1a1 co-localizes with Atp1b3a (Figure 4A-D, white arrow) suggesting that Atp1a1 and Atp1b3a can physically interact. Additionally, we observed Atp1a1 alone (Figure A1.4 A-D, blue arrow) and Atp1b3a alone (Figure A1.4A-D, yellow arrow) demonstrating that these

subunits can be present either together, individually or potentially with other unlabeled beta subunits. We could not directly assess whether Fxyd1 co-localizes with Atp1b3a since tagged versions of this protein were not compatible with tagged Atp1b3a, however we have demonstrated that both Atp1b3a (Figure A1.4A-D) and Fxyd1 (Chapter 2) can interact with Atp1a1. These data show that zebrafish Atp1b3a physically interacts with Atp1a1 and likely Fxyd1.

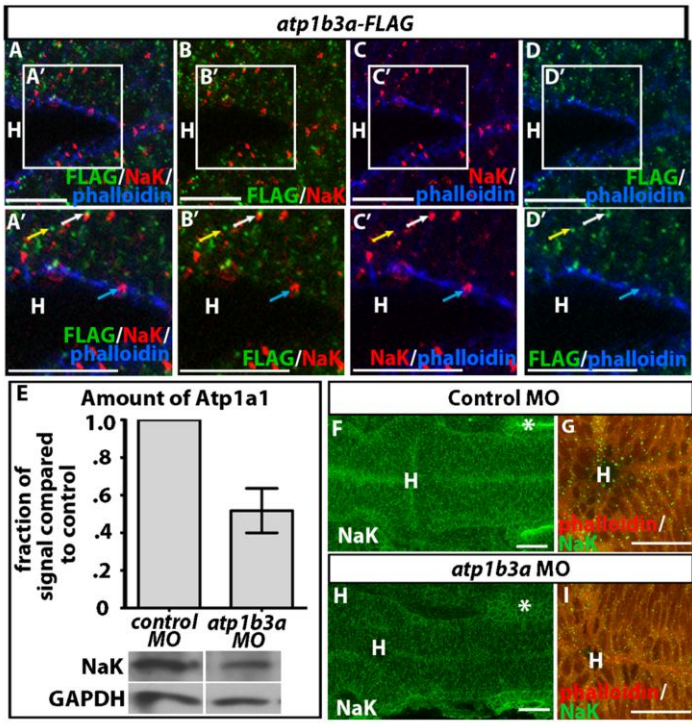

Figure A1.4: Atp1b3a interaction with Atp1a1. (A-D) Atp1b3a-FLAG (green) Na,K-ATPase (NaK, red) and actin (phalloidin, blue). Co-localization (white arrow), Atp1a1 alone (blue arrow) Atp1b3a alone (yellow arrow). (A'-D') magnification of A-D. Scale bars = 10 μm. (E) Western blot of Atp1a1, in 24 hpf whole embryo in *atp1b3a* MO vs. control MO. Data from at least 3 experiments and represented as mean +/- SEM. (F-I) Atp1a1 localization in 18 hpf control (F-G) vs. *atp1b3a* MO (H-I). NaK alone (F,H) or with phalloidin (G,I). Anterior to the left. Asterisk = ear. H = hindbrain. Scale bars = 50 μm.

The Na,K-ATPase beta subunits stabilize alpha subunit protein, prevent its degradation, and correctly localize it to the appropriate side of the cell. To further investigate interactions between Atp1a1 and Atp1b3a, we measured changes in levels of Atp1a1, after loss of Atp1b3a. Using a western blot, we quantified the Atp1a1 protein in *atp1b3a* loss-of-function embryos at 24 hpf. This assay revealed decreased amounts of Atp1a1 in *atp1b3a* morphants relative to wild type (Figure A1.4E). Because these experiments required the use of whole embryos, we could not determine if Atp1a1 levels were specifically decreased in the neuroepithelium. To address this question, we detected Atp1a1 by immunohistochemistry in the zebrafish embryonic brain at 18 hpf. In embryos injected with a control morpholino, Atp1a1 appeared as puncta localized throughout the length of the neuroepithelium and was enriched at the apical surface (Figure A1.4F-G). However, despite the reduction in the amount of Atp1a1 in *atp1b3a* morphants, the Atp1a1 protein remaining was not mis-localized compared to controls (Figure A1.4H-I). Thus, either Atp1b3a regulates levels of Atp1a1 protein but not localization or *atp1b3a* loss of function can

be compensated by other beta subunits to correctly localize Atp1a1. Furthermore, the data are consistent with the hypothesis that zebrafish Atp1b3a regulates levels of Atp1a1 protein, and these subunits functionally interact during brain ventricle development.

To determine whether *atp1b3a* functionally interacts with Atp1a1 and Fxyd1 during brain ventricle development, we asked whether *atp1b3a* synergizes with *atp1a1* and *fxyd1*. Embryos

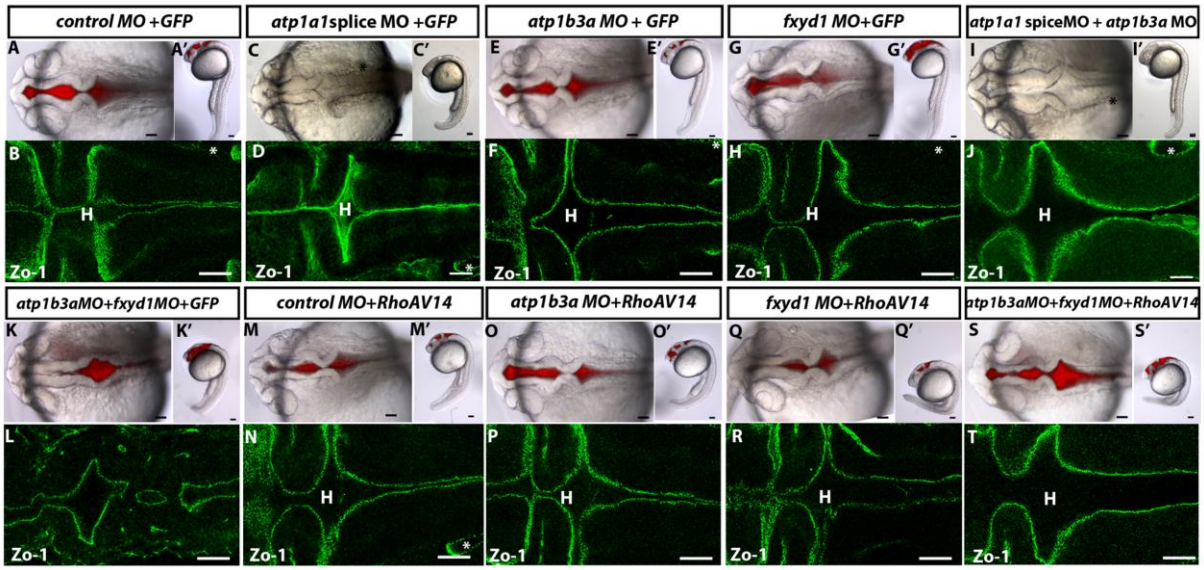

Figure A1.5: *atp1b3a* synergizes with *fxyd1* and is rescued by *RhoA*. (A-B) Control MO compared to low levels of (C-D) *atp1a1* splice site MO, (E-F) *atp1b3a* MO or (G-H) *fxyd1* MO. (I-J) *atp1a1* splice MO and *atp1b3a* MO synergy, (K-L) *atp1b3a* MO and *fxyd1* MO synergy. (M-T) Overexpression of *RhoAV14* in (M-N) control MO, low levels of (O-P) *atp1b3a*MO or (Q-R) *fxyd1* MO and (S-T) *atp1b3a* MO and *fxyd1* MO synergy. Dorsal (A,C,E,G,I,K,M,O,Q,S) and lateral A'-S' brightfield images of ventricle injected embryos. Zo-1 (B,D,F,H,J,L,N,P,R,T). All images of 24 hpf, anterior to the left. Asterisk = ear. H = hindbrain. Scale bars = 50 μm.

injected with low levels of individual *atp1a1* splice site MO (10/10 wild type), *atp1b3a* MO (27/27 wild type), or *fxyd1* MO (25/25 wild type) showed normal inflated brain ventricles, with continuous junctions (Figure A1.5A-H, control MO = 25/25 wild type). In combination, low levels of both *atp1a1* splice site and *atp1b3a* MOs did not affect apical junction localization or brain ventricle inflation (Figure A1.5I-J, 15/15 wild type,). However, combination of *atp1b3a* and *fxyd1* MOs severely disrupted apical junction localization (Figure A1.5K-L, 0/20 wild type). These results show that a partial loss of *fxyd1* in combination with a partial loss *atp1b3a* results in synergistic defects.

We have previously demonstrated that RhoA acts upstream of neuroepithelial formation and downstream of Fxyd1 (Chapter 2). Therefore we asked whether RhoA could rescue the

atp1b3a/fxyd1 synergy. Expression of constitutively active *RhoAV14* in embryos expressing low levels of *atp1b3a* MO or *fxyd1* MO does not disrupt neuroepithelial formation (Figure A1.5M-Q, fraction wild type in control MO + *RhoAV14* = 19/25, *atp1b3a* MO+ *RhoAV14* = 22/22, *fxyd1* MO + *RhoAV14* = 17/22) compared to controls (Figure A1.5A-B,E-H). However, expression of *RhoAV14* in combination with *atpb3a/fxyd1* synergy rescued neuroepithelial formation (Figure A1.5S-T, 20/25 wild type) compared to control RNA injected *atpb3a/fxyd1* synergy embryos (Figure A1.5K-L). This suggests that RhoA acts downstream of the Atp1b3a and Fxyd1 interaction to regulate neuroepithelial permeability. Further, since Atp1b3a alone does not have a significant effect on apical junctions, we propose that *atp1b3a* loss of function reduces the amount of Atp1a1 available to Fxyd1 thus disrupting formation of a continuous apical junction complex. However, a direct interaction between Fxyd1 and Atp1b3a cannot be excluded. Thus, RhoA appears to bypass the upstream requirement of the Na,K-ATPase to rescue the junctions.

In sum, although *atp1b3a* loss of function decreases levels of Atp1a1, we do not observe synergy, likely a result of functional redundancy of the beta subunits. In contrast, Atp1b3a and Fxyd1 synergize in a RhoA dependent manner to regulate neuroepithelial formation.

DISCUSSION AND FUTURE DIRECTIONS

Together these data suggest that Atp1b3a functions in conjunction with Atp1a1 and Fxyd1 during brain ventricle development. Due to functional redundancy, we cannot completely identify the role of Atp1b3a during neuroepithelial formation, permeability or brain ventricle inflation. However, our data does suggest that this subunit, in concert with others, plays a major role during CSF production (Figure A1.6). We propose that Atp1b3a directly contributes to CSF production and exhibits synergistic defects on apical junction localization with Fxyd1 by decreasing Atp1a1 levels. We cannot, however, rule out the possibility that Atp1b3a affects these processes in an Atp1a1 independent manner or directly interacts with Fxyd1. To fully investigate the role of the Atp1b3a during brain ventricle development, a complete characterization of the other beta subunits and identification of their functional redundancy must be performed.

One question that remains is why *atp1b3a* loss of function results in normal neuroepithelial formation and permeability. One possibility is that Atp1b3a is only required for CSF production and plays no role in the remaining developmental steps. Alternatively, Atp1b3a could be involved in neuroepithelial formation and permeability, but the phenotype of *atp1b3a* morphants is masked by other compensatory beta subunits. This latter hypothesis is supported by wild type $[Na^+]_i$ and ventricle size observed in *atp1b3a* morphants (Figure A1.3). However, we must investigate neuroepithelial permeability, $[Na^+]_i$, Atp1a1 levels and localization, and synergy between the other betas and Atp1a1 or Fxyd1 to completely characterize the role of the beta subunits during brain ventricle development. These results are interesting, as functional redundancy has previously been identified in mouse blastocysts (Barcroft et al., 2004; MacPhee et al., 2000). Mouse and humans contain only four beta subunits, and thus it is possible that the additional subunits found in zebrafish (seven in total) allow for compensation.

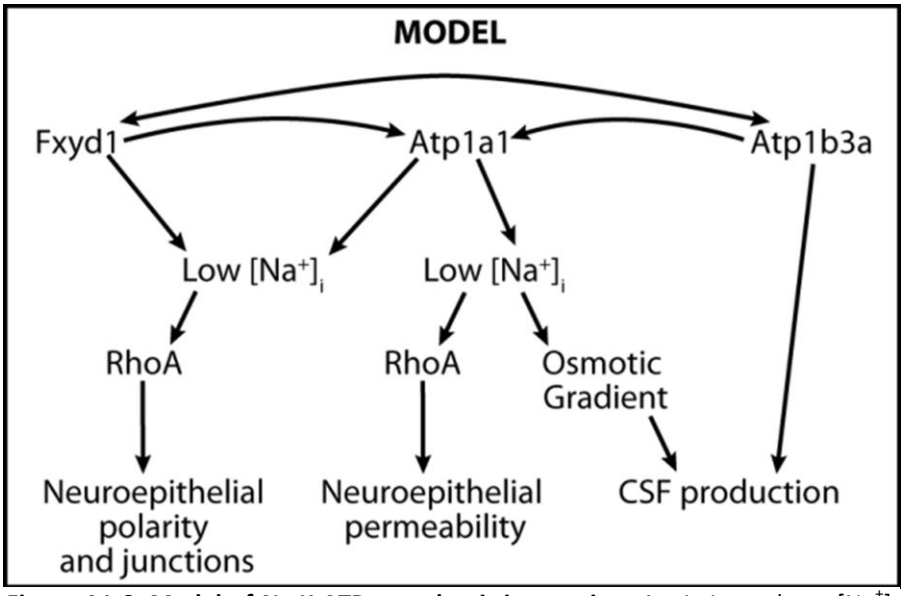

Figure A1.6: Model of Na,K-ATPase subunit interaction. Atp1a1 regulates $[Na^+]_i$ and which regulates osmotic gradient and thus CSF production or neuroepithelial permeability and polarity and junctions through RhoA. Fxyd1 can act via Atp1a1 or independently to regulate neuroepithelial junctions. Atp1b3a is required for CSF production and likely regulates Atp1a1 to affect CSF production.

Although we do not address the mechanism by which Atp1b3a maintains levels of Atp1a1, several studies have suggested that beta subunits can regulate Atp1a1 translation, stability and integration into the membrane (Geering, 2001; Rajasekaran et al., 2003). Our observation that Atp1b3a is necessary for maintaining wild type levels of Atp1a1 supports this hypothesis. However, localization of the remaining Atp1a1 protein is not perturbed in *atp1b3a* morphants.

In *Drosophila*, the alpha subunits bears a basolateral targeting sequence suggesting an alternative mechanisms to target alpha subunits to the plasma membrane (Muth et al., 1998). Therefore one possibility is that the zebrafish alpha subunit contains an apical targeting sequence allowing for proper localization in the absence of Atp1b3a. A second possibility is that a different beta subunit accompanies the remaining alpha subunit to the appropriate side of the cell. Future experiments will be done to identify whether other beta subunits are required to target the alpha to the apical surface.

An interesting hypothesis that remains to be tested is that Atp1a1 is the critical subunit necessary for brain ventricle development and phenotypes observed in *fxyd1* or *atp1b3a* loss of function embryos occur due to abnormal regulation of Atp1a1. Several lines of evidence support this hypothesis. First, *atp1b3a* morphants have decreased Atp1a1 levels and a reduction in CSF production and brain ventricle size. Therefore, it is possible that the reduction in Atp1a1 protein, due to the *atp1b3*a loss of function, reduces CSF production. Conversely, in *atp1b3a* gain-of-function embryos, brain ventricle size does not increase suggesting that Atp1b3a does not directly produce CSF but rather stabilizes Atp1a1 which produces CSF. However, we cannot rule out an Atp1b3a independent regulation of brain ventricle inflation. Finally, in embryos with partial loss of both *atp1b3a* and *fxyd1* (synergy), we propose that a partial loss of Atp1b3a slightly reduces Atp1a1 levels, in combination with a partial loss of Fxyd1 which further reduces remaining Atp1a1 pumping would result in abnormal neuroepithelial formation. If our hypothesis is true, we would expect that $[Na^+]_i$ levels would be elevated in embryos with partial loss of both *atp1b3a and fxyd1*. These data wound support the hypothesis that instead of interacting independent of the alpha subunit, Atpb3a and Fxyd1 synergize by simultaneously affecting Atp1a1's concentration (Atp1b3a-specific effects) and pumping activity (Fxyd1-specific effects). Further examination of Atp1a1 levels in embryos with a partial loss of function in both *atp1b3a* and *fxyd1* and *atp1b3a* gain of function will begin to test this hypothesis.

The Na,K-ATPase plays a role in regulating fluid production in many tubular organs. In humans, mice and zebrafish, abnormal Na,K-ATPase localization other ionic pump activity lead to

disorders such as polycystic kidney disorder, which is characterized by fluid filled cysts in the kidney epithelium and hydrocephalus, an excess of CSF within the brain ventricles. Further investigation of the interactions between Atp1a1, beta and Fxyd1 subunits, and a characterization of how the cell determines which subunits to use, will be important in dissecting the mechanism and etiology of these fluid production disorders.

ACKNOWLEDGEMENTS

This work was supported by the National Institute for Mental Health, and National Science Foundation. Special thanks to Laura Anne Lowery and Jenny Ruan who started the project, Joey Davis for comments on the manuscript, and Sive lab members for useful discussions and constructive criticism.

REFERENCES

Barcroft, L. C., Moseley, A. E., Lingrel, J. B., Watson, A. J., 2004. Deletion of the Na/K-ATPase alpha1-subunit gene (Atp1a1) does not prevent cavitation of the preimplantation mouse embryo. Mech Dev. 121**,** 417-26.

Canfield, V. A., Loppin, B., Thisse, B., Thisse, C., Postlethwait, J. H., Mohideen, M. A., Rajarao, S. J., Levenson, R., 2002. Na,K-ATPase alpha and beta subunit genes exhibit unique expression patterns during zebrafish embryogenesis. Mech Dev. 116**,** 51-9.

Draper, B. W., Morcos, P. A., Kimmel, C. B., 2001. Inhibition of zebrafish fgf8 pre-mRNA splicing with morpholino oligos: a quantifiable method for gene knockdown. Genesis. 30**,** 154-6.

Geering, K., 2001. The functional role of beta subunits in oligomeric P-type ATPases. J Bioenerg Biomembr. 33**,** 425-38.

Gloor, S., Antonicek, H., Sweadner, K. J., Pagliusi, S., Frank, R., Moos, M., Schachner, M., 1990. The adhesion molecule on glia (AMOG) is a homologue of the beta subunit of the Na,K-ATPase. J Cell Biol. 110**,** 165-74.

Gutzman, J. H., Sive, H., 2009. Zebrafish brain ventricle injection. J Vis Exp.

Gutzman, J. H., Sive, H., 2010. Epithelial relaxation mediated by the myosin phosphatase regulator Mypt1 is required for brain ventricle lumen expansion and hindbrain morphogenesis. Development. 137**,** 795-804.

Harland, R. M., 1991. In situ hybridization: an improved whole-mount method for Xenopus embryos. Methods Cell Biol. 36**,** 685-95.

Harrington, M. J., Hong, E., Brewster, R., 2009. Comparative analysis of neurulation: first impressions do not count. Mol Reprod Dev. 76**,** 954-65.

Hong, E., Brewster, R., 2006. N-cadherin is required for the polarized cell behaviors that drive neurulation in the zebrafish. Development. 133**,** 3895-905.

Jaisser, F., Jaunin, P., Geering, K., Rossier, B. C., Horisberger, J. D., 1994. Modulation of the Na,K-pump function by beta subunit isoforms. J Gen Physiol. 103**,** 605-23.

Kimmel, C. B., Ballard, W. W., Kimmel, S. R., Ullmann, B., Schilling, T. F., 1995. Stages of embryonic development of the zebrafish. Dev Dyn. 203**,** 253-310.

Lian, W. N., Wu, T. W., Dao, R. L., Chen, Y. J., Lin, C. H., 2006. Deglycosylation of Na+/K+-ATPase causes the basolateral protein to undergo apical targeting in polarized hepatic cells. J Cell Sci. 119**,** 11-22.

Lowery, L. A., Sive, H., 2005. Initial formation of zebrafish brain ventricles occurs independently of circulation and requires the nagie oko and snakehead/atp1a1a.1 gene products. Development. 132**,** 2057-67.

MacPhee, D. J., Jones, D. H., Barr, K. J., Betts, D. H., Watson, A. J., Kidder, G. M., 2000. Differential involvement of Na(+),K(+)-ATPase isozymes in preimplantation development of the mouse. Dev Biol. 222**,** 486-98.

Madan, P., Rose, K., Watson, A. J., 2007. Na/K-ATPase beta1 subunit expression is required for blastocyst formation and normal assembly of trophectoderm tight junction-associated proteins. J Biol Chem. 282**,** 12127-34.

Muth, T. R., Gottardi, C. J., Roush, D. L., Caplan, M. J., 1998. A basolateral sorting signal is encoded in the alpha-subunit of Na-K-ATPase. Am J Physiol. 274**,** C688-96.

Nasevicius, A., Ekker, S. C., 2000. Effective targeted gene 'knockdown' in zebrafish. Nat Genet. 26**,** 216-20.

Paul, S. M., Palladino, M. J., Beitel, G. J., 2007. A pump-independent function of the Na,K-ATPase is required for epithelial junction function and tracheal tube-size control. Development. 134**,** 147-55.

Paul, S. M., Ternet, M., Salvaterra, P. M., Beitel, G. J., 2003. The Na+/K+ ATPase is required for septate junction function and epithelial tube-size control in the Drosophila tracheal system. Development. 130**,** 4963-74.

Rajasekaran, S. A., Gopal, J., Rajasekaran, A. K., 2003. Expression of Na,K-ATPase beta-subunit in transformed MDCK cells increases the translation of the Na,K-ATPase alpha-subunit. Ann N Y Acad Sci. 986**,** 652-4.

Rajasekaran, S. A., Palmer, L. G., Quan, K., Harper, J. F., Ball, W. J., Jr., Bander, N. H., Peralta Soler, A., Rajasekaran, A. K., 2001. Na,K-ATPase beta-subunit is required for epithelial polarization, suppression of invasion, and cell motility. Mol Biol Cell. 12**,** 279-95.

Sagerstrom, C. G., Grinbalt, Y., Sive, H., 1996. Anteroposterior patterning in the zebrafish, Danio rerio: an explant assay reveals inductive and suppressive cell interactions. Development. 122**,** 1873-83.

Shoshani, L., Contreras, R. G., Roldan, M. L., Moreno, J., Lazaro, A., Balda, M. S., Matter, K., Cereijido, M., 2005. The polarized expression of Na+,K+-ATPase in epithelia depends on the association between beta-subunits located in neighboring cells. Mol Biol Cell. 16**,** 1071-81.

Vagin, O., Sachs, G., Tokhtaeva, E., 2007a. The roles of the Na,K-ATPase beta 1 subunit in pump sorting and epithelial integrity. J Bioenerg Biomembr. 39**,** 367-72.

Vagin, O., Tokhtaeva, E., Sachs, G., 2006. The role of the beta1 subunit of the Na,K-ATPase and its glycosylation in cell-cell adhesion. J Biol Chem. 281**,** 39573-87.

Vagin, O., Tokhtaeva, E., Yakubov, I., Shevchenko, E., Sachs, G., 2008. Inverse correlation between the extent of N-glycan branching and intercellular adhesion in epithelia. Contribution of the Na,K-ATPase beta1 subunit. J Biol Chem. 283**,** 2192-202.

Vagin, O., Turdikulova, S., Tokhtaeva, E., 2007b. Polarized membrane distribution of potassium-dependent ion pumps in epithelial cells: different roles of the N-glycans of their beta subunits. Cell Biochem Biophys. 47**,** 376-91.

Westerfield, M., Sprague, J., Doerry, E., Douglas, S., Grp, Z., 2001. The Zebrafish Information Network (ZFIN): a resource for genetic, genomic and developmental research. Nucleic Acids Research. 29**,** 87-90.

Wilson, P. D., Devuyst, O., Li, X., Gatti, L., Falkenstein, D., Robinson, S., Fambrough, D., Burrow, C. R., 2000. Apical plasma membrane mispolarization of NaK-ATPase in polycystic kidney disease epithelia is associated with aberrant expression of the beta2 isoform. Am J Pathol. 156**,** 253-68.

Wilson, P. D., Sherwood, A. C., Palla, K., Du, J., Watson, R., Norman, J. T., 1991. Reversed polarity of Na(+) -K(+) -ATPase: mislocation to apical plasma membranes in polycystic kidney disease epithelia. Am J Physiol. 260**,** F420-30.